Alma Mater Studiorum – Università di Bologna

DOTTORATO DI RICERCA IN

TECNOLOGIE INNOVATIVE E USO SOSTENIBILE DELLE RISORSE DI PESCA E BIOLOGICHE DEL MEDITERRANEO (FISHMED-PHD)

Ciclo 35

Settore Concorsuale: 03/D1 – CHIMICA E TECNOLOGIE FARMACEUTICHE, TOSSICOLOGICHE E NUTRACEUTICO - ALIMENTARI

Settore Scientifico Disciplinare: CHIM/11 – CHIMICA E BIOTECNOLOGIA DELLE FERMENTAZIONI

BIOREMEDIATION OF POLYCHLORINATED BIPHENYLS (PCBs) POLLUTED MARINE SEDIMENTS: A STUDY OF THE EFFECTIVENESS OF BIOAUGMENTATION AND BIOSTIMULATION VIA MICROBIAL ELECTROCHEMICAL TECHNOLOGIES AND POLYHYDROXYALKANOATES

Presentata da: Alberto Botti

Coordinatore Dottorato

Stefano Goffredo

Supervisore

Giulio Zanaroli

Co-supervisore

Marco Candela

Esame finale anno 2023

INDEX

This page is intentionally left blank

ABSTRACT

Polychlorinated biphenyls (PCBs) are chemicals largely employed in the industry, banned at the end of the last century yet still persistent in the environment. Microbial remediation exploits bacteria to reduce PCBs' toxicity and it is currently receiving attention as a promising technique to remediate polluted site *in situ*. Yet, natural microbial remediation is constrained by several factors as the low amount of the required nutrients and growth substrates (e.g. electron donors, oxygen) and the scarcity of bacteria able to metabolize the pollutants. In this regard, use of biodegradable polymers or microbial electrochemical technologies (METs) have been demonstrated effective in priming bioremediation of freshwater environments (e.g. river sediments) polluted by chlorinated solvents or PCBs. Still, little is known regarding their application in marine sediments, where the abundance of anaerobic competitors (i.e. sulfate reducing bacteria) and the different sediment's features might affect the bioremediation process.

In this PhD thesis, two approaches were studied for the first time to stimulate the bioremediation of PCBs polluted marine sediments. Polyhydroxyalkanoates (PHAs), a class of biodegradable polymers synthesizable from organic waste streams, were employed as slow hydrogen release compounds. METs, which couple electrodes with bacterial activity, were used to provide a constant and prolonged release of reducing equivalents in time. The influence of PHAs was studied on the main anaerobic metabolisms and on the microbial community of the heavily polluted sediments coming from the Pialassa della Baiona, a micro-tidal coastal lagoon in Ravenna, and from Mar Piccolo, the marine basin aside Taranto. The impact of METs was deepened by monitoring the physical-chemical parameters and the main anaerobic metabolisms of the sediments coming from Ravenna. Biostimulation with PHAs was effective in priming PCBs reductive dechlorination in sediment from Ravenna whereas it inhibited the process in sediment from Taranto. Thus, the outcome of the remediation was strictly dependent on the features of the treated site, being related to the availability of the amendments and to the competition of the indigenous microbial communities. As for the bioelectrochemical stimulation, we observed that the potential applied inhibited the bioremediation process, due to the competition of sulfate reducing bacteria and to the variation of pH, a side effect of the electrochemical input. In both cases, the key factor required to perform bioremediation of the polluted sites was the presence of an inoculated bacterial community. Therefore, the collected results led us to a comprehensive analysis of the available literature, questioning what could be the further approaches for an effective *in situ* bioremediation of PCBs polluted sites.

Chapter 1

Polychlorinated biphenyls (PCBs)

1.1 Polychlorinated biphenyls, an environmental concern

Many industrial processes require potential toxic and harmful substances that during the course of the years have been spread into the environment (Abraham et al., 2002; Antizar-Ladislao, 2010; Cappello et al., 2007). Polychlorinated biphenyls (PCBs) are a class of 209 synthetic compounds, characterized by the presence of chlorine atoms bonded to the aromatic ring (Fig. 1). The different PCBs molecules are usually addressed as congeners, identified by a specific number and position of halogen atoms. They were employed as mixtures, mostly known with their commercial names. For instance, in U.S.A. the Monsanto Corporation produced PCBs mixtures labeled as Aroclor, classified with a 4 digits numbering system where the first two digits usually refers to the number of the carbon atoms of the ring structure and the second two digits to the mass percentage of chlorine in the mixture. Thus resulting in several commercial products as Aroclor 1260, 1254 or 1242 (Mattes et al., 2018). PCBs are characterized by properties such as lipophilicity, chemical and thermal inertia, low dielectric constant, which have made them perfect candidates for different industrial processes (Fig. 2). However, the same properties make them poorly degradable, persisting in the environment and resulting in bioaccumulation and biomagnification into the food chain (Cho et al., 2007). For these reasons, after the 80' their usage in the industry was restricted and subsequently banned at the end of the last century (Abraham Wolf-Reiner et al., 2002). Later on, PCBs were defined as Persistent Organic Pollutants (POPs) by the Stockholm convention, in 2001 (Schuster et al., 2021). Indeed, besides their environmental persistence, PCBs have been classified as teratogens, carcinogenic to humans (Group 1) (Lauby-secretan et al., 2013) and endocrine disruptors (Baldigo et al., 2006; Gonzalez et al., 2016) since they can induce several adverse effects on the nervous, immune and endocrine systems. Despite all PCBs can cause toxic effects through different pathways (Lauby-secretan et al., 2013), a level of toxicity can be identified according to the type of congener. In particular, PCBs can be classified as non dioxine-like PCBs, or *orto*-congeners, and dioxine-like PCBs, with the second ones characterized by chlorine atoms in *meta* and *para* positions (Fig. 1). Dioxin-like PCBs have a stronger affinity to the aryl hydrocarbon receptor (AhR), identified also as dioxin receptor,

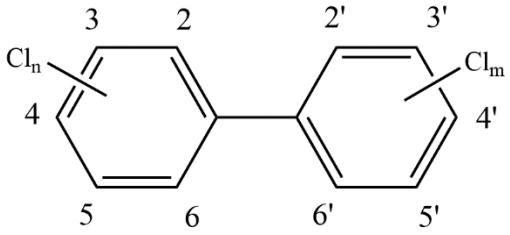

Figure 1 *General chemical structure of a PCB molecule. n,m= 1÷5; 2,2',6,6' are defined as orto positions; 3,3',5,5' are defined as meta positions; 4,4' are defined as para positions (Bedard, 2003)*

resulting in higher hazard quotients compared to non dioxine-like congeners (Giesy and Kannan, 1998). Considering the risks that this class of compounds poses to the environment, it is necessary to develop an efficient way to remove these pollutants reducing the toxicity of the contaminated sites (Carpenter, 2011; Nicolopoulou-Stamati and Pitsos, 2001).

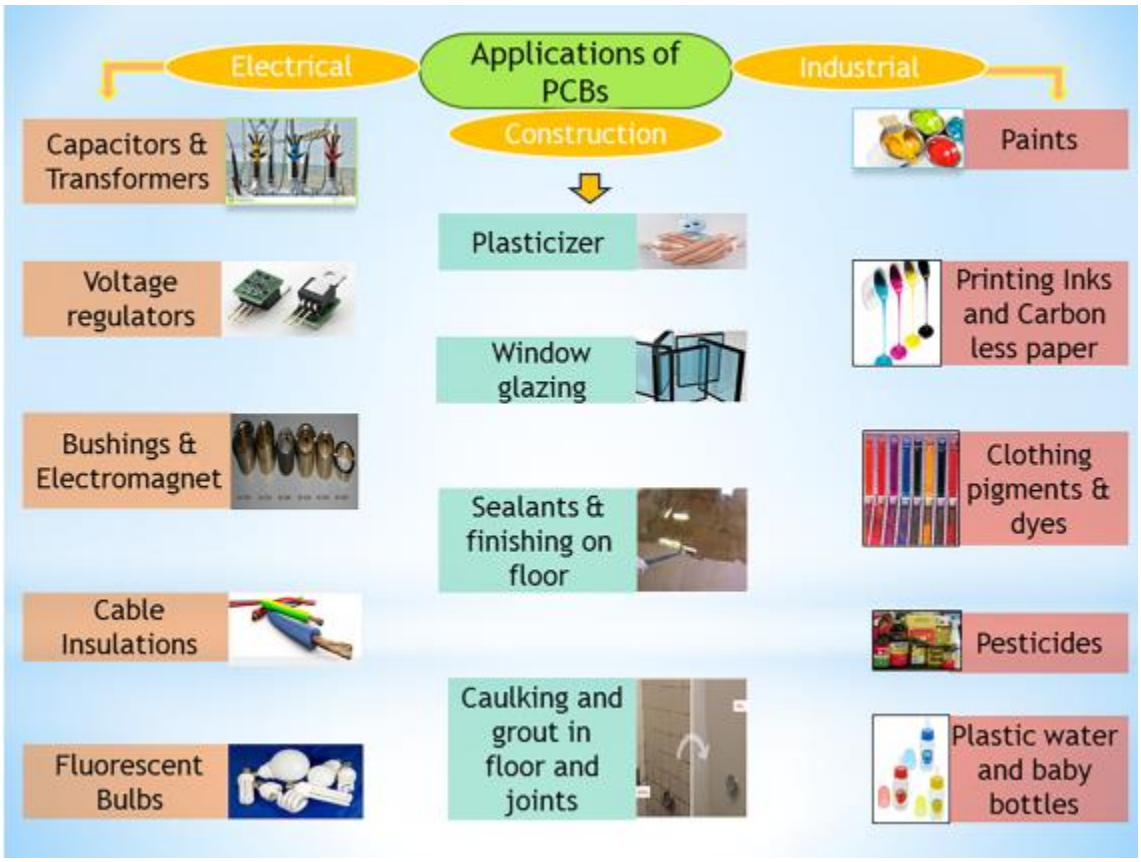

Figure 2 *Industrial applications of PCBs* (Reddy et al., 2019)

1.1.1 Pollution levels and current legislation for contaminated sediments

PCBs environmental concentrations can range from few $\mu g \cdot Kg^{-1}_{drysediment}$ to thousands of $mg \cdot Kg^{-1}_{drysediment}$ (Kjellerup et al., 2012; Nogales et al., 1999), being a worldwide burden with polluted areas that spatial from soils to river and marine sediments (IARC, 2016). Levels of contamination in Chinese soils were reported to be in the order of magnitude of 10^{-1} $mg \cdot Kg^{-1}_{drysediment}$ (Sun et al., 2018; Zhu et al., 2022), whereas higher concentrations were found in European or American sites, reaching several

mg·Kg$^{-1}_{drysediment}$ (Kjellerup et al., 2012; Nogales et al., 1999). The estimated amount of total PCBs pollution in soil sums up to 21'000 tons (Meijer et al., 2003). Urbanization and intensive industrialization led to the dispersion of pollutants also in aquatic environments as river sediments. For instance, the metropolitan region of Pearl River Delta (China) was subjected to industrial discharges from shipyards and heavy metals manufacturers, leading to PCBs concentrations of 0.1-0.5 mg·Kg$^{-1}_{drysediment}$ (Wang et al., 2019). Recently, a spatio-temporal assessment of the PCBs distribution in the four major French river corridors linked the pollution of the streams to the commercial and industrial activities of the area (Dendievel et al., 2020). In this context, river sediments act as sources of contamination for the marine environment. In fact, despite the relative low levels of contamination found in the studied river sediments (10^{-2}-10^{-3} mg·Kg$^{-1}_{drysediment}$) (Dendievel et al., 2020), values exceeding the regulatory benchmarks for consumption were found in mussels on the adjacent coasts (Amiard et al., 2011), highlighting the role of rivers in polluting marine biota and sediments (Dendievel et al., 2020). Indeed, PCBs abound in marine ecosystems, where surface sediments act as final repository of the pollutants, promoting their adsorption thanks to the high content of organic matter (Fig. 3) (Ngoubeyou et al., 2022; Reddy et al., 2019). Regarding the European continent, PCBs pollution has been assessed in the whole Mediterranean basin, with level of contaminations up to 20 mg·Kg$^{-1}_{drysediment}$ and higher values in proximity of industrial sites as Marseille (France) (Merhaby et al., 2019). As for Italian polluted sites, the pressure of the industrial poles led to the contamination of areas as the Pialassa della Baiona (Ravenna), a micro tidal coastal lagoon, and of the Mar Piccolo (Taranto), a semi-enclosed basin, with values of PCBs up to 7 mg·Kg$^{-1}_{drysediment}$ (Bellucci et al., 2016; Cotecchia et al., 2021; Guerra, 2012; Guerra et al., 2014; Mali et al., 2017; Quero et al., 2015; Todaro et al., 2020). Considering the high level of pollution of marine sediments, appropriate remediation strategies and regulations are needed.

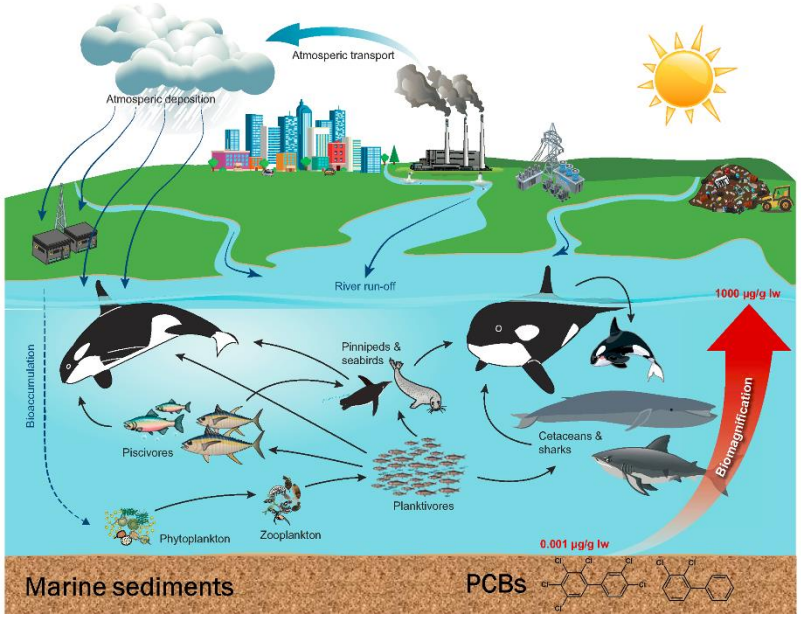

Figure 3 *PCBs transport and pollution from sources to biomagnification inside the food chain, adapted from (Bondo, 2018)*

Currently, a worldwide regulation for sediment's pollution hasn't been set yet (APAT, 2006). Level of PCBs in sediments are regulated by identifying guidelines and standard values to assess quality of the polluted sites, which can vary of order of magnitudes from one country to another (Alzieu et al., 2003; APAT, 2006; Bergemann and Gaumert, 2008; Brien et al., 2003; Canadian Council of Ministers of the Environment, 1999; MacDonald et al., 2000, 2003) (Table 1). European standard values can vary from 0.02 $mg \cdot Kg^{-1}_{drysediment}$ for single congeners, identified by the Germany government (Bergemann and Gaumert, 2008), to 1-4 $mg \cdot Kg^{-1}_{drysediment}$ for the total PCBs content, as indicated by French and Italian guidelines (Alzieu et al., 2003; APAT, 2006). On the contrary, American countries as Canada, Florida and Wisconsin, identified values of total PCBs between 0.02 and 0.06 $mg \cdot Kg^{-1}_{drysediment}$ as concentrations below which adverse effects are unlikely to occur (Brien et al., 2003; Canadian Council of Ministers of the Environment, 1999; MacDonald et al., 2003, 2000). It should be noted that even if sediment concentrations meet the quality guidelines, level of pollution in biota living next to the contaminated sites might exceed the limit for the consumption of fish and shellfish by wildlife species and human, still posing a risk to the environment (Arblaster et al., 2015).

Table 1 *Sediment quality guidelines for PCBs polluted sediments*

Country	**Sediment quality guideline ($mg \cdot Kg^{-1}_{drysediment}$)**	**Reference**
Canada	Threshold effect concentration: 0.0215(MS), 0.0341(FS) Probable effect levels: 0.189 (MS), 0.277 (FS)	(Canadian Council of Ministers of the Environment, 1999)
Florida (U.S.A.)	Probable effect concentration: 0.676 (FS) Threshold effect concentration: 0.060 (FS)	(MacDonald et al., 2003, 2000)
Wisconsin (U.S.A.)	Probable effect concentration: 0.676 (FS) Threshold effect concentration: 0.060 (FS)	(Brien et al., 2003; MacDonald et al., 2000)
Taiwan	0.09	(Chang et al., 2019a)
France	Threshold effect concentration: 0.500 Probable effect levels: 1	(Alzieu et al., 2003)
Germany	0.020 (for single congeners)	(Bergemann and Gaumert, 2008)
Italy	4	(APAT, 2006)

MS: marine sediment; FS: freshwater sediment

1.2 Remediation of PCBs polluted sediments

Currently, polluted sites are mainly treated by dredging, followed by *ex-situ* physical-chemical treatments or a disposal of the sediment (Helena I. Gomes et al., 2013). The least advisable approach to treat the dredged sediment is landfilling, since it does not provide a remediation of the polluted site (Šrédlová and Cajthaml, 2022). On the other hand incineration is one of the most effective techniques, despite being suitable only for low amount of highly contaminated matrix and possibly generating toxic compounds as polychlorinated dibenzo(p)dioxin and furans (PCDD/F) (Šrédlová and Cajthaml, 2022). Generally, *ex situ* approaches are highly impacting for the ecosystem, requiring large amount of energy, increasing the risks of diffusing the pollutants, for instance during the excavation process, and compromising the treated matrix due to the aggressive applied techniques (e.g. incineration). Consequently, they cannot be considered environmentally sustainable processes (Carberry and Wik, 2001; Helena I. Gomes et al., 2013; Vidali, 2001). *In situ* remediation does not require the physical removal of the contaminated matrix, reducing costs of treatments and lowering the risk of diffusion of the toxic substances. It is however necessary to avoid aggressive techniques such as the use of oxidant agents (Helena I Gomes et al., 2013), to preserve the treated site. Conventional capping, consisting in covering the surface sediment with a layer of clean material, has been applied to reduce the exposure of leaving organisms to the pollutants via a physical isolation (Zeller and Cushing, 2006). Carbonaceous material able to adsorb the contaminants, like activated carbon, were employed as capping layers and proved to be effective even at full scale applications, showing minor harmful effects compared to conventional capping (Janssen and Beckingham, 2013; Lillicrap et al., 2015; Patmont et al., 2020). Yet, capping reduces the bioavailability of the pollutants without remediating the site, thus leaving the polluted layer in the matrix. In this regard, bioremediation has been targeted as a promising approach for *in situ* applications since by exploiting living organisms as plants, fungi or bacteria it is possible to reduce the toxicity of the compounds. The first signs of PCBs biodegradability were reported in 1973 (Ahmed and Focht, 1973). Subsequently, several experiments demonstrated the role of living organisms in remediating the polluted sites. Phytoremediation relies on plants and bacteria to improve biodegradation of PCBs thanks to the interactions between roots and indigenous microbial community (Ancona et al., 2017). Still, it is applicable only on soils and few demonstrations were given at a large scale (Ancona et al., 2017; Šrédlová and Cajthaml, 2022). Fungi can degrade PCBs as well, given the low specific intracellular and extracellular enzymes, able to interact with several class of organic compounds (Šrédlová and Cajthaml, 2022). However, fungi have been mainly employed on polluted soils and require

operational conditions, as mechanical agitations, difficult to apply *in situ* (Sage et al., 2014; Siracusa et al., 2017; Šrédlová and Cajthaml, 2022). A further bioremediation approach occurs via microbial degradation. Natural attenuation of polluted sediments can take place via the indigenous microbial species able to metabolize the contaminants (Pakdeesusuk et al., 2005). Considering the adaptability of bacteria, able to sustain bioremediation processes in different water environments as river or marine sediments and under real *in situ* conditions, microbial degradation of PCBs has been targeted as a promising approach for bioremediation of polluted sediments (Payne et al., 2019; Šrédlová and Cajthaml, 2022).

1.2 Microbial degradation of PCBs

Microbial biodegradation of PCBs takes place via two sequential steps, respectively named as reductive dechlorination and oxidative degradation. In the following sections, the main features of the two processes will be deepened.

1.2.1 Reductive dehalogenation of PCBs

1.2.1.1 General features

The reductive dechlorination of PCBs is a process through which anaerobic bacteria use polychlorinated biphenyls as terminal electron acceptors of the respiration chain (Häggblom and Bossert, 2003). To do so, bacteria defined as dechlorinating bacteria or organohalide respiring bacteria (OHRB) require a source of protons and electrons so as to reduce the congener, by substituting the chlorine atom with a proton (Fig. 4). From an environmental point of view, the advantage of the reductive dechlorination is the possibility to reduce the toxicity of the chlorinated pollutants (Bedard, 2003). Indeed, OHRB are capable to transform *dioxine-like* PCBs to less toxic congeners as *non dioxine-like* PCBs, by reducing the carbon atoms at the *meta* and *para* positions which are the most commonly attacked. In this regard, several

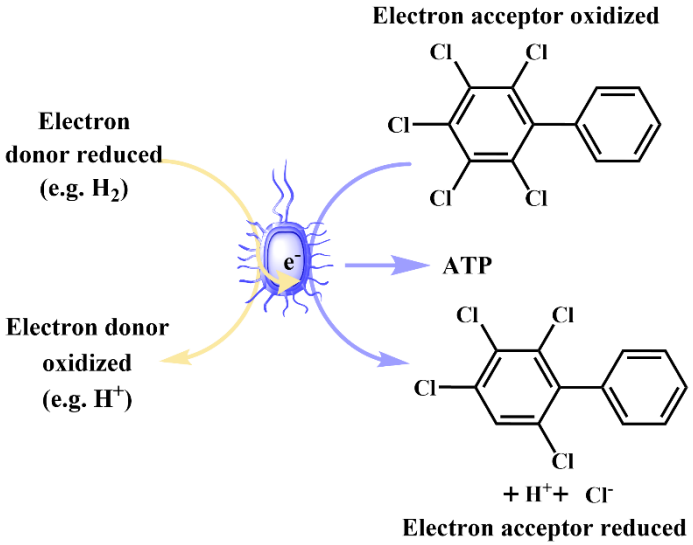

Figure 4 *Example of reductive dehalogenation of the 2,3,4,5-tetrachlorobiphenyl, resulting in the formation of 2,3,5-trichlorobiphenyl, adapted from* (Häggblom and Bossert, 2003)

patterns of dehalogenation were identified and classified according to the position of the chlorine atom involved in the reductive reaction (Häggblom and Bossert, 2003). For instance, dechlorination processes which remove singly flanked *para* chlorines are labelled patterns P, H, and H' whereas processes which remove singly flanked *meta* atoms are defined as N. The dechlorination processes that reduce congeners with unflanked chlorines are less common and are named M, Q and LP.

1.2.1.2 Key players of reductive dechlorination, organohalide respiring bacteria

Nowadays, several bacteria have been linked to reductive dechlorination of PCBs (Hiraishi, 2008; Steffan and Schaefer, 2016). Through phylogenetic analysis of enriched microbial community, it was confirmed that bacteria considered key-players in PCBs reductive dechlorination process belonged to Chloroflexi (Zanaroli et al., 2012a), *Dehalococcoides* and *Dehalogenimonas* (Wang and He, 2013), *Desulfitobacterium* (Baba et al., 2007) and *Dehalobacter* (Yan et al., 2006a). A better comprehension of this class of microbes was possible only after the isolation of pure cultures. The first pure culture of an anaerobic PCB-respiring bacterium was obtained from a tidal estuary of Charleston Harbour, and it was named *Dehalobium chlorocoercia* DF-1. It belonged to the phylum of *Chloroflexi* and it could reduce doubly flanked *meta* and *para* chlorines only in the presence of a non-dechlorinating *Desulfovibrio* species (May et al., 2008). Subsequently, pure cultures of *Dehalococcoides mccartyi* were identified, reporting their ability to reduce mixtures of PCBs, with a predominant activity towards *meta* and *para* chlorines (Adrian et al., 2009; Laroe et al., 2014). Instead, the more rare *orto* dechlorination was observed in presence of the *D. mccartyi o-17*, obtained in coculture with a non-dechlorinating *Desulfovibrio* species (Steffan and Schaefer, 2016). Studying the different dechlorinating cultures and characterizing the spectrum of congeners that they can dechlorinate has become essential to predict the effectiveness of a bioremediation strategy on a PCBs polluted site. Up to now, the knowledge of OHRB able to reductively dechlorinate PCBs is still limited due to the difficulties in growing them at high concentration and as pure culture (Wang et al., 2014).

1.2.1.3 Enrichment of OHRB able to reductively dechlorinate PCBs

At a laboratory phase, obtaining high cell densities culture of OHRB is an essential step to study PCBs reductive dehalogenation and to plan an appropriate *in situ* bioremediation action. Enriched culture can be obtained starting from real matrixes and growing the microbial community on sediments (Zanaroli et al., 2010) or on synthetic medium, defined as sediment-free culture, using sterile silica as support for the

microbial growth (Wang and He, 2013). In both cases, sequential dilutions of the starting matrix in sterile sediment or synthetic medium spiked at high concentrations of PCBs are performed, in the presence of a carbon source either coming from the indigenous sediment or externally added (e.g. acetate or formate) (Richardson, 2016). The large amount of electron acceptor can help to stimulate the bacteria's growth exerting a selective action. Synthetic media are more appropriate for laboratory studies and single cultures cultivation. Yet, it is possible that the enriched cultures lose their ability to dechlorinate PCBs during the sequential dilution process, due to the loss of nutritional factors that cannot be found in the synthetic medium (Wang and He, 2013). Additionally, cultivating bacteria on PCBs requires long incubation times and it does not yield to concentrated cultures. The low and slow growth yield is linked to two factors. First of all to the scarce solubility of PCBs, 2.4-3·10^3 µg·L^{-1}, largely lower compared to other common chlorinated pollutants as PCE (tetrachloroethylene), 1.5·10^5 µg·L^{-1} (Lombard et al., 2014). Secondly, to the low free energy Gibbs of the reduction reaction, -145/-168 kJ·mol^{-1} for PCBs compared to -192 kJ·mol^{-1} for PCE (Chen and He, 2018; Holmes et al., 1993). Hence, up to now, the most studied PCBs dechlorinating bacteria are the one provided with reductive dehalogenases (RDase) active both on PCBs and PCE and that can still metabolize PCBs even after a long period of growth on sole PCE (Adrian et al., 2009; Chen and He, 2018; May et al., 2008). With these kinds of bacteria, the growth strategy starts with transferring a sediment-free culture into a PCBs-free medium with PCE as sole electron acceptor (Payne et al., 2019). The PCE allows to obtain microbial cultures up to 10^2 times more concentrated than on PCBs, dramatically reducing the cultivation time (Wang et al., 2014). Subsequently, the PCE and its dechlorination products can be easily removed via nitrogen purging resulting in a solution free from organochlorinated compound that can be used for molecular studies or for bioremediation purposes. Yet, not all the microbial species are characterized by RDase that can retain their PCBs reduction activity through the sequential dilutions or after the growth on PCE.

1.2.1.4 Competing bacteria of OHRB

When working with synthetic medium or pure cultures of OHRB, the advantage is not only given by the possibility to tune the medium composition to favor growth of OHRB but also by the absence of other anaerobic competitors. Indeed, in real anaerobic environments several class of bacteria can compete with PCBs dechlorinating bacteria for the electron source (Häggblom and Bossert, 2003). Sulfate reducers (SRB) and methanogenic bacteria (MB) are commonly found in marine habitats, where the former class is usually the most competitive (Oremland and Taylor, 1978). PCBs OHRB are thought to specifically use hydrogen as electron donor, whereas SRB and MB can employ other molecules as acetate

(Richardson, 2016; Steffan and Schaefer, 2016). In this regard, the H_2 concentration can regulate the mechanism of competition of other anaerobic respiring bacteria (Dolfing, 2003). The minimum concentration of hydrogen to observe the electron accepting process is defined as the threshold value of H_2, which is known to be lower for OHRB compared to SRB or MB, making them more competitive at relatively low hydrogen concentration (Table 2). Yet, high amount of electron acceptors, as sulfates for SRB or acetate/carbon dioxide for MB, can change the thermodynamic of the process favoring this kind of bacteria in respect to OHRB (Dolfing, 2003). Additionally, the hydrophobicity of the organohalogenated electron acceptors leads to low aqueous concentrations decreasing the competitiveness of OHRB. In this complex conditions, OHRB bacteria struggle to get the necessary reducing equivalents (Mccarty, 1997). External supply of electron donors can help triggering the reductive dechlorination (Fennell and Gossett, 2003). However, the exogenous electron donors can prime other metabolisms too, as sulfate reduction, iron (III) reduction, acetotrophic and hydrogenotrophic methanogenesis (Fennell and Gossett, 2003). Hence, it is important to take into account that any unspecific action which aims to stimulate dechlorinating bacteria can favor other species as well (Aldera et al., 1993). Moreover, anaerobic respiring bacteria as SRB can exert a toxic effects towards other bacteria, as OHRB, due to the release in the environment of by-products of their metabolisms. Sulfate, thiosulfate, sulfite or sulfide are known to inhibit enzymes involved in dehalogenation (Fennell and Gossett, 2003; Hoelen and Reinhard, 2004). A partial attenuation of the inhibition exerted by SRB can be given by the presence of the sediment, for example thanks to the precipitation of iron sulfides which eliminate the toxic byproducts (Hoelen and Reinhard, 2004).

Table 2 *Hydrogen threshold concentrations for the different electron acceptor processes* (Bossert et al., 2003)

Electron acceptor process	**Hydrogen concentration (nM)**
Denitrification	<0.1
Iron (III) reduction	0.2-0.6
Dehalorespiration	0.3
Sulfate reduction	1-4
Methanogenesis	>5
Acetogenesis	>336

1.2.1.5 *In situ* natural attenuation of PCBs pollution via reductive dechlorination

Regarding the natural microbial process occurring *in situ*, a partial bioremediation of the polluted site can take place via the spontaneous reductive dechlorination of the PCBs mixture. For instance, Bzdusek *et al*. (2006) observed a shift in the pattern of PCBs (0-58 $mg \cdot Kg^{-1}_{drysediment}$) of polluted sediments of Lake Hartwell (South Carolina, U.S.A.) over a period of 11 years (1987-1998), resulting in profile of the single congeners not resembling the one employed in the commercial mixture (e.g. Aroclor 1254 and 1242). Similarly, in an emergency wastewater overflow lagoon in Virgina (U.S.A.) highly contaminated with PCBs (6-12'800 $mg \cdot Kg^{-1}_{drysediment}$), the accumulation of low-chlorinated congeners was observed and linked to the relative abundance of Chloroflexi phylum, putative dechlorinating bacteria (Mattes et al., 2018). Also, the less common reductive dechlorination of *orto*-congeners was observed *in situ* in PCBs polluted sediments (0.016-42.5 $mg \cdot Kg^{-1}_{drysediment}$) of the Hudson river (New York, U.S.A.) (Chitsaz et al., 2020). Yet, natural attenuation of PCBs contamination requires long times, up to several years (Bzdusek et al., 2006; Pakdeesusuk et al., 2005), due to factors as the low amount of indigenous electron donors and the relatively low abundance of OHRB. Additionally, spontaneous *in situ* PCBs microbial degradation is thought to reach a plateau after some time (Bzdusek et al., 2006; Pakdeesusuk et al., 2005), leading to the accumulation of low-chlorinated congeners that are not furtherly metabolized by OHRB. Indeed it should be noted that the reductive dechlorination process leaves the aromatic rings intact. Consequently, the presence of bacteria able to degrade the organic structure is mandatory for a complete PCBs removal process.

1.2.2 Oxidative degradation of PCBs

1.2.2.1 General features

To further reduce the toxicity of PCBs, reductive dehalogenation needs to be followed by the *oxidative degradation*, an aerobic process which cleaves the aromatic structure via the biphenyl degradation pathway producing chlorinated benzoic acid and other aliphatic chlorinated compounds (Mondello, 1989) (Fig. 5). Chlorobenzoate (CBAs) can then be mineralized by other bacteria, via the catechol pathway (Fava et al., 1993; Furukawa K and Chakrabarty AM, 1982; Kim and Picardal, 2002). Oxidative degradation has been mostly observed when remediating low-chlorinated PCBs, since it appeared that these are the easiest congeners to be aerobically degraded (Abramowicz, 1990). It should be noted that the main factor affecting the aerobic degradation is the position of the halogen substituent rather than the

number of chlorine atoms (Arnett et al., 2000), which can hinder the enzymatic attack or lead to the formation of toxic substances (Bartels et al., 1984).

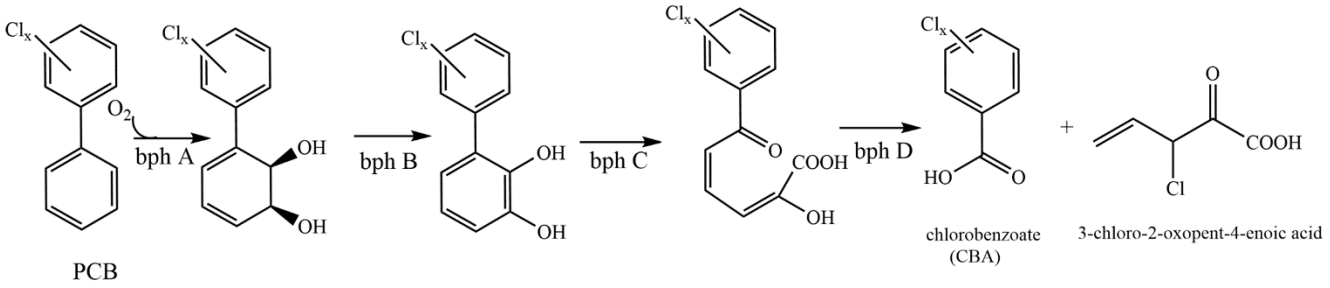

Figure 5 *Aerobic degradation of PCBs via the biphenyl pathway. bph A: biphenyl 2,3-dioxygenase; bph B: dihydrodiol deoxygenase; bph C: 2,3-dihydroxybiphenyl dioxygenase; bph D: 2-hydroxy-6-oxo-6-phenylhexa-2,4-dienoic acid; x=1÷5* (Mohn, 2004; Mondello, 1989)

Aerobic degraders can grow directly on PCBs or bioconvert them co-metabolically (Field and Sierra-Alvarez, 2008). The latter process is possible thanks to a low specificity of the enzymes that can thus interact with the pollutants. For this reason, the co-metabolism is active only in presence of biphenyl or other aromatic compounds as benzoic acids, acting as growth substrates (Mohn, 2004).

1.2.2.2 Aerobic PCBs degraders

Bacteria able to aerobically degrade PCBs are widely distributed in the environment, going from Canada to Antarctica and Africa (Adebusoye et al., 2008; Lambo and Patel, 2006; Papale et al., 2017). Several bacteria were found able to grow on PCBs as sole carbon source or co-metabolically, such as: *Pseudomonas, Burkholderia, Comamonas, Rhodococcus, Ralstonia, Acinetobacter,* etc. (Field and Sierra-Alvarez, 2008), with a number of isolated species constantly increasing (Xiang et al., 2020). Aerobic degradation can occur on high-chlorinated mixtures, as Aroclor 1260, as well as on low chlorinated congeners (Xiang et al., 2020). The substrate specificity is what determines the spectrum of congeners that can be degraded. Thanks to its broad specificity, *Burkholderia xenovorans LB400* is one of the most studied and employed PCBs aerobic degraders (Cagnetta et al., 2015; Field and Sierra-Alvarez, 2008; Payne et al., 2019). The cultivation of these bacteria is faster than dehalorespiring ones thanks to the higher solubility of the growth substrates (e.g. benzoic acids). The enrichment of PCBs aerobic degraders requires oxygen and a carbon source, which can be easily controlled at laboratory scale using bioreactors and obtaining high concentrated culture (Payne et al., 2019).

1.2.2.3 *In situ* natural attenuation of PCBs contamination via aerobic degradation

Only few reports assessed the natural occurrence of PCBs aerobic degradation in aquatic environments as freshwater or marine sediments, possibly due to the anoxic conditions of the polluted sites and to the low abundance of aerobic bacteria. In sediments of the Hudson river (New York, U.S.A.), products of the aerobic degradation of PCBs as CBAs and other chlorinated aliphatic acids were detected in the surface layer of the samples (2-5 cm) (Flanagan and May, 1993). Still, PCBs aerobic degradation is thought to occur spontaneously (Bedard, 2003), even though at scarce rates which might require external oxygen supply to prime the gene expression (Harkness et al., 1993).

1.2.3 Techniques to prime *in situ* microbial remediation of PCBs polluted sediments: biostimulation and bioaugmentation

Natural attenuation of PCBs contamination via microbial degradation is a slow and often uncomplete process (Šrédlová and Cajthaml, 2022). Consequently, so as to perform an effective microbial remediation strategy two main factors need to be taken into account. First of all, the substrates required for the bioremediation processes (e.g. electron donors, oxygen). Secondly, the presence of a sufficient amount of anaerobic respiring bacteria or aerobic degraders in the polluted sediment. In the last years, researches focused on two main different approaches to enhance *in situ* microbial remediation. The first approach aims to stimulate the indigenous microbial community, i.e. by providing a large amount of electron donors to prime dechlorinating bacteria. Such technique is referred as biostimulation. On the other hand, in case the indigenous microbial community of the polluted site does not include bacteria able to bioremediate PCBs or it is difficult to stimulate them due to a large competition of other species, it is often possible to insert exogenous species that can help removing the pollutants. The action of inoculating bacteria is defined as bioaugmentation.

1.2.3.1 Biostimulation of PCBs reductive dechlorination

It is known that natural attenuation of PCBs can occur at laboratory scale on a reasonable experimental time scale. Anaerobic microcosms were prepared with wastewater overflow lagoon sediments and incubated for 430 days, observing up to 70% removal of high-chlorinated single congeners without the addition of electron donors or inoculating the sediment (Ewald et al., 2020). Similarly, the ability of the indigenous microbial community of sediment from Mar Piccolo (Taranto) was evaluated in anerobic microcosms containing a weathered mixture of PCBs at 0.4 $mg \cdot Kg_{drysediment}^{-1}$ over a period of 1 year, resulting in the reduction of high-chlorinated congeners (Matturro et al., 2016). Also, Zanaroli *et al*. (

2006) observed reductive dechlorination of a weathered PCBs mixture (1.6 mg·$Kg_{drysediment}^{-1}$) of sediment from Porto Marghera (Venice, Italy) after 16 months of microcosms' incubation, yet only after the complete depletion of sulfate. Conversely, at real conditions, *in situ* reductive dechlorination proceeds at rates that would require several decades for a natural attenuation process (Needham et al., 2019). It is thought that one of the main key factor responsible for the modest extent of *in situ* reductive dechlorination is the low amount of indigenous organic fermentable matter required to supply the electron donors for the anaerobic metabolisms (Kjellerup et al., 2008; Yan et al., 2006b). In this regard, several electron donors were employed as stimulating agents to prime PCBs reductive dechlorination at a laboratory scale (Table 3). Direct application of hydrogen to selectively stimulate OHRB is difficult to perform, due to the risks of stimulating other anaerobic respiring bacteria as MB and SRB and to the need of frequent replenishment of the electron donors (Fennell and Gossett, 2003). Hence, the addition of small-chain volatile fatty acids (VFAs) as acetate, propionate or butyrate, that prime the H_2 production at low levels (Fennell and Gossett, 2003) is more practical. VFAs have been largely studied to sustain PCBs reductive dechlorination in lab scale microcosms (Chang et al., 2006; Di Gregorio et al., 2013; Fagervold et al., 2011; Krumins et al., 2009; Sudjarid et al., 2012; Zanaroli et al., 2012a). Although being effective to stimulate the bioremediation of PCBs river sediments (Chang et al., 2006; Di Gregorio et al., 2013; Krumins et al., 2009), some studies reported that the addition of VFAs exerted an inhibitory effect on OHRB (Sudjarid et al., 2012; Zanaroli et al., 2012a). Indeed, the organic electron donors added to freshwater sites (Sudjarid et al., 2012) and marine sediments (Zanaroli et al., 2012a) stimulated sulfate reduction lengthening the lag-phase of the reductive dechlorination and reducing the dechlorination rate. To mitigate the strong competition of SRB, lower levels of hydrogen are needed. In this perspective, use of electron donor molecules, as zero valent iron, biodegradable polymers or vegetable matrixes, which can release hydrogen at slower rates is more effective. Indeed, these molecules can provide lower amount of reducing equivalents, being more selective, and they can exert a stimulation effect on a longer time-scale, thus reducing the frequency of replenishment of the amendment in the treated site and decreasing the application costs (Zanaroli et al., 2012b). Zero-valent iron acts as cathodic hydrogen source thanks to the oxidation of the metal, thus being applied as slow hydrogen release compound to sustain PCBs microbial dechlorination (Xu et al., 2021; Zanaroli et al., 2012b). Vegetable matrixes as cellulose were employed as exogenous organic matter to sustain the fermentative processes, being effective in priming the reductive dechlorination process (Payne et al., 2019, 2017). As for biodegradable polymers, applications focused on the remediation of freshwater sediments polluted with chlorinated solvents and little is known regarding their use in marine environments (Bhola et al., 2021; Koenigsberg et al., 2006;

Pierro et al., 2017). Additionally, biostimulation as sole approach to prime *in situ* reductive dechlorination has been studied only at a laboratory scale, without finding optimal stimulating agents for field applications.

1.2.3.2 Biostimulation of aerobic degradation

As previously stated, aerobic degradation is strictly related to the presence of oxygen, which cleaves the aromatic ring and acts as terminal electron acceptor. Due to the anoxic conditions of aquatic sediments, oxidative degradation is mostly absent in these environments. Therefore, it becomes necessary to supply oxygen *in situ*. Delivering oxygen via mechanical aeration is the technically simplest approach, despite being an expensive operation (Harkness et al., 1993). One of the first *in situ* pilot scale studies of biostimulation of aerobic degradation was performed by Harkness *et al.* (1993), which employed several mechanical agitators to stimulate the indigenous microbial community of Hudson river sediments (New York). Another possibility to provide the required oxygen is via chemical agents. For instance, addition of peroxides results in the oxygenation of the sediment with the consequent stimulation of PCBs aerobic degradation (Anid et al., 1993). However, chemical oxidant agents have two disadvantages, since they need to be periodically added to the sediments and they can be harmful for the living organisms (Nebe et al., 2009). The carbon source constitutes the second essential nutritional factor for oxidative degradation. Considering that the majority of the aerobic species degrade PCBs co-metabolically, specific substrates such as biphenyls or benzoic acids are needed to trigger the aerobic degradation. In the past years, the efficacy of biphenyl as biostimulating agent was showed in river sediments (Harkness et al., 1993). Yet, the toxicity of biphenyl discourage its use as priming agent. Considering the technical and environmental challenges to perform an economically sustainable aeration of the sediment and to sustain the growth of aerobic degraders, biostimulation of PCBs aerobic degradation to enhance *in situ* bioremediation of PCBs polluted sediment has been scarcely deepened. On the other hand, proceeding via bioaugmentation has been demonstrated a more feasible approach (Payne et al., 2019, 2013).

1.2.3.3 Bioaugmentation of PCBs organohalide respiring bacteria and aerobic degraders

Despite the relatively high PCBs environmental concentrations, largely over the sediment quality guidelines, for a long time the recalcitrance of these compounds was linked to their low concentration and bioavailability (Bedard, 2003; Passatore et al., 2014). For instance, threshold values of 40 $mg \cdot Kg^{-1}_{drysediment}$ were identified as the minimum concentration required to observe reductive dehalogenation (Cho et al., 2003; Rhee et al., 2001). Only recently, Lombard *et al.* (2014) demonstrated that the reductive

PCBs dechlorination can proceed at concentrations typically found in contaminated sediment porewater. They suggested that the main factor that limits *in situ* bioremediation is the cell density of the OHRB or aerobic degraders, rather than the pollutants' concentration. In fact, the typical population densities of existing OHRB are $10^1 \div 10^3$ CFU·mL^{-1}, while densities of 10^6 CFU·mL^{-1} would be required to observe removal of PCBs in short time scale (month-years) (Needham et al., 2019). Starting from these considerations, it can be comprehended why bioaugmentation has revealed an effective approach. Indeed, inoculating PCBs organohalide respiring bacteria primed the dehalogenation of freshly spiked mixture as well as weathered mixture of contaminants in freshwater (Fagervold et al., 2011; Krumins et al., 2009; Payne et al., 2011; Sudjarid et al., 2012; Yan et al., 2006b) and marine sediments (Yan et al., 2006b; Zanaroli et al., 2012a). Additionally, concomitantly inoculating OHRB and aerobic degraders furtherly increased the efficacy of the bioremediation approach. Payne *et al.* (2013) inoculated DF-1 and LB400 in lab-scale microcosms containing marine sediments, observing the removal of weathered PCBs from 8 to 2 mg·Kg$_{drysediment}^{-1}$ in the microcosms with no added electron donors. Interestingly, OHRB reduced the lag-phase of the process, without resulting in a significant difference compared when inoculating the sole LB400. The same approach allowed a scale up of the technique to treat river sediments going from laboratory mesocosms (Payne et al., 2017) to a pilot-scale study (Payne et al., 2019). The applicability of the technique was demonstrated reducing the pollutants level of a watershed drainage pond in Abraham's creek (Pennsylvania, U.S.A) from 2.5 ± 0.3 mg·Kg$^{-1}_{drysediment}$ to 1.2 ± 0.3 mg·Kg$^{-1}_{drysediment}$.

1.2.3.4 Perspectives for *in situ* microbial remediation of PCBs polluted sediments

Up to now, several attempts were made to assess the real applicability of bioaugmentation and biostimulation approaches, as well as to compare their effectiveness. Yet, a clear pattern so as to identify the best treatment was not pointed out. The external addition of electron donors or organic molecules to stimulate PCBs bioremoval was largely demonstrated to be effective (Dudášová et al., 2016; Xu et al., 2021). However, often biostimulation was not sufficient and it needed to be coupled with bioaugmentation. Biostimulating the sediments of the Baltimore Harbor with zero valent iron or lactate sorted negligible effects, whereas inoculating with OHRB and aerobic degraders reduced the level of pollution (Payne et al., 2013). Similarly, adding zero valent iron to river sediments did not stimulate reductive dechlorination over a period of one year and the bioremediation process started only after the inoculation of OHRB (Winchell and Novak, 2008). Yet, the inoculated bacteria are not always able to exert their bioremoval action. For instance, lab-scale microcosms prepared with sediment collected from Mar Piccolo (Taranto, Italy) and inoculated with *Dehalococcoides mccartyi* showed no differences in the

reductive dehalogenation of PCBs compared to the not inoculated sediments (Matturro et al., 2016). A study of the applicability of bioaugmentation on different sites revealed the dependency of the efficacy of the inoculated culture to the treated sediment (Yan et al., 2006b). Indeed, the effectiveness of the inoculum is related to several factors and features of the treated site, as the presence of nutrients (Kjellerup et al., 2008; Yan et al., 2006b). In this perspective, combining approaches as biostimulation and bioaugmentation might help overcoming the deficiencies of individual methods (Jing et al., 2018) thus obtaining successful strategies for *in situ* PCBs microbial remediation (Payne et al., 2019, 2017). Yet, several attempts still need to be done to assess the usefulness of biostimulating agents and the versatility of the inoculum so as to remediate harsher environments as marine sediments, where the different biogeochemical conditions and microbiota might lead to unsuccessful stimulation or inhibition of the remediation process (Zanaroli et al., 2012a).

Table 3 *Biostimulation and bioaugmentation approaches for the microbial remediation of PCBs polluted sediments*

Environment and scale (L)	**PCBs concentration ($mg \cdot Kg_{drysediment}^{-1}$)**	**Inoculum**	**Amendment**	**Duration (d)**	**Mechanism**	**Degradation/ Dechlorination rate**	**Reference**
Bioaugmentation							
Seawater and freshwater sediments, lab scale (0.16)	[c]532, Freshly spiked single congener	Culture enriched with OHRB	No	189	R.D.	[c]0.007 $mol_{Cl} \cdot mol_{biphenyl}^{-1} \cdot d^{-1}$, [c]12.6 $\mu mol_{Cl} \cdot Kg_{drysediment}^{-1} \cdot d^{-1}$	(Yan et al., 2006b)
Freshwater sediment, lab scale (0.125)	0.54-204, Weathered mixture	Culture enriched with OHRB	[a] Fe^0	80	R.D.	[c]0.023-0.025 $mol_{Cl} \cdot mol_{biphenyl}^{-1} \cdot d^{-1}$; [c]0.05-20 $\mu mol_{Cl} \cdot Kg_{drysediment}^{-1} \cdot d^{-1}$	(Winchell and Novak, 2008)
Freshwater sediment, lab scale (0.25)	2.1 ± 1.4 Weathered mixture	Culture enriched with OHRB	no	415	R.D.	[c]0.001 $mol_{Cl} \cdot mol_{biphenyl}^{-1} \cdot d^{-1}$, [c]0.009 $\mu mol_{Cl} \cdot Kg_{drysediment}^{-1} \cdot d^{-1}$	(Krumins et al., 2009)

Seawater sediment, lab scale (0.02)	100, freshly spiked mixture	DF-1, SF1-, DEH10, o-17	Acetate, propionate, butyrate	300	R.D.	[c]0.006 $mol_{Cl} \cdot mol_{biphenyl}^{-1} \cdot d^{-1}$, [c]1.6 $\mu mol_{Cl} \cdot Kg_{drysediment}^{-1} \cdot d^{-1}$	(Fagervold et al., 2011)
Seawater sediment, lab scale (2)	1.3 ± 0.2 Weathered mixture	DF-1	no	120	R.D.	0.007 $mol_{Cl} \cdot mol_{biphenyl}^{-1} \cdot d^{-1}$, [c]0.07 $\mu mol_{Cl} \cdot Kg_{drysediment}^{-1} \cdot d^{-1}$	(Payne et al., 2011)
Freshwater sediment, lab scale (0.1)	Not reported, Freshly spiked single congener	Culture enriched with OHRB	No	98	R.D.	Not reported (reduction of the lag-phase)	(Sudjarid et al., 2012)
Seawater sediment, lab scale (0.05)	1000 Freshly spiked mixture	Culture enriched with OHRB	[b]H_2, formate, acetate, propionate, butyrate	210	R.D.	21 $\mu mol_{Cl} \cdot Kg_{drysediment}^{-1} \cdot d^{-1}$, [c]0.005 $mol_{Cl} \cdot mol_{biphenyl}^{-1} \cdot d^{-1}$	(Zanaroli et al., 2012a)
Seawater sediment, lab scale (2)	8.0 ± 2.3 Weathered mixture	DF-1 + LB400	no	365	R.D. + O.D.	[c]50 $\mu g_{PCB} \cdot Kg_{drysediment}^{-1} \cdot d^{-1}$	(Payne et al., 2013)
Freshwater sediment, lab scale (1.75)	3.4 ± 0.5 Weathered mixture	DF-1 + LB400	Cellulose	375	R.D. + O.D.	22 $\mu g_{PCB} \cdot Kg_{drysediment}^{-1} \cdot d^{-1}$	(Payne et al., 2017)
Freshwater sediment, lab scale application *in situ* (31)	0.168 ± 0.04 Weathered mixture	Culture enriched with OHRB	Hot temperature (80 °C) inversion emulsification (soybean oil, surfactants) and nutrients (vitamin)	70	R.D.	[c]2 $\mu g_{PCB} \cdot Kg_{drysediment}^{-1} \cdot d^{-1}$ (no difference when bioaugmenting and biostimulating compared to the sole inverse emulsification)	(Chang et al., 2019b)
Freshwater sediment, pilot scale *in situ* (30'000)	3.4 ± 0.5 (average) 2.5 ± 0.3 (treated plot)	DF-1 + LB400	Cellulose	409	R.D. + O.D.	3.2 $\mu g_{PCB} \cdot Kg_{drysediment}^{-1} \cdot d^{-1}$	(Payne et al., 2019)

	Weathered mixture						
Biostimulation							
Freshwater sediment, lab scale (0.12)	135, Freshly spiked mixture reductively dechlorinated	No	Hydrogen peroxide	96	O.D.	[c]1198 $\mu g_{PCB} \cdot Kg_{drysediment}^{-1} \cdot d^{-1}$	(Anid et al., 1993)
Freshwater sediment, pilot scale *in situ* (12'700)	39 ± 102 Weathered mixture	No	Biphenyl, aeration (mechanical)	73	O.D.	[c]370-490 $\mu g_{PCB} \cdot Kg_{drysediment}^{-1} \cdot d^{-1}$	(Harkness et al., 1993)
Freshwater sediment, lab scale (0.125)	1, Freshly spiked single congener	No	Acetate, lactate, pyruvate	Not reported	R.D.	[c]0.02-0.18 $\mu mol_{Cl} \cdot Kg_{drysediment}^{-1} \cdot d^{-1}$	(Chang et al., 2006)
Freshwater sediment, lab scale (0.25)	2.1 ± 1.4 Weathered mixture	No	Acetate, lactate, propionate and butyrate	415	R.D.	[c]0.0007 $mol_{Cl} \cdot mol_{biphenyl}^{-1} \cdot d^{-1}$, [c]0.005 $\mu mol_{Cl} \cdot Kg_{drysediment}^{-1} \cdot d^{-1}$	(Krumins et al., 2009)
Freshwater sediment, lab scale (0.1)	[c]15, Freshly spiked single congener	No	[b]Acetate, lactate, pyruvate	168	R.D.	Negative effect	(Sudjarid et al., 2012)
Seawater sediment, lab scale (0.1)	1000 Freshly spiked mixture	No	Fe^0 (Nano zero valent iron particles)	245	R.D.	[c]0.001 $mol_{Cl} \cdot mol_{biphenyl}^{-1} \cdot d^{-1}$, 5.5 $\mu mol_{Cl} \cdot Kg_{drysediment}^{-1} \cdot d^{-1}$	(Zanaroli et al., 2012b)
Freshwater sediment, lab scale (volume not reported)	6.290 ± 0.009 Weathered mixture	No	acetate	270	R.D.	[c]6 $\mu g_{PCB\ dechlorinated} \cdot Kg_{drysediment}^{-1} \cdot d^{-1}$	(Di Gregorio et al., 2013)
Freshwater sediment, lab scale (0.03)	50 Freshly spiked mixture	No	Fe^0 (Nano zero valent iron particles)	357	R.D.	[c]94 $\mu g_{PCB} \cdot Kg_{drysediment}^{-1} \cdot d^{-1}$	(Xu et al., 2021)

[a]microbial remediation was not effective without bioaugmenting; [b]microbial remediation was inhibited by the amendments; [c]calculated based on the reported data; R.D.: reductive dechlorination; O.D.: oxidative degradation; DF-1: *Dehalobium chlorocoercia* DF-1; LB400: *Burkholderia xenovorans* LB400;

CG1: *Dehalococcoides mccartyi* CG1; DEH10, SF1, o-17: Chloroflexi phylotypes DEH10,SF1, o-17 respectively

1.3 Bibliography

Abraham, W.-R., Nogales, B., Golyshin, P.N., Pieper, D.H., Timmis, K.N., 2002. Polychlorinated biphenyl degrading microbial communities. Curr. Opin. Microbiol. 5, 246–253. https://doi.org/https://doi.org/10.1016/S1369-5274(02)00323-5

Abraham Wolf-Reiner, Nogales Balbina, Golyshin Peter N, Pieper Dietmar H, Timmis Kenneth N, 2002. Polychlorinated biphenyl-degrading microbial communities in soils and sediments. Curr. Opin. Microbiol. 5, 246–253. https://doi.org/10.1016/s1369-5274(02)00323-5 Abstract

Abramowicz, D.A., 1990. Aerobic and anaerobic biodegradation of PCBs: A review. Crit. Rev. Biotechnol. 10, 241–251. https://doi.org/10.3109/07388559009038210

Adebusoye, S.A., Picardal, F.W., Ilori, M.O., Amund, O.O., Fuqua, C., 2008. Characterization of multiple novel aerobic polychlorinated biphenyl (PCB)-utilizing bacterial strains indigenous to contaminated tropical African soils. Biodegradation 19, 145–159. https://doi.org/10.1007/s10532-007-9122-x

Adrian, L., Dudková, V., Demnerová, K., Bedard, D.L., 2009. "Dehalococcoides" sp. strain CBDB1 extensively dechlorinates the commercial polychlorinated biphenyl mixture Aroclor 1260. Appl. Environ. Microbiol. 75, 4516–4524. https://doi.org/10.1128/AEM.00102-09

Ahmed, M., Focht, D.D., 1973. Degradation of polychlorinated biphenyls by two species of Achromobacter. Can. J. Microbiol. 19, 47–52. https://doi.org/10.1139/m73-007

Aldera, A.C., Häggblom, M.M., Oppenheimer, S.R., Young, L.Y., 1993. Reductive Dechlorination of Polychlorinated Biphenyls in Anaerobic Sediments. Environ. Sci. Technol. 27, 530–538. https://doi.org/10.1021/es00040a012

Alzieu, C., Bocquené, G., Régis, D., Dhainaut-Courtois, N., Empis, A., Forget, J., Glémarec, M., Jean François, Pavillon Chrystèle, P., Françoise, Q., 2003. Evaluation des risques liés à l'immersion des boues de dragage des ports maritimes.

Amiard, J., Arnich, N., Badot, P., 2011. Shellfish and Residual Chemical Contaminants : Hazards , Monitoring , and Archimer. Rev. Environ. Contam. Toxicol. 213, 55–111. https://doi.org/10.1007/978-1-4419-9860-6

Ancona, V., Barra Caracciolo, A., Grenni, P., Di Lenola, M., Campanale, C., Calabrese, A., Uricchio, V.F., Mascolo, G., Massacci, A., 2017. Plant-assisted bioremediation of a historically PCB and heavy metal-contaminated area in Southern Italy. N. Biotechnol. 38, 65–73. https://doi.org/10.1016/j.nbt.2016.09.006

Anid, P.J., Ravest-Webster, B.P., Vogel, T.M., 1993. Effect of hydrogen peroxide on the biodegradation of PCBs in anaerobically dechlorinated river sediments. Biodegradation 4, 241–248. https://doi.org/10.1007/BF00695972

Antizar-Ladislao, B., 2010. Bioremediation: Working with bacteria. Elements 6, 389–394. https://doi.org/10.2113/gselements.6.6.389

APAT, 2006. Diossine Furani e PCB. Rome, Italy.

Arblaster, J., Ikonomou, M.G., Gobas, F.A.P.C., 2015. Toward ecosystem-based sediment quality guidelines for polychlorinated biphenyls (PCBs). Integr. Environ. Assess. Manag. 11, 689–700. https://doi.org/10.1002/ieam.1638

Arnett, C.M., Parales, J. V., Haddock, J.D., 2000. Influence of chlorine substituents on rates of oxidation of chlorinated biphenyls by the biphenyl dioxygenase of Burkholderia sp. Strain LB400. Appl. Environ. Microbiol. 66, 2928–2933. https://doi.org/10.1128/AEM.66.7.2928-2933.2000

Baba, D., Yasuta, T., Yoshida, N., Kimura, Y., Miyake, K., Inoue, Y., Toyota, K., Katayama, A., 2007. Anaerobic biodegradation of polychlorinated biphenyls by a microbial consortium originated from uncontaminated paddy soil. World J. Microbiol. Biotechnol. 23, 1627–1636. https://doi.org/10.1007/s11274-007-9409-4

Baldigo, B.P., Sloan, R.J., Smith, S.B., Denslow, N.D., Blazer, V.S., Gross, T.S., 2006. Polychlorinated biphenyls, mercury, and potential endocrine disruption in fish from the Hudson River, New York, USA. Aquat. Sci. 68, 206–228. https://doi.org/10.1007/s00027-006-0831-8

Bartels, I., Knackmuss, H.J., Reineke, W., 1984. Suicide inactivation of catechol 2,3-dioxygenase from Pseudomonas putida mt-2 by 3-halocatechols. Appl. Environ. Microbiol. 47, 500–505. https://doi.org/10.1128/aem.47.3.500-505.1984

Bedard, D.L., 2003. Polychlorinated Biphenyls in Aquatic Sediments: Environmental Fate and Outlook for Biological Treatment, in: Häggblom, M.M., Bossert, I.D. (Eds.), Dehalogenation, Microbial Processes and Environmental Applications. Rutgers University, USA, pp. 443–465. https://doi.org/10.1007/0-306-48011-5_17

Bellucci, L.G., Cassin, D., Giuliani, S., Botter, M., Zonta, R., 2016. Sediment pollution and dynamic in the Mar Piccolo of Taranto (southern Italy): insights from bottom sediment traps and surficial sediments. Environ. Sci. Pollut. Res. 23, 12554–12565. https://doi.org/10.1007/s11356-016-6738-6

Bergemann, M., Gaumert, T., 2008. Elbebericht 2008.

Bhola, S., Arora, K., Kulshrestha, S., Mehariya, S., Bhatia, R.K., Kaur, P., Kumar, P., 2021. Established and Emerging Producers of PHA: Redefining the Possibility. Appl. Biochem. Biotechnol. 193, 3812–3854. https://doi.org/10.1007/s12010-021-03626-5

Bondo, P., 2018. PCB pollution threatens to wipe out killer whales [WWW Document]. Arct. Res. Cent. - Aarhus Univ. - News. URL https://arctic.au.dk/news-and-events/news/show/artikel/pcb-pollution-threatens-to-wipe-out-killer-whales

Bossert, I.D., Haggblom, M., Young, L.Y., 2003. Microbial Ecology of Dehalogenation, in: Häggblom, M.M., Bossert, I.D. (Eds.), Dehalogenation, Microbial Processes and Environmental Applications. Rutgers University, USA, pp. 33–52.

Brien, G.O., Behnke, H.F., Poulson, H.D., Ela, J.P., Willett, S.D., Hassett, S., 2003. Consensus-Based Sediment Quality Guidelines Recommendations for Use & Application Interim Guidance Developed by the Contaminated Sediment Standing Team James Tiefenthaler Jr ., Vice Chair Wisconsin Department of Natural Resources, Wisconsin department of natural resources.

Bzdusek, P.A., Christensen, E.R., Lee, C.M., Pakdeesusuk, U., Freedman, D.L., 2006. PCB congeners

and dechlorination in sediments of Lake Hartwell, South Carolina, determined from cores collected in 1987 and 1998. Environ. Sci. Technol. 40, 109–119. https://doi.org/10.1021/es050194o

Cagnetta, G., Intini, G., Liberti, L., Boldyrev, V. V., Lomovskiy, O.I., 2015. The Biomec process for mechanochemically assisted biodegradation of PCBs in marine sediments. J. Soils Sediments 15, 240–248. https://doi.org/10.1007/s11368-014-1009-y

Canadian Council of Ministers of the Environment, 1999. Canadian Sediment Quality Guidelines for the Protection of Aquatic Life- PCBs.

Cappello, S., Caruso, G., Zampino, D., Monticelli, L.S., Maimone, G., Denaro, R., Tripodo, B., Troussellier, M., Yakimov, M., Giuliano, L., 2007. Microbial community dynamics during assays of harbour oil spill bioremediation: A microscale simulation study. J. Appl. Microbiol. 102, 184–194. https://doi.org/10.1111/j.1365-2672.2006.03071.x

Carberry, J.B., Wik, J., 2001. Comparison of ex situ and in situ bioremediation of unsaturated soils contaminated by petroleum. J. Environ. Sci. Heal. - Part A Toxic/Hazardous Subst. Environ. Eng. 36, 1491–1503. https://doi.org/10.1081/ESE-100105726

Carpenter, D.O., 2011. Polychlorinated Biphenyls (PCBs): Routes of Exposure and Effects on Human Health. Rev. Environ. Health 21, 1–24. https://doi.org/10.1515/reveh.2006.21.1.1

Chang, B.-V., Chiu, T.-C., Yuan, S.-Y., 2006. Dechlorination of Polychlorinated Biphenyl Congeners by Anaerobic Microorganisms From River Sediment. Water Environ. Res. 78, 764–769. https://doi.org/10.2175/106143006x107380

Chang, S.C., Yeh, C.W., Lee, S.K., Chen, T.W., Tsai, L.C., 2019a. Efficient remediation of river sediments contaminated by polychlorinated biphenyls and hexachlorobenzene by coupling in situ phase-inversion emulsification and biological reductive dechlorination. Int. Biodeterior. Biodegrad. 140, 133–143. https://doi.org/10.1016/j.ibiod.2019.02.007

Chang, S.C., Yeh, C.W., Lee, S.K., Chen, T.W., Tsai, L.C., 2019b. Efficient remediation of river sediments contaminated by polychlorinated biphenyls and hexachlorobenzene by coupling in situ phase-inversion emulsification and biological reductive dechlorination. Int. Biodeterior. Biodegrad. 140, 133–143. https://doi.org/10.1016/j.ibiod.2019.02.007

Chen, C., He, J., 2018. Strategy for the Rapid Dechlorination of Polychlorinated Biphenyls (PCBs) by Dehalococcoides mccartyi Strains. Environ. Sci. Technol. 52, 13854–13862. https://doi.org/10.1021/acs.est.8b03198

Chitsaz, M., Fennell, D.E., Rodenburg, L.A., 2020. Sources of polychlorinated biphenyls to Upper Hudson River sediment post-dredging. Chemosphere 259, 127438. https://doi.org/10.1016/j.chemosphere.2020.127438

Cho, Y.C., Sokol, R.C., Frohnhoefer, R.C., Rhee, G.Y., 2003. Reductive Dechlorination of Polychlorinated Biphenyls: Threshold Concentration and Dechlorination Kinetics of Individual Congeners in Aroclor 1248. Environ. Sci. Technol. 37, 5651–5656. https://doi.org/10.1021/es034600k

Cho, Y.M., Smithenry, D.W., Ghosh, U., Kennedy, A.J., Millward, R.N., Bridges, T.S., Luthy, R.G., 2007. Field methods for amending marine sediment with activated carbon and assessing treatment

effectiveness. Mar. Environ. Res. 64, 541–555. https://doi.org/10.1016/j.marenvres.2007.04.006

Cotecchia, F., Vitone, C., Sollecito, F., Mali, M., Miccoli, D., Petti, R., Milella, D., Ruggieri, G., Bottiglieri, O., Santaloia, F., De Bellis, P., Cafaro, F., Notarnicola, M., Todaro, F., Adamo, F., Di Nisio, A., Lanzolla, A.M.L., Spadavecchia, M., Moretti, M., Agrosì, G., De Giosa, F., Fago, P., Lacalamita, M., Lisco, S., Manzari, P., Mesto, E., Romano, G., Scardino, G., Schingaro, E., Siniscalchi, A., Tempesta, G., Valenzano, E., Mastronuzzi, G., Cardellicchio, N., Di Leo, A., Spada, L., Giandomenico, S., Calò, M., Uricchio, V.F., Mascolo, G., Bagnuolo, G., Ciannarella, R., Tursi, A., Cipriano, G., Cotugno, P., Sion, L., Carlucci, R., Capasso, G., De Chiara, G., Pisciotta, G., Velardo, R., Corbelli, V., 2021. A geo-chemo-mechanical study of a highly polluted marine system (Taranto, Italy) for the enhancement of the conceptual site model. Sci. Rep. 11, 1–26. https://doi.org/10.1038/s41598-021-82879-w

Dendievel, A.M., Mourier, B., Coynel, A., Evrard, O., Labadie, P., Ayrault, S., Debret, M., Koltalo, F., Copard, Y., Faivre, Q., Gardes, T., Vauclin, S., Budzinski, H., Grosbois, C., Winiarski, T., Desmet, M., 2020. Spatio-temporal assessment of the polychlorinated biphenyl (PCB) sediment contamination in four major French river corridors (1945-2018). Earth Syst. Sci. Data 12, 1153–1170. https://doi.org/10.5194/essd-12-1153-2020

Di Gregorio, S., Azaizeh, H., Lorenzi, R., 2013. Biostimulation of the autochthonous microbial community for the depletion of polychlorinated biphenyls (PCBs) in contaminated sediments. Environ. Sci. Pollut. Res. 20, 3989–3999. https://doi.org/10.1007/s11356-012-1350-x

Dolfing, J., 2003. Thermodynamic considerations for dehalogenation, in: Häggblom, M.M., Bossert, I.D. (Eds.), Dehalogenation, Microbial Processes and Environmental Applications. Kluwer Academic Publishers, Rutgers University, USA, pp. 89–114.

Dudášová, H., Lászlová, K., Lukáčová, L., Balaščáková, M., Murínová, S., Dercová, K., 2016. Bioremediation of PCB-contaminated sediments and evaluation of their pre- and post-treatment ecotoxicity. Chem. Pap. 70, 1049–1058. https://doi.org/10.1515/chempap-2016-0041

Ewald, J.M., Humes, S. V., Martinez, A., Schnoor, J.L., Mattes, T.E., 2020. Growth of Dehalococcoides spp. and increased abundance of reductive dehalogenase genes in anaerobic PCB-contaminated sediment microcosms. Environ. Sci. Pollut. Res. 27, 8846–8858. https://doi.org/10.1007/s11356-019-05571-7

Fagervold, S.K., Watts, J.E.M., May, H.D., Sowers, K.R., 2011. Effects of bioaugmentation on indigenous PCB dechlorinating activity in sediment microcosms. Water Res. 45, 3899–3907. https://doi.org/10.1016/j.watres.2011.04.048

Fava, F., Di Gioia, D., Marchetti, L., Quattroni, G., Marraffa, V., 1993. Aerobic mineralization of chlorobenzoates by a natural polychlorinated biphenyl-degrading mixed bacterial culture. Appl. Microbiol. Biotechnol. 40, 541–548. https://doi.org/10.1007/BF00175746

Fennell, D.E., Gossett, J.M., 2003. Microorganisms for site-specific evaluation of enhanced biological reductive dehalogenation, in: Häggblom, M.M., Bossert, I.D. (Eds.), Dehalogenation, Microbial Processes and Environmental Applications. Rutgers University, USA, pp. 385–420.

Field, J.A., Sierra-Alvarez, R., 2008. Microbial transformation and degradation of polychlorinated biphenyls. Environ. Pollut. 155, 1–12. https://doi.org/10.1016/j.envpol.2007.10.016

Flanagan, W.P., May, R.J., 1993. Metabolite Detection as Evidence for Naturally Occurring Aerobic

PCB Biodegradation in Hudson River Sediments. Environ. Sci. Technol. 27, 2207–2212. https://doi.org/10.1021/es00047a030

Furukawa K, Chakrabarty AM, 1982. Involvement of plasmids in total degradation of Chlorinated Biphenls. Appl. Environ. Microbiol. 44, 619–626.

Giesy, J.P., Kannan, K., 1998. Dioxin-like and non-dioxin like effects of polychlorinated biphenyls: Implications for risk assessment. Crit. Rev. Toxicol. 28, 511–569. https://doi.org/10.1046/j.1440-1770.2002.00185.x

Gomes, Helena I, Dias-ferreira, C., Ribeiro, A.B., 2013. Overview of in situ and ex situ remediation technologies for PCB-contaminated soils and sediments and obstacles for full-scale application. Sci. Total Environ. 445–446, 237–260. https://doi.org/10.1016/j.scitotenv.2012.11.098

Gomes, Helena I., Dias-Ferreira, C., Ribeiro, A.B., 2013. Overview of in situ and ex situ remediation technologies for PCB-contaminated soils and sediments and obstacles for full-scale application. Sci. Total Environ. 445–446, 237–260. https://doi.org/10.1016/j.scitotenv.2012.11.098

Gonzalez, S.T., Remick, D., Creton, R., Colwill, R.M., 2016. Effects of embryonic exposure to polychlorinated biphenyls (PCBs) on anxiety-related behaviors in larval zebrafish. Neurotoxicology 53, 93–101. https://doi.org/10.1016/j.neuro.2015.12.018

Guerra, R., 2012. Polycyclic aromatic hydrocarbons, polychlorinated biphenyls and trace metals in sediments from a coastal lagoon (Northern Adriatic, Italy). Water. Air. Soil Pollut. 223, 85–98. https://doi.org/10.1007/s11270-011-0841-6

Guerra, R., Pasteris, A., Lee, S. hyung, Park, N. jin, Ok, G., 2014. Spatial patterns of metals, PCDDs/Fs, PCBs, PBDEs and chemical status of sediments from a coastal lagoon (Pialassa Baiona, NW Adriatic, Italy). Mar. Pollut. Bull. 89, 407–416. https://doi.org/10.1016/j.marpolbul.2014.10.024

Häggblom, M.M., Bossert, I.D., 2003. Dehalogenation, Microbial processes and environmental applications. Kluwer Academic Publishers, Rutgers University, USA.

Harkness, M.R., McDermott, J.B., Abramowicz, D.A., Salvo, J.J., Flanagan, W.P., Stephens, M.L., Mondello, F.J., May, R.J., Lobos, J.H., Carroll, K.M., Brennan, M.J., Bracco, A.A., Fish, K.M., Warner, G.L., Wilson, P.R., Dietrich, D.K., Lin, D.T., Morgan, C.B., Gately, W.L., 1993. In situ stimulation of aerobic PCB biodegradation in Hudson River sediments. Science (80-.). 259, 503–507. https://doi.org/10.1126/science.8424172

Hiraishi, A., 2008. Biodiversity of dehalorespiring bacteria with special emphasis on polychlorinated biphenyl/dioxin dechlorinators. Microbes Environ. 23, 1–12. https://doi.org/10.1264/jsme2.23.1

Hoelen, T.P., Reinhard, M., 2004. Complete biological dehalogenation of chlorinated ethylenes in sulfate containing groundwater. Biodegradation 15, 395–403. https://doi.org/10.1023/B:BIOD.0000044592.33729.d6

Holmes, D.A., Harrison, B.K., Dolfing, J., 1993. Estimation of Gibbs Free Energies of Formation for Polychlorinated Biphenyls. Environ. Sci. Technol. 27, 725–731. https://doi.org/10.1021/es00041a017

IARC, 2016. Polychlorinated Biphenyls and Polybrominated Biphenyls - IARC monographs on the evaluation of carcinogenic risks to humans, POLYCHLORINATED BIPHENYLS AND

POLYBROMINATED BIPHENYLS - IARC monographs on the evaluation of carcinogenic risks to humans.

Janssen, E.M.L., Beckingham, B.A., 2013. Biological responses to activated carbon amendments in sediment remediation. Environ. Sci. Technol. 47, 7595–7607. https://doi.org/10.1021/es401142e

Jing, R., Fusi, S., Kjellerup, B. V., 2018. Remediation of Polychlorinated Biphenyls (PCBs) in contaminated soils and sediment: State of knowledge and perspectives. Front. Environ. Sci. 6, 1–17. https://doi.org/10.3389/fenvs.2018.00079

Kim, S., Picardal, F.W., 2002. A novel bacterium that utilizes monochlorobiphenyls and 4-chlorobenzoate as growth substrates. FEMS Microbiol. Lett. 185, 225–229. https://doi.org/10.1016/s0378-1097(00)00091-4

Kjellerup, B. V., Paul, P., Ghosh, U., May, H.D., Sowers, K.R., 2012. Spatial distribution of PCB dechlorinating bacteria and activities in contaminated soil. Appl. Environ. Soil Sci. 2012, 1–12. https://doi.org/10.1155/2012/584970

Kjellerup, B. V., Sun, X., Ghosh, U., May, H.D., Sowers, K.R., 2008. Site-specific microbial communities in three PCB-impacted sediments are associated with different in situ dechlorinating activities. Environ. Microbiol. 10, 1296–1309. https://doi.org/10.1111/j.1462-2920.2007.01543.x

Koenigsberg, S., Willett, A., Sutherland, M., 2006. Controlled release electron donors: Hydrogen release compound (HRC)-an overview of a decade of case studies. Bioremediat. J. 10, 45–57. https://doi.org/10.1080/10889860600842837

Krumins, V., Park, J.W., Son, E.K., Rodenburg, L.A., Kerkhof, L.J., Häggblom, M.M., Fennell, D.E., 2009. PCB dechlorination enhancement in Anacostia River sediment microcosms. Water Res. 43, 4549–4558. https://doi.org/10.1016/j.watres.2009.08.003

Lambo, A.J., Patel, T.R., 2006. Isolation and characterization of a biphenyl-utilizing psychrotrophic bacterium, Hydrogenophaga taeniospiralis IA3-A, that cometabolize dichlorobiphenyls and polychlorinated biphenyl congeners in Aroclor 1221. J. Basic Microbiol. 46, 94–107. https://doi.org/10.1002/jobm.200510006

Laroe, S.L., Fricker, A.D., Bedard, D.L., 2014. Dehalococcoides mccartyi strain JNA in pure culture extensively dechlorinates aroclor 1260 according to polychlorinated biphenyl (PCB) dechlorination process N. Environ. Sci. Technol. 48, 9187–9196. https://doi.org/10.1021/es500872t

Lauby-secretan, B., Loomis, D., Grosse, Y., Ghissassi, F. El, Bouvard, V., Benbrahim-tallaa, L., Guha, N., Baan, R., Mattock, H., Straif, K., Agency, I., Working, M., Iarc, G., 2013. Carcinogenicity of polychlorinated biphenyls and polybrominated biphenyls. Lancet Oncol. 14, 287–288. https://doi.org/10.1016/S1470-2045(13)70104-9

Lillicrap, A., Schaanning, M., Macken, A., 2015. Assessment of the direct effects of biogenic and petrogenic activated carbon on benthic organisms. Environ. Sci. Technol. 49, 3705–3710. https://doi.org/10.1021/es506113j

Lombard, N.J., Ghosh, U., Kjellerup, B. V., Sowers, K.R., 2014. Kinetics and threshold level of 2,3,4,5-tetrachlorobiphenyl dechlorination by an organohalide respiring bacterium. Environ. Sci. Technol. 48, 4353–4360. https://doi.org/10.1021/es404265d

MacDonald, D.D., Dipinto, L.M., Field, J., Ingersoll, C.G., Long, E.R., Swartz, R.C., 2000. Development and evaluation of consensus-based sediment effect concentrations for polychlorinated biphenyls. Environ. Toxicol. Chem. 19, 1403–1413. https://doi.org/10.1002/etc.5620190524

MacDonald, D.D., Ingersoll, C.G., Smorong, D.E., Lindskoog, R.A., Sloane, G., Biernacki, T., 2003. Development and Evaluation of Numerical Sediment Quality Assessment Guidelines for Florida Inland Waters Development and Evaluation of Numerical Sediment Quality Assessment Guidelines for Florida Inland Waters, Technical Report for Florida Department of Environmental Protection.

Mali, M., Dell'Anna, M.M., Notarnicola, M., Damiani, L., Mastrorilli, P., 2017. Combining chemometric tools for assessing hazard sources and factors acting simultaneously in contaminated areas. Case study: "Mar Piccolo" Taranto (South Italy). Chemosphere 184, 784–794. https://doi.org/10.1016/j.chemosphere.2017.06.028

Mattes, T.E., Ewald, J.M., Liang, Y., Martinez, A., Awad, A., Richards, P., Hornbuckle, K.C., Schnoor, J.L., 2018. PCB dechlorination hotspots and reductive dehalogenase genes in sediments from a contaminated wastewater lagoon. Environ. Sci. Pollut. Res. 25, 16376–16388. https://doi.org/10.1007/s11356-017-9872-x

Matturro, B., Ubaldi, C., Grenni, P., Caracciolo, A.B., Rossetti, S., 2016. Polychlorinated biphenyl (PCB) anaerobic degradation in marine sediments: microcosm study and role of autochthonous microbial communities. Environ. Sci. Pollut. Res. 23, 12613–12623. https://doi.org/10.1007/s11356-015-4960-2

May, H.D., Miller, G.S., Kjellerup, B. V., Sowers, K.R., 2008. Dehalorespiration with polychlorinated biphenyls by an anaerobic ultramicrobacterium. Appl. Environ. Microbiol. 74, 2089–2094. https://doi.org/10.1128/AEM.01450-07

Mccarty, P.L., 1997. Breathing with chlorinated solvents. Science (80-.). 276, 1521–1522. https://doi.org/https://doi.org/10.1126/science.276.5318.1521

Meijer, S.N., Ockenden, W.A., Sweetman, A., Breivik, K., Grimalt, J.O., Jones, K.C., 2003. Global distribution and budget of PCBs and HCB in background surface soils: Implications for sources and environmental processes. Environ. Sci. Technol. 37, 667–672. https://doi.org/10.1021/es025809l

Merhaby, D., Rabodonirina, S., Net, S., Ouddane, B., Halwani, J., 2019. Overview of sediments pollution by PAHs and PCBs in mediterranean basin: Transport, fate, occurrence, and distribution. Mar. Pollut. Bull. 149, 110646. https://doi.org/10.1016/j.marpolbul.2019.110646

Mohn, W.W., 2004. Biodegradation and Bioremediation of Halogenated Organic Compounds, in: Singh, A., Ward, O.P. (Eds.), Biodegradation and Bioremediation. Springer Berlin, Heidelberg, pp. 125–148.

Mondello, F.J., 1989. Cloning and expression in Escherichia coli of Pseudomonas strain LB400 genes encoding polychlorinated biphenyl degradation. J. Bacteriol. 171, 1725–1732. https://doi.org/10.1128/jb.171.3.1725-1732.1989

Nebe, J., Baldwin, B.R., Kassab, R.L., Nies, L., Nakatsu, C.H., 2009. Quantification of aromatic oxygenase genes to evaluate enhanced bioremediation by oxygen releasing materials at a gasoline-

contaminated site. Environ. Sci. Technol. 43, 2029–2034. https://doi.org/10.1021/es900146f

Needham, T.P., Payne, R.B., Sowers, K.R., Ghosh, U., 2019. Kinetics of PCB microbial dechlorination explained by freely dissolved concentration in sediment microcosms. Environ. Sci. Technol. 53, 7432–7441. https://doi.org/10.1021/acs.est.9b01088

Ngoubeyou, P.S.K., Wolkersdorfer, C., Ndibewu, P.P., Augustyn, W., 2022. Toxicity of polychlorinated biphenyls in aquatic environments – A review. Aquat. Toxicol. 251, 106284. https://doi.org/10.1016/j.aquatox.2022.106284

Nicolopoulou-Stamati, P., Pitsos, M.A., 2001. The impact of endocrine disrupters on the female reproductive system. Hum. Reprod. Update 7, 323–330. https://doi.org/10.1093/humupd/7.3.323

Nogales, B., Moore, E.R.B., Abraham, W.R., Timmis, K.N., 1999. Identification of the metabolically active members of a bacterial community in a polychlorinated biphenyl-polluted moorland soil. Environ. Microbiol. 1, 199–212. https://doi.org/10.1046/j.1462-2920.1999.00024.x

Oremland, R.S., Taylor, B.F., 1978. Sulfate reduction and methanogenesis in marine sediments. Geochim. Cosmochim. Acta 42, 209–214. https://doi.org/10.1016/0016-7037(78)90133-3

Pakdeesusuk, U., Lee, C.M., Coates, J.T., Freedman, D.L., 2005. Assessment of natural attenuation via in situ reductive dechlorination of polychlorinated biphenyls in sediments of the Twelve Mile Creek arm of Lake Hartwell, SC. Environ. Sci. Technol. 39, 945–952. https://doi.org/10.1021/es0491228

Papale, M., Giannarelli, S., Francesconi, S., Di Marco, G., Mikkonen, A., Conte, A., Rizzo, C., De Domenico, E., Michaud, L., Giudice, A. Lo, 2017. Enrichment, isolation and biodegradation potential of psychrotolerant polychlorinated-biphenyl degrading bacteria from the Kongsfjorden (Svalbard Islands, High Arctic Norway). Mar. Pollut. Bull. 114, 849–859. https://doi.org/10.1016/j.marpolbul.2016.11.011

Passatore, L., Rossetti, S., Juwarkar, A.A., Massacci, A., 2014. Phytoremediation and bioremediation of polychlorinated biphenyls (PCBs): State of knowledge and research perspectives. J. Hazard. Mater. 278, 189–202. https://doi.org/10.1016/j.jhazmat.2014.05.051

Patmont, E., Jalalizadeh, M., Bokare, M., Needham, T., Vance, J., Greene, R., Cargill, J., Ghosh, U., 2020. Full-Scale Application of Activated Carbon to Reduce Pollutant Bioavailability in a 5-Acre Lake. J. Environ. Eng. 146, 1–10. https://doi.org/10.1061/(asce)ee.1943-7870.0001667

Payne, R.B., Fagervold, S.K., May, H.D., Sowers, K.R., 2013. Remediation of polychlorinated biphenyl impacted sediment by concurrent bioaugmentation with anaerobic halorespiring and aerobic degrading bacteria. Environ. Sci. Technol. 47, 3807–3815. https://doi.org/10.1021/es304372t

Payne, R.B., Ghosh, U., May, H.D., Marshall, C.W., Sowers, K.R., 2019. A Pilot-Scale Field Study: In Situ Treatment of PCB-Impacted Sediments with Bioamended Activated Carbon. Environ. Sci. Technol. 53, 2626–2634. https://doi.org/10.1021/acs.est.8b05019

Payne, R.B., Ghosh, U., May, H.D., Marshall, C.W., Sowers, K.R., 2017. Mesocosm Studies on the Efficacy of Bioamended Activated Carbon for Treating PCB-Impacted Sediment. Environ. Sci. Technol. 51, 10691–10699. https://doi.org/10.1021/acs.est.7b01935

Payne, R.B., May, H.D., Sowers, K.R., 2011. Enhanced reductive dechlorination of polychlorinated

biphenyl impacted sediment by bioaugmentation with a dehalorespiring bacterium. Environ. Sci. Technol. 45, 8772–8779. https://doi.org/10.1021/es201553c

Pierro, L., Matturro, B., Rossetti, S., Sagliaschi, M., Sucato, S., Alesi, E., Bartsch, E., Arjmand, F., Papini, M.P., 2017. Polyhydroxyalkanoate as a slow-release carbon source for in situ bioremediation of contaminated aquifers: From laboratory investigation to pilot-scale testing in the field. N. Biotechnol. 37, 60–68. https://doi.org/10.1016/j.nbt.2016.11.004

Quero, G.M., Cassin, D., Botter, M., Perini, L., Luna, G.M., 2015. Patterns of benthic bacterial diversity in coastal areas contaminated by heavy metals, polycyclic aromatic hydrocarbons (PAHs) and polychlorinated biphenyls (PCBs). Front. Microbiol. 6, 1–15. https://doi.org/10.3389/fmicb.2015.01053

Reddy, A.V.B., Moniruzzaman, M., Aminabhavi, T.M., 2019. Polychlorinated biphenyls (PCBs) in the environment: Recent updates on sampling, pretreatment, cleanup technologies and their analysis. Chem. Eng. J. 358, 1186–1207. https://doi.org/10.1016/j.cej.2018.09.205

Rhee, G.Y., Sokol, R.C., Bethoney, C.M., Cho, Y.C., Frohnhoefer, R.C., Erkkila, T., 2001. Kinetics of polychlorinated biphenyl dechlorination and growth of dechlorinating microorganisms. Environ. Toxicol. Chem. 20, 721–726. https://doi.org/10.1002/etc.5620200405

Richardson, R.E., 2016. Organohalide-Respiring Bacteria as Members of Microbial Communities: Catabolic Food Webs and Biochemical Interactions, in: Adrian, L., Löffler, F.E. (Eds.), Organohalide- Respiring Bacteria. Springer Berlin, Heidelberg, pp. 309–344.

Sage, L., Périgon, S., Faure, M., Gaignaire, C., Abdelghafour, M., Mehu, J., Geremia, R.A., Mouhamadou, B., 2014. Autochthonous ascomycetes in depollution of polychlorinated biphenyls contaminated soil and sediment. Chemosphere 110, 62–69. https://doi.org/10.1016/j.chemosphere.2014.03.013

Schuster, J.K., Harner, T., Eng, A., Rauert, C., Su, K., Hornbuckle, K.C., Johnson, C.W., 2021. Tracking POPs in Global Air from the First 10 Years of the GAPS Network (2005 to 2014). Environ. Sci. Technol. 55, 9479–9488. https://doi.org/10.1021/acs.est.1c01705

Siracusa, G., Becarelli, S., Lorenzi, R., Gentini, A., Di Gregorio, S., 2017. PCB in the environment: bio-based processes for soil decontamination and management of waste from the industrial production of Pleurotus ostreatus. N. Biotechnol. 39, 232–239. https://doi.org/10.1016/j.nbt.2017.08.011

Šrédlová, K., Cajthaml, T., 2022. Recent advances in PCB removal from historically contaminated environmental matrices. Chemosphere 287, 132096. https://doi.org/10.1016/j.chemosphere.2021.132096

Steffan, R.J., Schaefer, C.E., 2016. Current and Future Bioremediation Applications: Bioremediation from a Practical and Regulatory Perspective, in: Adrian, L., Löffler, F.E. (Eds.), Organohalide-Respiring Bacteria. Springer Berlin Heidelberg, pp. 517–540.

Sudjarid, W., Chen, I.M., Monkong, W., Anotai, J., 2012. Reductive dechlorination of 2,3,4-chlorobiphenyl by biostimulation and bioaugmentation. Environ. Eng. Sci. 29, 255–261. https://doi.org/10.1089/ees.2011.0228

Sun, J., Pan, L., Tsang, D.C.W., Zhan, Y., Zhu, L., Li, X., 2018. Organic contamination and

remediation in the agricultural soils of China: A critical review. Sci. Total Environ. 615, 724–740. https://doi.org/10.1016/j.scitotenv.2017.09.271

Todaro, F., De Gisi, S., Notarnicola, M., 2020. Contaminated marine sediment stabilization/solidification treatment with cement/lime: leaching behaviour investigation. Environ. Sci. Pollut. Res. 27, 21407–21415. https://doi.org/10.1007/s11356-020-08562-1

Vidali, M., 2001. Bioremediation. An overview. Pure Appl. Chem. 73, 1163–1172. https://doi.org/https://doi.org/10.1351/pac200173071163

Wang, S., Chng, K.R., Wilm, A., Zhao, S., Yang, K.L., Nagarajan, N., He, J., 2014. Genomic characterization of three unique Dehalococcoides that respire on persistent polychlorinated biphenyls. Proc. Natl. Acad. Sci. 111, 12103–12108. https://doi.org/10.1073/pnas.1404845111

Wang, S., He, J., 2013. Phylogenetically Distinct Bacteria Involve Extensive Dechlorination of Aroclor 1260 in Sediment-Free Cultures. PLoS One 8. https://doi.org/10.1371/journal.pone.0059178

Wang, W., Bai, J., Zhang, G., Jia, J., Wang, X., Liu, X., Cui, B., 2019. Occurrence, sources and ecotoxicological risks of polychlorinated biphenyls (PCBs) in sediment cores from urban, rural and reclamation-affected rivers of the Pearl River Delta, China. Chemosphere 218, 359–367. https://doi.org/10.1016/j.chemosphere.2018.11.046

Winchell, L.J., Novak, P.J., 2008. Enhancing polychlorinated biphenyl dechlorination in fresh water sediment with biostimulation and bioaugmentation. Chemosphere 71, 176–182. https://doi.org/10.1016/j.chemosphere.2007.10.021

Xiang, Y., Xing, Z., Liu, J., Qin, W., Huang, X., 2020. Recent advances in the biodegradation of polychlorinated biphenyls. World J. Microbiol. Biotechnol. 36, 1–10. https://doi.org/10.1007/s11274-020-02922-2

Xu, Y., Tang, Y., Xu, L., Wang, Y., Liu, Z., Qin, Q., 2021. Effects of iron-carbon materials on microbial-catalyzed reductive dechlorination of polychlorinated biphenyls in Taihu Lake sediment microcosms: Enhanced chlorine removal, detoxification and shifts of microbial community. Sci. Total Environ. 792, 148454. https://doi.org/10.1016/j.scitotenv.2021.148454

Yan, T., LaPara, T.M., Novak, P.J., 2006a. The effect of varying levels of sodium bicarbonate on polychlorinated biphenyl dechlorination in Hudson River sediment cultures. Environ. Microbiol. 8, 1288–1298. https://doi.org/10.1111/j.1462-2920.2006.01037.x

Yan, T., LaPara, T.M., Novak, P.J., 2006b. The impact of sediment characteristics on polychlorinated biphenyl-dechlorinating cultures: Implications for bioaugmentation. Bioremediat. J. 10, 143–151. https://doi.org/10.1080/10889860601021381

Zanaroli, G., Balloi, A., Negroni, A., Borruso, L., Daffonchio, D., Fava, F., 2012a. A Chloroflexi bacterium dechlorinates polychlorinated biphenyls in marine sediments under in situ-like biogeochemical conditions. J. Hazard. Mater. 209–210, 449–457. https://doi.org/10.1016/j.jhazmat.2012.01.042

Zanaroli, G., Balloi, A., Negroni, A., Daffonchio, D., Young, L.Y., Fava, F., 2010. Characterization of the microbial community from the marine sediment of the Venice lagoon capable of reductive dechlorination of coplanar polychlorinated biphenyls (PCBs). J. Hazard. Mater. 178, 417–426. https://doi.org/10.1016/j.jhazmat.2010.01.097

Zanaroli, G., Negroni, A., Vignola, M., Nuzzo, A., Shu, H.Y., Fava, F., 2012b. Enhancement of microbial reductive dechlorination of polychlorinated biphenyls (PCBs) in a marine sediment by nanoscale zerovalent iron (NZVI) particles. J. Chem. Technol. Biotechnol. 87, 1246–1253. https://doi.org/10.1002/jctb.3835

Zanaroli, G., Pérez-Jiménez, J.R., Young, L.Y., Marchetti, L., Fava, F., 2006. Microbial reductive dechlorination of weathered and exogenous co-planar polychlorinated biphenyls (PCBs) in an anaerobic sediment of Venice Lagoon. Biodegradation 17, 19–27. https://doi.org/10.1007/s10532-005-3752-7

Zeller, C., Cushing, B., 2006. Panel discussion: remedy effectiveness: what works, what doesn't? Integr. Environ. Assess. Manag. 2, 75–79. https://doi.org/10.1897/1551-3793(2006)2[75:PDREWW]2.0.CO;2

Zhu, M., Yuan, Y., Yin, H., Guo, Z., Wei, X., Qi, X., Liu, H., Dang, Z., 2022. Environmental contamination and human exposure of polychlorinated biphenyls (PCBs) in China: A review. Sci. Total Environ. 805, 150270. https://doi.org/10.1016/j.scitotenv.2021.150270

Chapter 2

Microbial Electrochemical Technologies (METs)

2.1 Microbial Electrochemical Technologies (METs)

Microbial electrochemical technologies (METs), a branch of bioelectrochemical systems (BES) (Schröder et al., 2015), couple bacterial activities with electrodes, using the latter as inexhaustible source of electron donors or acceptors (Logan et al., 2019). In METs, oxidation reactions take place at the anode and provide electrons to reductive reactions at the cathode. Given the flexibility of the technology, METs can be employed for several purposes as production of chemicals, valorization of waste streams or bioremediation of polluted matrixes (Dessì et al., 2021; Logan et al., 2008; Osset-Álvarez et al., 2019; Wang et al., 2020). The main constituting elements of METs are electrodes and bacteria. Electrodes are solid or liquid state materials which act as conductors for the electron exchanges between bacteria and the surrounding environment. Bacteria able to interact with the electrodes are identified as electroactive bacteria and exchange electrons via an extracellular electron transfer (EET) (Paquete et al., 2022). In the next paragraphs the fundamentals aspects of an electrochemical cell and electroactive bacteria will be highlighted and illustrated, setting the bases for a better comprehension of the processes which regulate the fascinating interaction between electrodes and bacteria.

2.2 Fundamentals of an electrochemical set-up

Despite electrochemistry exerts astonishment between scientists and students, often being seen as a magic world where unexplainable phenomena take place, most of the basic processes which regulate the electron exchanges can be understood with principle of physic and chemistry. It is not the purpose of these paragraphs to deeply go through the aspects of the electrochemistry, which would require much greater knowledge and competences that the ones I own. Still, I would like to summarize the main features of an electrochemical experiment, so as to clarify the contents that will be furtherly illustrated. To do so, I collected the aspects described in (Bard and Faulkner., 2001) that I consider the essential ones and I reported them below.

2.2.1 The electrochemical cell

In the electrochemical systems, all the processes that take place involve and define a flow of electrons between two species. The electron flow can proceed through an electronic conductor, the electrode, or through an ionic conductor, the electrolyte. Ideally, both the conductors should pose low resistance to the flow of electrons. Hence, electrodes can be made of metals, either at solid (e.g. Pt) or liquid state (e.g. Hg), of carbon (e.g. graphite) or of semiconductors materials (e.g. Si). As for the electrolyte, which is

commonly an aqueous solution, the movement of the electrons is guaranteed by the presence of ions, with the most employed electrolytes being NaCl, $NaNO_3$, etc. . The flow of the electrons is regulated by the difference in energy between the two electrodes. The voltage, or the electric potential (E) ($V = J \cdot C^{-1}$), is a measure of the amount of energy available to drive the electron exchange process. The electron flow goes from higher energy states (more negative potentials or voltages) to lower energy states (more positive potentials or voltages) (Fig. 1). Consequently, an electrode posed at a negative potential sufficiently more energetic compared to a species A in the adjacent solution will lead to the reduction of the species A observing the flow of a reduction/cathodic current. On the contrary, an electrode posed at a positive potential sufficiently less energetic compared to a species A will lead to the oxidation of the species observing the flow of an oxidation/anodic current. Therefore, the presence of a difference in energy between two species, namely a difference in potential, is mandatory to observe an electron flow. Yet, the presence of a difference in potential and of a current flow is not sufficient to observe a chemical reduction or oxidation. Indeed, two processes occur at the interface between the electrode and the electrolyte, namely nonfaradaic and faradaic processes. Nonfaradaic processes can generate a current without changing the chemical composition of the studied environment. Processes as adsorption, desorption and migration of ions from the bulk of the solution to the electrode surface are called nonfaradaic processes. Instead, faradaic processes are the ones which involve the exchange of electrons between one species to another. Ideally, if the electrode is posed at a potential not negative enough to supply electrons to a species A, or not positive enough to withdraw electrons from a species A, only nonfaradaic processes are involved since the thermodynamic barrier prevents the electron exchange.

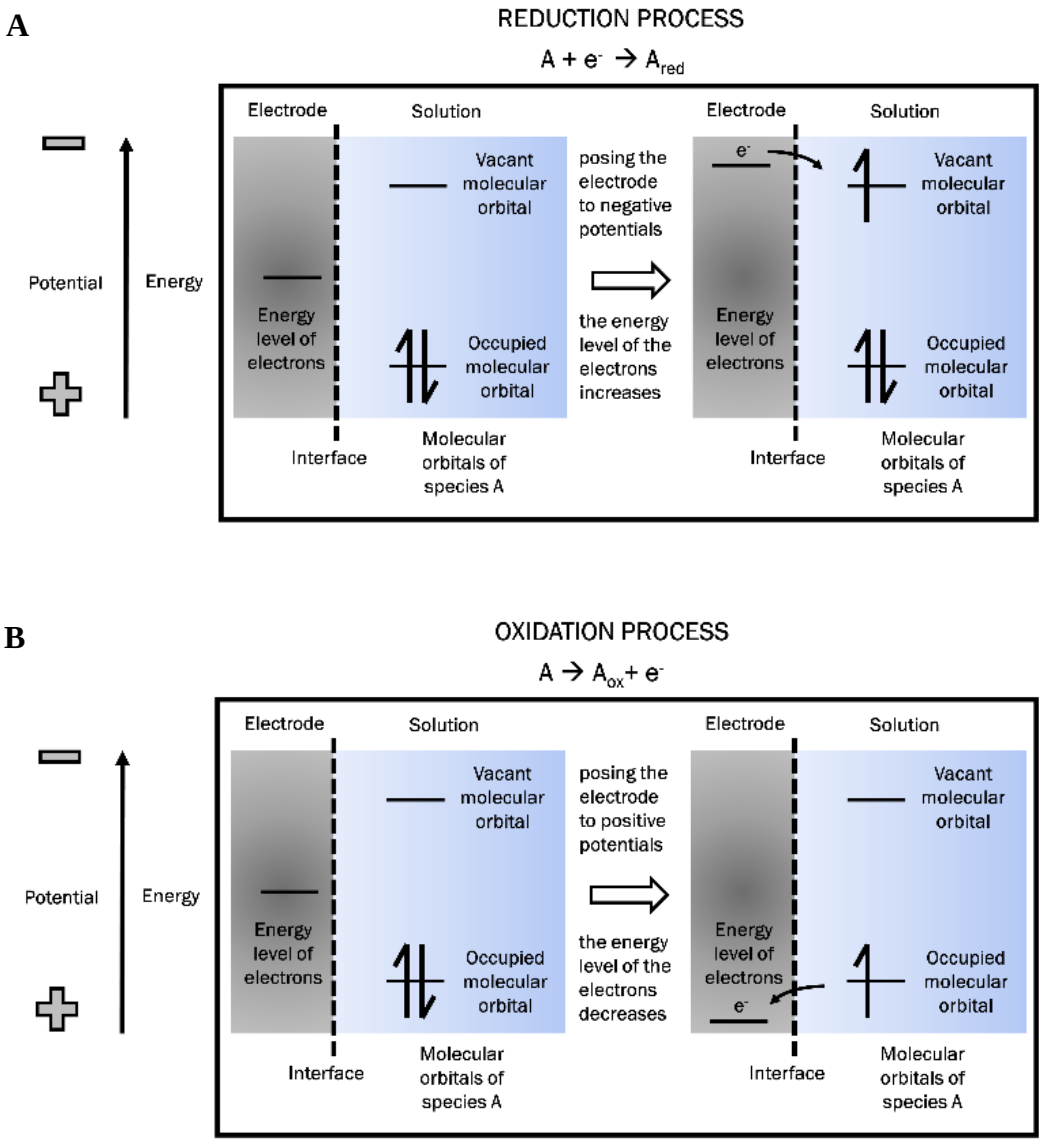

Figure 1 *Representation of reduction (panel A) and oxidation (panel B) processes of species A, mediated by an electrode, adapted from* (Bard and Faulkner., 2001)

The potential of an electrode or of a species is not an absolute value yet it is always expressed in respect to another electrode, namely reference electrode (RE). The voltage, i.e. a difference in the energy of two species, inevitably implicates the presence of a reference point, used to measure this difference. Ideally, to perform an electrochemical experiment two electrodes would be required. However, most of the electrochemical experiments are performed using three electrodes systems. Such systems involve a working electrode (WE), a counter electrode (CE) and a reference electrode (RE) (Fig. 2). The WE is usually the one where the reaction of interest occurs. The current flows between the WE and the CE. The CE is required so as to close the circuit, guaranteeing the supply or the withdrawal of electrons. Instead, an additional circuit connects the RE to the WE, so as to measure more accurately the voltage of the WE. In fact, in the circuit connecting the RE to the WE no current flows. Doing so, it is possible to avoid the voltage drop, namely the amount of energy required to flow the current in a circuit. Consequently, the difference of potential between the WE and the RE is solely due to the energetic states of the two electrodes. From a practical point of view, in an electrochemical experiment an accurate control of the WE potential can be performed thanks to the RE. Whereas the potential of the CE is defined dependently according to the imposed potential of the WE and to the features of the system.

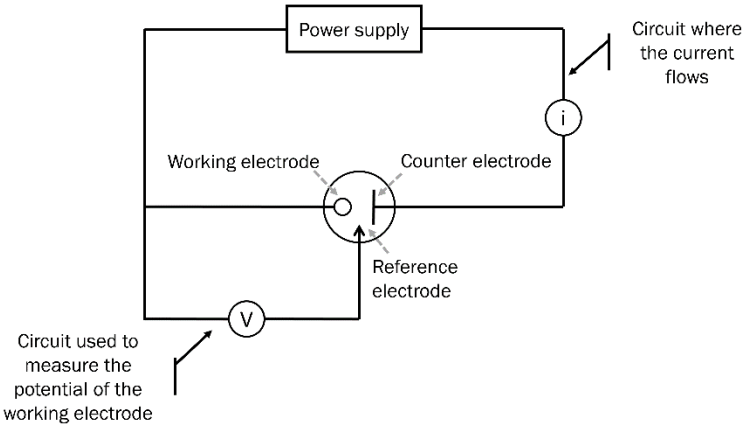

Figure 2 *Three electrode cell, adapted from* (Bard and Faulkner., 2001)

2.2.2 Mass transfers

Similarly to all the chemical equilibrium, also in an electrochemical system thermodynamic and kinetic combine to define the outcome of the process. The thermodynamic of the process is linked to the Nernst equation (eq. 1), which relates the concentration of the reactants to the specific energy of each reaction.

$$E = E° + \frac{R \cdot T}{n \cdot F} ln \frac{C_O}{C_R} \qquad O + n\,e^- \rightleftharpoons R \tag{1}$$

Where E° is the standard potential of the reaction, R is the gas constant, F is the Faraday constant identifying the number of Coulomb (charge) per mole of electron, n is the number of electron exchanged in the redox process, C_O and C_R indicates respectively the concentration of reactants and products. As for

the kinetic of the process, several chemical and physical aspects can contribute in identifying them. Within the kinetic aspect of an electrochemical equilibrium, mass transfer can play an important role. In a solution, the modes of mass transfer can be migration, diffusion and convection. Migration is the movement of a charged particle driven by an electric field. Diffusion depends on the presence of a chemical gradient, as a concentration gradient. Convection can be classified as natural convection, driven by hydrodynamic (i.e. the transport that take place in the presence of a density gradient), or as forced convection, driven by mechanical agitation. Identifying the contribution of each mode to the total diffusion process is not an easy task. Often, electrochemical systems are designed to consider one mode negligible, simplifying the calculation. It is important to keep in mind what differs from one mode to another. Specifically, the main differentiation is between stirred systems, in the presence of a convection mode, and static systems. Avoiding the rigorous modelling of mathematical expressions that define the mass transport, we can still understand the influence of mass transfer on an electrochemical process. Let's consider a stirred system, with a species O converted to R at the electrode surface. In such a system, we can assume that the stirring is ineffective at the electrode surface, thus leaving a thin layer attached to the electrode where the C_O decreases (Nernst diffusion layer). Consequently, C_O goes from the highest value of the bulk solution to a lower value next to the electrode (Fig. 3A). After an initial equilibration time, C_O in the proximity to the electrode reaches a constant value depending on the entity of the stirring, on the applied potential and on the kinetic of the reaction. Similarly does the current profile, following a trend analogue to the variation of the C_O and reaching a plateau (Fig. 3B). Conversely, in a static system the diffusion layer tends to grow in time, reducing the current flow. In the absence of convection, the

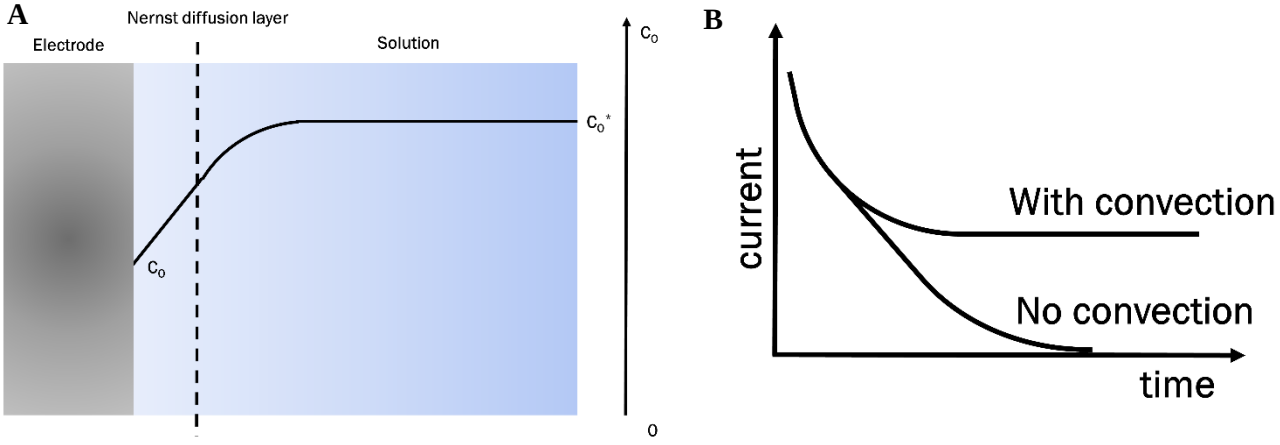

Figure 3 *Panel A: Concentration profile and diffusion layer approximation, Panel B: Current profile for a potential applied to a stationary electrode (no convection) and to an electrode in a stirred solution (with convection) where a steady-state current is attained, adapted from* (Bard and Faulkner., 2001)

kinetic of the process is mainly driven by the mass transfers, which proceed preferentially via migration and diffusion, thus limiting the current flow (Fig. 3B).

2.2.3 Bulk electrolysis methods

Electrochemical techniques have several ways of operation and many applications. Within this large group of functioning, bulk electrolysis methods are often applied in METs. In bulk electrolysis methods a power supply is applied, for instance, for removal of components from a solution. The advantage of coupling bulk electrolysis methods and biological systems is reducing the energetic costs to achieve the desired reaction thanks to the catalytic action of the bacteria. Two approaches for bulk electrolysis methods exist. The first one is defined as controlled-potential technique (potentiostatic), based on maintaining the potential of the WE constant in respect to the RE for all the length of the experiment. The current flow is then a consequence of the imposed potential. The second approach is named controlled-current technique (galvanostatic), obtained by imposing a constant current flow. The potential of the electrodes is then a consequence of the applied current flow. To evaluate the efficacy of the bulk electrolysis methods, coulombic efficiency is commonly calculated, i.e. the amount of electrons involved in the desired reaction compared to the total electron flow. Usually, potentiostatic techniques are employed for a finer tuning of the process and are characterized by higher coulombic efficiencies. Indeed, when the potential applied is the one required for the target reaction, the current flow is a consequence of such reaction. Thus, the number of electrons involved in the target reaction is approximately the total number of electrons flowed. On the contrary, in galvanostatic techniques the potential can vary according to the amount of current imposed. Doing so, the electrodes can reach values of potentials that allow parallel reactions to take place, reducing the selectivity and the coulombic efficiency.

2.3 Electrodes

The electrode is a key aspect of METs, since it enhances the electron exchanges with bacteria. Thus, electrodes should guarantee good conductivity, good compatibility with bacteria and reasonable prices. In this regard, an incredible variety of electrode materials has been studied and it is not the purpose of this section to illustrate the various materials that can be applied in METs. On the contrary, I will illustrate only the main elements behind the application of an electrode and its functioning, reporting few relevant examples and achievements for the comprehension of this PhD thesis. Indeed, electrodes can be classified in two main groups, respectively named bio-electrodes and chemical-electrodes according to the presence

or not of bacteria as catalysts (Wei et al., 2011). When working with bio-electrode, the goal is to obtain high current densities (Xie et al., 2015). Thus the porosity of the electrode is extremely relevant since the available surface area guarantees the contact with the bacteria, affecting the current density. The main drawback of high porosity structures is the possibility of clogging, due to the excessive growth of bacteria. Considering that biofilm can reach thickness of up to hundreds of μm (Baudler et al., 2015), only electrodes with pores size of several hundreds of μm are expected to prevent clogging (Xie et al., 2015). One of the most employed material for bio-electrodes is carbon, given the good biocompatibility, the good stability and the reasonable price (Wei et al., 2011; Xie et al., 2015). Several carbonaceous materials are available on the market, as graphite rod, graphite granules, carbon cloth, glassy carbon, carbon paper, carbon nanotubes, graphene, with a variety of chemical-physical properties. Metals and oxide metals are characterized by higher conductivity, even though they are less employed due to the lower biocompatibility and higher costs (Wei et al., 2011). Recently, the advantages of carbonaceous materials and metals were exploited by covering stainless steel with a graphite layer or carbon nanotubes, obtaining high porosity biocompatible structures with excellent mechanical properties (Amade et al., 2015; Xu et al., 2020). Regarding chemical-electrodes, they can be employed for the production of chemicals, e.g. O_2/H_2 via water electrolysis or Cl_2 (Botti et al., 2023; Lai et al., 2017), or to guarantee a constant supply of electrons for the cathodic reactions, thus being defined as sacrificial anodes (Mao et al., 2011). If chemical-electrodes are used for the production of chemicals, their stability should be sufficient to prevent their corrosion within the voltage working range. For instance, when trying to produce oxygen via the electrolysis of water, carbonaceous materials easily oxidize to CO_2 whereas more stable metal oxides, as titanium covered with mixed-metal oxides (Ti-MMO), are preferred (Lai et al., 2017). On the other hand, chemical-electrodes that are meant to be sacrificial anodes have to supply electrons with a minimum energy expense and avoiding excessive positive potential to prevent parallel reactions. Thus they should be characterized by oxidation potentials lower than the chemical species mostly abundant in the surrounding environment (Mao et al., 2011).

2.4 The interaction between bacteria and electrodes

Electron transfers in biological systems are essential processes for the cell growth, regulating the energy transfers of the cell (Bartlett, 2008). The biological electron transfer relies on electron transport chains, where several cell components contribute in exchanging the electrons. Considering the importance of such process in biological systems, it is not surprisingly that bacteria can exchange electrons also with abiotic elements as electrodes. Bacteria that are able to communicate with electrodes are identified as

electroactive bacteria and the exchange mechanism is defined as extracellular electron transfer (EET) (Paquete et al., 2022). EET can be classified in two main categories: direct and indirect EET. Direct electron transfer can be performed via outer membrane multiheme c-type cytochromes (OMC), pili or outer membrane vesicles (OMV) (Logan et al., 2019; Paquete et al., 2022) (Fig. 4). Outer membrane multiheme c-type cytochromes are peripheral proteins localized at the membrane surface and responsible for the transfer of electrons (Hianik, 2008). Pili were reported to be electrically conductive filamentous, typically 10-20 µm long, responsible for long-range electron transfers between bacteria and other electron donor/acceptor (Lovley, 2011), which can contain cytochromes so as to facilitate the electron exchange process (Liu et al., 2015; Lovley, 2011). OMV are 100-300 nm vesicles containing lipopolysaccharides (LPS), phospholipids, peptidoglycan, outer membrane proteins (OMPs) as OMCs, cell wall components, proteins, DNA, RNA and have been associated to several functions, playing a role in the bacterial adherence (Jan, 2017). Indirect transfer is possible thanks to mediator as extracellular enzymes or electron shuttles (Logan et al., 2019; Paquete et al., 2022). Regarding extracellular enzymes, the role of hydrogenases and dehydrogenases was pointed out in the electron exchange process (Deutzmann et al., 2015). Electron shuttles, or redox mediator, are exogenous compounds secreted by microorganisms that facilitate the electron transfer or chemicals with redox properties (Zhu et al., 2022). Molecules as flavins (Von Canstein et al., 2008) or humic substances (Piepenbrock and Kappler, 2013) were reported to be involved in external electron transfer processes. External electron shuttles can also be employed to guarantee a connection between bacteria and the electrodes, thus allowing electrochemically inactive bacteria to play active role in METs (Aulenta et al., 2007; Zheng et al., 2020). For instance H_2 is a common redox mediator used for electrochemically inactive bacteria, given the possibility to produce it via electrolysis (Zhu et al., 2022).

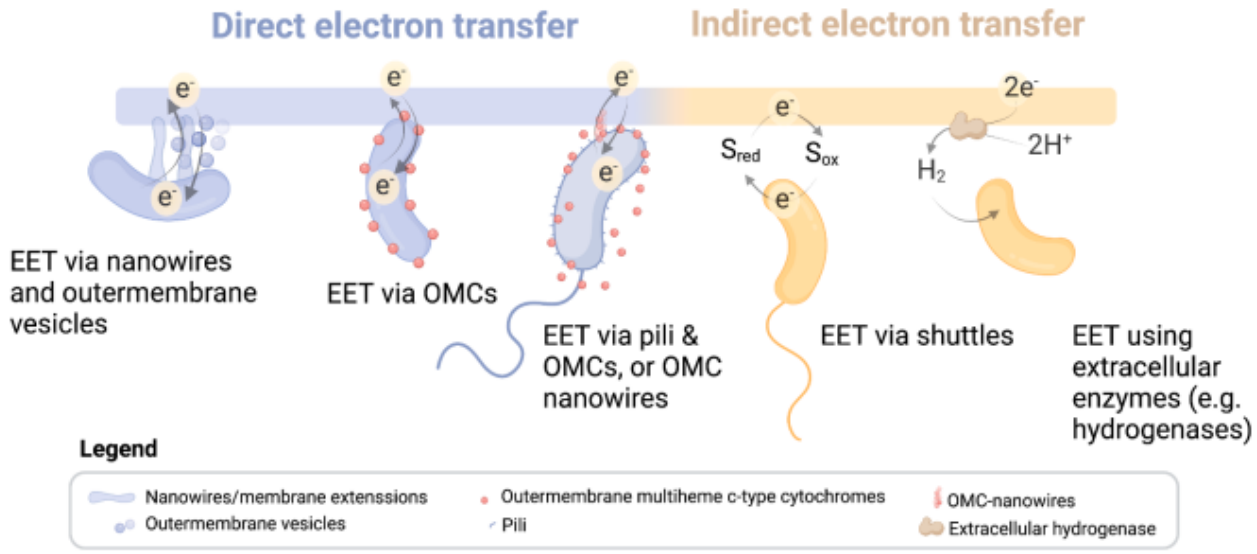

Figure 4 *Extracellular electron transfer mechanisms performed by electroactive bacteria. Electron transfer can occur through a direct process using nanowires, OMVs, pili or cell-surface cytochromes (OMCs), or by an indirect process using electron shuttles or extracellular enzymes* (Paquete et al., 2022)

2.5 Classification of METs and applications for bioremediation of polluted matrixes

The interaction between bacteria and electrodes is at the bases of METs. A main classification of these systems is performed according to the presence or not of an external potential. In particular, METs can be divided in microbial fuel cells (MFC) or microbial electrolysis cells (MEC) respectively requiring the absence or presence of an external applied potential (Hamelers et al., 2010) (Fig. 5). MFC relies on spontaneous reaction to metabolize nutrients or to convert pollutants, producing chemicals or electricity (Hamelers et al., 2010; Logan, 2008). Conversely in MEC, bulk electrolysis methods are combined with the bio catalytic action of bacteria to favor non-spontaneous reactions (Hamelers et al., 2010). Both the systems are characterized by versatility and can be employed for several applications. In this regard, a typical use of MFC and MEC is for bioremediation purposes. For instance, MFC have been largely studied for wastewater treatment, reducing the high content of organic matter, nitrogen or chemicals (e.g. pharmaceuticals) and possibly valorizing the by-product via energy production (Do et al., 2018; Doherty et al., 2015; Fu et al., 2022). MFC have also been employed for desalination, removal of heavy metals or remediation of soils (Abbas and Rafatullah, 2021; Verma et al., 2021). Similarly, MEC have been applied for the remediation of polluted liquid streams, soils or sediments (Wang et al., 2020). Some uses

of METs employed in MEC configurations will be illustrated in the next paragraphs so as to highlight and anticipate the applications studied during this PhD thesis.

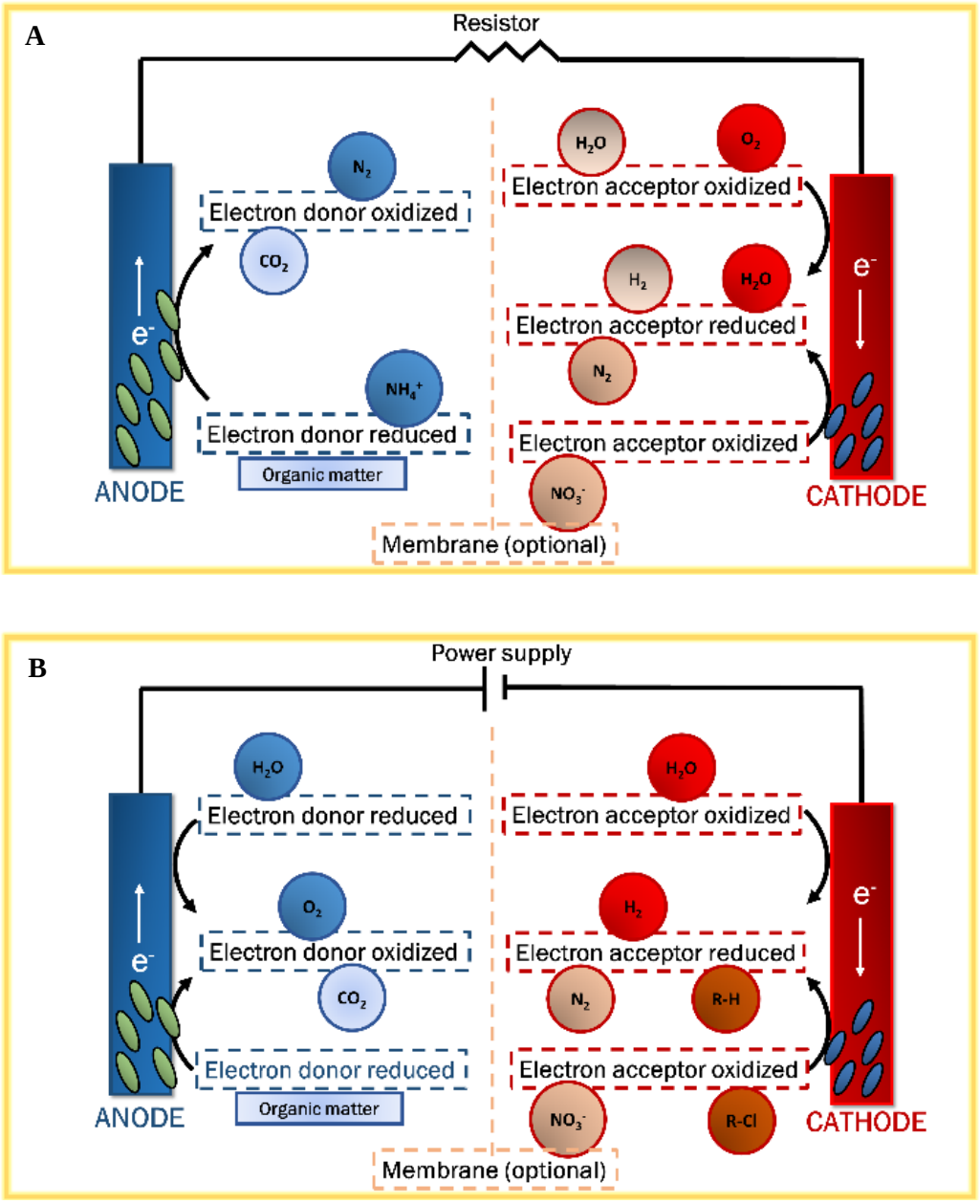

Figure 5 *Schematic illustration of a microbial fuel cell (MFC), panel A, and a microbial electrolysis cell (MEC), panel B, and examples of anodic and cathodic redox processes involved, adapted from* (Wang and Ren, 2013; Wang et al., 2020)

2.5.1 Bioelectrochemical stimulation for the removal of chlorinated compounds

Chlorinated contaminants that need to be removed from the environment range from aliphatic hydrocarbons, as tetrachloroethylene (PCE), trichloroethylene (TCE), dichloroethylene (DCE) and vinylchloride (CV), to aromatic hydrocarbons, as chlorinated phenols or PCBs. Often, chlorinated pollutants require a first anaerobic reduction which decreases the chlorination degree of the contaminant and a second aerobic oxidation to cleave the organic skeleton. METs appear to perfectly fit into the biostimulation approach since they can simultaneously prime the reductive dechlorination and the oxidative degradation. Regarding the stimulation of reductive dechlorination, the cathode can supply the electrons required from the bacteria to reduce the chlorinated compounds. The ability of OHRB to respire on chlorinated solvents as PCE or TCE using electrodes as sole electron source was proven either using redox mediator as methyl viologen or by direct contact (Aulenta et al., 2009, 2007; Chen et al., 2019). Reduction of TCE was demonstrated also using hydrogen as redox mediator (Aulenta et al., 2011). Cathodic stimulation was effective also for other chlorinated compounds as chloroform (Fernández-Verdejo et al., 2022) or polychlorophenols (Lin et al., 2019). Additionally, by employing METs it is possible to control the rate of the stimulation exerting a more selective effect by tuning the potential (Aulenta et al., 2011). Following, the anode can stimulate the oxidative degradation of low chlorinated pollutants by supplying the required oxygen via water electrolysis, enhancing the removal of the pollutants. The electrolysis of water can in principle guarantee a constant oxygen production, avoiding the high costs of mechanical aeration or the toxicity of chemical oxidant agents used to produce oxygen. Recently, this configuration was applied for an *ex situ* treatment of real groundwater contaminated with a mixture of PCE, TCE, DCE, VC, showing the efficacy of the process in priming the reductive dechlorination and oxidative degradation (Dell'Armi et al., 2022).

2.5.1.1 A focus on METs applied for the bioremediation of PCBs polluted sediments

Theoretically, METs for the bioremediation of PCBs polluted sediments can guarantee a long lasting stimulating effect, in line with the time scale of the PCBs reductive dechlorination and oxidative degradation processes. Up to now, the proof of concept of electrostimulated bioremediation of PCBs polluted sediments has been done on single congeners and PCBs mixtures in freshwater sediments or synthetic medium (Table 1). Cathodes polarized at -0.46 V vs Ag/AgCl (3M KCl) primed the reductive dechlorination of a freshly spiked single congener (PCB 61) in river sediments (Liu et al., 2017; Yu et al., 2017). Carbon paper bioanode poised at 0.24 V vs Ag/AgCl (3M KCl) (Yu et al., 2016) and graphite felt biocathode polarized at -0.65 V vs Ag/AgCl (3M KCl) (Wan et al., 2018) enhanced the

bioremediation of PCB 61 in river sediments. More recently, Zhang *et al.* (2021) stimulated a marine-originated dechlorinating culture increasing the dechlorination rate of Aroclor 1260 spiked in synthetic medium. The only example of concomitant stimulation of reductive dechlorination and aerobic degradation was reported by Chun *et al.*(2013) and illustrated in the theoretical experimental scheme of Fig. 6. The application of constant cell voltages was studied on river sediments contaminated both with freshly spiked single congeners and a weathered mixture of PCB. The imposed potential speeded up the dechlorination of PCBs and reduced the accumulation of low chlorinated congeners. Still, METs has never been studied to remediate PCB polluted marine sediments, where chemical-physical parameters and the indigenous microbiota profoundly differ from freshwater sites.

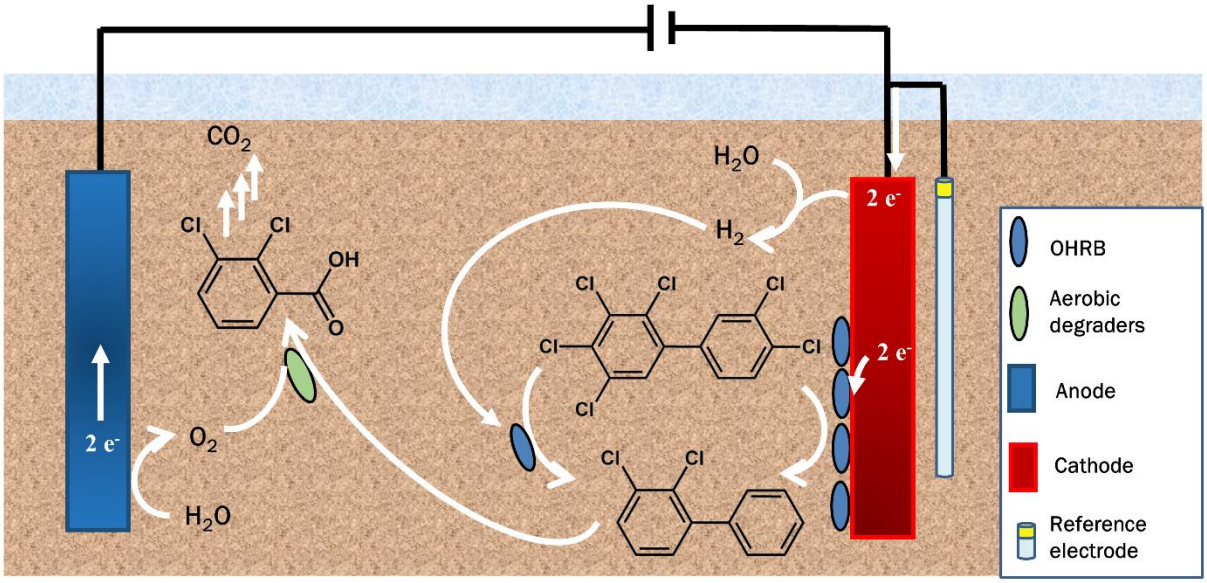

Figure 6 *Theoretical experimental scheme of the concomitant reductive dechlorination and oxidative degradation of PCBs in a static in situ MET for the bioremediation of PCBs polluted sediments*

Little is known about the interaction between electrodes and PCBs respiring bacteria. A direct electron transfer between OHRB and graphite electrodes was inferred to explain the enhanced dechlorination rate observed when working at negative potential without electrochemical hydrogen production (Liu et al., 2017; Yu et al., 2016; Zhang et al., 2021). Furthermore, it was speculated that *Chloroflexi* phylum and *Desulfovibrio* genus can reductive dechlorinate PCBs using H_2 as mediator for indirect EET (Field and Sierra-Alvarez, 2008; MacAskie et al., 2012). A direct electron transfer between electrodes and bacteria can be preferred since it involves milder potential and it has a lower impact on the treated sites. Indeed, electrochemical water hydrolysis is required to produce either H_2 or O_2. Consequently, when

bioelectrochemical stimulation is applied as *in situ* technique at static conditions, the water hydrolysis rapidly leads to severe variations of the sediment pH due to the mass transfer limitations (Bellagamba et al., 2017; Chun et al., 2013). Harmful conditions for bacterial growth could take place, representing one of the main drawbacks of bioelectrochemical stimulation for *in situ* bioremediation of PCBs for which a proper solution has not been found yet.

Table 4 *Summary of the literature regarding application of METs to stimulate the microbial degradation of PCBs in aquatic sediments*

Environment and scale (L)	**PCB concentration ($mg \cdot Kg_{drysediment}^{-1}$)**	**Bioaugmentation**	**METs' parameters and amendment**	**Duration (d)**	**Mechanism**	**Degradation/ Dechlorination rate**	**Reference**
Freshwater sediment, lab scale (0.4)	Freshly spiked single congeners (26, 100) and weathered mixture (20)	No	Cell voltage difference: 1.5, 2, 3 V	88	R.D. + O.D.	$^{c}0.022$ $mol_{Cl} \cdot mol_{biphenyl}^{-1} \cdot d^{-1}$, $^{c}0.34$ $\mu mol_{PCB} \cdot Kg_{drysediment}^{-1} \cdot d^{-1}$ (removal rates reported are relative to the freshly spiked single congeners)	(Chun et al., 2013)
Freshwater sediment, lab scale (0.1)	26 Freshly spiked single congener	No	Bioanode: 0.24 V vs Ag/AgCl (3M KCl) and acetate	130	R.D.	$^{c}0.007$ $mol_{Cl} \cdot mol_{biphenyl}^{-1} \cdot d^{-1}$, $^{c}0.7$ $\mu mol_{Cl} \cdot Kg_{drysediment}^{-1} \cdot d^{-1}$	(Yu et al., 2016)
Freshwater sediment, lab scale (0.21)	26 Freshly spiked single congener	No	Biocathode: -0.46 V vs Ag/AgCl (3M KCl)) and iron oxide	120	R.D.	$^{c}0.005$ $mol_{Cl} \cdot mol_{biphenyl}^{-1} \cdot d^{-1}$, $^{c}0.5$ $\mu mol_{Cl} \cdot Kg_{drysediment}^{-1} \cdot d^{-1}$	(Liu et al., 2017)
Freshwater sediment,	13 Freshly spiked single congener	No	Biocathode: -0.46 V vs Ag/AgCl	290	R.D.	$^{c}0.0027$ $mol_{Cl} \cdot mol_{biphenyl}^{-1} \cdot d^{-1}$, $^{c}0.23$	(Yu et al., 2017)

lab scale (0.11)			(3M KCl)) and acetate			$\mu mol_{Cl} \cdot Kg_{drysediment}^{-1} \cdot d^{-1}$	
Freshwater sediment, lab scale (0.3)	26 Freshly spiked single congener	No	Biocathode: -0.65 V vs Ag/AgCl (3M KCl)) and iron oxide	180	R.D.	[c]0.006 $mol_{Cl} \cdot mol_{biphenyl}^{-1} \cdot d^{-1}$, [c]0.6 $\mu mol_{Cl} \cdot Kg_{drysediment}^{-1} \cdot d^{-1}$	(Wan et al., 2018)
Synthetic medium, lab scale (0.15)	25 $mg \cdot L^{-1}$ Freshly spiked mixtures	Yes	Biocathode: -0.55 V vs Ag/AgCl (3M KCl)), lactate and humins	35	R.D.	[c]0.025 $mol_{Cl} \cdot mol_{biphenyl}^{-1} \cdot d^{-1}$	(Zhang et al., 2021)

[c]calculated based on the reported data; R.D.: reductive dechlorination; O.D.: oxidative degradation

2.5.2 A focus on METs applied for the bioremediation of nitrogen polluted water matrixes

Nitrogen contamination due to the intensive industrial and agricultural activities is a current problem, requiring economic and sustainable solutions. The catalytic activity of bacteria can help reducing the energy burden demanded for the removal of pollutants. Consequently, one of the most common application of METs for bioremediation purposes is the removal of nitrogen, either in form of ammonium or nitrate which are two common pollutants present in wastewaters (Council Directive, 1991). Anodic oxidation of ammonium mediated by electrodes has been demonstrated by Shaw *et al.* (2020) and Osset-Álvarez *et al.* (2022), reporting the conversion of NH_4^+ to N_2 highlighting the role of electrodes in enhancing the bioremediation process. Cathodic stimulation has been largely proven effective in stimulating the removal of nitrate from groundwater or wastewater, overcoming the typical lack of electrons in the polluted matrixes (Ceballos-Escalera et al., 2021; Molognoni et al., 2017; Sander et al., 2017). The application of METs for the bioremediation of nitrogen polluted wastewater will be further deepened in the last chapter of this PhD thesis.

2.6 Bibliography

Abbas, S.Z., Rafatullah, M., 2021. Recent advances in soil microbial fuel cells for soil contaminants remediation. Chemosphere 272, 129691. https://doi.org/10.1016/j.chemosphere.2021.129691

Amade, R., Vila-Costa, M., Hussain, S., Casamayor, E.O., Bertran, E., 2015. Vertically aligned carbon nanotubes coated with manganese dioxide as cathode material for microbial fuel cells. J. Mater. Sci. 50, 1214–1220. https://doi.org/10.1007/s10853-014-8677-2

Aulenta, F., Canosa, A., Reale, P., Rossetti, S., Panero, S., Majone, M., 2009. Microbial reductive dechlorination of trichloroethene to ethene with electrodes serving as electron donors without the external addition of redox mediators. Biotechnol. Bioeng. 103, 85–91. https://doi.org/10.1002/bit.22234

Aulenta, F., Catervi, A., Majone, M., Panero, S., Reale, P., Rossetti, S., 2007. Electron transfer from a solid-state electrode assisted by methyl viologen sustains efficient microbial reductive dechlorination of TCE. Environ. Sci. Technol. 41, 2554–2559. https://doi.org/10.1021/es0624321

Aulenta, F., Tocca, L., Verdini, R., Reale, P., Majone, M., 2011. Dechlorination of Trichloroethene in a Continuous-Flow Bioelectrochemical Reactor : Effect of Cathode Potential on Rate , Selectivity , and Electron Transfer Mechanisms. Environ. Sci. Technol. 45, 8444–8451. https://10.1021/es202262y

Bard, A.J., Faulkner., L.R., 2001. Electrochemical Methods Fundamentals and Applications, Second. ed, Physics. John Wiley & Sons, Texas, Austin.

Bartlett, P., 2008. Bioenergetics and Biological Electron Transport, in: Bartlett, P. (Ed.), Bioelectrochemistry: Fundamentals, Experimental Techniques and Applications. Wiley & Sons, Southampton, UK, pp. 1–33.

Baudler, A., Schmidt, I., Langner, M., Greiner, A., Schröder, U., 2015. Does it have to be carbon? Metal anodes in microbial fuel cells and related bioelectrochemical systems. Energy Environ. Sci. 8, 2048–2055. https://doi.org/10.1039/c5ee00866b

Bellagamba, M., Viggi, C.C., Ademollo, N., Rossetti, S., Aulenta, F., 2017. Electrolysis-driven bioremediation of crude oil-contaminated marine sediments. N. Biotechnol. 38, 84–90. https://doi.org/10.1016/j.nbt.2016.03.003

Botti, A., Pous, N., Cheng, H.Y., Colprim, J., Zanaroli, G., Puig, S., 2023. Electrifying secondary settlers to enhance nitrogen and pathogens removals. Chem. Eng. J. 451. https://doi.org/10.1016/j.cej.2022.138949

Ceballos-Escalera, A., Pous, N., Chiluiza-Ramos, P., Korth, B., Harnisch, F., Bañeras, L., Balaguer, M.D., Puig, S., 2021. Electro-bioremediation of nitrate and arsenite polluted groundwater. Water Res. 190, 116748. https://doi.org/10.1016/j.watres.2020.116748

Chen, F., Li, Z.L., Liang, B., Yang, J.Q., Cheng, H.Y., Huang, C., Nan, J., Wang, A.J., 2019. Electrostimulated bio-dechlorination of trichloroethene by potential regulation: Kinetics, microbial community structure and function. Chem. Eng. J. 357, 633–640. https://doi.org/10.1016/j.cej.2018.09.191

Chun, C.L., Payne, R.B., Sowers, K.R., May, H.D., 2013. Electrical stimulation of microbial PCB

degradation in sediment. Water Res. 47, 141–152. https://doi.org/10.1016/j.watres.2012.09.038

Council Directive, 1991. Council Directive 91/271/EEC, Official Journal of the European Communities. https://doi.org/10.1039/AP9842100196

Dell'Armi, E., Zeppilli, M., Di Franca, M.L., Matturro, B., Feigl, V., Molnár, M., Berkl, Z., Németh, I., Yaqoubi, H., Rossetti, S., Papini, M.P., Majone, M., 2022. Evaluation of a Bioelectrochemical Reductive/Oxidative Sequential Process for Chlorinated Aliphatic Hydrocarbons (Cahs) Removal from a Real Contaminated Groundwater. J. Water Process Eng. 49, 103101. https://doi.org/10.2139/ssrn.3981653

Dessì, P., Rovira-Alsina, L., Sánchez, C., Dinesh, G.K., Tong, W., Chatterjee, P., Tedesco, M., Farràs, P., Hamelers, H.M.V., Puig, S., 2021. Microbial electrosynthesis: Towards sustainable biorefineries for production of green chemicals from CO2 emissions. Biotechnol. Adv. 46. https://doi.org/10.1016/j.biotechadv.2020.107675

Deutzmann, J.S., Sahin, M., Spormann, A.M., 2015. Extracellular enzymes facilitate electron uptake in biocorrosion and bioelectrosynthesis. MBio 6, 1–8. https://doi.org/10.1128/mBio.00496-15

Do, M.H., Ngo, H.H., Guo, W.S., Liu, Y., Chang, S.W., Nguyen, D.D., Nghiem, L.D., Ni, B.J., 2018. Challenges in the application of microbial fuel cells to wastewater treatment and energy production: A mini review. Sci. Total Environ. 639, 910–920. https://doi.org/10.1016/j.scitotenv.2018.05.136

Doherty, L., Zhao, Y., Zhao, X., Hu, Y., Hao, X., Xu, L., Liu, R., 2015. A review of a recently emerged technology: Constructed wetland - Microbial fuel cells. Water Res. 85, 38–45. https://doi.org/10.1016/j.watres.2015.08.016

Fernández-Verdejo, D., Cortés, P., Guisasola, A., Blánquez, P., Marco-Urrea, E., 2022. Bioelectrochemically-assisted degradation of chloroform by a co-culture of Dehalobacter and Dehalobacterium. Environ. Sci. Ecotechnology 12, 0–5. https://doi.org/10.1016/j.ese.2022.100199

Field, J.A., Sierra-Alvarez, R., 2008. Microbial transformation and degradation of polychlorinated biphenyls. Environ. Pollut. 155, 1–12. https://doi.org/10.1016/j.envpol.2007.10.016

Fu, J., Zhao, Y., Yao, Q., Addo-Bankas, O., Ji, B., Yuan, Y., Wei, T., Esteve-Núñez, A., 2022. A review on antibiotics removal: Leveraging the combination of grey and green techniques. Sci. Total Environ. 838. https://doi.org/10.1016/j.scitotenv.2022.156427

Hamelers, H.V.M., Ter Heijne, A., Sleutels, T.H.J.A., Jeremiasse, A.W., Strik, D.P.B.T.B., Buisman, C.J.N., 2010. New applications and performance of bioelectrochemical systems. Appl. Microbiol. Biotechnol. 85, 1673–1685. https://doi.org/10.1007/s00253-009-2357-1

Hianik, T., 2008. Biological Membranes and Membrane Mimics, in: Bartlett, P. (Ed.), Bioelectrochemistry: Fundamentals, Experimental Techniques and Applications. Wiley & Sons, Southampton, UK, pp. 87–156.

Jan, A.T., 2017. Outer Membrane Vesicles (OMVs) of gram-negative bacteria: A perspective update. Front. Microbiol. 8, 1–11. https://doi.org/10.3389/fmicb.2017.01053

Lai, A., Aulenta, F., Mingazzini, M., Palumbo, M.T., Papini, M.P., Verdini, R., Majone, M., 2017. Bioelectrochemical approach for reductive and oxidative dechlorination of chlorinated aliphatic hydrocarbons (CAHs). Chemosphere 169, 351–360.

https://doi.org/10.1016/j.chemosphere.2016.11.072

Lin, X.Q., Li, Z.L., Liang, B., Zhai, H.L., Cai, W.W., Nan, J., Wang, A.J., 2019. Accelerated microbial reductive dechlorination of 2,4,6-trichlorophenol by weak electrical stimulation. Water Res. 162, 236–245. https://doi.org/10.1016/j.watres.2019.06.068

Liu, F., Rotaru, A.E., Shrestha, P.M., Malvankar, N.S., Nevin, K.P., Lovley, D.R., 2015. Magnetite compensates for the lack of a pilin-associated c-type cytochrome in extracellular electron exchange. Environ. Microbiol. 17, 648–655. https://doi.org/10.1111/1462-2920.12485

Liu, X., Wan, H., Xue, Y., Feng, C., Wei, C., 2017. Addition of iron oxides in sediments enhances 2,3,4,5-tetrachlorobiphenyl (PCB 61) dechlorination by low-voltage electric fields. RSC Adv. 7, 26019–26027. https://doi.org/10.1039/c7ra02849k

Logan, B.E., 2008. Microbial Fuel Cells. Wiley & Sons, Pennsylvania.

Logan, B.E., Call, D., Cheng, S., Hamelers, H.V.M., Sleutels, T.H.J.A., Jeremiasse, A.W., Rozendal, R.A., 2008. Microbial electrolysis cells for high yield hydrogen gas production from organic matter. Environ. Sci. Technol. 42, 8630–8640. https://doi.org/10.1021/es801553z

Logan, B.E., Rossi, R., Ragab, A., Saikaly, P.E., 2019. Electroactive microorganisms in bioelectrochemical systems. Nat. Rev. Microbiol. 17, 307–319. https://doi.org/10.1038/s41579-019-0173-x

Lovley, D.R., 2011. Live wires: Direct extracellular electron exchange for bioenergy and the bioremediation of energy-related contamination. Energy Environ. Sci. 4, 4896–4906. https://doi.org/10.1039/c1ee02229f

MacAskie, L.E., Humphries, A.C., Mikheenko, I.P., Baxter-Plant, V.S., Deplanche, K., Redwood, M.D., Bennett, J.A., Wood, J., 2012. Use of Desulfovibrio and Escherichia coli Pd-nanocatalysts in reduction of Cr(VI) and hydrogenolytic dehalogenation of polychlorinated biphenyls and used transformer oil. J. Chem. Technol. Biotechnol. 87, 1430–1435. https://doi.org/10.1002/jctb.3763

Mao, X., Ciblak, A., Amiri, M., Alshawabkeh, A.N., 2011. Redox control for electrochemical dechlorination of trichloroethylene in bicarbonate aqueous media. Environ. Sci. Technol. 45, 6517–6523. https://doi.org/10.1021/es200943z

Molognoni, D., Devecseri, M., Cecconet, D., Capodaglio, A.G., 2017. Cathodic groundwater denitrification with a bioelectrochemical system. J. Water Process Eng. 19, 67–73. https://doi.org/10.1016/j.jwpe.2017.07.013

Osset-Álvarez, M., Pous, N., Chiluiza-Ramos, P., Bañeras, L., Balaguer, M.D., Puig, S., 2022. Unveiling microbial electricity driven anoxic ammonium removal. Bioresour. Technol. Reports 17. https://doi.org/10.1016/j.biteb.2022.100975

Osset-Álvarez, M., Rovira-Alsina, L., Pous, N., Blasco-Gómez, R., Colprim, J., Balaguer, M.D., Puig, S., 2019. Niches for bioelectrochemical systems on the recovery of water, carbon and nitrogen in wastewater treatment plants. Biomass and Bioenergy 130, 105380. https://doi.org/10.1016/j.biombioe.2019.105380

Paquete, C.M., Rosenbaum, M.A., Baneras, L., Rotaru, A., Puig, S., 2022. Let ' s chat : Communication between electroactive microorganisms. Bioresour. Technol. 347. https://doi.org/10.1016/j.biortech.2022.126705

Piepenbrock, A., Kappler, A., 2013. Humic Substances and Extracellular Electron Transfer, in: Gescher, J., Kappler, A. (Eds.), Microbial Metal Respiration: From Geochemistry to Potential Applications. Springer Berlin, Heidelberg, pp. 107–128. https://doi.org/10.1007/978-3-642-32867-1

Sander, E.M., Virdis, B., Freguia, S., 2017. Bioelectrochemical nitrogen removal as a polishing mechanism for domestic wastewater treated effluents. Water Sci. Technol. 76, 3150–3159. https://doi.org/10.2166/wst.2017.462

Schröder, U., Harnisch, F., Angenent, L.T., 2015. Microbial electrochemistry and technology: Terminology and classification. Energy Environ. Sci. 8, 513–519. https://doi.org/10.1039/c4ee03359k

Shaw, D.R., Ali, M., Katuri, K.P., Gralnick, J.A., Reimann, J., Mesman, R., van Niftrik, L., Jetten, M.S.M., Saikaly, P.E., 2020. Extracellular electron transfer-dependent anaerobic oxidation of ammonium by anammox bacteria. Nat. Commun. 11. https://doi.org/10.1038/s41467-020-16016-y

Verma, J., Kumar, D., Singh, N., Katti, S.S., Shah, Y.T., 2021. Electricigens and microbial fuel cells for bioremediation and bioenergy production: a review, Environmental Chemistry Letters. Springer International Publishing. https://doi.org/10.1007/s10311-021-01199-7

Von Canstein, H., Ogawa, J., Shimizu, S., Lloyd, J.R., 2008. Secretion of flavins by Shewanella species and their role in extracellular electron transfer. Appl. Environ. Microbiol. 74, 615–623. https://doi.org/10.1128/AEM.01387-07

Wan, H., Yi, X., Liu, X., Feng, C., Dang, Z., Wei, C., 2018. Time-dependent bacterial community and electrochemical characterizations of cathodic biofilms in the surfactant-amended sediment-based bioelectrochemical reactor with enhanced 2,3,4,5-tetrachlorobiphenyl dechlorination. Environ. Pollut. 236, 343–354. https://doi.org/10.1016/j.envpol.2018.01.048

Wang, H., Ren, Z.J., 2013. A comprehensive review of microbial electrochemical systems as a platform technology. Biotechnol. Adv. 31, 1796–1807. https://doi.org/10.1016/j.biotechadv.2013.10.001

Wang, X., Aulenta, F., Puig, S., Esteve-Núñez, A., He, Y., Mu, Y., Rabaey, K., 2020. Microbial electrochemistry for bioremediation. Environ. Sci. Ecotechnology 1. https://doi.org/10.1016/j.ese.2020.100013

Wei, J., Liang, P., Huang, X., 2011. Recent progress in electrodes for microbial fuel cells. Bioresour. Technol. 102, 9335–9344. https://doi.org/10.1016/j.biortech.2011.07.019

Xie, X., Criddle, C., Cui, Y., 2015. Design and fabrication of bioelectrodes for microbial bioelectrochemical systems. Energy Environ. Sci. 8, 3418–3441. https://doi.org/10.1039/c5ee01862e

Xu, D.C., Zhai, S.Y., Cheng, H.Y., Guadie, A., Wang, H.C., Han, J.L., Liu, C.Y., Wang, A.J., 2020. Wire-drawing process with graphite lubricant as an industrializable approach to prepare graphite coated stainless-steel anode for bioelectrochemical systems. Environ. Res. 191, 110093. https://doi.org/10.1016/j.envres.2020.110093

Yu, H., Feng, C., Liu, X., Yi, X., Ren, Y., Wei, C., 2016. Enhanced anaerobic dechlorination of polychlorinated biphenyl in sediments by bioanode stimulation. Environ. Pollut. 211, 81–89.

https://doi.org/10.1016/j.envpol.2015.12.039

Yu, H., Wan, H., Feng, C., Yi, X., Liu, X., Ren, Y., Wei, C., 2017. Microbial polychlorinated biphenyl dechlorination in sediments by electrical stimulation: The effect of adding acetate and nonionic surfactant. Sci. Total Environ. 580, 1371–1380. https://doi.org/10.1016/j.scitotenv.2016.12.102

Zhang, D., Li, X., Zhang, C., Xiao, Z., Li, Y., Liang, Y., Dang, H., 2021. Electrostimulated bio-dechlorination of a PCB mixture (Aroclor 1260) in a marine-originated dechlorinating culture. Environ. Pollut. 291, 118157. https://doi.org/10.1016/j.envpol.2021.118157

Zheng, T., Li, J., Ji, Y., Zhang, W., Fang, Y., Xin, F., Dong, W., Wei, P., Ma, J., Jiang, M., 2020. Progress and Prospects of Bioelectrochemical Systems: Electron Transfer and Its Applications in the Microbial Metabolism. Front. Bioeng. Biotechnol. 8, 1–10. https://doi.org/10.3389/fbioe.2020.00010

Zhu, X., Wang, X., Li, N., Wang, Q., Liao, C., 2022. Bioelectrochemical system for dehalogenation: A review. Environ. Pollut. 293, 118519. https://doi.org/10.1016/j.envpol.2021.118519

Chapter 3

Polyhydroxyalkanoates to enhance reductive dehalogenation of microbial communities in marine sediment

3.1 Introduction

Polychlorinated biphenyls (PCBs) are widespread persistent organic pollutants in marine sediments, for which a sustainable remediation approach is still lacking (Šrédlová and Cajthaml, 2022). Indeed, it is known that PCBs may undergo microbial reductive dechlorination processes in marine sediments, but the time scale of such process is usually of months/years (Payne et al., 2019; Zanaroli et al., 2010). Reductive dechlorination can be primed via the addition of organic substrates that upon fermentation release electron donors for organohalide respiring bacteria (OHRB) (Chang et al., 2006). One of the key points of biostimulation is to attain a long lasting release of reducing equivalents in time, so as to lower the application costs reducing the frequency of the amendments' replenishment (Koenigsberg et al., 2006). Starting from these considerations, the use of biodegradable polymers is a promising approach for the stimulation of OHRB. Indeed, the hydrolysis step can slow down the release of readily fermentable organic matter over time, thus ensuring a prolonged, slow release of the electron donors used by OHRB (Koenigsberg and Sandefur, 1999). An additional important aspect of biostimulation is the presence of other anaerobic bacteria respiring different electron acceptors and competing with OHRB for hydrogen, such as sulfate-reducing (SRB), methanogenic (MB) and acetogenic bacteria (AB) (Bedard, 2003; Wiegel and Wu, 2000; Zanaroli et al., 2012). From a kinetic point of view, OHRB appear to be favored thanks to their higher affinity for hydrogen compared to their competitors (Bedard, 2003). Yet, the abundance of electron acceptors used by competitors can favor the latter when high concentrations of reducing equivalents are supplied. Hence, thanks to the hydrolysis step, biodegradable biopolymers could release the necessary amount of reducing equivalents in a longer time, resulting in lower hydrogen concentration (Aulenta et al., 2006). In this regard, PLA (polylactic acid) and sorbitol polylactate esters were successfully used to remediate groundwater sites polluted by perchloroethenes (Koenigsberg et al., 2006; Koenigsberg and Sandefur, 1999). More recently, attention has been paid to polyhydroxyalkanoates (PHAs), a family of microbial biopolyesters that can be produced with pure and mixed cultures using a wide range of organic waste streams as feedstock. For instance, PHAs production was obtained from municipal wastewaters (Morgan-Sagastume et al., 2014) and from agro-industrial by-products such as grape pomace (Martinez et al., 2022). As for bioremediation purposes, the commercial homopolymer poly-3-hydroxybutyrate (PHB) and PHAs heteropolymers (poly(3-hydroxybutyrate-co-3-hydrolyvalerate)), have been proven effective in enhancing the microbial reductive dechlorination of chlorinated aliphatic hydrocarbons in polluted groundwater in laboratory and pilot-scale tests (Baric et al., 2014; Pierro et al., 2017). Conversely, no information is available on the effect of PHAs on microbial

reductive dechlorination processes in marine environments, where the biodegradation of PHAs has been reported to be faster than in freshwater ecosystems (Kasuya et al., 1998; Mergaert et al., 1994) and may thus provide electron donors at higher concentrations to OHRB and their competitors. In addition, the anaerobic microbial community of marine sediments profoundly differs from freshwater environments. While in the latter MB and AB are the mostly active anaerobic microbes (Aulenta et al., 2008), in marine sediments the large amount of sulfates favors the growth of SRB, which are potentially stronger competitors of OHRB due their high affinity for hydrogen (Isa et al., 1986; Lovley et al., 1982; Lovley and Klug, 1983). Finally, limited information is available on the effect of PHAs composition on their biodegradation rate in marine environments. Indeed, it is not clear if the polymer composition can affect its hydrolysis rate, resulting in faster or slower degradation. For example, a faster hydrolysis has been reported for PHAs with higher content in the monomer 3-hydroxyvalerate in marine environment (Kaplan et al., 1994; Kasuya et al., 1998; Mergaert et al., 1994). However, other studies both in field (Doi et al., 1992; Volova et al., 2010) and in aquarium mimicking marine dynamic conditions (Thellen et al., 2008) did not show significant differences in the hydrolysis rate of films of heteropolymers with different compositions.

Experimental objectives of this study were: i) to assess the suitability of PHAs as long-term, slow releasing electron donors to stimulate the microbial reductive dechlorination of PCBs in marine sediments; ii) to evaluate the effects of the supplemented PHAs on the main anaerobic competing metabolisms of dehalorespiration (sulfate reduction, methanogenesis); and iii) to identify the influence of the polymer composition on their stimulation effects. To this aim, we investigated the effects of two PHAs with different composition (ratio of 3-hydroxybutyrate to 3-hydroxyvalerate 75:25 and 88:12 mol %, respectively), and of their main monomer 3-hydroxybutyrate as a rapidly fermentable control, on the reductive dechlorination activities of a PCBs-dechlorinating marine microbial culture inoculated in sediment microcosms mimicking the biogeochemical conditions of the marine environment. Specifically, microcosms were set up using sediments and waters from two different and representative Italian coastal sites in the Northwestern Adriatic Sea and in the Ionian Sea, *i.e.* two shallow basins within the Mediterranean Sea, highly anthropized and bordered by several urban areas and large industrial sites. Chosen locations were, respectively, (i) a salt marsh located in Ravenna (Pialassa Baiona), previously reported as presenting certain level of PCBs contamination (9-634 ug/kg of sediment) (Guerra et al., 2014) and influenced by high freshwater inputs from the Po river (Ponti and Airoldi, 2009), draining a heavily anthropized and extensive cultivated inland, and (ii) a semi enclosed lagoon in Taranto (Mar

Piccolo) with scarce water circulation that encourages organic matter sedimentation and accumulation of pollutants, *i.e.* organic compounds and heavy metals deriving from the high urbanization and the massive industrialization of the surrounding area (Cardellicchio et al., 2016). Such approach allowed to gain insights into the impact of the sediments' environmental history (*i.e.* present and past contamination events, which shaped the current chemical and biochemical pattern of the sediment, as well as its resident microbial community composition) on the efficacy of proposed bioaugmentation/biostimulation strategies for bioremediation.

3.2 Material and methods

3.2.1 Microcosms preparation, sampling and maintenance

Sediments were collected in the Mar Piccolo, Taranto, Italy (T-sediments) and in Piallassa della Baiona, Ravenna, Italy (R-sediments). Main chemical-physical parameters of the two sediments are reported in supplementary Tables S1-S2, as collection of the recent data available in the literature (from 2010 on). Microcosms were prepared in 100 mL glass serum bottles with 70 mL of sediment slurry (20% w/v of sediment and overlaying water) under anaerobic conditions (nitrogen gas in the headspace) and sealed with butyl rubber stopper and aluminum crimp. Under stirring and nitrogen flow, the anaerobic slurry was spiked with a 20'000 $mg \cdot L^{-1}$ stock solution of Aroclor 1254 in acetone to a final PCBs concentration of 100 $mg \cdot kg_{dry\ sediment}^{-1}$ and inoculated (5% v/v) with a previously obtained marine culture enriched in OHRB able to reductively dechlorinate PCBs (Nuzzo et al., 2017). Microcosms were then amended with one of the following organic electron donors (final concentration 20 mM): 3-hydroxybutyric acid (3HB) (from a 2.3 M stock solution in sterile distilled water), poly-3-hydroxybutyrate-co-3-hydroxyvalerate having a 3-hydroxybutyrate:3-hydroxyvalerate molar ratio 75:25 (PHBHV75) and poly-3-hydroxybutyrate-co-3-hydroxyvalerate having a 3-hydroxybutyrate:3-hydroxyvalerate molar ratio 88:12 (PHBHV88) (both added as powder). Microcosms inoculated with the dechlorinating culture were set up as controls (CTR). Microcosms were incubated statically in the dark at 30°C for 89 days. Periodic sampling (after 0, 30, 61, 75 and 89 days of incubation) was performed to analyze the volume and the composition of the head-space gas, the concentration of SO_4^{2-} in the water phase and the concentration of PCBs in the sediment. Each electron donor was supplied at the beginning of the incubation (day 0) and then monthly (*i.e.*, on days 30 and 61), since 1 month was the estimated time required to completely ferment the added PHAs, as observed in the preliminary test (Supplementary Figure S1). In addition,

consumed SO_4^{2-} were replenished periodically to maintain microcosms under actual site biogeochemical conditions, avoiding the alteration of the natural competition for electron donors between different terminal-electron accepting processes. In particular, sulfates were replenished by adding a 2.1 M stock solution of Na_2SO_4, on days 30, 61 and 75.

3.2.2 Preliminary test to estimate the time required to ferment the PHAs

The CO_2 production was identified as key parameter to evaluate the fermentation activities stimulated by the PHAs. To do so, lab-scale microcosms were set-up as described in the previous section. The stimulation effect of the PHAs was compared to microcosms with no amendments, labeled as controls. PHAs were added to the microcosms at the beginning of the experiment. Head-space gas was measured to monitor the CO_2 production. PHAs were considered to be completely degraded when the carbon dioxide production rate became equal to the one of the unamended control (Supplementary Figure S1) (Harrison et al., 2018).

3.2.3 Extraction and analysis of PCBs

PCBs in the sediment were extracted following a modified method from Rosato *et al.* (2020). Batch extraction was performed overnight at 30°C and 150 rpm from 1 mL of sediment slurry, with 3 mL of a hexane:acetone (9:1) mixture and octachloronaphtalene (OCN) (0.04 $mg \cdot L^{-1}$) as internal standard. The recovered organic phase was filtered on an Extrabond® Silica column (Scharlab, Barcelona, Spain) and added with 10 mg of elemental copper (Sigma Aldrich, St. Luis, Missouri, USA) as described in (Riis and Babel, 1999). An aliquot of the sample was placed in 1.5 mL vials for gas-chromatography (GC) equipped with Teflon coated screw caps (LLG-Labware, Meckenheim, Germany). The qualitative and quantitative analysis of the extracted PCBs was performed with a gas chromatograph (6890 series II) equipped with a HP-5 capillary column (30 m by 0.25 mm), a ^{63}Ni electron capture detector (µECD) and a 6890 series II automatic sampler (Agilent Technologies, Santa Clara, CA, USA). The column was operated at the following conditions: initial temperature 60°C; isothermal for 1 min; initial temperature rate 40°C/min; final temperature 140°C; isothermal for 2 min; initial temperature rate 1.5°C/min; final temperature 185°C; initial temperature rate 4.5°C/min; final temperature 275°C; isothermal for 5 min; injector (splitless mode), 250°C; detector ECD, 320°C; carrier gas flow rate (N_2) 1.5 mL/min; sample volume 1 µl. Aroclor PCBs, injected in the presence of OCN, were identified as described in Fava *et al.* (2003) by matching the detected peaks with the chromatographic profiles of the standard PCBs mixtures

Aroclor 1254 and Aroclor 1242 previously characterized (Frame et al., 1996) and comparing the retention time (relative to OCN) of each peak with those of PCBs of the same standard Aroclors analyzed under identical conditions. Quantitative analysis of the freshly spiked PCBs and their possible dechlorination products was performed by using the GC-ECD response factor of each target PCB congener or group of co-eluting congeners obtained from six-points calibration curves (0.5-50 $mg \cdot L^{-1}$) of Aroclors 1254 and 1242 and the weight percentage of each congener occurring in the same Aroclors reported elsewhere (Frame, 1997). PCBs concentrations were expressed as μmol of $PCBs \cdot kg_{dry\ sediment}^{-1}$. The chlorination degree was calculated as average number of chlorines per biphenyl molecule, as follows,

(**1**) $$Chlorination\ degree = \frac{\mu mol\ of\ organic\ chlorine}{\mu mol\ of\ total\ PCBs} = \frac{\sum C_i \times n_i}{\sum C_i}$$

where C_i is the molar concentration of each detected PCB congener ($\mu mol \cdot kg_{dry\ sediment}^{-1}$) and n_i is the number of its Cl substituents.

3.2.4 Analysis of sulfates, head-space gas and 3HB

Gas production in the microcosms was measured with an airtight syringe while its composition in CH_4, CO_2, N_2 and O_2 was analysed with a μGC (model 3000 A – Agilent Technologies, Milano, Italy) under the following conditions: injector temperature 90 °C; column temperature 60 °C; sampling time 20 s; injection time 50 ms; column pressure 25 psi; run time is 45 s and the carrier gas was nitrogen. The concentration of SO_4^{2-} in the water phase of the sediment slurry was determined using a Dionex ICS-1000 ion chromatograph equipped with an IonPac AS14 4 mm × 250 mm column, a conductivity detector combined to an AERS-500 suppressor system (Dionex, Sunnyvale, CA, USA). Quantitative analysis were performed by using the conductivity detector response factor obtained from a five points calibration curve (0.5-50 $mg \cdot L^{-1}$) of Na_2SO_4. 3HB was determined by HPLC-RID equipped with a Varian Hi-Plex H column (300 x 7.7 mm), under the following conditions: mobile phase, sulfuric acid 5 mM; flow rate, 0.6 mL/min; operating temperature, 65°C.

3.2.5 Electron and mass balances

The electrons equivalents supplied by each electron donor were calculated considering the moles of electron donor supplemented and its composition (i.e., the molar ratio of the monomeric units present in the two PHBHV polymers) and the stoichiometry of the chemical equations reported below (eq. 2, 3 and

4), assuming the complete oxidation of electron donors to CO_2 by fermenting communities including short-chain fatty acids oxidizing syntrophic bacteria (Leeson et al., 2004):

(2) 3-hydroxybutyric acid $C_4H_8O_3 + 5\,H_2O \rightarrow 4\,CO_2 + 9\,H_2$

(3) 3-hydroxyvaleric acid $C_5H_{10}O_3 + 7\,H_2O \rightarrow 5\,CO_2 + 12\,H_2$

(4) Hydrogen $H_2 \rightarrow 2\,H^+ + 2\,e^-$

The moles of electrons consumed by each metabolism were calculated considering the moles of electron acceptor reduced (i.e., moles of SO_4^{2-} reduced to H_2S for SRB; moles of organic Cl removed from the PCBs mixture for OHRB) or of reduction product generated (i.e., moles of CH_4 produced from CO_2 reduction for MB), and the corresponding electrons required for the reduction of one mole of electron acceptor (8 electrons for SO_4^{2-} reduction, 2 electrons for PCBs reduction and 8 electrons for methanogenesis). It has to be considered that PHAs are not directly used as reducing agents, but they are initially hydrolyzed and subsequently fermented to acetate and hydrogen, which act as the main electron donors for anaerobic respiring metabolisms (Amanat et al., 2021; Aulenta et al., 2008). The two main pathways, using H_2 or acetate, supply the same reducing power. In particular, CH_4 can be produced: i) by acetoclastic methanogens, which directly convert acetate to CH_4 and CO_2 (eq. 5); ii) via syntrophic acetate oxidation to CO_2 and H_2 (eq. 6), subsequently converted to methane (eq. 7) (Conrad, 2020). In both routes, one mole of methane is produced from one mole of acetate, which supplies 8 electrons.

(5) acetoclastic methanogenesis $C_2H_4O_2 \rightarrow CH_4 + CO_2$

(6) syntrophic acetate oxidation $C_2H_4O_2 + 2\,H_2O \rightarrow 4\,H_2 + 2\,CO_2$

(7) methanogenic conversion $CO_2 + 4\,H_2 \rightarrow CH_4 + 2\,H_2O$

Similarly, sulfate reducing bacteria can use hydrogen (eq. 8), as the product of syntrophic acetate oxidation (eq. 6), or directly acetate (eq. 9) as electron donors, requiring 8 electrons in the reduction process (Liamleam and Annachhatre, 2007).

(8) sulfate reduction via hydrogen $4\,H_2 + SO_4^{2-} + 2\,H^+ \rightarrow H_2S + 4\,H_2O$

(9) sulfate reduction via acetate $C_2H_4O_2 + SO_4^{2-} + 2\,H^+ \rightarrow H_2S + 2\,CO_2 + 2\,H_2O$

The stimulation yield (%) was calculated as the ratio between the moles of electrons consumed by each metabolism and the moles of electrons provided by the electron donor, multiplied times 100. It has to be noted that reducing equivalents can accumulate in the form of acetate, not being furtherly metabolized by anaerobic respiring bacteria (Aulenta et al., 2008; Liamleam and Annachhatre, 2007).

3.2.6 Chemicals

Aroclor 1242, Aroclor 1254 and octachloronaphtalene were provided by Ultra-Scientific. Inorganic ions for IC analysis, 3-hydroxybutyric acid and poly(3-hydroxybutyrate-*co*-3-hydroxyvalerate) with 25 mol% 3 HV units (PHBHV75, powder, custom grade) and with 12 mol% 3 HV units (PHBHV88, powder, custom grade) were supplied by Sigma Aldrich. Acetone and hexane (both for pesticide analysis in capillary column GC systems) as well as the ultra-resi analyzed water for ion chromatography were supplied by Mallinckrodt-Baker.

3.2.7 Bacterial DNA extraction, 16S rRNA gene amplification and sequencing

Approximately 300 mg of sediment samples taken from the inoculated sediment at the beginning of the experiment (0 day) and from all the microcosms at the end of the experiment (89 days) were used for characterization of the inhabiting microbial community. Samples of the marine culture previously enriched with OHRB able to reductively dechlorinate PCBs used as inoculum were included. DNA extraction was performed using DNeasy PowerSoil Kit (Qiagen, Hilden, Germany) following the manufacturer's instructions. Extracted DNA samples were quantified using Qubit 3.0 fluorimeter (Invitrogen, Waltham, MA, USA) and stored at –20 °C until further processing. The V3-V4 hypervariable region of the 16S rRNA gene was PCR amplified in 50 uL final volume containing 25 ng of microbial DNA, 2X KAPA HiFi HotStart ReadyMix (Roche, Basel, Switzerland), and 200 nmol/L of microbial 341F and 785R primers carrying Illumina overhang adapter sequences (Klindworth et al., 2013). Thermal cycle was set as follows: 3 min at 95°C, 25 cycles of 30 s at 95°C, 30 s at 55°C, and 30 s at 72°C, and a final 5-min step at 72°C (Palladino et al., 2022). PCR products were purified using Agencourt AMPure XP magnetic beads (Beckman Coulter, Brea, CA, United States). Indexed libraries were prepared by limited-cycle PCR with Nextera technology and cleaned-up with the same magnetic beads protocol. Libraries were then normalized to 4 nM and pooled, prior to denaturation with 0.2 N NaOH. Sequencing was performed on Illumina MiSeq platform using a 2 × 250 bp paired-end protocol, following the manufacturer's instructions (Illumina, San Diego, CA, United States).

3.2.8 Bioinformatics and statistics

Paired-end sequenced reads were merged using the VSEARCH algorithm (v2.15.2) (Rognes et al., 2016) and analyzed using QIIME2 (version 2022.8) (Bolyen et al., 2019). Briefly, the DADA2 (Divisive Amplicon Denoising Algorithm 2) (Hall and Beiko, 2018) plugin was used to remove noise, chimeras, and to generate Amplicon Sequence Variants (ASVs). ASVs were taxonomically assigned using the SILVA reference database version 138 (Yilmaz et al., 2014). Normalization by rarefaction to the number of sequences in the sample with the least coverage was performed. Microbial community relative abundance profiles at different phylogenetic level were obtained. Statistical analysis was performed using the R statistical software (www.r-project.org), v. 4.0.4. Two different metrics were used to evaluate alpha diversity: Faith's Phylogenetic Diversity (PD) (Haard et al., 1975) and the Simpson diversity index. Weighted and unweighted Unifrac distances were computed to explore samples beta-diversity and plotted as Principal Coordinates Analyses (PCoA) using the R package "vegan". Data separation on PCoA plots was tested using a permutation test with pseudo-F ratios (function "adonis2" in the vegan package). T-test was used to assess significance of differences in microbial community profiles among groups of samples. Sequence reads were deposited in the National Center for Biotechnology Information Sequence Read Archive (NCBI SRA; BioProject ID PRJ PRJNA884891; PRJNA926484).

3.3 Results

3.3.1 Methanogenic activities

Methanogenic activity is reported in Fig. 1 as cumulative amount of methane (mM) produced over time. In the control microcosms (CTR), the final CH_4 concentrations were similar for both the sediments, with values of 0.29 ± 0.06 mM and 0.29 ± 0.14 mM in the Pialassa della Baiona (Ravenna) and Mar Piccolo (Taranto) sediments, respectively. A remarkably higher CH_4 production was observed when stimulating both R-sediments and T-sediments with 3HB (53.1 ± 4.5 and 45.8 ± 11.6 mM, respectively). No methanogenic activities were observed in the cultures amended with 3HB after day 75 (two weeks later having replenished the amendments) indicating a complete depletion of the fatty acid during the first two weeks of incubation after replenishment of 3HB (day 75). In the microcosms amended with PHAs, a lower stimulation of the methanogenic activity was detected compared to those amended with the monomer. In R-sediments, cumulative concentrations at the end of the incubation obtained with the two PHAs were not significantly different (p-value = 0.6), being 13.9 ± 3.5 mM and 16.4 ± 2.2 mM for PHBHV88 and PHBHV75. As for the T-sediments, methane cumulative concentration for PHBHV88

was 6.4 ± 1.1 mM, almost 50 % less than with PHBHV75, 13.0 ± 3.6 mM. Furthermore, differently from 3HB, amending with PHAs led to a more constant CH_4 production during the third month of incubation suggesting a slower fermentation rate of the amendments.

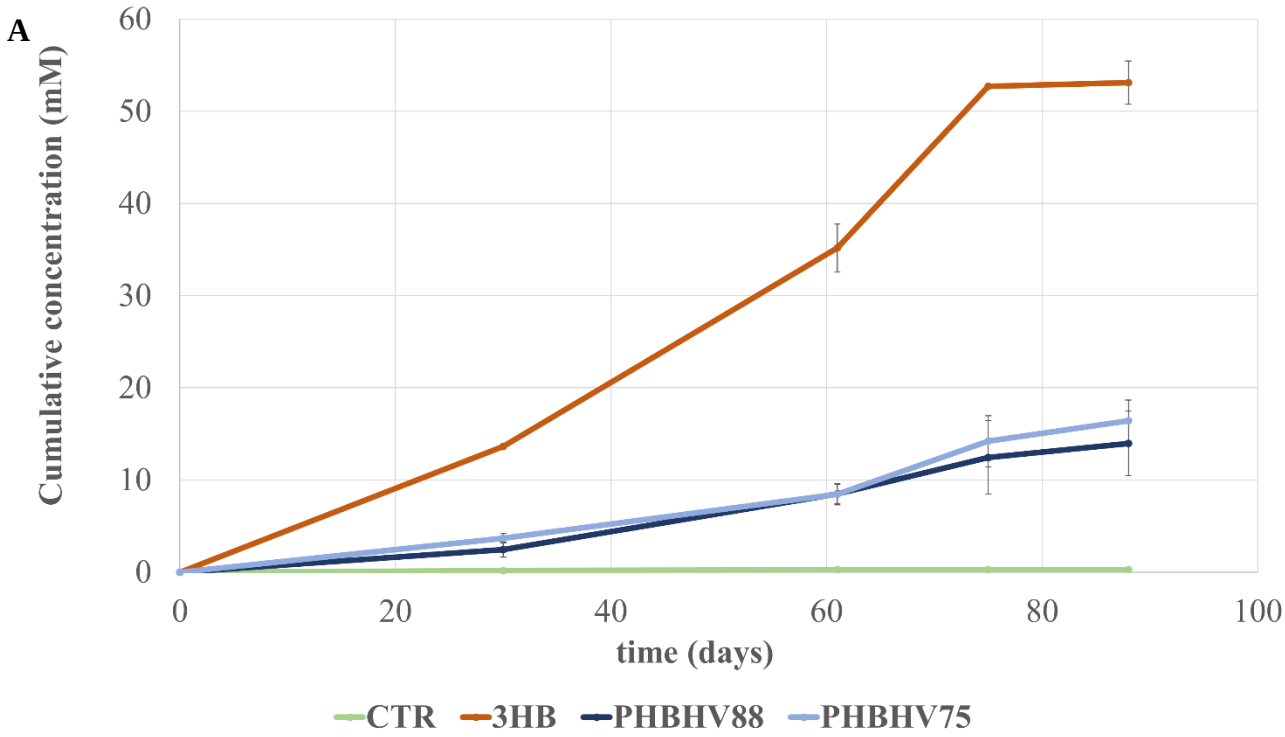

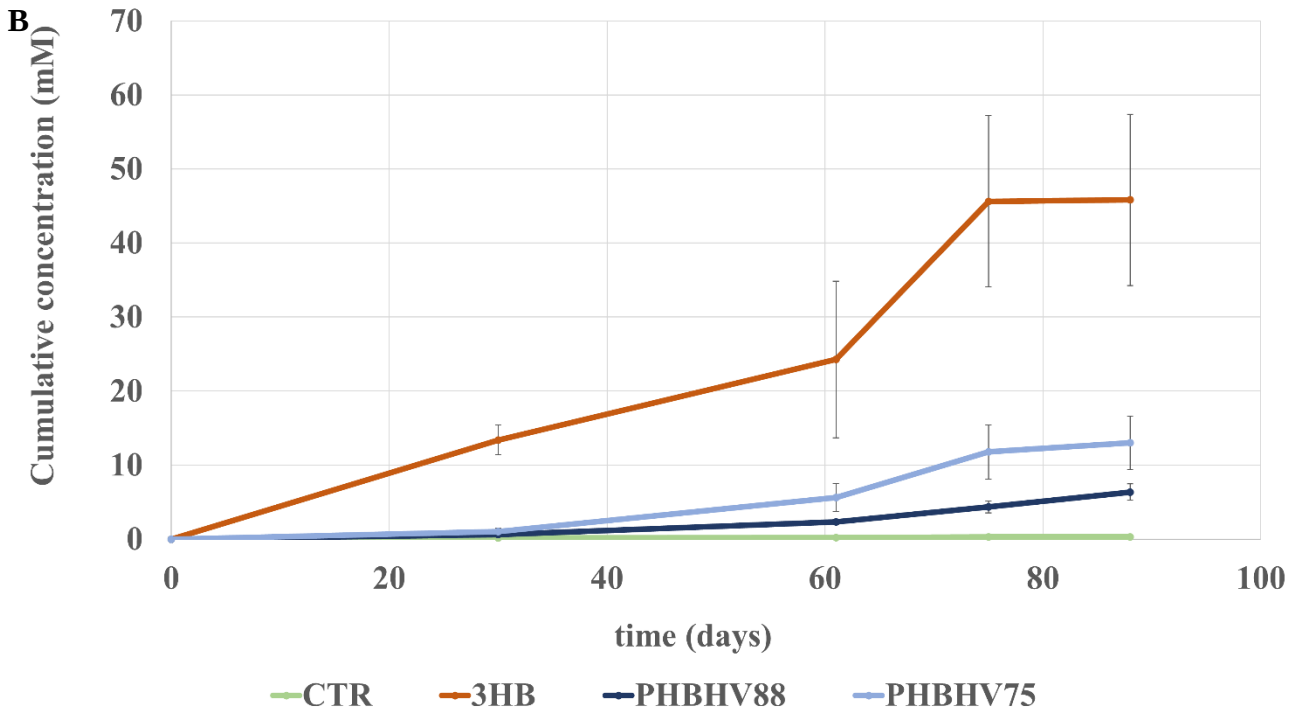

Figure 1 *Cumulative methane concentration measured in the headspace gas of the microcosms with sediments collected in Pialassa della Baiona, Ravenna (R-sediments) (A), and in Mar Piccolo, Taranto (T-sediments) (B).*

3.3.2 Sulfate reduction activities

Sulfate depletion was detected in the control microcosms only during the first month with an average depletion rate of 0.046 ± 0.001 $g \cdot L^{-1} \cdot d^{-1}$ and 0.042 ± 0.001 $g \cdot L^{-1} \cdot d^{-1}$ in R-sediments and T-sediments, respectively (Supplementary Figure S2). In the following months, the sulfate reduction activity was negligible in the absence of external electron donors. In parallel, a complete removal of sulfates was observed in all the amended microcosms after 30 days (Supplementary Figure S2), corresponding to an apparent average depletion rate of at least 0.099 $g \cdot L^{-1} \cdot d^{-}1$ in R-sediments and 0.11 $g \cdot L^{-1} \cdot d^{-1}$ in T-sediments. The complete consumption of sulfate (replenished to its original concentration at day 30, along with the electron donors) within one month of incubation in all the amended microcosms was confirmed at day 61 as well. The sulfate depletion rate in the microcosms amended with the different electron donors was thus assessed more accurately during the third month of experiment, when microcosms were sampled both two weeks (75 days) and one month (89 days) after sulfate replenishment to its original concentration at day 61 (along with electron donors). During the interval of time 61-75 days, 3HB remarkably primed sulfate reduction in both the sediments, showing depletion rates over 0.19

$g \cdot L^{-1} \cdot d^{-1}$ (Fig. 2). After further replenishment of the original sulfate concentration (day 75), negligible sulfate removal was detected in the period 75-89 days. Conversely, in the R-sediments, both PHAs constantly stimulated sulfate reduction to a lesser extent than 3HB throughout the whole month, with values around 0.12 $g \cdot L^{-1} \cdot d^{-1}$ (Fig. 2). In the T-sediments, PHBHV88 stimulated sulfate reduction similarly to R-sediments. Instead, PHBHV75 showed a stimulating effect that resembled the one obtained using the monomer. Removal rates were 0.17 ± 0.01 $g \cdot L^{-1} \cdot d^{-1}$ during the first half of the month and 0.03 ± 0.01 $g \cdot L^{-1} \cdot d^{-1}$ during the second half.

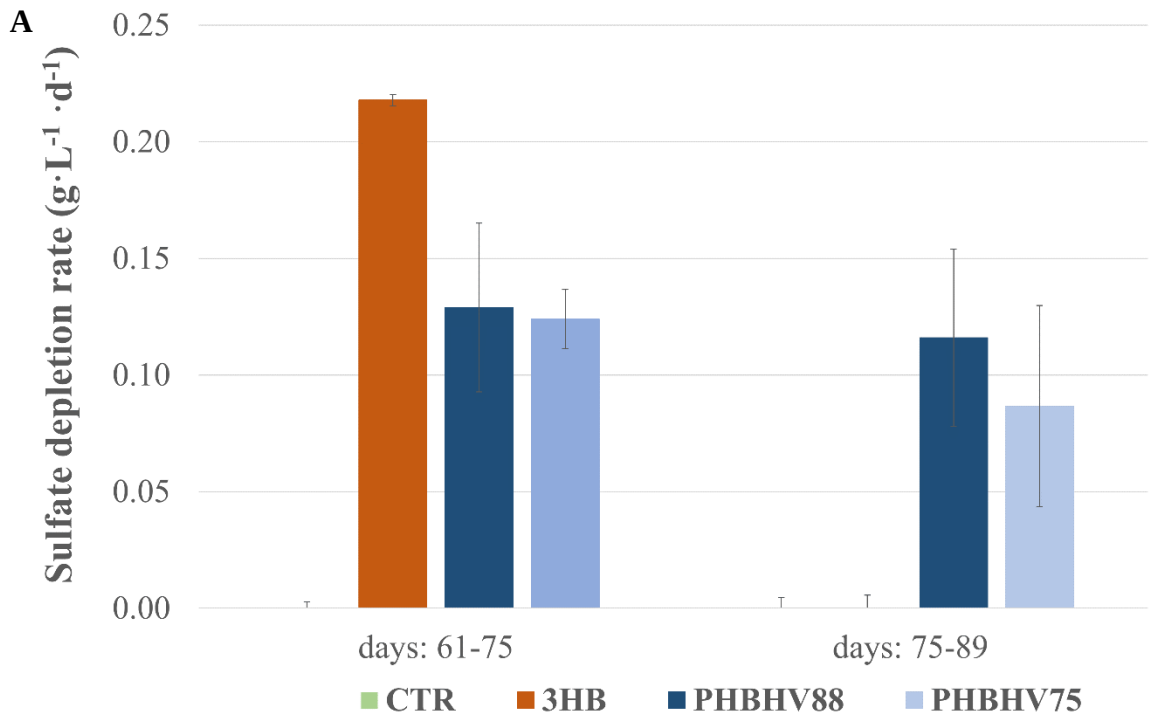

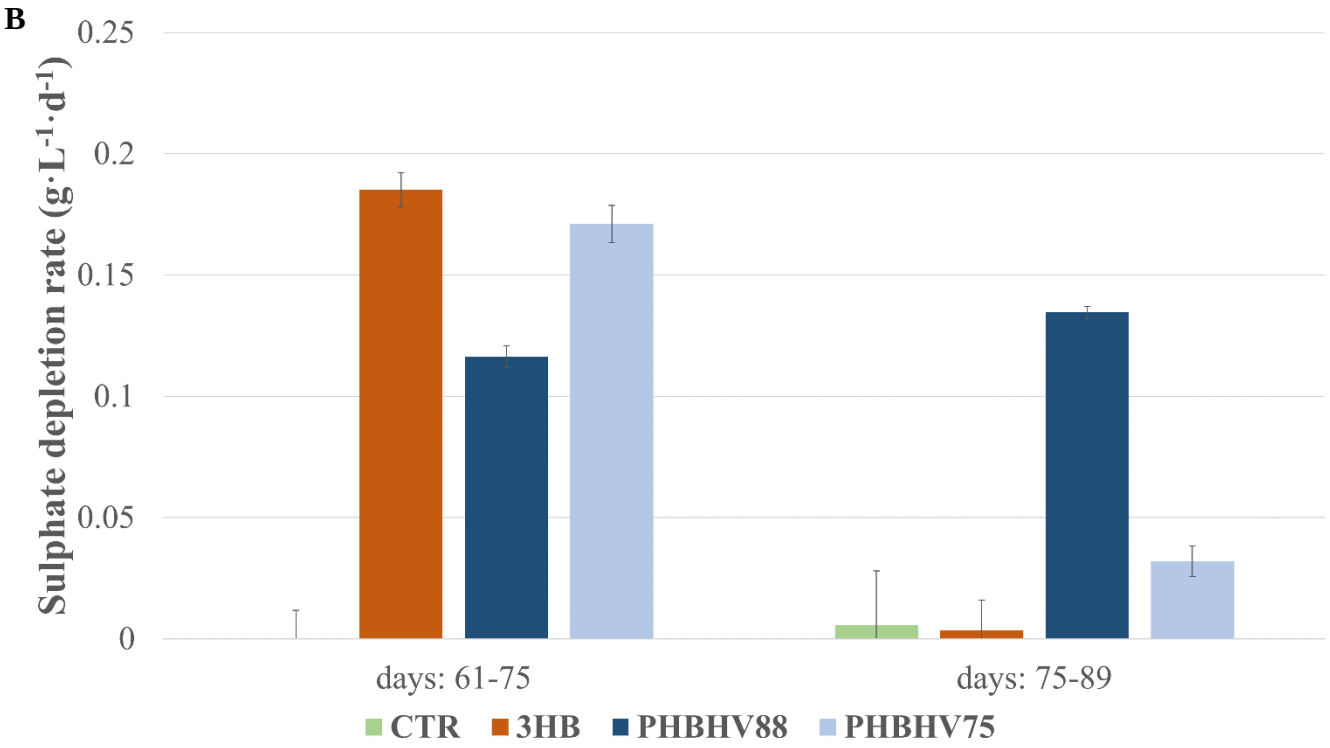

Figure 2 *Sulfate depletion rate detected in the first two weeks (days 61-75) and in the following two weeks (days 75-89) of the third month of experiment (days 61-89), of microcosms with sediments collected in Pialassa della Baiona, Ravenna (R-sediments) (A) and in Mar Piccolo, Taranto (T-sediments) (B). Sulfate consumed during the first two weeks was replenished to its original concentration on day 75.*

3.3.3 PCBs reductive dechlorination

Reductive dechlorination of the PCBs mixture in the control microcosms took place to a different extent in the two sediments. In R-sediments, at the end of the incubation (day 89) hexa- and penta-chlorinated congeners were depleted of 43 ± 11 and 49 ± 2 %, respectively, with a consequent increase of tetra-, tri- and di-chlorinated congeners (Fig. 3A). While being negligible during the first month of incubation (0.9 ± 0.3 % reduction of the chlorination degree of the PCBs mixture on day 30), PCBs dechlorination started from month 2, progressively leading to a 14.4 ± 1.7 % reduction of the chlorination degree of the PCBs mixture at the end of the incubation (Fig. 4A). Instead, in T-sediments hexa- and penta-chlorinated congeners were reduced of only 8 ± 8 and 21 ± 9 % (Fig. 3B). No signs of bioconversion were detected during the first 30 days of incubation and the chlorination degree was reduced only of 4.6 ± 1.8 % after 3 months (Fig. 4B).

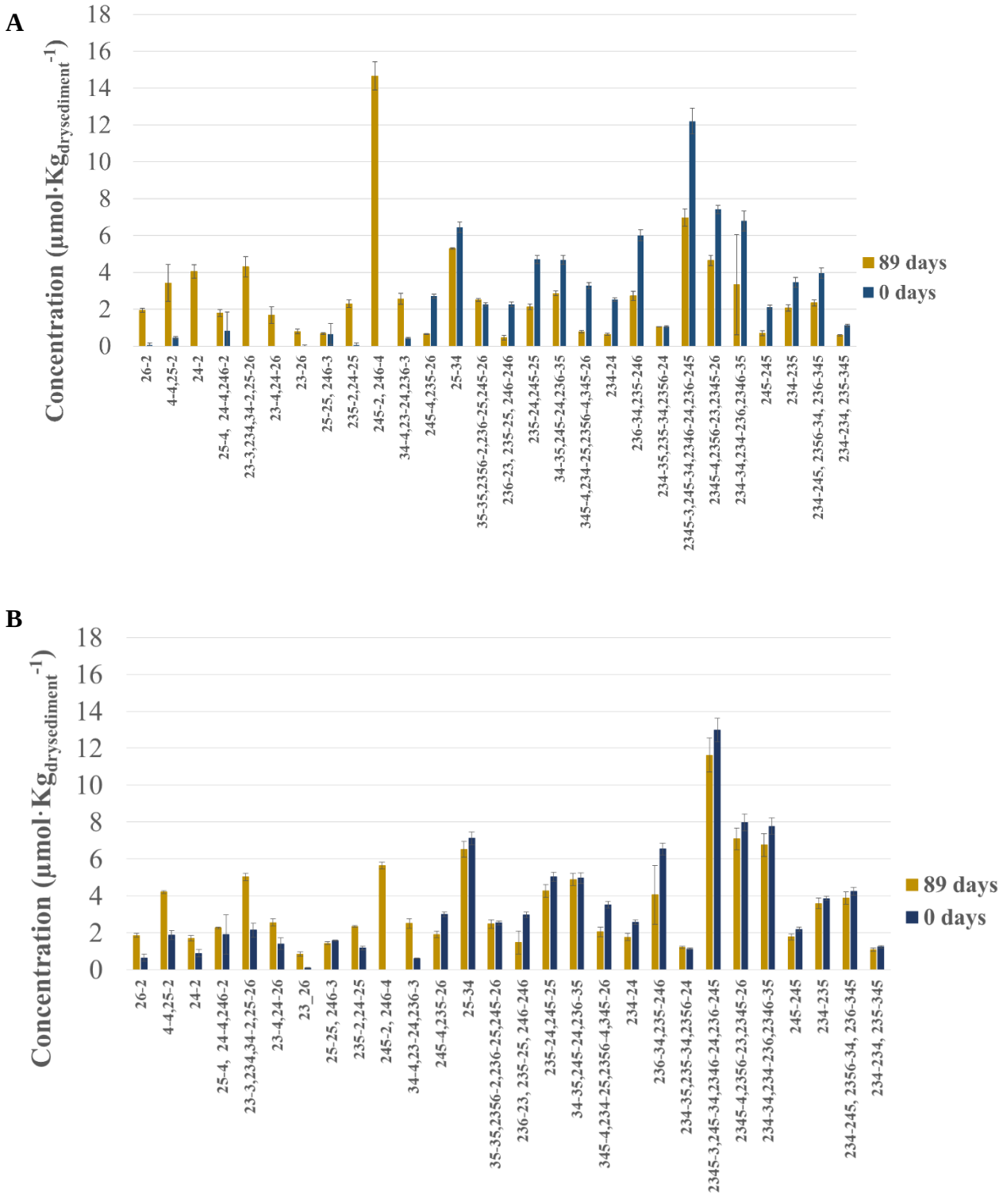

Figure 3 *Concentration of PCB congeners detected in the control microcosms (CTR) at the beginning and at the end of the incubation (day 89) of microcosms with sediments collected in Pialassa della Baiona, Ravenna (R-sediments) (A) and in Mar Piccolo, Taranto (T-sediments) (B).*

As for the amended microcosms of the R-sediments, the supplementation of 3HB, PHBHV75 and PHBHV88 stimulated a faster onset of PCBs dechlorination, leading to a significantly higher decrease of the chlorination degree after 30 days of incubation with respect to the control (7.4 ± 0.6 %, 5.3 ± 1.7 % and 7.0 ± 0.5 %, in the microcosms supplemented with 3HB, PHBHV88 and PHBHV75, respectively (3HB, p-value = 0.0005; PHBHV75, p-value = 0.0002; PHBHV88, p-value = 0.04) (Fig. 4A). However, at the end of the incubation (89 days) the reduction of the chlorination degree did not significantly differ between amended microcosms and control (Fig. 4A). Conversely, in the T-sediments, biostimulating via PHAs exerted a negative influence on the inoculum, since after 2 months no average reduction of the chlorination degree was observed in microcosms biostimulated with PHBHV75 and 3HB. After 89 days, the chlorination degree was reduced of 2.8 ± 3.7 %, 0.9 ± 1.4 % and 2.7 ± 0.3 % with respect to control microcosms, when biostimulating with 3HB, PHBHV75 and PHBHV88, respectively (not significant).

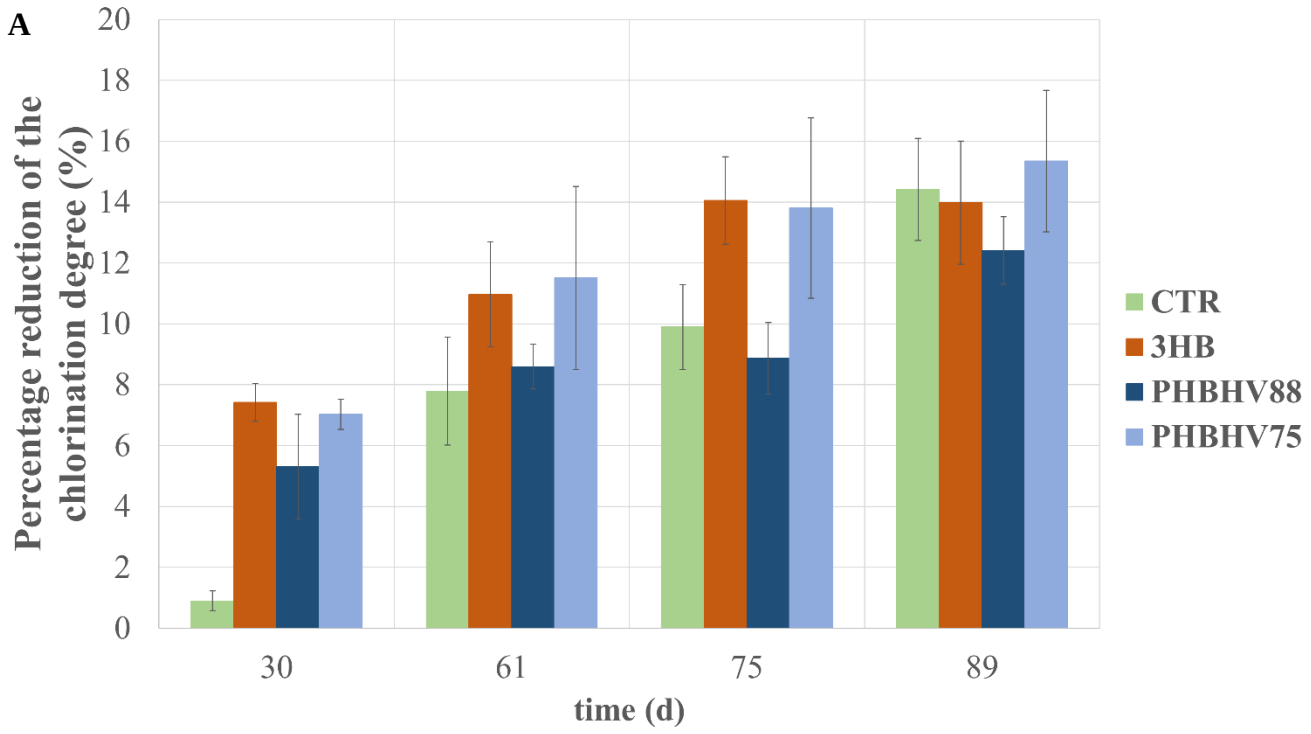

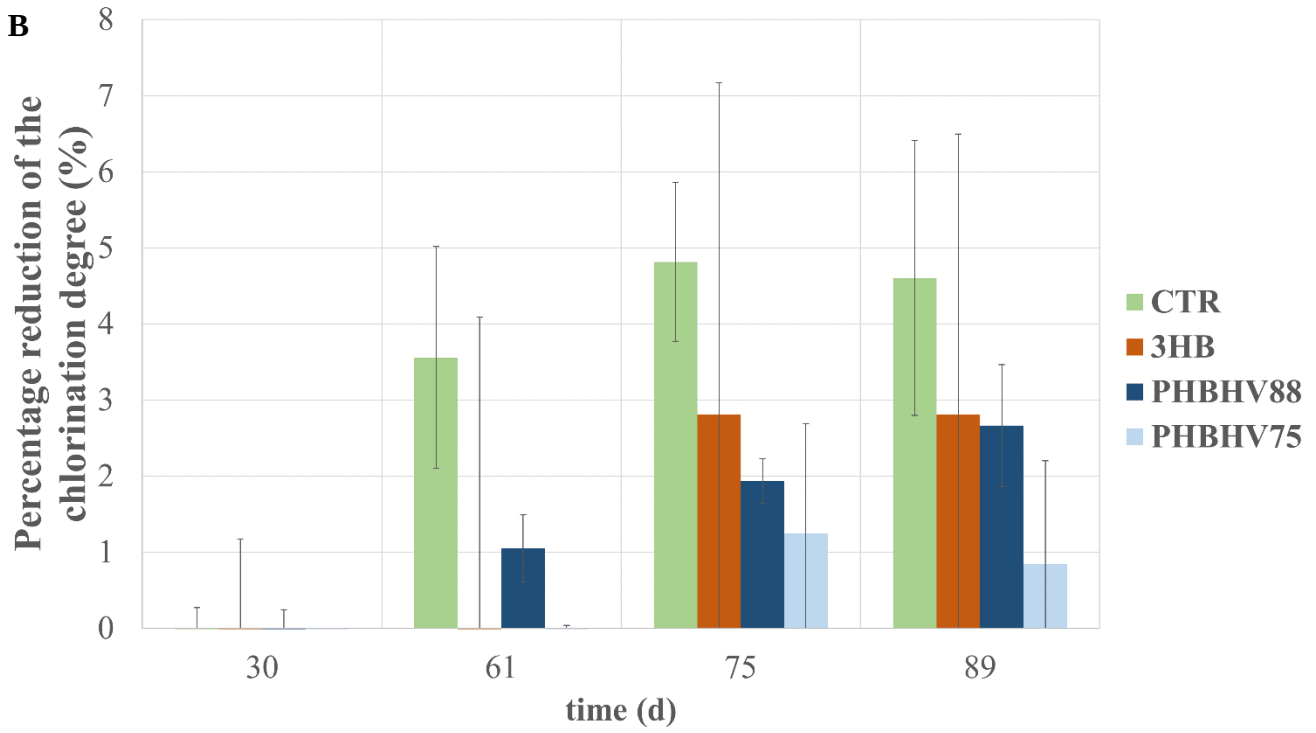

Figure 4 *Percentage reduction of the chlorination degree of the PCBs mixture during incubation of microcosms with sediments collected in Pialassa della Baiona, Ravenna (R-sediments) (A) and in Mar Piccolo, Taranto (T-sediments) (B).*

3.3.4 Electron balances and stimulation yield of the PHAs amended to the marine microbial community

To better understand and to compare the effects of electron donors on the different terminal electron accepting processes, the balance between the electrons supplied by each amendment and the electrons consumed by each metabolism was calculated. The electrons provided by the complete oxidation to CO_2 of the electron donors were calculated under the following assumptions: i) the monomer was depleted within two weeks; ii) the heteropolymers were depleted in one month, with a constant degradation rate. Regarding the monomer, the complete consumption within two weeks was supported by the absence of sulfate reduction and methanogenic activities in the interval 75-89 days, *i.e.* 15 days after the amendment with 3HB. To confirm the assumption, at the end of the experiment, 3HB was re-supplied to the microcosms and the concentration of 3HB in time was monitored, confirming its complete degradation within 8 days (Supplementary Figure S3). As for the polymers, the degradation time was estimated considering the results of the preliminary fermentation test (Supplementary Figure S1). Given the similar methanogenic and sulfate-reduction rates detected during the first 2 weeks (days 61-75) after PHAs

supplementation and the following 2 weeks (days 75-89), PHAs were assumed to be consumed constantly during the month, thus supplying half of the amended moles every two weeks. It should be noted that this assumption might be partially correct in the case of PHBHV75 amended to the Taranto sediment, since sulfate depletion rate was not constant throughout the third month of incubation. Stimulation yield for reductive dehalogenation were calculated only for Ravenna sediments, since the process was inhibited in Taranto sediment thus assuming that no reducing equivalent was delivered to OHRB. Subsequently, the stimulation yield for each metabolism was calculated considering the first 2 weeks after the supplementation of the amendments on day 61 (days 61-75) and the following 2 weeks (days 75-89).

The majority of electron equivalents was consumed through sulfate reduction, with no remarkable differences between the electron donors (Fig. 5). During the third month sulfate reduction processes consumed more than 50 and 44 % of the electrons provided by the amendments in the sediment of Ravenna and Taranto, respectively. Conversely, in R sediments the process of methanogenesis consumed a higher fraction of the electron equivalents provided by the monomer (31.0 ± 0.9%) compared to those provided by the polymers (13 ± 3 % and 9 ± 7 % of electron equivalents provided by PHBHV75 and PHBHV88, respectively). An analogue profile was observed in sediment from Taranto, since methanogenesis depleted the 16.0 ± 9 %, 8 ± 2 % and 5 ± 2 % of the equivalents supplied by 3HB, PHBHV75 and PHBHV88. Reductive dechlorination accounted for a negligible consumption of the reducing equivalents supplied by both the polymers and the monomer (0.01-0.02%).

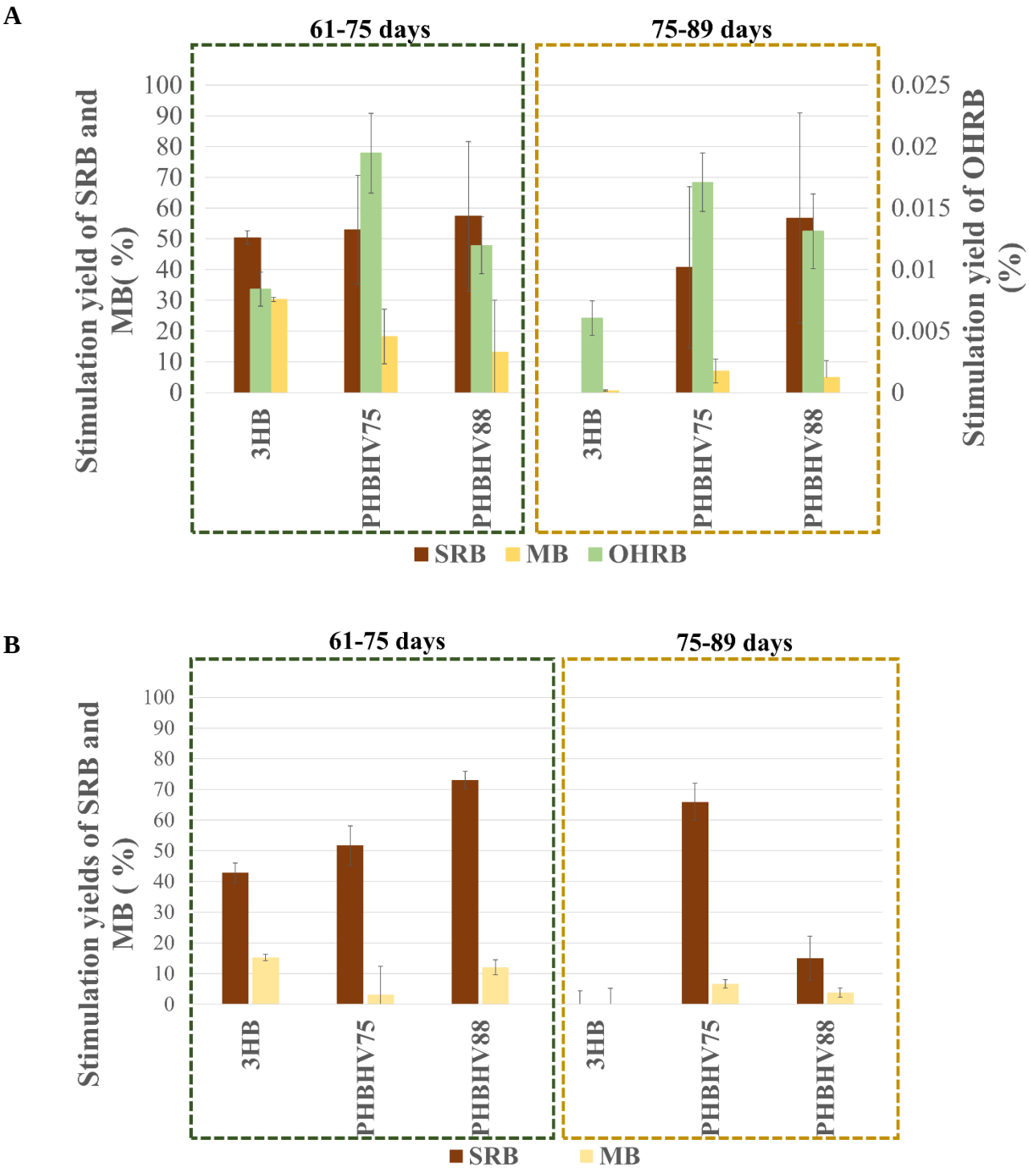

Figure 5 *Stimulation yields of SRB, MB and OHRB for each electron donor in the 15-day period immediately after replenishment of electron donors (61-75 days, green rectangle) and in the following one (75-89 days, yellow rectangle), of microcosms with sediments collected in Pialassa della Baiona, Ravenna (R-sediments) (A) and in Mar Piccolo, Taranto (T-sediments) (B).*

3.3.6 Microbial community characterization

The composition of the bacterial communities of the microbial culture used as inoculum, the inoculated sediment at the beginning of the experiment, and of all the microcosms at the end of the experiment (89 days), was analyzed by sequencing of the V3-V4 hypervariable region of the 16S rRNA gene. The sequencing yield per sample ranged between 90,038 and 153,802 high quality reads.

The microbial communities of unamended sediments after three months of incubation showed higher alpha diversity with respect to the microbial communities at day 0, in microcosms assembled using both Ravenna and Taranto sediments (t-test, p values 0.1 and 0.003 for Simpson and faith's PD indexes of R-sediments, 0.22 and 0.07 for Simpson and faith's PD indexes of T-sediments) (Fig. 6). Amendments tended to have a decreasing effect on the alpha diversity of the sediment community, especially for what concern heteropolymers in the Taranto sediments (t test, p values 0.009 and 0.03 for Simpson index and 0.5 and 0.5 for faith's PD index when amending respectively with PHBHV88 and PHBHV75) (Fig. 6). At the compositional level, the microbial community of unamended sediments (both at day 0 and day 89) clustered separately, along the first coordination axis, from all samples taken at day 89 from amended microcosms (Adonis test, p value = 0.001 using both weighted and unweighted Unifrac distances, Fig. 7), independently from the origins of the sediments (Ravenna or Taranto). Conversely, along the second coordination axis, which explain a smaller percentage of variation in the dataset with respect to the first axis, separation between sediments from Ravenna and Taranto is evident only on the PCoA plot based on unweighted Unifrac distances (Adonis test, p value = 0.001, Fig. 7A), hinting at a relevant impact of subdominant community members on the difference between the sediment's microbiomes from the two sites. On the contrary, the sediment microbial communities in samples belonging to different groups of treatment (controls, 3HB and polymers) cluster separately on the PCoA based on weighted Unifrac distances (Adonis test, p value = 0.001, Fig. 7B), with samples amended with monomer and polymers separating along the second coordination axis.

Family-level community profile showed that amending with 3HB and PHBHV resulted in a pervasive modification of the community composition (Fig. 8). Indeed, after 89 days of incubation with 3HB, the microbial community in R-sediments featured a significant dominance of *Dethiosulfatibacteraceae* (29 ± 7 %) with respect to day 0 (1.0 ± 0.8 %). On the other hand, the content of *Dethiosulfatibacteraceae* in T-sediments increased to a less extent (11 ± 5 %, with respect to 1.9 ± 0.5 % at day 0). T-sediments

amended with 3HB were characterized by the appearance of a relevant percentage of *Synergistaceae* (6 ± 3 %), with sequences mostly belonging to the genera *Thermovirga* (3 ± 2 %) and *Aminobacterium* (3 ± 1 %). R-sediments showed the same, but less evident, pattern with abundances equal to 3 ± 1 % for family of *Synergistaceae*, divided in *Thermovirga* (1.6 ± 0.8 %) and *Aminobacterium* (1.4 ± 0.1 %). Moreover, 3HB amended microcosms were the only ones in which sequences assigned to the methanogenic Archaea genus *Methanosaeta* were detectable (0.7 ± 0.6 % and 0.5 ± 0.9 % in R and T-sediments). For what concern both PHBHV75 and PHBHV88, at day 89 a microbial community significantly dominated by *Spirochaetaceae* (23 ± 5 % and 26 ± 5 % for PHBHV75 in R and T-sediments, 20 ± 12 % and 26 ± 1 % for PHBHV88 in R and T-sediments, compared to 0.6 ± 0.5 and 1.1 ± 0.9 at day 0 in R and T-sediments) was found. *Petrotogaceae* were enriched by all the amendments. Abundances in R-sediments were 0.6 ± 0.4 % for 3HB, 1.7 ± 0.7 % for PHBHV75 and 1.1 ± 0.1 % for PHBHV88, while abundances in T-sediments were 2 ± 1 % for 3HB, 5 ± 1% for PHBHV75 and 2.2 ± 0.2 % for PHBHV88, whereas no sequences assigned to *Petrotogaceae* were detected in the control even after 3 months of incubation. *Marinilabiliaceae* (all sequences assigned to uncultured bacteria) and *Williamwhitmaniaceae* (all sequences assigned to "Blvii28_wastewater-sludge_group"), which are families of the phylum Bacteroidetes, were initially present in the inoculated sediments at abundances < 0.2% and subsequently enriched in all the amended sediments with no remarkable growth in the control microcosms. Relative abundances of *Marinilabiliaceae* in R sediments reached up to 5 ± 1 % when amending with 3HB while not being detected in the control. As for T-sediments, percentages ranged from 5.2 ± 0.6 (PHBHV75) to 13 ± 1 % (3HB) compared to 2 ± 2 % of the control. Regarding *Williamwhitmaniaceae*, no sequences were detected in the controls. Percentages below 1.5 % were identified in R-sediments whereas in sediment of Mar Piccolo they grew up to 10 % (PHBHV75). Conversely, the control microcosms maintained family-level community structures similar to the ones of the inoculated sediments at day 0, without noticeable dominance, confirming the above mentioned increased alfa diversity. For instance, within the group of bacteria showing higher initial abundances, sequences assigned to *Anaerolineae* (uncultered), *Flavobacteriaceae* and *Sulfurovaceae* were identified. Regarding sequences assigned to uncultured members of *Anaerolineae,* larger amounts were detected in T-sediments (6 ± 1 %) compared to R-sediments (0.4 ± 0.7 %), which maintained similar percentages at the end of the incubation (5.7 ± 0.6 %, T-sediments; 3.0 ± 0.1 %, R-sediments). *Flavobacteriaceae* were more abundant in R-sediments (10 ± 1 %) compared to T-sediments (5 ± 2 %) at the beginning of the incubation and found at comparable values at the end of the experiment, being 6 ± 2 % and 4 ± 1 %. Lastly, *Sulfurovaceae* were present at similar relative percentages in both the sediments (< 6%),

maintaining comparable abundances after the incubation without amendments while being reduced below 2% in R-sediments and disappearing in T-sediments in all the stimulated microcosms.

For what concerns bacteria commonly associated to reductive dehalogenation, *Dehalococcoidaceae* were abundant in the inoculum (approximately 7 %) and present to a lower percentage in the inoculated sediments (0.8 ± 0.4 % and 0.8 ± 0.2 in R and T-sediments), coherently with the inoculum ratio. In microcosms with R-sediments, after 89 days sequences assigned to the inoculated *Dehalococcoidaceae* were maintained in the unamended control (0.9 ± 0.1 %), whereas relative abundances below 0.1 % were detected in amended microcosms. For T-sediments, the abundance of inoculated *Dehalococcoidaceae* decreased in the control (0.3 ± 0.3 %) and, even more strikingly, in the amended microcosms (<0.1%). Conversely, indigenous group *Dehalococcoidia* AB-539-J10 was identified at the beginning of the experiment in both R and T-sediments, with percentages of 0.5 ± 0.9 % and 4 ± 3 %, respectively. After 89 days, in control mesocosms the abundance of such indigenous group was maintained (0.4 ± 0.4 % and 3 ± 2 in R and T-sediments), whilst in the amended microcosms, relative abundances were <0.2 % and approximately 0.5% in R and T sediments, respectively.

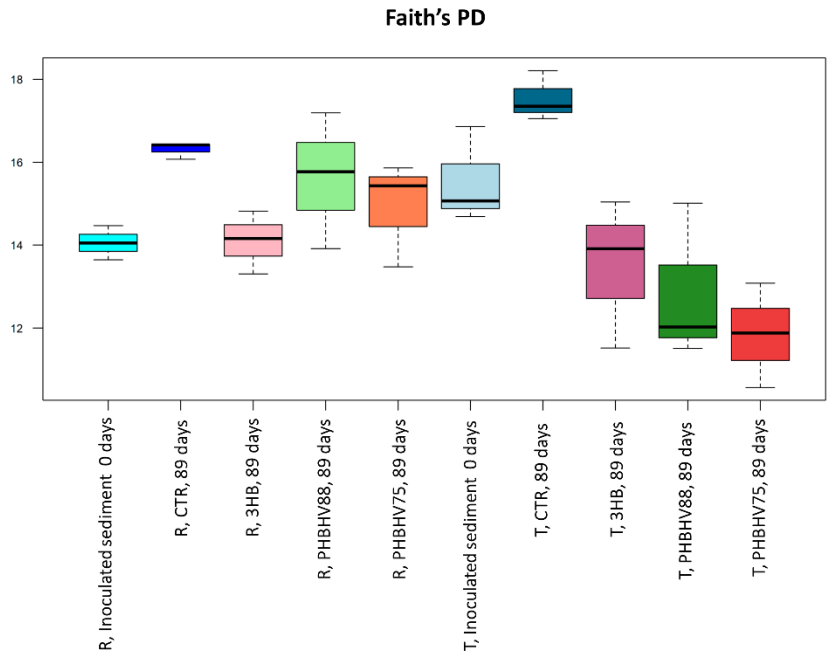

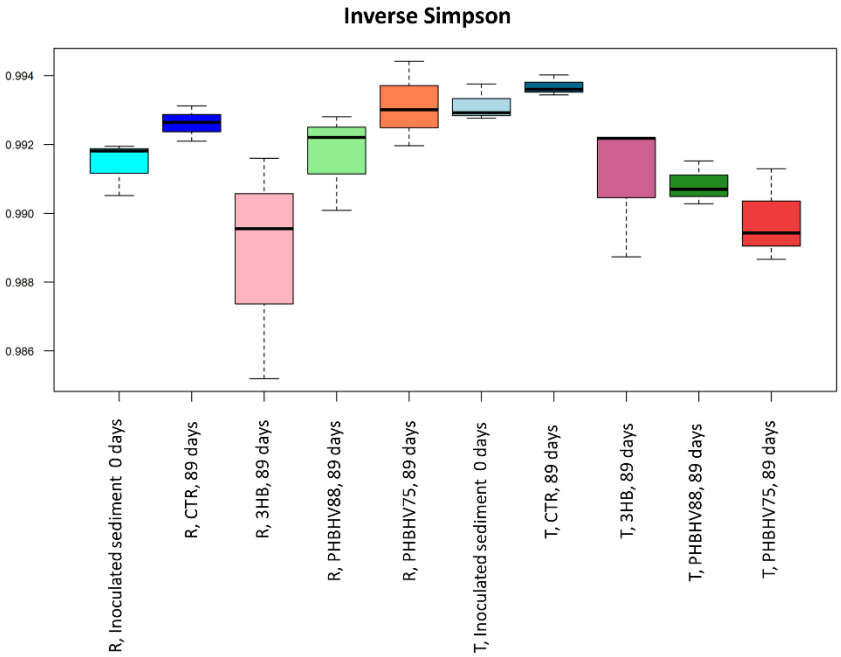

Figure 6 *Microbial community biodiversity of marine sediment in samples taken at the beginning (0 days) and at the end of the experiment (89 days). Boxplot representation of alpha diversity calculated using the phylogenetic Faith's PD index and Inverse Simpson index. Biodiversity significantly increases between R-sediments at 0 and 89 days without amendments, while decrease in T-sediments amended with PHBHV88 and PHBHV75 compared to those at the beginning (0 days) (t-test, p values<0.05).*

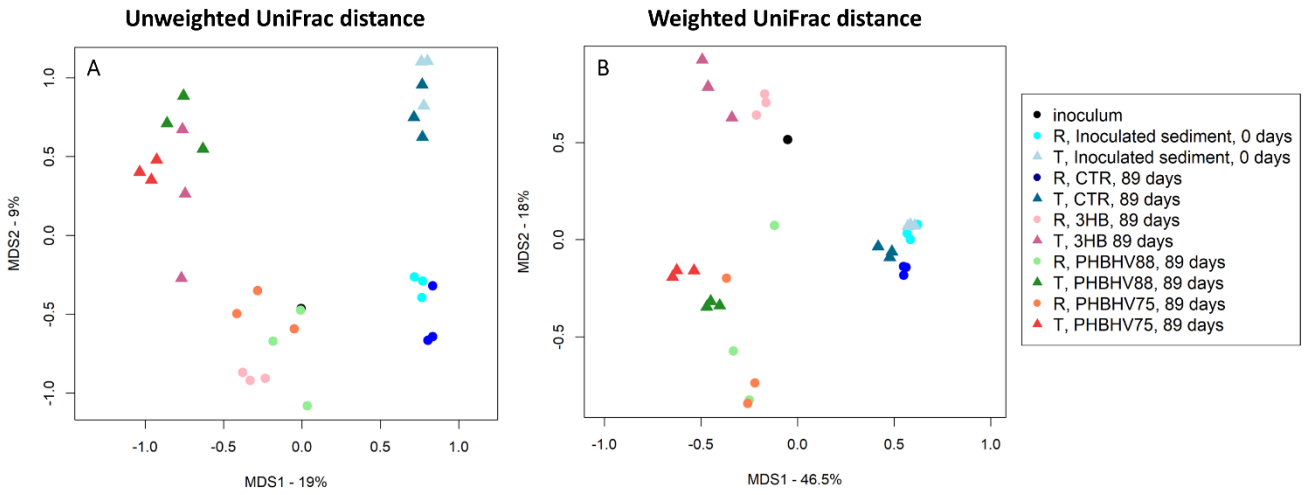

Figure *7 PCoA based on unweighted (left) and weighted (right) UniFrac distances of microbiota profiles of samples collected at the beginning (0 days) and at the end of the experiment (89 days). First and second coordination axes (MDS1 and MDS2) are plotted for each analysis. Percentages of variance in the dataset accounted for by MDS1 and MDS2 are reported.*

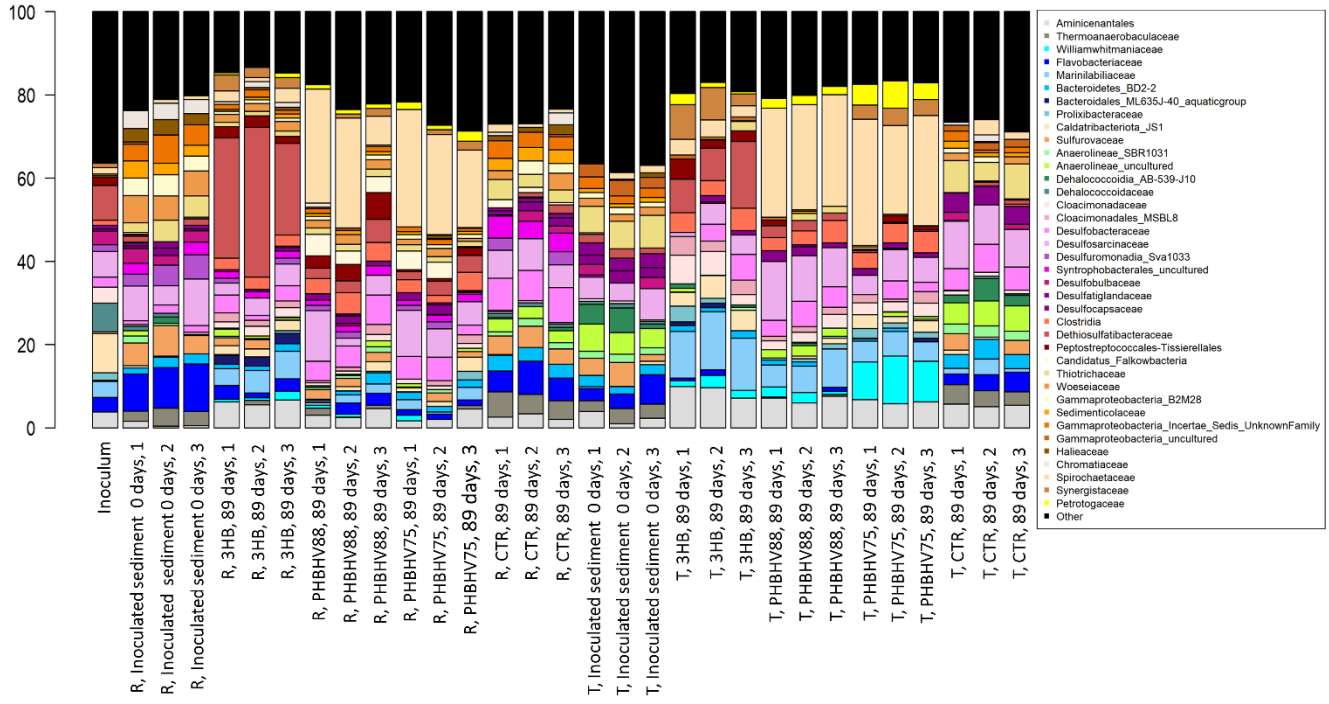

Figure 8 *Microbial community phylogenetic profiles at the family level of the inoculum, inoculated sediments from Ravenna (R) and Taranto (T) at the beginning of the experiment (0 day) and sediments from all the studied microcosms (R and T) at the end of the experiment (89 days). Bacterial families*

having relative abundance >2% in at least 1 sample are depicted. Color legend is shown in the right panel. Black color is used to indicate the percentage of "Other" reads, including unassigned sequences and families with a relative abundance which did not pass the mentioned threshold.

3.4 Discussion

Within the landscape of contaminated sites which require sustainable remediation processes, PCBs polluted marine sediments still represent an unresolved problem (Kaya et al., 2019; Šrédlová and Cajthaml, 2022). In this perspective, this study contributed in broadening the current knowledge about applicability of biostimulation of reductive dechlorination processes with a class of slow hydrogen release compounds currently poorly applied for this purpose (Bhola et al., 2021; Pierro et al., 2017) and that might represent good candidates thanks to their environmentally sustainable production process (Martinez et al., 2022; Morgan-Sagastume et al., 2014). Our comparative approach, which included starting sedimentary materials from two highly anthropized coastal sites in the Mediterranean basin, obtained contradictory results in biostimulating the dechlorination in marine sediments, highlighting once more the need to deepen the comprehension on how different factors, *i.e.* the composition of resident microbial community and the chemical-physical parameters of the starting environment, interact among each other and with both the biostimulating agent and the exogenous OHRB, to determine the outcome of the bioremediation strategy.

Indeed, in our experiment starting sediments from Ravenna and Taranto coastal regions (Italy), spiked with PCBs, were both bioaugmented, using a marine microbial community enriched with OHRB able to reductively dechlorinate PCBs, and biostimulated via the addiction of slow fermenting compounds of environmental and industrial interest. While the anaerobic metabolisms of OHRB's competitors (*i.e.* sulfate reduction and methane production) were stimulated similarly in both the studied sediments, reductive dechlorination proceeded to a different extent in sediment from Pialassa della Baiona compared to Taranto's ones, supporting the onset of reductive dehalogenation in the first case while inhibiting it in the second. Thus, it appeared that the sediments chemical characteristics and/or the biodiversity and composition of the indigenous microbial community, might have played a key role in determining the outcome of the bioremediation strategy. For instance, sediments of Pialassa differ from Mar Piccolo's one for the granulometry, with the former notoriously being richer in sand content compared to the latter ones which has a higher fraction of mud (Di Leo et al., 2016; Guerra, 2012; Guerra et al., 2014; Mali et al., 2020, 2017; Ponti et al., 2011; Quero et al., 2015; Todaro et al., 2020; Vitone et al., 2016). Sandy

sediment are characterized by a higher permeability (Huettel et al., 2014), which favors mass transport resulting in higher carbon bacterial uptake (Woulds et al., 2016). As for muddy sediments, they are usually more anoxic, richer in organic matter, and consequently able to guarantee higher microbial load and biodiversity (Boey et al., 2022). Indeed, the available literature showed that sediments from Mar Piccolo can reach higher values of total organic carbon (TOC) (Borghesi et al., 2016; Di Leo et al., 2016; Guerra, 2012; Guerra et al., 2022, 2014, 2013; Mali et al., 2020, 2017; Ponti et al., 2011; Quero et al., 2015; Sfriso et al., 2020; Sollecito et al., 2019; Todaro et al., 2020, 2019). Thus, concerning the differences in the extent of reductive dehalogenation, the higher sand content of Ravenna sediments might have supported the bacterial carbon uptake and the fermentation of organic matter. As for the inhibition observed in T-sediments, beside the less effective biostimulation due to the sediment's composition, the resident microbial community might have contributed in affecting the chances for the inoculated OHRB to become active, even if subdominant, members of the sediment microbiota. Indeed, Taranto sediments were characterized by higher percentage of indigenous *Dehalococcoidia* AB-539-J10, a particular group of bacteria that may have competed with the inoculated ones for the same ecological niche, possibly thanks to similar affinity for hydrogen, but without reductively dechlorinating PCBs due to the lack of dehalogenases in their genome (Wasmund et al., 2014). The presence of more abundant Chloroflexi (Anaerolineae and Dehalococcoidia) in the sediments from Mar Piccolo might be related to the higher Pb contamination reported for this site with respect to the Pialassa della Baiona (Bellucci et al., 2016; Borghesi et al., 2016; Mali et al., 2020, 2017; Quero et al., 2015; Todaro et al., 2020, 2019) as a positive correlation between this lineage and Pb concentration has previously been reported (Li et al., 2020). As for the equally low abundance of inoculated OHRB in both Ravenna and Taranto sediments, it might be worth to remark that DNA-based molecular characterization techniques do not distinguish between active and non-active bacterial community members. Sandy sediments have been previously associated to indigenous microbial communities able to respond more rapidly to changing environmental conditions with respect to muddier ones (Boey et al., 2022). It is tempting to hypothesize that, along the relatively short timeframe of the microcosm experiment, the microbial community from the sandier location (Ravenna) might have been able to promptly reestablish a functioning microbial metabolic network in which even low-abundant members fulfill their ecological role.

In terms of biochemistry, in spite of the reported early phase stimulation of reductive dechlorination by PHAs, the majority of the reducing equivalents provided by the amendments were consumed by other anaerobic competing processes. Sulfate-reduction was the main metabolism stimulated by the

amendments and sulfate-reducing taxa (*Desulfobacteraceae, Desulfosarcinaceae, Desulfuromonadia, Syntrophobacterales, Desulfobulbaceae, Desulfatiglandaceae, Desulfocapsaceae*) (Plugge et al., 2011; Waite et al., 2020; Wasmund et al., 2017) represented an important fraction of the microbial community under all tested conditions. Considering that OHRB can outcompete SRB at low hydrogen concentrations (Hoelen and Reinhard, 2004), reducing the fermentation rate of PHAs might avoid the hyperproliferation of competitors by means of slower release of electron donors. Fermentation rate could be tuned by adjusting the specific surface area, being polymers degradation a surface process (Chinaglia et al., 2018). For example, a reduction in PHAs degradation rate of up to 10 times was reported using thin films instead of polymer powder (Modelli et al., 1999). On the contrary, in this study PHAs were added to the sediment as powder, resulting in a too quick fermentation and fast release of reducing equivalents, supporting the need to further investigate the effects of granulometry, shape, and size (Colwell et al., 2017) on PHAs fermentation rate and ability to stimulate more selectively OHRB in the marine environment. Moreover, we confirmed the previously highlighted complexity of the role of the polymer composition in defining the degradation rate (Doi et al., 1992; Kaplan et al., 1994; Kasuya et al., 1998; Mergaert et al., 1994; Thellen et al., 2008; Volova et al., 2010). In this study, the polymer's composition did not affect significantly its biostimulation effects when added to sediments from Ravenna, whereas in sediments from Taranto the heteropolymer with a higher content of 3-hydroxyvalerate was more promptly fermented. This is in line with biodegradation tests reporting faster weight losses for heteropolymers with higher content of 3HV (Kasuya et al., 1998; Mergaert et al., 1994). Yet, other experiments showed a slower fermentation of PHAs according to an increasing content of 3-hydroxyvalerate (Amanat *et al.*, 2022; Kaplan *et al*, 1994). Considering these conflicting results reported in the literature and the data obtained in this experiment, the fermentation rate of the PHAs might be dependent on the features of the original sediments and further studies would be required to deepen the relationship between the polymer's composition and its degradation rate in different biogeochemical and ecosystem contexts.

Indeed, two levels of complexity are appreciable in data obtained from the microbial community characterization, since both sediment-specific and amendment-specific features were detected in the dataset. Site-specific microbial features resided within the subdominant fraction of the sediments microbial community, as sediment-wise clusterization in amended microbial communities (after three month of microcosm experiment) occurred when using statistics that do not take into account the abundance of the single species (*i.e.* unweighted Unifrac metric). Conversely, abundant members of the microbial communities responded to the use of either polymers or monomers as amendment, determining

the noticeable separation of the two types of samples when weighted statistical analyses (*i.e.* weighted Unifrac metric, which takes into account the abundance of each microbial species) were performed.

Concerning site-specific features, coherently with the previously reported highest percentage of silt and clay in the sediments from Mar Piccolo (Di Leo et al., 2016; Mali et al., 2020, 2017; Quero et al., 2015; Todaro et al., 2020; Vitone et al., 2016), such samples were initially characterized by higher alpha diversity compared to sediments from Ravenna. Taranto samples showed compositional features previously associated to muddy sediments, such as higher abundances of *Anaerolineae* (Aldeguer-Riquelme et al., 2022) and decreased *Flavobacteriaceae* (Chen et al., 2022). These features, as well as the levels of alpha diversity, were maintained during the three months incubation in microcosms in absence of biostimulation (control experiments), whereas the different types of amendments led to the selection of specific microbial communities with decreased alpha diversity, particularly marked in Taranto sediments.

Indeed, the addition of monomer and polymers led to the enrichment of specific fermenting bacteria in both sediments, with the instauration of a dominance in the microbial community profile. As expectable, the monomer-based amendment enriched fermenting and syntrophic bacteria, such as those belonging to the family *Dethiosulfatibacteraceae* or the genus *Thermovirga (Synergistaceae),* both in Ravenna and Taranto sediments. This bacterial lineage belongs to the Firmicutes phylum, and it is known to ferment hydroxyl-fatty acids (An et al., 2017; Matturro et al., 2017), explaining the preferential enrichment with the monomer addition. Also, this group is able to reduce thiosulfate and elemental sulfur to sulfide (Takii et al., 2007), with thiosulfate being an inorganic intermediate of sulfur cycle that is only accumulated in sediments with particularly high organic load and sulfide production, such as salt marsh beds (Zopfi et al., 2004). Moreover, the genus *Dethiosulfatibacter* have been reported to potentially thrive in presence of a large number of aliphatic and aromatic hydrocarbons, since it is equipped with genes for their anaerobic degradation (Vigneron et al., 2021). It is tempting to link the more striking dominance of *Dethiosulfatibacteraceae* obtained in the sediments from Ravenna with the higher PAH contamination reported for this location (Guerra, 2012). *Thermovirga* is a syntrophic bacteria able to oxidize acetate and sustain the growth of hydrogenotrophic methanogens, that were not enriched in the studied sediments. However, *Thermovirga* has also been found in cooperative association in anaerobic reactors with *Methanosaeta*, an acetoclastic methanogen (Ito et al., 2011; Xu et al., 2018), confirming the instauration of a functioning and cooperative microbial community based on fermentative processes when amending with readily fermentable monomers. Conversely, the amended heteropolymers led to a

proliferation of *Spirochaetaceae* in both sediments. This family was previously highlighted as enriched when amending microbial communities with PHAs (Matturro et al., 2018; Pinnell and Turner, 2019; Yang et al., 2020) and have been reported among lineages encoding PHAs depolymerases (Viljakainen and Hug, 2021). *Spirochaetes* were also addressed as possible acetogens in an enriched microbial community able to reductively dechlorinate TCE (Ziv-El et al., 2011). Thus, they might have possibly acted as first degraders of the added complex organic matter, subsequently leading to the stimulation of other anaerobic species as sulfate reducing bacteria, as speculated by Pinnell and Turner (2019). In both monomer and polymer amended microcosms, the hyper proliferation of specific bacteria able to exploit the added carbon source was accompanied by a reduction in the relative quantification of other species whose metabolism was not directly stimulated, as the chemolithoautotrophic *Sulfurovaceae* (Waite et al., 2017) that were present in initial sediments, maintained in controls but markedly decreased or disappeared in amended microcosms.

Trying to combine the two levels of complexity ("sediment effect" and "amendment specificity") is harder task. For instance, in both Ravenna and Taranto sediments, the amendments (both polymers and monomer) caused a shrinkage of the relative abundance of members of *Flavobacteraceae* (phylum Bacteroidetes), which was not detected in control microcosms. However, only in amended sediments from Taranto the Bacteroidetes population is replenished by a proliferation of other families within the same phylum, namely *Marinilabiliaceae* and, especially in the case of PHBHV75 amendment, *Williamwhitmaniaceae*. The available literature did not offer clear suggestions neither about the ecological role of such bacterial families in marine sediment ecosystems, nor on possible links with biogeochemical features of the Taranto sediments that might not have been present in Ravenna site. Interestingly, members of the *Marinilabiliaceae* family have been reported as lipolytic bacteria (Shalley et al., 2013) and the lipolysis process is strictly linked to the metabolism of PHAs, not only in PHA producing bacteria but also in degraders-only (Bashiri et al., 2022). Bacterial group "Blvii28_wastewater-sludge_group", to which all sequences attached to the family *Williamwhitmaniaceae* were assigned, was reported as able to perform β/ω-oxidation (de Melo Pirete et al., 2022), a metabolic pathway involved in the degradation of oligomers and monomers generated by PHAs hydrolysis (Altaee et al., 2016; Prieto et al., 2016).

From a community ecology standpoint, the changes in the microbial community profile of the amended microcosms likely mirror rearrangements in the metabolic network. Indeed, *Flavobacteriaceae* are known primary degraders in marine ecosystems, often keystone species of modules controlled by - and

specialized in the degradation of - the most abundant and available carbon source (Enke et al., 2019; Gralka et al., 2020). The decrease or disappearance of such group in amended microcosms is a direct consequence of the change in the main available macromolecular carbon source, because of which other types of primary degraders take over and becomes dominant (*i.e.* fermenters in the case of microcosms provided with simple monomers, macromolecules-degrading *Spirochateaceae* in the case of polymers). Marine communities are also equipped with secondary modules of bacteria independent from the nature and abundance of the major complex substrate, whose dynamics are less predictable and determined by inter-species metabolic interactions, *e.g.* cross-feeding. Members of these secondary modules lack hydrolytic capability and rely on other community members for provision of metabolic intermediates: organic acids, oligosaccharides, nucleotides, amino acids, as well as other secondary metabolites such as signaling molecules and antimicrobial compounds, which emerge from the interaction of the microbial community members and specific biogeochemical features of the environment (Enke et al., 2019; Gralka et al., 2020). The construction of the amended microcosms creates the opportunity for the sedimentary microbial community to re-assemble, with a structure centered on a common module of primary degraders selected by the exogenous primary carbon source (PHB monomers or polymers), but with decentralized modules of subdominant, secondary consumers which is idiosyncratic to the two different sediments (Gralka et al., 2020). In the present model, the Bacteroidetes families with unclear ecological role (*Marinilabialiaceae* and *Williamwhitmaniaceae*) that only enrich in amended microcosms built using sediments from Taranto might represent an example of those secondary functional clusters. In fact, they were selected starting from the plethora of subdominant microrganisms provided by the original material, and they thrived in the specific novel environment resulting from the shift in the primary metabolism, with consequent changes in released secondary metabolites, within the peculiar biochemical and granulometric context of the Mar Piccolo.

3.5 Conclusions

In the present study, the complexity of the factors involved in a bioremediation action under *in situ*-like conditions were highlighted by monitoring the influence of PHAs, employed as novel amendments, on the anaerobic metabolisms of OHRB, on their anaerobic competitors and on the microbial community of two heavily anthropogenically impacted marine sediments. According to our data, biological, chemical and physical features of the treated sediments played a key role in determining the outcome of the biostimulation approach. Indeed, in microcosms built with sediment from Ravenna, PHAs primed PCBs reductive dechlorination by anticipating the onset of the process. On the other hand, in Mar Piccolo's

sediment, the same treatment led to a severe inhibition of the reductive dechlorination process which adversely affected the bioremediation outcome. In all cases, PHAs degradation proceeded rapidly, favoring the metabolisms of competitive bacteria and underlying the need of an optimization of the fermentation rate. Furthermore, the influence of PHAs' composition on the degradation rate was site specific, being null when studying sediment from Ravenna and having a relevant impact in the sediment of Mar Piccolo. The site's specific features (*i.e.* granulometry) and the indigenous microbial community were identified as fundamental factors to explain the discrepancy in the obtained data. In fact, the diverse chemical-physical environments could have interacted differently with the metabolites released by the newly arranged microbial core of polymers degraders (or monomers fermenters), shaping the composition of the fraction of the microbial community that includes cross-feeders and secondary degraders. Moreover, the subdominant indigenous species might have furtherly competed with the organohalide respiring bacteria, reducing the efficacy of the biostimulation approach. Concluding, our comparative approach highlighted the complexity of the interaction among the features of the polluted site, with its autochthonous microbiota, the inoculated microbial culture, and the nature of the biostimulant agent. We proved that such interactions and our lack of understanding of its mechanisms, can determine the failing of bioremediation strategies that showed promising elsewhere. Moreover, our results demonstrated that PHAs can have a pervasive effect on the composition of sediment microbiota, heavily impacting the abundance of primary degraders. In a perspective scenario in which biobased plastic materials are meant to take over traditional undegradable plastics, it is reasonable to picture that an increasing load of such polymers will reach the natural environment in the next future where, becoming an abundant source of carbon-based macromolecules, they will have the potential to change the structure of autochthonous microbial communities with consequent effects on the natural biogeochemical cycles.

3.6 Bibliography

Aldeguer-Riquelme, B., Rubio-Portillo, E., Álvarez-Rogel, J., Giménez-Casalduero, F., Otero, X.L., Belando, M.D., Bernardeau-Esteller, J., García-Muñoz, R., Forcada, A., Ruiz, J.M., Santos, F., Antón, J., 2022. Factors structuring microbial communities in highly impacted coastal marine sediments (Mar Menor lagoon, SE Spain). Front. Microbiol. 13, 1–18. https://doi.org/10.3389/fmicb.2022.937683

Altaee, N., El-Hiti, G.A., Fahdil, A., Sudesh, K., Yousif, E., 2016. Biodegradation of different formulations of polyhydroxybutyrate films in soil. Springerplus 5. https://doi.org/10.1186/s40064-016-2480-2

Amanat, N., Matturro, B., Rossi, M.M., Valentino, F., Villano, M., Papini, M.P., 2021. Assessment of long-term fermentability of pha-based materials from pure and mixed microbial cultures for potential environmental applications. Water (Switzerland) 13, 897. https://doi.org/10.3390/w13070897

Amanat, N., Matturro, B., Villano, M., Lorini, L., Rossi, M.M., Zeppilli, M., Rossetti, S., Petrangeli Papini, M., 2022. Enhancing the biological reductive dechlorination of trichloroethylene with PHA from mixed microbial cultures (MMC). J. Environ. Chem. Eng. 10, 107047. https://doi.org/10.1016/j.jece.2021.107047

An, B.A., Shen, Y., Voordouw, G., 2017. Control of sulfide production in high salinity Bakken shale oil reservoirs by halophilic bacteria reducing nitrate to nitrite. Front. Microbiol. 8. https://doi.org/10.3389/fmicb.2017.01164

Aulenta, F., Fuoco, M., Canosa, A., Papini, M.P., Majone, M., 2008. Use of poly-β-hydroxy-butyrate as a slow-release electron donor for the microbial reductive dechlorination of TCE. Water Sci. Technol. 57, 921–925. https://doi.org/10.2166/wst.2008.073

Aulenta, F., Majone, M., Tandoi, V., 2006. Enhanced anaerobic bioremediation of chlorinated solvents: environmental factors influencing microbial activity and their relevance under field conditions. J. Chem. Technol. Biotechnol. 81, 1463–1474. https://doi.org/10.1002/jctb

Baric, M., Pierro, L., Pietrangeli, B., Papini, M.P., 2014. Polyhydroxyalkanoate (PHB) as a slow-release electron donor for advanced in situ bioremediation of chlorinated solvent-contaminated aquifers. N. Biotechnol. 31, 377–382. https://doi.org/10.1016/j.nbt.2013.10.008

Bashiri, R., Allen, B., Shamurad, B., Pabst, M., Curtis, T.P., Ofiţeru, I.D., 2022. Looking for lipases and lipolytic organisms in low-temperature anaerobic reactors treating domestic wastewater. Water Res. 212. https://doi.org/10.1016/j.watres.2022.118115

Bedard, D.L., 2003. Polychlorinated biphenyls in acquatic sediments: environmental fate and outlook for biological treatment, in: Häggblom, M.M., Bossert, I.D. (Eds.), Dehalogenation, Microbial Processes and Environmental Applications. Kluwer Academic Publishers, Rutgers University,

USA.

Bellucci, L.G., Cassin, D., Giuliani, S., Botter, M., Zonta, R., 2016. Sediment pollution and dynamic in the Mar Piccolo of Taranto (southern Italy): insights from bottom sediment traps and surficial sediments. Environ. Sci. Pollut. Res. 23, 12554–12565. https://doi.org/10.1007/s11356-016-6738-6

Bhola, S., Arora, K., Kulshrestha, S., Mehariya, S., Bhatia, R.K., Kaur, P., Kumar, P., 2021. Established and Emerging Producers of PHA: Redefining the Possibility. Appl. Biochem. Biotechnol. 193, 3812–3854. https://doi.org/10.1007/s12010-021-03626-5

Boey, J.S., Mortimer, R., Couturier, A., Worrallo, K., Handley, K.M., 2022. Estuarine microbial diversity and nitrogen cycling increase along sand–mud gradients independent of salinity and distance. Environ. Microbiol. 24, 50–65. https://doi.org/10.1111/1462-2920.15550

Bolyen, E., Rideout, J.R., Dillon, M.R., Bokulich, N.A., Abnet, C.C., Al-Ghalith, G.A., Alexander, H., Alm, E.J., Arumugam, M., Asnicar, F., Bai, Y., Bisanz, J.E., Bittinger, K., Brejnrod, A., Brislawn, C.J., Brown, C.T., Callahan, B.J., Caraballo-Rodríguez, A.M., Chase, J., Cope, E.K., Da Silva, R., Diener, C., Dorrestein, P.C., Douglas, G.M., Durall, D.M., Duvallet, C., Edwardson, C.F., Ernst, M., Estaki, M., Fouquier, J., Gauglitz, J.M., Gibbons, S.M., Gibson, D.L., Gonzalez, A., Gorlick, K., Guo, J., Hillmann, B., Holmes, S., Holste, H., Huttenhower, C., Huttley, G.A., Janssen, S., Jarmusch, A.K., Jiang, L., Kaehler, B.D., Kang, K. Bin, Keefe, C.R., Keim, P., Kelley, S.T., Knights, D., Koester, I., Kosciolek, T., Kreps, J., Langille, M.G.I., Lee, J., Ley, R., Liu, Y.X., Loftfield, E., Lozupone, C., Maher, M., Marotz, C., Martin, B.D., McDonald, D., McIver, L.J., Melnik, A. V., Metcalf, J.L., Morgan, S.C., Morton, J.T., Naimey, A.T., Navas-Molina, J.A., Nothias, L.F., Orchanian, S.B., Pearson, T., Peoples, S.L., Petras, D., Preuss, M.L., Pruesse, E., Rasmussen, L.B., Rivers, A., Robeson, M.S., Rosenthal, P., Segata, N., Shaffer, M., Shiffer, A., Sinha, R., Song, S.J., Spear, J.R., Swafford, A.D., Thompson, L.R., Torres, P.J., Trinh, P., Tripathi, A., Turnbaugh, P.J., Ul-Hasan, S., van der Hooft, J.J.J., Vargas, F., Vázquez-Baeza, Y., Vogtmann, E., von Hippel, M., Walters, W., Wan, Y., Wang, M., Warren, J., Weber, K.C., Williamson, C.H.D., Willis, A.D., Xu, Z.Z., Zaneveld, J.R., Zhang, Y., Zhu, Q., Knight, R., Caporaso, J.G., 2019. Reproducible, interactive, scalable and extensible microbiome data science using QIIME 2. Nat. Biotechnol. 37, 852–857. https://doi.org/10.1038/s41587-019-0209-9

Borghesi, F., Migani, F., Dinelli, E., 2016. Geochemical characterization of surface sediments from the

northern Adriatic wetlands around the Po River delta. Part II: aqua regia results. J. Geochemical Explor. 169, 13–29. https://doi.org/10.1016/j.gexplo.2016.06.012

Cardellicchio, N., Annicchiarico, C., Di Leo, A., Giandomenico, S., Spada, L., 2016. The Mar Piccolo of Taranto: an interesting marine ecosystem for the environmental problems studies. Environ. Sci. Pollut. Res. 23, 12495–12501. https://doi.org/10.1007/s11356-015-4924-6

Chang, B.-V., Chiu, T.-C., Yuan, S.-Y., 2006. Dechlorination of Polychlorinated Biphenyl Congeners by Anaerobic Microorganisms From River Sediment. Water Environ. Res. 78, 764–769. https://doi.org/10.2175/106143006x107380

Chen, Y.J., Leung, P.M., Cook, P.L.M., Wong, W.W., Hutchinson, T., Eate, V., Kessler, A.J., Greening, C., 2022. Hydrodynamic disturbance controls microbial community assembly and biogeochemical processes in coastal sediments. ISME J. 16, 750–763. https://doi.org/10.1038/s41396-021-01111-9

Chinaglia, S., Tosin, M., Degli-Innocenti, F., 2018. Biodegradation rate of biodegradable plastics at molecular level. Polym. Degrad. Stab. 147, 237–244. https://doi.org/10.1016/j.polymdegradstab.2017.12.011

Colwell, J.M., Gauthier, E., Halley, P., Laycock, B., Nikoli, M., Bottle, S., George, G., 2017. Lifetime prediction of biodegradable polymers. Prog. Polym. Sci. 71, 144–189. https://doi.org/10.1016/j.progpolymsci.2017.02.004

Conrad, R., 2020. Importance of hydrogenotrophic, aceticlastic and methylotrophic methanogenesis for methane production in terrestrial, aquatic and other anoxic environments: A mini review. Pedosphere 30, 25–39. https://doi.org/10.1016/S1002-0160(18)60052-9

Cotecchia, F., Vitone, C., Sollecito, F., Mali, M., Miccoli, D., Petti, R., Milella, D., Ruggieri, G., Bottiglieri, O., Santaloia, F., De Bellis, P., Cafaro, F., Notarnicola, M., Todaro, F., Adamo, F., Di Nisio, A., Lanzolla, A.M.L., Spadavecchia, M., Moretti, M., Agrosì, G., De Giosa, F., Fago, P., Lacalamita, M., Lisco, S., Manzari, P., Mesto, E., Romano, G., Scardino, G., Schingaro, E., Siniscalchi, A., Tempesta, G., Valenzano, E., Mastronuzzi, G., Cardellicchio, N., Di Leo, A., Spada, L., Giandomenico, S., Calò, M., Uricchio, V.F., Mascolo, G., Bagnuolo, G., Ciannarella, R., Tursi, A., Cipriano, G., Cotugno, P., Sion, L., Carlucci, R., Capasso, G., De Chiara, G., Pisciotta, G., Velardo, R., Corbelli, V., 2021. A geo-chemo-mechanical study of a highly polluted

marine system (Taranto, Italy) for the enhancement of the conceptual site model. Sci. Rep. 11, 1–26. https://doi.org/10.1038/s41598-021-82879-w

de Melo Pirete, L., Camargo, F.P., Dornelles, H.S., Granatto, C.F., Sakamoto, I.K., Grosseli, G.M., Fadini, P.S., Silva, E.L., Varesche, M.B.A., 2022. Biodegradation of diclofenac and ibuprofen in Fluidized Bed Reactor applied to sanitary sewage treatment in acidogenic and denitrifying conditions. J. Water Process Eng. 49. https://doi.org/10.1016/j.jwpe.2022.102964

Di Leo, A., Annicchiarico, C., Cardellicchio, N., Cibic, T., Comici, C., Giandomenico, S., Spada, L., 2016. Mobilization of trace metals and PCBs from contaminated marine sediments of the Mar Piccolo in Taranto during simulated resuspension experiment. Environ. Sci. Pollut. Res. 23, 12777–12790. https://doi.org/10.1007/s11356-015-5472-9

Doi, Y., Kanesawa, Y., Tanahashi, N., Kumagai, Y., 1992. Biodegradation of microbial polyesters in the marine environment. Polym. Degrad. Stab. 36, 173–177. https://doi.org/10.1016/0141-3910(92)90154-W

Enke, T.N., Datta, M.S., Schwartzman, J., Cermak, N., Schmitz, D., Barrere, J., Pascual-García, A., Cordero, O.X., 2019. Modular Assembly of Polysaccharide-Degrading Marine Microbial Communities. Curr. Biol. 29, 1528-1535.e6. https://doi.org/10.1016/j.cub.2019.03.047

Fava, F., Zanaroli, G., Young, L.Y., 2003. Microbial reductive dechlorination of pre-existing PCBs and spiked 2,3,4,5,6-pentachlorobiphenyl in anaerobic slurries of a contaminated sediment of Venice Lagoon (Italy). FEMS Microbiol. Ecol. 44, 309–318. https://doi.org/10.1016/S0168-6496(03)00069-2

Frame, G.M., 1997. A collaborative study of 209 PCB congeners and 6 Aroclors on 20 different HRGC columns: 1. Retention and coelution database. Fresenius. J. Anal. Chem. 357, 701–713. https://doi.org/10.1007/s002160050237

Gralka, M., Szabo, R., Stocker, R., Cordero, O.X., 2020. Trophic Interactions and the Drivers of Microbial Community Assembly. Curr. Biol. 30, R1176–R1188. https://doi.org/10.1016/j.cub.2020.08.007

Guerra, R., 2012. Polycyclic aromatic hydrocarbons, polychlorinated biphenyls and trace metals in sediments from a coastal lagoon (Northern Adriatic, Italy). Water. Air. Soil Pollut. 223, 85–98. https://doi.org/10.1007/s11270-011-0841-6

Guerra, R., Pasteris, A., Lee, S. hyung, Park, N. jin, Ok, G., 2014. Spatial patterns of metals, PCDDs/Fs, PCBs, PBDEs and chemical status of sediments from a coastal lagoon (Pialassa Baiona, NW Adriatic, Italy). Mar. Pollut. Bull. 89, 407–416. https://doi.org/10.1016/j.marpolbul.2014.10.024

Guerra, R., Pistocchi, R., Vanucci, S., 2013. Dynamics and sources of organic carbon in suspended particulate matter and sediments in Pialassa Baiona lagoon (NW Adriatic Sea, Italy). Estuar. Coast. Shelf Sci. 135, 24–32. https://doi.org/10.1016/j.ecss.2013.06.022

Guerra, R., Simoncelli, S., Pasteris, A., 2022. Carbon accumulation and storage in a temperate coastal lagoon under the influence of recent climate change (Northwestern Adriatic Sea). Reg. Stud. Mar. Sci. 53, 102439. https://doi.org/10.1016/j.rsma.2022.102439

Haard, N.F., Chism, G., Nagle, N., 1975. A fluorometric method for the kinetic assay of indole-3-acetic acid oxidase. Anal. Biochem. 69, 627–631. https://doi.org/10.1016/0003-2697(75)90168-2

Hall, M., Beiko, R.G., 2018. 16S rRNA Gene Analysis with QIIME2, in: Methods in Molecular Biology. Humana Press Inc., pp. 113–129.

Harrison, J.P., Boardman, C., O'Callaghan, K., Delort, A.M., Song, J., 2018. Biodegradability standards for carrier bags and plastic films in aquatic environments: A critical review. R. Soc. Open Sci. 5. https://doi.org/10.1098/rsos.171792

Hoelen, T.P., Reinhard, M., 2004. Complete biological dehalogenation of chlorinated ethylenes in sulfate containing groundwater. Biodegradation 15, 395–403. https://doi.org/10.1023/B:BIOD.0000044592.33729.d6

Huettel, M., Berg, P., Kostka, J.E., 2014. Benthic exchange and biogeochemical cycling in permeable sediments. Ann. Rev. Mar. Sci. 6, 23–51. https://doi.org/10.1146/annurev-marine-051413-012706

Isa, Z., Grusenmeyer, S., Verstraete, W., 1986. Sulfate Reduction Relative to Methane Production in High-Rate Anaerobic Digestion : Microbiological Aspects. Appl. Environ. Microbiol. 51, 580–587.

Ito, T., Yoshiguchi, K., Ariesyady, H.D., Okabe, S., 2011. Identification of a novel acetate-utilizing bacterium belonging to Synergistes group 4 in anaerobic digester sludge. ISME J. 5, 1844–1856. https://doi.org/10.1038/ismej.2011.59

Kaplan, D.L., Mayer, J.M., Greenberger, M., Gross, R., McCarthy, S., 1994. Degradation methods and degradation kinetics of polymer films. Polym. Degrad. Stab. 45, 165–172. https://doi.org/10.1016/0141-3910(94)90133-3

Kasuya, K.I., Takagi, K.I., Ishiwatari, S.I., Yoshida, Y., Doi, Y., 1998. Biodegradabilities of various aliphatic polyesters in natural waters. Polym. Degrad. Stab. 59, 327–332. https://doi.org/10.1016/s0141-3910(97)00155-9

Kaya, D., Sowers, K.R., Demirtepe, H., Stiell, B., Baker, J.E., Imamoglu, I., Kjellerup, B. V., 2019. Assessment of PCB contamination, the potential for in situ microbial dechlorination and natural attenuation in an urban watershed at the East Coast of the United States. Sci. Total Environ. 683, 154–165. https://doi.org/10.1016/j.scitotenv.2019.05.193

Klindworth, A., Pruesse, E., Schweer, T., Peplies, J., Quast, C., Horn, M., Glöckner, F.O., 2013. Evaluation of general 16S ribosomal RNA gene PCR primers for classical and next-generation sequencing-based diversity studies. Nucleic Acids Res. 41, 1–11. https://doi.org/10.1093/nar/gks808

Koenigsberg, S., Willett, A., Sutherland, M., 2006. Controlled release electron donors: Hydrogen release compound (HRC)-an overview of a decade of case studies. Bioremediat. J. 10, 45–57. https://doi.org/10.1080/10889860600842837

Koenigsberg, S.S., Sandefur, A.C., 1999. The Use of Hydrogen Release Compound for the Accelerated Bioremediation of Anaerobically Degradable Contaminants : The Advent of The-Release Electron Donors. Remediation 10, 31–53.

Leeson, A., Beevar, E., Bruce, H., Fortenberry, J., Coyle, C., 2004. Principles and Practices of Enhanced Anaerobic Bioremediation of Chlorinated Solvents.

Li, C., Quan, Q., Gan, Y., Dong, J., Fang, J., Wang, L., Liu, J., 2020. Effects of heavy metals on microbial communities in sediments and establishment of bioindicators based on microbial taxa and function for environmental monitoring and management. Sci. Total Environ. 749, 141555. https://doi.org/10.1016/j.scitotenv.2020.141555

Liamleam, W., Annachhatre, A.P., 2007. Electron donors for biological sulfate reduction. Biotechnol. Adv. 25, 452–463. https://doi.org/10.1016/j.biotechadv.2007.05.002

Lovley, D.R., Dwyer, D.F., Klug, M.J., 1982. Kinetic Analysis of Competition Between Sulfate Reducers and Methanogens for Hydrogen in Sedimentst. Appl. Environ. Microbiol. 43, 1373–1379.

Lovley, D.R., Klug, M.J., 1983. Sulfate Reducers Can Outcompete Methanogens Sulfate Concentrationst at Freshwater. Appl. Environ. Microbiol. 45, 187–192.

Mali, M., Dell'Anna, M.M., Mastrorilli, P., Chiaia, G., Romanazzi, G., Damiani, L., 2020. Multivariate analyses for investigating highly polluted marine ecosystem: The case study of Mar Piccolo (Taranto, South Italy). Aquat. Ecosyst. Heal. Manag. 23, 436–444. https://doi.org/10.1080/14634988.2020.1807224

Mali, M., Dell'Anna, M.M., Notarnicola, M., Damiani, L., Mastrorilli, P., 2017. Combining chemometric tools for assessing hazard sources and factors acting simultaneously in contaminated areas. Case study: "Mar Piccolo" Taranto (South Italy). Chemosphere 184, 784–794. https://doi.org/10.1016/j.chemosphere.2017.06.028

Martinez, G.A., Puccio, S., Domingos, J.M.B., Morselli, E., Gioia, C., Marchese, P., Raspolli Galletti, A.M., Celli, A., Fava, F., Bertin, L., 2022. Upgrading grape pomace contained ethanol into hexanoic acid, fuel additives and a sticky polyhydroxyalkanoate: an effective alternative to ethanol distillation. Green Chem. 24, 2882–2892. https://doi.org/10.1039/d2gc00044j

Matturro, B., Frascadore, E., Rossetti, S., 2017. High-throughput sequencing revealed novel Dehalococcoidia in dechlorinating microbial enrichments from PCB-contaminated marine sediments. FEMS Microbiol. Ecol. 93, 1–10. https://doi.org/10.1093/femsec/fix134

Matturro, B., Pierro, L., Frascadore, E., Papini, M.P., Rossetti, S., 2018. Microbial community changes in a chlorinated solvents polluted aquifer over the field scale treatment with poly-3-hydroxybutyrate as amendment. Front. Microbiol. 9, 1–11. https://doi.org/10.3389/fmicb.2018.01664

Mergaert, J., Wouters, A., Anderson, C., Swings, J., 1994. In situ biodegradation of poly(3-hydroxybutyrate) and poly(3-hydroxybutyrate-co-3-hydroxyvalerate) in natural waters. Can. J. Microbiol. 41, 154–159. https://doi.org/10.1139/m95-182

Modelli, A., Calcagno, B., Scandola, M., 1999. Kinetics of aerobic polymer degradation in soil by means of the ASTM D 5988-96 standard method. J. Environ. Polym. Degrad. 7, 109–116.

Morgan-Sagastume, F., Valentino, F., Hjort, M., Cirne, D., Karabegovic, L., Gerardin, F., Johansson, P., Karlsson, A., Magnusson, P., Alexandersson, T., Bengtsson, S., Majone, M., Werker, A., 2014. Polyhydroxyalkanoate (PHA) production from sludge and municipal wastewater treatment. Water Sci. Technol. 69, 177–184. https://doi.org/10.2166/wst.2013.643

Nuzzo, A., Hosseinkhani, B., Boon, N., Zanaroli, G., Fava, F., 2017. Impact of bio-palladium nanoparticles (bio-Pd NPs) on the activity and structure of a marine microbial community. Environ. Pollut. 220, 1068–1078. https://doi.org/10.1016/j.envpol.2016.11.036

Palladino, G., Caroselli, E., Tavella, T., D'Amico, F., Prada, F., Mancuso, A., Franzellitti, S., Rampelli, S., Candela, M., Goffredo, S., Biagi, E., 2022. Correction to: Metagenomic shifts in mucus, tissue and skeleton of the coral Balanophyllia europaea living along a natural CO2 gradient. ISME Commun. 2, 2022. https://doi.org/10.1038/s43705-022-00165-w

Payne, R.B., Ghosh, U., May, H.D., Marshall, C.W., Sowers, K.R., 2019. A Pilot-Scale Field Study: In Situ Treatment of PCB-Impacted Sediments with Bioamended Activated Carbon. Environ. Sci. Technol. 53, 2626–2634. https://doi.org/10.1021/acs.est.8b05019

Pierro, L., Matturro, B., Rossetti, S., Sagliaschi, M., Sucato, S., Alesi, E., Bartsch, E., Arjmand, F., Papini, M.P., 2017. Polyhydroxyalkanoate as a slow-release carbon source for in situ bioremediation of contaminated aquifers: From laboratory investigation to pilot-scale testing in the field. N. Biotechnol. 37, 60–68. https://doi.org/10.1016/j.nbt.2016.11.004

Pignotti, E., Guerra, R., Covelli, S., Fabbri, E., Dinelli, E., 2018. Sediment quality assessment in a coastal lagoon (Ravenna, NE Italy) based on SEM-AVS and sequential extraction procedure. Sci. Total Environ. 635, 216–227. https://doi.org/10.1016/j.scitotenv.2018.04.093

Pinnell, L.J., Turner, J.W., 2019. Shotgun metagenomics reveals the benthic microbial community response to plastic and bioplastic in a coastal marine environment. Front. Microbiol. 10. https://doi.org/10.3389/fmicb.2019.01252

Plugge, C.M., Zhang, W., Scholten, J.C.M., Stams, A.J.M., 2011. Metabolic flexibility of sulfate-reducing bacteria. Front. Microbiol. 2, 1–8. https://doi.org/10.3389/fmicb.2011.00081

Ponti, M., Airoldi, L., 2009. The Pialassa Baiona Coastal Lagoon (Ravenna , Northern Adriatic Sea), in: Cecere, E., Petrocelli, A., Izzo, G., Sfriso, A. (Eds.), Flora and Vegetation of the Italian Transitional Water Systems. Copyright CoRiLa, Stampa "Multigraf" Spinea, pp. 1–15.

Ponti, M., Casselli, C., Abbiati, M., 2011. Anthropogenic disturbance and spatial heterogeneity of macrobenthic invertebrate assemblages in coastal lagoons: The study case of Pialassa Baiona (northern Adriatic Sea). Helgol. Mar. Res. 65, 25–42. https://doi.org/10.1007/s10152-010-0197-0

Prieto, A., Escapa, I.F., Martínez, V., Dinjaski, N., Herencias, C., de la Peña, F., Tarazona, N., Revelles, O., 2016. A holistic view of polyhydroxyalkanoate metabolism in Pseudomonas putida. Environ. Microbiol. 18, 341–357. https://doi.org/10.1111/1462-2920.12760

Quero, G.M., Cassin, D., Botter, M., Perini, L., Luna, G.M., 2015. Patterns of benthic bacterial diversity in coastal areas contaminated by heavy metals, polycyclic aromatic hydrocarbons (PAHs) and polychlorinated biphenyls (PCBs). Front. Microbiol. 6, 1–15. https://doi.org/10.3389/fmicb.2015.01053

Riis, V., Babel, W., 1999. Removal of sulfur interfering in the analysis of organochlorines by GC-ECD. Analyst 124, 1771–1773.

Rognes, T., Flouri, T., Nichols, B., Quince, C., Mahé, F., 2016. VSEARCH: A versatile open source tool for metagenomics. PeerJ 2016, 1–22. https://doi.org/10.7717/peerj.2584

Rosato, A., Barone, M., Negroni, A., Brigidi, P., Fava, F., Xu, P., Candela, M., Zanaroli, G., 2020. Microbial colonization of different microplastic types and biotransformation of sorbed PCBs by a marine anaerobic bacterial community. Sci. Total Environ. 705, 135790. https://doi.org/10.1016/j.scitotenv.2019.135790

Sfriso, A., Buosi, A., Tomio, Y., Juhmani, A.S., Chiesa, S., Greco, M., Gazzola, C., Mistri, M., Munari, C., Sfriso, A.A., 2020. Sediment carbon variations in the venice lagoon and other transitional water systems of the northern adriatic sea. Water (Switzerland) 12, 1–13. https://doi.org/10.3390/w12123430

Shalley, S., Pradip Kumar, S., Srinivas, T.N.R., Suresh, K., Anil Kumar, P., 2013. Marinilabilia nitratireducens sp. nov., a lipolytic bacterium of the family Marinilabiliaceae isolated from marine solar saltern. Antonie van Leeuwenhoek, Int. J. Gen. Mol. Microbiol. 103, 519–525. https://doi.org/10.1007/s10482-012-9834-8

Sollecito, F., Cotecchia, F., Mali, M., Miccoli, D., Vitone, C., 2019. Geo-chemo-mechanical characterization of a polluted marine basin. E3S Web Conf. 92. https://doi.org/10.1051/e3sconf/20199218001

Šrédlová, K., Cajthaml, T., 2022. Recent advances in PCB removal from historically contaminated environmental matrices. Chemosphere 287, 132096. https://doi.org/10.1016/j.chemosphere.2021.132096

Takii, S., Hanada, S., Tamaki, H., Ueno, Y., Sekiguchi, Y., Ibe, A., Matsuura, K., 2007. Dethiosulfatibacter aminovorans gen. nov., sp. nov., a novel thiosulfate-reducing bacterium isolated from coastal marine sediment via sulfate-reducing enrichment with Casamino acids. Int. J. Syst. Evol. Microbiol. 57, 2320–2326. https://doi.org/10.1099/ijs.0.64882-0

Thellen, C., Coyne, M., Froio, D., Auerbach, M., Wirsen, C., Ratto, J.A., 2008. A processing, characterization and marine biodegradation study of melt-extruded polyhydroxyalkanoate (PHA) films. J. Polym. Environ. 16, 1–11. https://doi.org/10.1007/s10924-008-0079-6

Todaro, F., de Gisi, S., Labianca, C., Notarnicola, M., 2019. Combined assessment of chemical and ecotoxicological data for the management of contaminated marine sediments. Environ. Eng. Manag. J. 18, 2287–2296.

Todaro, F., De Gisi, S., Notarnicola, M., 2020. Contaminated marine sediment stabilization/solidification treatment with cement/lime: leaching behaviour investigation. Environ. Sci. Pollut. Res. 27, 21407–21415. https://doi.org/10.1007/s11356-020-08562-1

Vigneron, A., Cruaud, P., Ducellier, F., Head, I.M., Tsesmetzis, N., 2021. Syntrophic hydrocarbon degradation in a decommissioned off-shore subsea oil storage structure. Microorganisms 9, 1–14. https://doi.org/10.3390/microorganisms9020356

Viljakainen, V.R., Hug, L.A., 2021. The phylogenetic and global distribution of bacterial polyhydroxyalkanoate bioplastic-degrading genes. Environ. Microbiol. 23, 1717–1731. https://doi.org/10.1111/1462-2920.15409

Vitone, C., Federico, A., Puzrin, A.M., Ploetze, M., Carrassi, E., Todaro, F., 2016. On the geotechnical characterisation of the polluted submarine sediments from Taranto. Environ. Sci. Pollut. Res. 23, 12535–12553. https://doi.org/10.1007/s11356-016-6317-x

Volova, T.G., Boyandin, A.N., Vasiliev, A.D., Karpov, V.A., Prudnikova, S. V., Mishukova, O. V., Boyarskikh, U.A., Filipenko, M.L., Rudnev, V.P., Bá Xuân, B., Vit Dũng, V., Gitelson, I.I., 2010. Biodegradation of polyhydroxyalkanoates (PHAs) in tropical coastal waters and identification of PHA-degrading bacteria. Polym. Degrad. Stab. 95, 2350–2359.

https://doi.org/10.1016/j.polymdegradstab.2010.08.023

Waite, D.W., Chuvochina, M., Pelikan, C., Parks, D.H., Yilmaz, P., Wagner, M., Loy, A., Naganuma, T., Nakai, R., Whitman, W.B., Hahn, M.W., Kuever, J., Hugenholtz, P., 2020. Proposal to reclassify the proteobacterial classes deltaproteobacteria and oligoflexia, and the phylum thermodesulfobacteria into four phyla reflecting major functional capabilities. Int. J. Syst. Evol. Microbiol. 70, 5972–6016. https://doi.org/10.1099/ijsem.0.004213

Waite, D.W., Vanwonterghem, I., Rinke, C., Parks, D.H., Zhang, Y., Takai, K., Sievert, S.M., Simon, J., Campbell, B.J., Hanson, T.E., Woyke, T., Klotz, M.G., Hugenholtz, P., 2017. Comparative genomic analysis of the class Epsilonproteobacteria and proposed reclassification to epsilonbacteraeota (phyl. nov.). Front. Microbiol. 8. https://doi.org/10.3389/fmicb.2017.00682

Wasmund, K., Mußmann, M., Loy, A., 2017. The life sulfuric: microbial ecology of sulfur cycling in marine sediments. Environ. Microbiol. Rep. 9, 323–344. https://doi.org/10.1111/1758-2229.12538

Wasmund, K., Schreiber, L., Lloyd, K.G., Petersen, D.G., Schramm, A., Stepanauskas, R., Jørgensen, B.B., Adrian, L., 2014. Genome sequencing of a single cell of the widely distributed marine subsurface Dehalococcoidia, phylum Chloroflexi. ISME J. 8, 383–397. https://doi.org/10.1038/ismej.2013.143

Wiegel, J., Wu, Q., 2000. Microbial reductive dehalogenation of polychlorinated biphenyls. Fems Microbiol. Ecol. 32, 1–15.

Woulds, C., Bouillon, S., Cowie, G.L., Drake, E., Middelburg, J.J., Witte, U., 2016. Patterns of carbon processing at the seafloor: The role of faunal and microbial communities in moderating carbon flows. Biogeosciences 13, 4343–4357. https://doi.org/10.5194/bg-13-4343-2016

Xu, S., Han, R., Zhang, Y., He, C., Liu, H., 2018. Differentiated stimulating effects of activated carbon on methanogenic degradation of acetate, propionate and butyrate. Waste Manag. 76, 394–403. https://doi.org/10.1016/j.wasman.2018.03.037

Yang, Z., Sun, H., Zhou, Q., Zhao, L., Wu, W., 2020. Nitrogen removal performance in pilot-scale solid-phase denitrification systems using novel biodegradable blends for treatment of waste water treatment plants effluent. Bioresour. Technol. 305, 122994. https://doi.org/10.1016/j.biortech.2020.122994

Yilmaz, P., Parfrey, L.W., Yarza, P., Gerken, J., Pruesse, E., Quast, C., Schweer, T., Peplies, J., Ludwig, W., Glöckner, F.O., 2014. The SILVA and "all-species Living Tree Project (LTP)" taxonomic frameworks. Nucleic Acids Res. 42, 643–648. https://doi.org/10.1093/nar/gkt1209

Zanaroli, G., Balloi, A., Negroni, A., Daffonchio, D., Young, L.Y., Fava, F., 2010. Characterization of the microbial community from the marine sediment of the Venice lagoon capable of reductive dechlorination of coplanar polychlorinated biphenyls (PCBs). J. Hazard. Mater. 178, 417–426. https://doi.org/10.1016/j.jhazmat.2010.01.097

Zanaroli, G., Negroni, A., Vignola, M., Nuzzo, A., Shu, H.Y., Fava, F., 2012. Enhancement of microbial reductive dechlorination of polychlorinated biphenyls (PCBs) in a marine sediment by nanoscale zerovalent iron (NZVI) particles. J. Chem. Technol. Biotechnol. 87, 1246–1253. https://doi.org/10.1002/jctb.3835

Ziv-El, M., Delgado, A.G., Yao, Y., Kang, D.W., Nelson, K.G., Halden, R.U., Krajmalnik-Brown, R., 2011. Development and characterization of DehaloR 2, a novel anaerobic microbial consortium performing rapid dechlorination of TCE to ethene. Appl. Microbiol. Biotechnol. 92, 1063–1071. https://doi.org/10.1007/s00253-011-3388-y

Zopfi, J., Ferdelman, T.G., Fossing, H., 2004. Thiosulfate, and elemental sulfur in marine sediments. Geol. Soc. Am. 379, 97–116.

3.7 Supplementary materials

Summary

S1 – Figure S1 - Cumulative CO_2 production

S2 – Figure S2 - Profile in time of the sulfate concentrations of the aqueous phase

S3 – Figure S3 - Profile in time of 3HB concentration in the aqueous phase

S4 – Table S1 - Summary of the main chemical-physical parameters reported in the literature for the studied sediments

S5 – Table S2 - Summary of the concentrations of heavy metals and polycyclic aromatic hydrocarbons reported in the literature for the studied sediments

S1

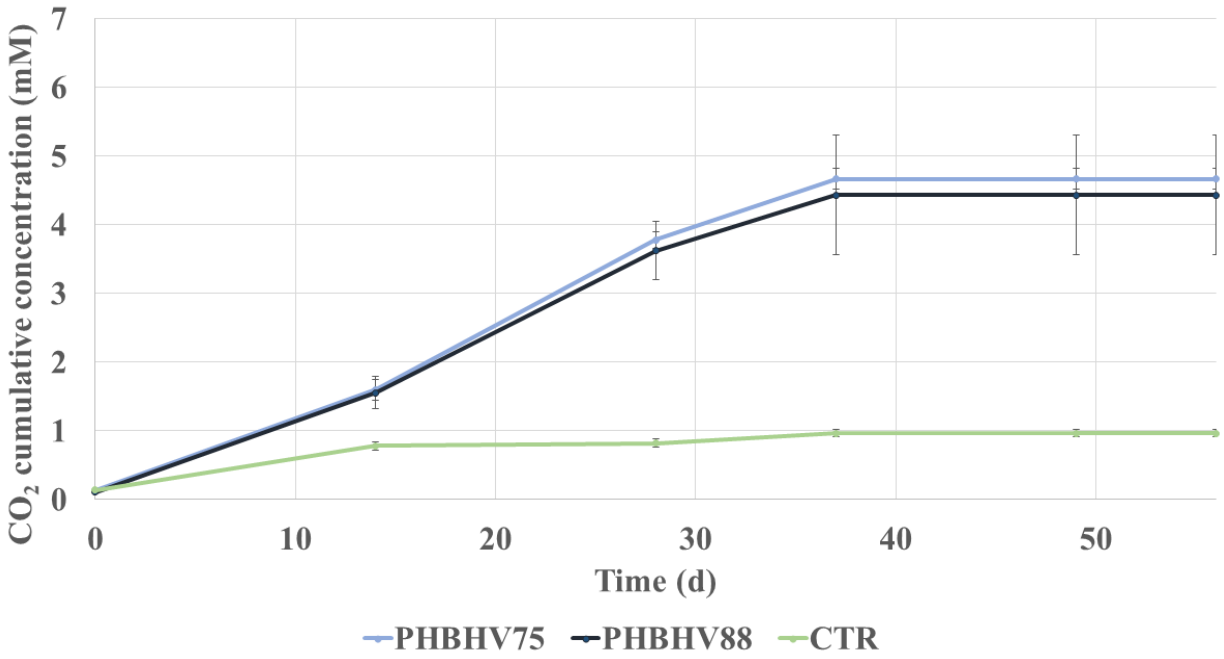

Figure S1. *Cumulative CO_2 production in the control, unamended microcosms (CTR), and in those amended with PHAs (PHBHV75 and PHBHV88).*

Fig. S1 illustrates the CO_2 cumulative production observed in lab-scale microcosms of a previous experiment. The incubation time required to complete degrade the heteropolymers was estimated from the gas profile. On day 37, the CO_2 cumulative concentrations were 4.7 ± 0.1 for PHBHV75, 4.4 ± 0.9 mM or PHBHV88 and 0.96 ± 0.06 mM for the control. A plateau in the gas production was observed after 37 days from the addition of the heteropolymers. Thus it was speculated that in the studied condition the polymers were depleted in less than 37 days.

S2

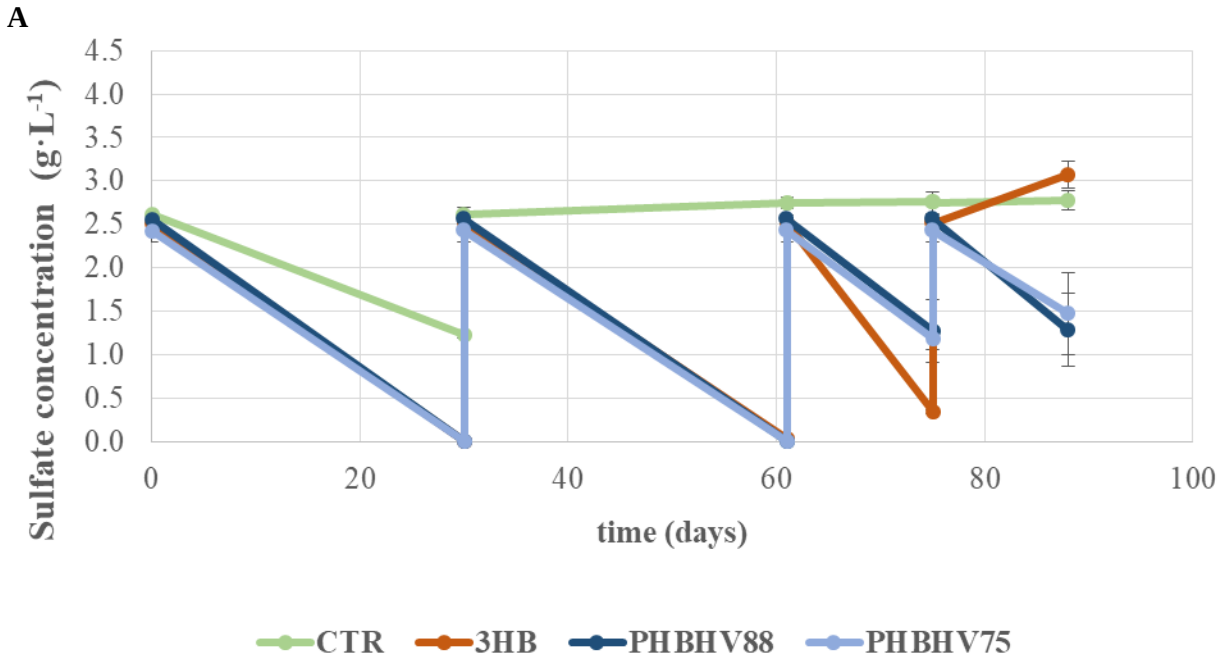

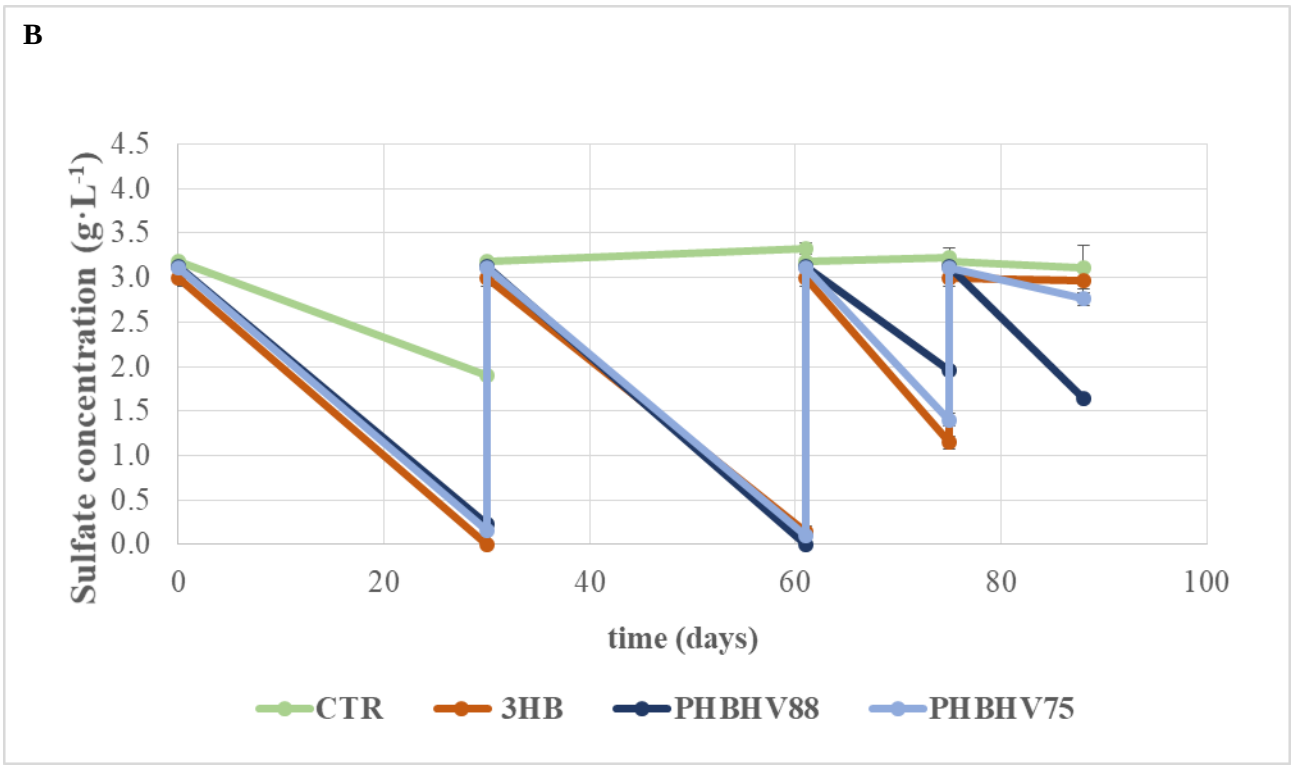

Figure S2. *Profile in time of the sulfate concentrations of the aqueous phase in the control, unamended microcosms (CTR), and in those amended with the monomer (3HB) and PHAs (PHBHV75 and PHBHV88) for R-sediments (A) and T-sediments (B). Sulfates were replenished on days 30 and 61.*

S3

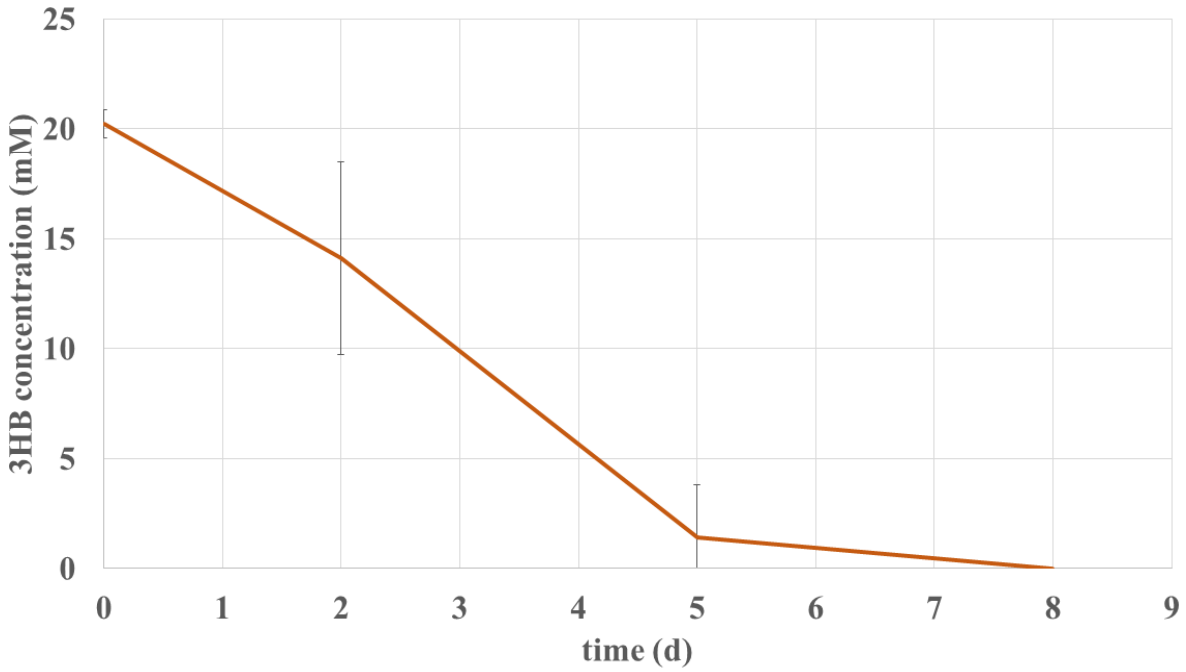

Figure S3*. Profile in time of 3HB concentration in the aqueous phase in the lab-scale microcosms*

S4

Table S1 *Summary of the main chemical-physical parameters reported in the literature for the studied sediments*

Reference	pH	TOC (%)	TN (%)	Sand (%)	Mud (Clay and Silt) %
Pialassa della Baiona, Ravenna					
(Ponti et al., 2011)		3.5-2.5[c]		12-90	
(Guerra, 2012)		2.81[a,d]			41[a]
(Guerra et al., 2013)		0.76-3.45[d]	0.1-0.48		
(Guerra et al., 2014)		5.4[c]			33
(Borghesi et al., 2016)		5.2[c]			
(Sfriso et al., 2020)	7.4	1.2[d]			
(Guerra et al., 2022)		2.3[d]			
Mar Piccolo, Taranto					
(Quero et al., 2015)		20.1[a,c]		29[a]	70[a]
(Vitone et al., 2016)				23[a]	76[a]
(Di Leo et al., 2016)	7.87	4.06[,d]		10	89.9
(Mali et al., 2017)	7.26	2.57[b]		19.5	77
(Todaro et al., 2019)		16.7[a,c]			
(Sollecito et al., 2019)		9-18[c]			
(Todaro et al., 2020)		21.3 [a,c]		8.5 [a]	91.5 [a]
(Mali et al., 2020)		2.5[d]	0.22	19.5	77

[a]value presented as average of the data reported in the article
[b]method used to determine TOC is not specified
[c]TOC determined via EPA 160.4 as loss of ignition (LOI)
[d]TOC determined with elemental analyzer

S5

Table S2 *Summary of the concentrations of heavy metals and polycyclic aromatic hydrocarbons reported in the literature for the studied sediments, expressed as* $mg \cdot Kg_{drysediment}^{-1}$

Reference	Al	As	Cd	Cr	Cu	Fe	Hg	Mn	Ni	Pb	V	Zn	PAH
Pialassa della Baiona (Ravenna)													
(Ponti et al., 2011)							0.1-41						
(Guerra, 2012)	46300			160	47	24700	46					270	14[a]
(Guerra et al., 2014)				84	38	21580	4	428	43			123	
(Borghesi et al., 2016)	13257	7	0.4		47	22943	5	546	51	21	31	141	
(Pignotti et al., 2018)					42		2		71		104	167	
Mar Piccolo (Taranto)													
(Quero et al., 2015)	24660[a]	14[a]	0.4[a]	57[a]	93[a]	28029[a]	3.9[a]	350[a]	41[a]	84[a]		261[a]	1.8[a]
(Bellucci et al., 2016)	26636[a]	15[a]	0.5[a]	61[a]	100[a]	30156[a]	4.2[a]	366[a]	44[a]	89[a]		281[a]	1.8[a]
(Mali et al., 2017)	31938	13	0.4	56	48	28823	2.5		50	63	56	168	1.1
(Todaro et al., 2019)		12	0.4		40		3.8		39	63	52	94	
(Mali et al., 2020)	31901	10	0.3	56	34	28791	0.9		47	47	56	2	
(Todaro et al., 2020)		44[a]	1[a]	75[a]	124[a]		14[a]		51[a]	247[a]	95[a]	440[a]	5.1[a]
(Cotecchia et al., 2021)													3.9[a]

[a]value presented as average of the data reported in the article

Chapter 4

Microbial electrochemical technologies to bioremediate PCBs polluted sediments

4.1 Introduction

In situ bioremediation of PCBs polluted marine sediments has been targeted as an economical and environmental sustainable approach to remove this class of pollutants from the environment (Sowers and May, 2013). The complete bioremoval of PCBs requires two sequential-steps mediated by bacteria which transforms high-chlorinated PCBs to, ideally, carbon dioxide and chlorine. The first step is defined as reductive dehalogenation. It is carried on by bacteria called organohalide respiring bacteria (OHRB) which anaerobically transform high-chlorinated PCBs to low-chlorinated PCBs (Häggblom and Bossert, 2003). To do so, OHRB need a source of protons and electrons, i.e. hydrogen. The second step is labeled as oxidative degradation. It is an aerobic process which converts low chlorinated PCBs to benzoic acids, via the biphenyl pathway, thanks to bacteria named PCBs aerobic degraders (Mondello, 1989). Given to the diverse operational conditions of the two mechanisms, it is unlikely to encounter a spontaneous complete bioremediation process in the environment (Sowers and May, 2013). Additionally, PCBs bioremoval requires a long time to take place since time scale of reductive dechlorination are of months/years (Fagervold et al., 2011). The process can be primed by supplying the needed growth substrates, adding fermentable molecules as acetic acids or lactic acids (Lu et al., 2021; Song et al., 2015). Yet, the addition of external molecules to the polluted site suffers from two main disadvantages: (i) the need of frequent replenishment of the amendments due to their fast depletion compared to the bioremediation time (Baric et al., 2014; Lu et al., 2021), (ii) the undiscriminating stimulation that can favor other species competing with OHRB in consuming the electron donors (e.g. H_2) , as methanogen producing bacteria (MB) or sulfate reducing bacteria (SRB) (Aulenta et al., 2008).

To overcome these drawbacks, Microbial Electrochemical Technologies (METs) have been identified as a possible alternatives to conventional electron donors (Chun et al., 2013). METs couple microbial activity with electrodes to use the former as biocatalyst and the latter as source or sink for electrons (Logan et al., 2019). In particular, METs can be used to prime both the reductive dehalogenation and the oxidative degradation of PCBs (Chun et al., 2013). The cathodic stimulation can supply the required electrons to reduce high-chlorinated PCBs to low-chlorinated PCBs. Electrons can be exchanged either via a direct electron transfer between electrodes and bacteria or via an indirect electron transfer, i.e. mediated by hydrogen (Paquete et al., 2022). Instead, the anodic electrolysis of water can provide *in situ* the oxygen required to cleave the aromatic structure of low-chlorinated PCBs. Additionally, the applied potential allows to tune the electrical stimulation so as to prime the target metabolism, guaranteeing a constant and selective stimulation of OHRB (Aulenta et al., 2011; Lin et al., 2019). For instance, the

application of METs systems has been demonstrated by Aulenta *et al.* (2011) and Lin *et al.* (2019) , who stimulated reductive dechlorination without priming other anaerobic metabolisms, as methanogenesis, by controlling the applied potential. Moreover, METs are stable systems that can perform a long lasting stimulation, optimal for priming microbial activities characterized by slow kinetic. In this regard, the endurance of the MET tested by Aulenta et al. (2011) was proved on a long term (570 days). Although the theoretical basis support the use of bioelectrochemical system to perform complete bioremediation of PCBs polluted sediment, to date the utilization of METs to specifically biostimulate PCBs bioremoval has been reported only as proof of concept in river sediments and mainly to stimulate reductive dechlorination. Cathodes polarized at -0.46 V vs Ag/AgCl (3M KCl) primed the reductive dechlorination of a freshly spiked single congener (PCB 61) (Liu et al., 2017; Yu et al., 2017). Carbon paper bioanode poised at 0.24 V vs Ag/AgCl (3M KCl) enhanced the reductive dechlorination of PCB 61 (Yu et al., 2016). The only proof of concomitant reductive dechlorination and oxidative degradation was given by Chun *et al.* (2013). They applied constant cell voltages to stimulate the bioremoval of indigenous weathered mixture and freshly spiked PCBs, observing an optimum of dechlorination rate according to the applied potential. Conversely, for what concern the marine environment, little evidence has been provided on the use of METs, especially for bioremediation of PCBs polluted sediments. Zhang *et al*. (2021) studied the bioelectrochemical stimulation of a microbial community obtained from marine sediments, in anaerobic synthetic medium. They reported a raise in dechlorination rate of Aroclor 1260 when working with graphite rod polarized at -0.55 V vs Ag/AgCl (3M KCl) compared to open circuit conditions.

It should be considered that marine environments profoundly differ from freshwater environments. For instance, microbiota of marine habitats is richer in sulfate reducing bacteria (SRB) (Wang et al., 2012), competitors of OHRB in up taking hydrogen thanks to their high affinity to it (Dolfing, 2003). Consequently, the bioelectrochemical stimulation needs to be as selective as possible. Marine waters are also characterized by high salt content that can lead to unwanted parallel reactions. At sufficient anodic potential (>1.1 V vs Ag/AgCl 3M KCl)(Bard and Faulkner., 2001), chlorine evolution reaction (CLER) can take place, resulting in the production of disinfectant agents and lowering the coulombic efficiency of the process since CLER competes with oxygen evolution reaction (OER) (Karlsson and Cornell, 2016). Currently, effective and easy to synthetize materials to enhance OER compared to CLER have not been identified. It is known that metal-oxides catalyst can have high selectivity for OER, although they usually require ideal conditions (pH > 12) (Dionigi et al., 2016; Jiang et al., 2022) not applicable in

real matrixes. A simple and effective electrode modification was suggested by Balaji *et al*. (2009), who covered metal anodes using a Nafion^{TM} membrane. They speculated that the cation exchange membrane acted as a barrier for the negative charged chlorine, inhibiting the CLER. Yet, no details were given about the durability of the modified electrode and its suitability in real system. Another strategy to avoid chlorine production might be the use of sacrificial anodes (Mao et al., 2011), though OER would be avoided too. On the other hand, the high salinity of marine waters guarantees a higher conductivity (Palacky, 1987) that could favour the electron exchanges compared to freshwater environments, where the addition of conductive materials as biochar might be needed to enhance electron transfers (Viggi et al., 2022). The high conductivity could also mitigate the pH gradient formation in proximity to the electrodes, which are likely to establish in groundwater due to the low conductivity (Logan et al., 2006; Puggioni et al., 2021). Indeed one of the main drawbacks of METs operated under static condition is the pH gradient in proximity of the electrodes. Chun *et al.* (2013) reported cathodic and anodic pH values >11 and <4, respectively, after only 54 days of operation when applying METs to enhance bioremediation of PCBs polluted river sediments. The extreme pH can alter the microbial community composition, inhibiting the survival of keystone species for bioremediation. A neutral pH is optimal for reductive dechlorination whereas more acidic or alkaline values can slow down or even completely inhibit the process (Chang et al., 2004; Holliger et al., 1998; Philips et al., 2013). Thus, strategies need to be developed to maintain pH as constant as possible considering the length of the bioremediation process. A possible solution to reduce pH variation is the periodic polarity inversion of the electrodes (Jiang et al., 2016; Li et al., 2014; Sun et al., 2015). Yet, appropriate electrode materials should be used to guarantee their stability within the range of working potential. A MET with an intermittent application of the voltage was studied by Bellagamba *et al.* (Bellagamba et al., 2017). The system was only partially effective since in 104 days, the sediment's pH decreased from 7.4 to 6.3 when applying the periodic stimulation, while the continuous system reduced the pH to 5.9. Up to now, a consolidate solution to control the pH variation in METs under batch conditions has not been identified.

Considering the lack of a consistent strategy to favor OER in seawater, in this experiment an initial study about anodes covered with Nafion^{TM} was carried on. After having assessed the not applicability of the electrodes due to their low endurance, iron plate were chosen as sacrificial anode to guarantee the stability of the METs for the stimulation of an enriched microbial community able to reductively dechlorinate PCBs in marine sediments, under *in situ* like conditions. A two-antiparallel circuits configuration (2AP-system) was compared to conventional METs set-up to evaluate the possibility to control the pH

variation. In the 2AP-system, the open and closed circuit were respectively and periodically switched on and off. During the experiment we aimed at evaluating the influence of the electrochemical input on the sediment, both from a chemical-physical and a microbial perspective. In particular, the impact of the METs was assessed on (i) the physical-chemical parameters, *i.e.* pH and redox potential (ORP), (ii) the main anaerobic bacterial metabolisms of interest, *i.e*. sulfate reduction and reductive dechlorination, by monitoring the means of metabolites and (ii) the overall biodiversity and composition of the sediment microbial community.

4.2 Materials and methods

4.2.1 Preliminary study to enhance the selectivity of OER in respect to CLER

H-cell (375 mL) were used to study the applicability of a Nafion^{TM} membrane to enhance the oxygen evolution reaction in respect to chlorine evolution reaction. Each chamber was filled with 325 mL volume of electrolyte, leaving 50 mL of headspace. Plates of stainless steel (SS) 316 (surface area 2.5 cm^2) were used both as anode and cathode. Three different tests were conducted: test I, II and III. The aim of test I was to assess the oxygen generated by pristine electrodes in marine synthetic water. Two different electrolytes were used: a control solution, $NaNO_3$ (0.5 M), and synthetic marine water, NaCl (0.5 M). A current of 5 $mA \cdot cm^{-2}$ was applied for 45 min and the amount of oxygen in the solution and in the headspace was monitored. Subsequently, in test II, it was evaluated the electrochemical oxygen production with modified SS anode in electrolyte rich of chlorine. The SS 316 electrode used as anode was covered with a Nafion^{TM} 117 membrane via hot pressing (175°C, 5000 psi, 10 min). Two different electrolytes were used: a control solution, $NaNO_3$ (0.5 M), and synthetic marine water, NaCl (0.5 M). A current of 5 $mA \cdot cm^{-2}$ was applied for 90, 150 and 210 min and the amount of oxygen in the solution and in the headspace was monitored. Finally, test III aimed to assess the durability of the modified electrode. A SS plate covered with Nafion membrane was used as anode. The electrolyte was synthetic marine water. A current of 5 $mA \cdot cm^{-2}$ was applied for 150 min and the amount of oxygen in the solution and in the headspace was monitored. After each cycle, electrolyte was changed and the electrode was left in distilled water overnight. The electrochemical cycle was repeated until the electrode was not compromised, i.e. the potentiometer gave a signal of over load due to the excessive potential required to flow the current. A system with no voltage applied was used to monitor the oxygen infiltration. Each test was run in triplicate. The results obtained in these trials were reported and discussed in the supplementary

materials (section S1). Considering the low durability of the modified anodes, the bioelectrochemical stimulation of bioremediation of PCBs polluted sediments focused on the sole reductive dechlorination via use of sacrificial anodes, as explained in the following paragraphs.

4.2.2 Microcosms set-up and operation

Laboratory scale microcosms were prepared using glass tanks (15x15x10 cm). Under continuous nitrogen flow and stirring, the marine sediment (collected in Pialassa della Baiona, Ravenna, Italy) was mixed with real seawater, inoculated (5% v/v) with a marine culture previously enriched with OHRB able to reductively dechlorinate PCBs (Nuzzo et al., 2017) and spiked with Aroclor 1254 to a final concentration of 100 $mg \cdot Kg_{drysediment}^{-1}$. The so prepared slurry was added to each glass tank up to 9 cm (approximately 1 Kg of wet sediment) and covered up to 12 cm with real seawater, reaching final microcosm volume of 1.8 L. A graphite rod (20 cm^2) was used as cathode (WE, working electrode) while an iron plate (20 cm^2) was used as anode (CE, counter electrode). The iron plate was chosen as sacrificial anode to avoid anodic chlorine production, using a configuration similar to the one suggested by Mao *et al.* (2011). Ag/AgCl (3M KCl) was used as reference electrode (RE) (unless stated otherwise, all the potentials reported in the manuscript will be expressed according to the reference electrode). The bioelectrochemical stimulation of the reductive dechlorination was studied applying a potential of -0.7 V vs Ag/AgCl, a current of 0.025 $mA \cdot cm^{-2}$ and of 0.05 $mA \cdot cm^{-2}$. The potentiostatic condition was studied using single circuit system. As for the galvanostatic conditions, the bioelectrochemical systems were studied in single and double circuit set-up to control the pH variation due to the higher current applied (Figure 1). In the double system, two antiparallel circuits (2AP-system) were placed in the microcosms. The system was operated with one circuit open and one closed. The open and closed antiparallel circuits were respectively closed and open if the value of pH in the proximity of the electrodes exceeded the range 6.5-8.5, typical interval for marine sediments (Widdicombe et al., 2011). Microcosms were sampled weekly to monitor pH and ORP and monthly to monitor PCBs and sulfates (each sample was collected in triplicate). In the 2AP-system area 1 and area 2 were defined as the sampling points next to the cathode and anode of the closed circuit at the beginning of the experiment (Figure 1). Microcosms were left at room temperature and exposed to the laboratory atmosphere. The evaporated overlaying water was periodically replenished with sterile deionized water previously flushed with nitrogen. The experiment lasted for 159 days.

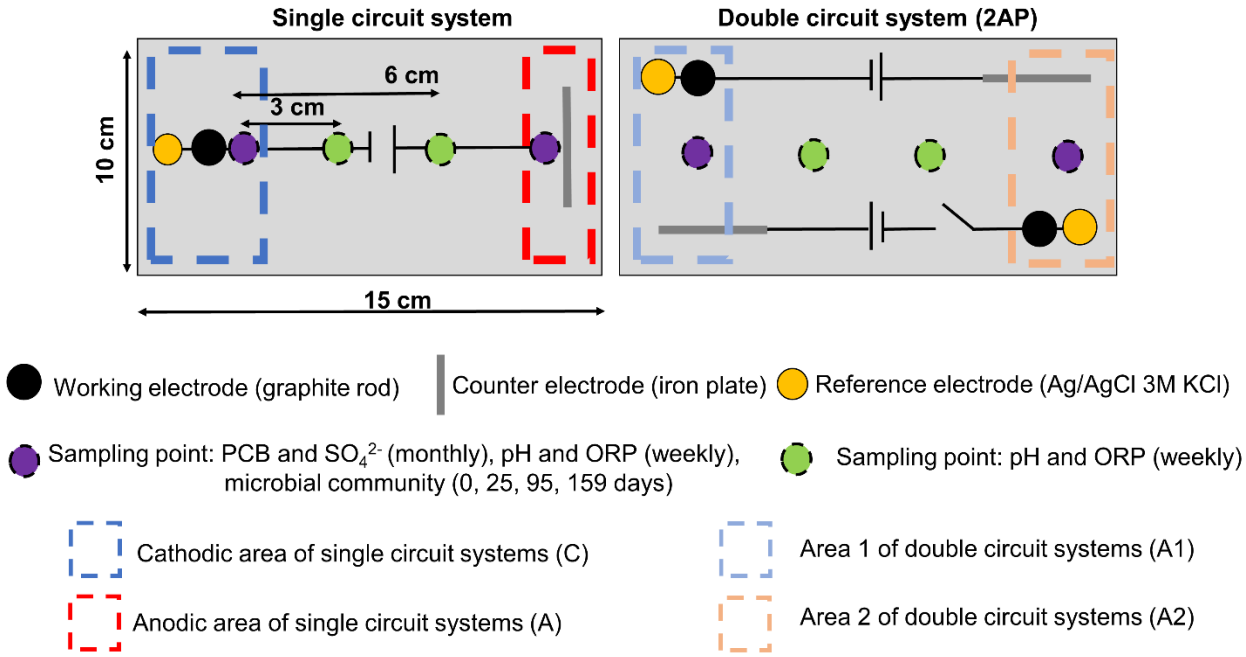

Figure 1 *Experimental design of single (both potentiostatic, P-0.7, and galvanostatic, G0.025 and G0.05) and double circuit (galvanostatic only, G0.025_2AP and G0.05_2AP) systems. Spatial distribution of electrodes (working electrode, counter electrode, reference electrode) and sampling points for PCB and SO_4^{2-} concentration, as well as for pH and ORP measurements and microbial community are indicated using different colors. Definition of cathodic (C) and anodic (A) areas in single circuit systems, as well as Areas 1 and 2 (A1 and A2) in double circuit systems, is here provided as blue-red and lightblue-pink dashed lined squares, respectively.*

4.2.3 Extraction and analysis of PCBs

PCBs in the sediment were extracted following a modified method from Rosato *et al.* (2020). Batch extraction was performed overnight at 30°C and 150 rpm from 1 mL of sediment slurry, with 3 mL of a hexane:acetone (9:1) mixture and octachloronaphtalene (OCN) (0.04 $mg \cdot L^{-1}$) as internal standard. The recovered organic phase was filtered on an Extrabond® Silica column (Scharlab, Barcelona, Spain) and added with 10 mg of elemental copper (Sigma Aldrich, St. Luis, Missouri, USA) as described in (Riis and Babel, 1999). An aliquot of the sample was placed in 1.5 mL vials for gas-chromatography (GC) equipped with Teflon coated screw caps (LLG-Labware, Meckenheim, Germany). The qualitative and quantitative analysis of the extracted PCBs was performed with a gas chromatograph (6890 series II) equipped with a HP-5 capillary column (30 m by 0.25 mm), a ^{63}Ni electron capture detector (µECD) and a 6890 series II automatic sampler (Agilent Technologies, Santa Clara, CA, USA). The column was

operated at the following conditions: initial temperature 60°C; isothermal for 1 min; initial temperature rate 40°C/min; final temperature 140°C; isothermal for 2 min; initial temperature rate 1.5°C/min; final temperature 185°C; initial temperature rate 4.5°C/min; final temperature 275°C; isothermal for 5 min; injector (splitless mode), 250°C; detector ECD, 320°C; carrier gas flow rate (N_2) 1.5 mL/min; sample volume 1 µl. Aroclor PCBs, injected in the presence of OCN, were identified as described in Fava *et al.* (2003) by matching the detected peaks with the chromatographic profiles of the standard PCBs mixtures Aroclor 1254 and Aroclor 1242 previously characterized (Frame et al., 1996) and comparing the retention time (relative to OCN) of each peak with those of PCBs of the same standard Aroclors analyzed under identical conditions. Quantitative analysis of the freshly spiked PCBs and their possible dechlorination products was performed by using the GC-ECD response factor of each target PCB congener or group of co-eluting congeners obtained from six-points calibration curves (0.5-50 $mg \cdot L^{-1}$) of Aroclors 1254 and 1242 and the weight percentage of each congener occurring in the same Aroclors reported elsewhere (Frame, 1997). PCBs concentrations were expressed as µmol of $PCBs \cdot kg_{dry\ sediment}^{-1}$. The chlorination degree and the reduction percentage of the chlorination degree were calculated as reported in eq. 1 and 2.

(1) $$Chlorination\ degree = \frac{\mu mol\ of\ organic\ chlorine}{\mu mol\ of\ total\ PCBs} = \frac{\sum C_i \times n_i}{\sum C_i}$$

(2) $$Reduction\ percentage\ of\ the\ chlorination\ degree = \frac{Chlorination\ degree\ (0\ days) - Chlorination\ degree\ (n\ days)}{Chlorination\ degree\ (0\ days)}\ x\ 100$$

Where n is the number of days of each sampling (25, 63, 95, 124, 159)

4.2.4 Analytical methods, instrumentation and calculations

Oxygen in the headspace was monitored using a a µGC (model 3000 A – Agilent Technologies, Milano, Italy) under the following conditions: injector temperature 90 °C; column temperature 60 °C; sampling time 20 s; injection time 50 ms; column pressure 25 psi; run time is 45 s and the carrier gas was nitrogen. Oxygen in the solution was monitored using a pO_2 sensor VisiFerm DO 225 (ECS) (Hamilton, Reno, Nevada, U.S.A.). The sensor was calibrated using a two points calibration curve, using water flushed with nitrogen and air as 0% and 100% points of air saturation, respectively. The concentration of SO_4^{2-} in the water phase of the sediment slurry was determined using a Dionex ICS-1000 ion chromatograph

equipped with an IonPac AS14 4 mm × 250 mm column, a conductivity detector combined to an AERS-500 suppressor system (Dionex, Sunnyvale, CA, USA). Quantitative analysis were performed using the conductivity detector response factor obtained from a five points calibration curve (0.5-50 $mg \cdot L^{-1}$) of Na_2SO_4. pH and ORP were measured using an XS sensor polymer S7 (XS Instruments, Carpi, Italy) and an Inlab Redox Micro (Mettler Toledo, Columbus, Ohio, U.S.A.). All the electrochemical experiments were performed using an Ivium-n-Stat multichannel (Ivium technologies, Eindhoven, Netherlands). Potentiostatic data are reported in Supplementary Figures S18-S22 and Supplementary Table S8. For statistical analysis of data, significant differences were tested using t-test, 0.05 as significance threshold and adjusting the obtained p-values. R statistical software (https://www.r-project.org/) was used to perform statistics. The electron balance (EB) for the sulfate reduction at the end of the experiment (159 days) was calculated considering the chemoorganotrophic contributions and the chemolithotrophic contributions (eq. 3) (Dai et al., 2022; Luo et al., 2014). The chemoorganotrophic contributions were estimated according to the activity of the open circuit microcosms and expressed as the ratio between the reducing equivalents, as coulombs, required for the sulfate reduction of the O.C.V. and of each bioelectrostimulated system (eq. 4). The chemolithotrophic contributions were calculated assuming that all the electrons supplied were delivered to sulfate reducers and expressed as the ratio between the accumulated charge and the reducing equivalents, as coulombs, required for the sulfate reduction in each bioelectrostimulated system (eq. 5). The electron balance of each bioelectrostimulated system was calculated as the average between cathode/anode or area1/area2 since no significant differences in terms of sulfate reduction were observed in each microcosms. Coulombic efficiencies (CE) were calculated considering only the chemolithotrophic sulfate contribution, as reported in eq. 6.

(3) $$Electron\ balance\ (EB) = Chemoorganotrophic\ contributions + Chemolithotrophic\ contributions$$

(4) *Chemoorganotrophic contributions*

$$= \frac{\left(C_{SO_4^{2-}\ 0\ days,\ O.C.V.} - C_{SO_4^{2-}\ 159\ days,\ O.C.V.}\right) * V * MM_{SO_4^{2-}}{}^{-1} * n_{SO_4{}^{2-}/S^{2-}} * F}{\left(C_{SO_4^{2-}\ 0\ days,\ METs_i} - C_{SO_4^{2-}\ 159\ days,\ METs_i}\right) * V * MM_{SO_4^{2-}}{}^{-1} * n_{SO_4{}^{2-}/S^{2-}} * F} x\ 100$$

(5) *Chemolithotrophic contributions*

$$= \frac{accumulated\ charge\ (C)}{\left(C_{SO_4^{2-}\ 0\ days,\ METs_i} - C_{SO_4^{2-}\ 159\ days,\ METs_i}\right) * V * MM_{SO_4^{2-}}{}^{-1} * n_{SO_4{}^{2-}/S^{2-}} * F} x\ 100$$

(6) Coulombic efficiency % (CE)

$$= \frac{\left(C_{SO_4^{2-}\ 0\ days,\ METs_i} - C_{SO_4^{2-}\ 159\ days,\ METs_i} - \left(C_{SO_4^{2-}\ 0\ days,\ O.C.V.} - C_{SO_4^{2-}\ 159\ days,\ O.C.V.}\right)\right) * V * MM_{SO_4^{2-}}{}^{-1} * n_{\frac{SO_4{}^{2-}}{S^{2-}}} * F}{accumulated\ charge\ (C)}$$

$$x\ 100$$

Where C_i is the molar concentration of each detected PCBs congener (µmol·kg$_{\text{dry sediment}}^{-1}$); n_i is the number of Cl substituents; $C_{SO_4^{2-}\ 0\ days}$, sulfate concentration at the beginning of the experiment (g·L^{-1}); $C_{SO_4^{2-}\ 159\ days}$, sulfate concentration at the end of the experiment (g·L^{-1}); V, total volume of the microcosm expressed as L; O.C.V. is the open circuit microcosms; METs$_i$ indicates the bioelectrochemical systems and i stands for: -0.7 V, 0.025 mA·cm^{-2}, 0.025 mA·cm^{-2}-2AP, 0.05 mA·cm^{-2}, 0.05 mA·cm^{-2}-2AP; F is the Faraday constant (96 485 C·mol^{-1}); $MM_{SO_4^{2-}}$ is the molecular weight of sulfate (96.06 g· mol^{-1}); $n_{SO_4{}^{2-}/S^{2-}}$ represent the equivalent electrons required for the redox reaction, 8.

4.2.5 Bacterial DNA extraction, 16S rRNA gene amplification and sequencing

Approximately 450 mg of sediment samples were used for characterization of the inhabiting microbial community. Samples of the slurry added to the lab-scale microcosms at the beginning of the experiment (Inoculated sediment) and of the sediment around the electrodes of each microcosm after 25 (25d), 95 (95d) and 159 (195d) days of incubation were analyzed. Each sample was collected, as reported in Fig 1., and analyzed in triplicates. DNA extraction was performed using DNeasy PowerSoil Kit (Qiagen, Hilden, Germany) following the manufacturer's instructions. Extracted DNA samples were quantified using Qubit 3.0 fluorimeter (Invitrogen, Waltham, MA, USA) and stored at –20 °C until further processing. The V3-V4 hypervariable region of the 16S rRNA gene was PCR amplified as described in Botti et al., (2023). PCR products were purified using Agencourt AMPure XP magnetic beads (Beckman Coulter, Brea, CA, United States). Indexed libraries were prepared by limited-cycle PCR with Nextera technology and cleaned-up with the same magnetic beads protocol. Libraries were then normalized to 4

nM and pooled, prior to denaturation with 0.2 N NaOH. Sequencing was performed on Illumina MiSeq platform using a 2 × 250 bp paired-end protocol, following the manufacturer's instructions (Illumina, San Diego, CA, United States).

4.2.6 Bioinformatics and statistics

Paired-end sequenced reads were merged using the VSEARCH algorithm (v2.15.2) (Rognes et al., 2016) and analysed using QIIME2 (version 2022.8) pipeline (Bolyen et al., 2019). The DADA2 (Divisive Amplicon Denoising Algorithm 2) (Hall and Beiko, 2018) plugin was used to remove noise, chimeras, and to generate Amplicon Sequence Variants (ASVs). ASVs were taxonomically assigned using the SILVA reference database version 138 (Yilmaz et al., 2014). The number of high-quality reads in samples ranged between 1,058 and 24,082 per sample, resulting in a rarefaction to the lowest number of sequences (1058). Beta-diversity was measured by calculating the weighted or unweighted UniFrac distances among samples. Microbial community relative abundance profiles at different phylogenetic levels were obtained; family level was chosen for graphical representation. Statistical analyses were performed using the R statistical software (www.r-project.org), v. 4.2.2, and the libraries vegan, made4 and rstatix. Sequence reads were deposited in the National Center for Biotechnology Information Sequence Read Archive (NCBI SRA; BioProject ID PRJ PRJNA956431).

4.3 Results

4.3.1 Impact of the electrochemical input on chemical-physical parameters and sediment microbial communities

Chemical-physical parameters (i.e. pH and ORP) of the sediment were monitored to explore the influence of the bioelectrochemical stimulation on the studied sediments. Considering that the values of pH and ORP obtained at the intermediate sampling points (3 and 6 cm, Fig. 1) were in line with the expected trend (Supplementary Figures S2-S13), to clarify the content of this paragraph the showed results will focus on the variations in proximity of the electrodes. At the beginning of the experiment, pH of the sediment was 7.5 ± 0.1. After 159 days, in the open circuit voltage control (OCV), pH reached values that were averagely more alkaline (7.9 ± 0.2, Fig. 2A; Supplementary Figure S2). In the closed circuit systems, pH changed proportionally to the intensity of the electrochemical input. Posing the cathode at -0.7 V had a limited effect on the sediments with final cathodic and anodic pH respectively equal to 7.9

and 7.4 (Fig. 2B; Supplementary Figure S3). On the contrary, applying current density of 0.025 and 0.05 $mA \cdot cm^{-2}$ reduced the anodic pH below 6.5 and increased the cathodic pH above 8.5 in both the single circuit systems (Fig. 2C and 2E; Supplementary Figures S4 and S6). Microbial community structure, explored using 16S rRNA gene sequencing, reflected this trend, as Principal Coordinates Analysis (PCoA) based on both weighted and unweighted UniFrac distances (Fig. 3) showed that as the cathodic pH progressively increased, microbial communities in cathode samples of microcosm stimulated under galvanostatic conditions (G0.025_C and G0.05_C) clustered separately from all the other samples. Furthermore, weighted UniFrac based PCoA performed separately on samples taken from each MET (Supplementary Figure S23) confirmed the progressive clusterization of cathode samples from the anodic ones after 95 and 159 days of experiment in single circuit galvanostatic conditions. In the 2AP, one circuit was operating at a time, leaving the remaining circuit opened. As the pH exceeded the range of value 6.5-8.5, the closed and open circuits were inverted mitigating the impact of the bioelectrochemical stimulation on sediments pH (Fig. 2D and 2F; Supplementary Figure S5 and S7). Average pH of A1 and A2 were equal to 7.1 ± 0.3 and 7.1 ± 0.5 in the system with 0.025 $mA \cdot cm^{-2}$ applied and 7.3 ± 0.7 and 7.1 ± 0.7 in the system with 0.05 $mA \cdot cm^{-2}$ applied. PCoA based on both weighted and unweighted UniFrac distances (Fig. 3) confirmed that the inversion of the circuits led to a more stable microbial community across time and between the areas around the electrodes, as the microbial community of samples showing a temporarily elevated pH at 159 days did not show separation in the PCoA plots from neutral and acidic samples (Fig. 3E and 3F).

Regarding the redox potential of the sediment, the initial ORP was -232 ± 14 mV. In the open circuit system, redox potential decreased to a final value of -425 ± 25 mV after 159 days (Supplementary Figure S8). As for the bioelectrochemically stimulated microcosms, the sediment in proximity to the anode showed higher potentials compared to the OCV (Table 1, Supplementary Figure S8-S12). Conversely, the potential of the sediment around the cathode decreased according to the intensity of the electrical stimulation (Supplementary Figure S9-S13). The lowest ORP value was observed after 118 days, applying 0.05 $mA \cdot cm^{-2}$ (-738 mV). In the 2AP, the inversion of the circuits mitigated the ORP gradient, with redox potential around -370 mV (Table 1). Conversely, cathodic and anodic redox potentials in single circuit systems ranged from -270 to -738 mV.

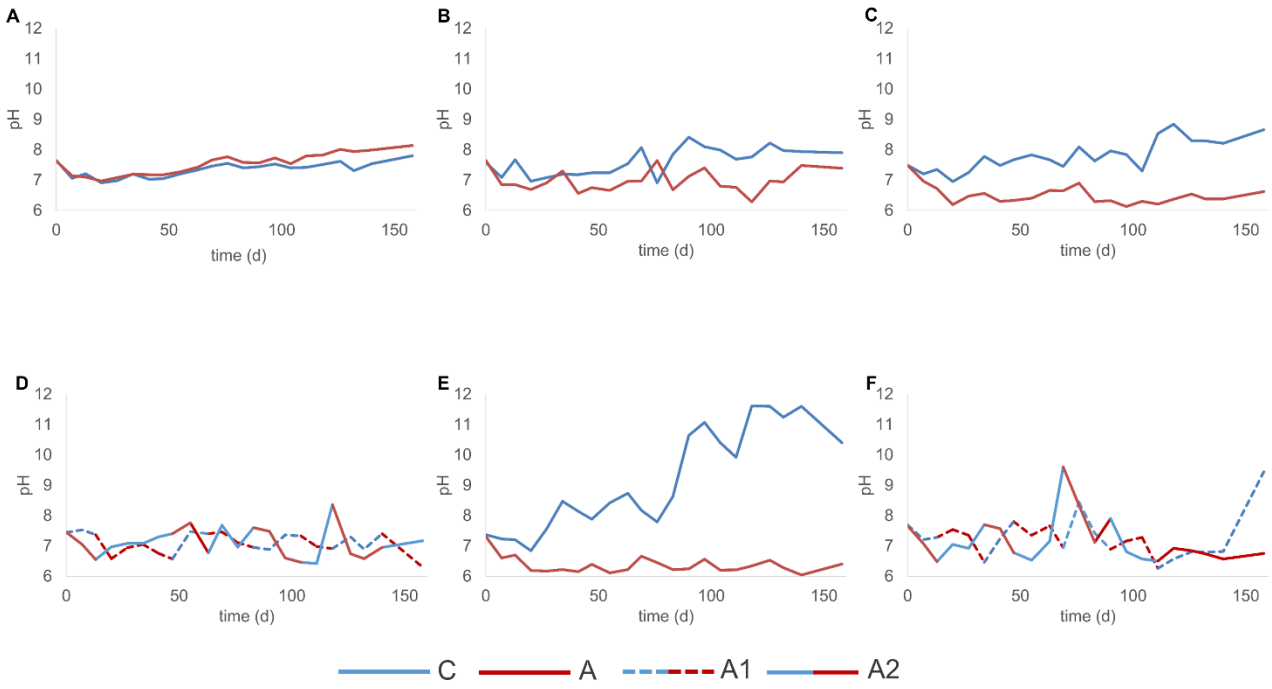

Figure 2 *pH dynamics in open circuit (OCV) microcosm (A), MET poised at -0.7 V (P-0.7) (B), single circuit MET stimulated with an applied current of 0.025 mA·cm^{-2} (G0.025) (C) and 0.05 mA·cm^{-2} (G0.05) (E), double circuit MET stimulated with an applied current of 0.025 mA·cm^{-2} (G0.025_2AP) (D) and 0.05 mA·cm^{-2} (G0.05_2AP) (F). Continuous blue and red lines indicate the area next to the cathode (C) and to the anode (A), respectively, in single circuit systems. Dashed blue and red lines indicate the area next to area 1 (A1) in double circuit systems, whereas alternated continuous blue and red lines indicate the area next to area 2 (A2) in double circuit systems; blue and red colors indicate a cathodic and an anodic polarization.*

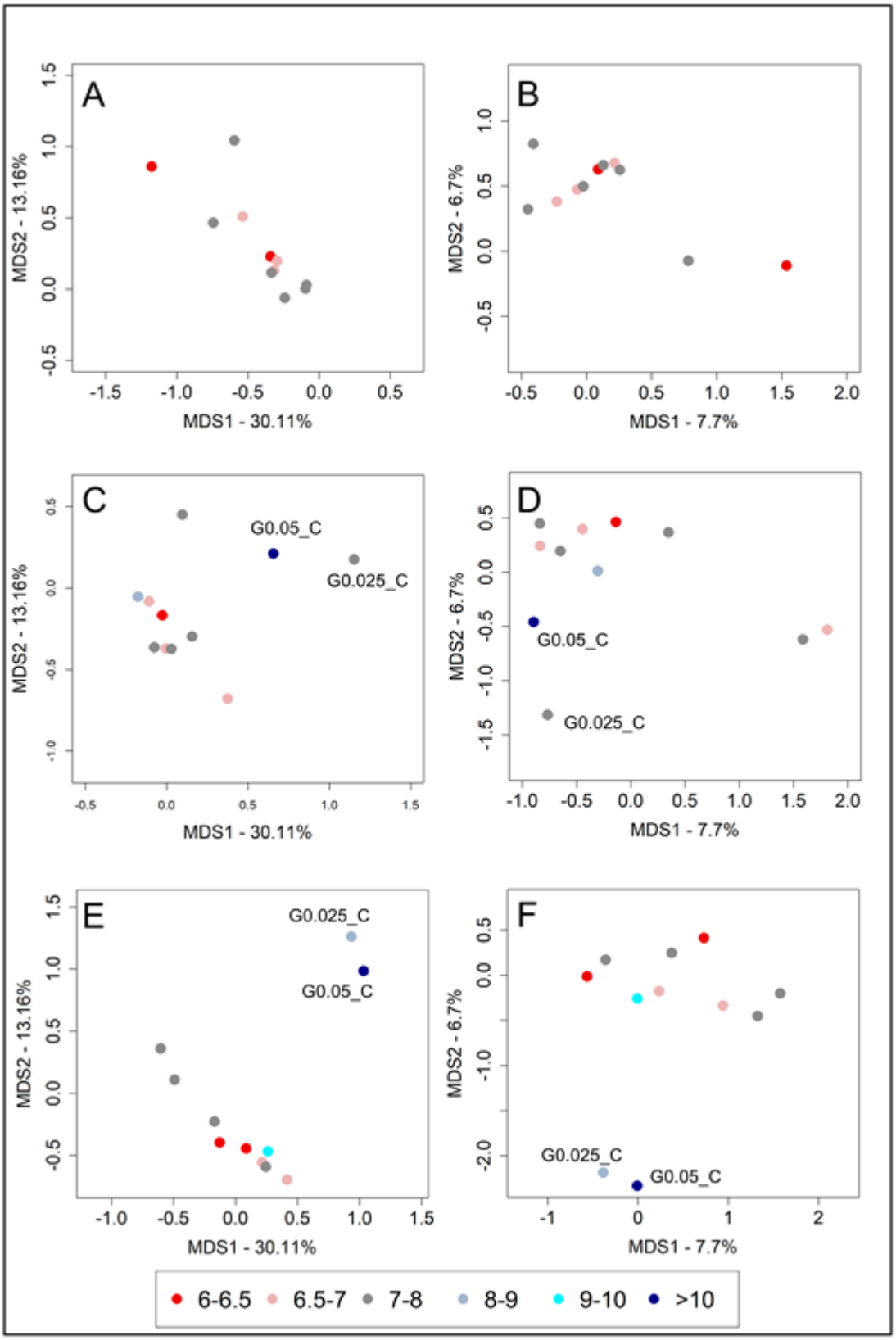
A
MDS2 - 13.16%
MDS1 - 30.11%
B
MDS2 - 6.7%
MDS1 - 7.7%
C
G0.05_C
G0.025_C
MDS2 - 13.16%
MDS1 - 30.11%
D
G0.05_C
G0.025_C
MDS2 - 6.7%
MDS1 - 7.7%
E
G0.025_C
G0.05_C
MDS2 - 13.16%
MDS1 - 30.11%
F
G0.025_C
G0.05_C
MDS2 - 6.7%
MDS1 - 7.7%
6-6.5
6.5-7
7-8
8-9
9-10
>10

Figure 3 *Impact of pH on the composition of the sediments' microbial community. PCoA based on weighted (A-C-E) and unweighted (B-D-F) UniFrac distances among sediments microbiota profiles of samples collected at 25 (A-B), 95 (C-D), and 159 days (E-F) from all METs evaluated in the present experiments. Samples are displayed according to the pH value recorded at the sampling time. Color legend for samples representation is reported (bottom). First and second coordination axes (MDS1 and MDS2) are plotted for each analysis. Percentages of variance in the dataset accounted for by MDS1 and MDS2 are reported. Label of samples that cluster separately are added for clarity: G0.025_C, cathodic area of the single circuit MET stimulated with an applied current of 0.025 mA·cm^{-2}; G0.05_C, cathodic area of the single circuit MET stimulated with an applied current of 0.05 mA·cm^{-2}.*

Table 1 *ORP of the lab-scale microcosms in the proximity to the electrodes at the end of the experiment (159 days) and as average values observed during the whole length of the experiment.*

Conditions[a]	ORP at 159 days (mV)	ORP along the experiment (mV, average ± standard deviation)
OCV	-425 ± 25[b]	-410 ± 55[b]
P-0.7_C	-315	-401 ± 62
P-0.7_A	-326	-354 ± 64
G0.025_C	-399	-433 ± 61
G0.025_A	-383	-341 ± 66
G0.025_A1	-393	-370 ± 75
G0.025_A2	-394	-367 ± 65
G0.05_C	-488	-563 ± 129
G0.05_A	-270	-318 ± 49
G0.05_A1	-552	-367 ± 75
G0.05_A2	-417	-378 ± 71

[a]*OCV indicates open circuit control. P-0.7 indicates MET poised at -0.7 V. G0.025 indicates MET stimulated with an applied current of 0.025 mA·cm^{-2}. G0.05 indicates MET stimulated with an applied current of 0.05 mA·cm^{-2}. C indicates the cathode. A indicates the anode. A1 indicates area 1 in double circuit systems. A2 indicates area 2 in double circuit systems.*
[b]*Data for the OCV are presented as average values of the sampling points.*

4.3.2 Anaerobic metabolisms progression and microbial community compositional dynamics

Inoculated starting sediment was mainly composed of sequences assigned to the families *Sulfurovaceae, Woeseiaceae* and *Desulfosarcinaceae* (Supplementary Figure S25). Along the five-months experiment

most appreciable changes in terms of microbial composition occurred in the microbial community around the cathode area of the single circuit systems stimulated with a current density of 0.025 and 0.05 $mA \cdot cm^{-2}$ compared to the OCV. In those samples (G0.025_C and G0.05_C), reads assigned to uncultured members of the Peptostreptococcales-Tissierellales group and of *Synergistaceae* reached 18% and 4.8% respectively, compared to the very low relative abundance in the OCV (0.03% and under detection limits, respectively). Moreover, members belonging to the family *Chlorobiaceae*, initially present below the detection limit, were enriched across the time of the experiment mainly in cathode area of MET with 0.025 $mA \cdot cm^{-2}$ applied current, reaching at 159 days a relative abundance of 15.7% compared to the 6.4 % of the open circuit. Nevertheless, in each studied condition a large portion of the sediments' biodiversity was represented by members of the phylum Desulfobacterota. Aiming at exploring the composition and dynamics of the sediments' microbiota members involved in sulfate reduction, a focus on phylogenetic groups commonly listed as potential SRB is provided at 25, 95 and 159 days, in relation to the temporal dynamic of sulfate decrease in the studied microcosms (Fig. 4). According to the literature, we selected as putative SRB in marine sediments members of Desulfobacterota phylum (Waite et al., 2020), few families from the phyla Firmicutes (*Desulfitobacteriaceae, Desulfotomaculales, Desulfallas-Sporotomaculum, Fusibacteraceae* and reads ascribed to the order Thermoanaerobacterales) and Nitrospirota (Thermodesulfovibrionia) (Zhou et al., 2011) (Supplementary Tables S9-S11). For this analysis, it is important to remember that during the incubation period, sulfates, present at an initial concentration of 2.8 ± 0.3 $g \cdot L^{-1}$, were not replenished in order to maintain the static condition of the sediment and observe the variations in pH and redox potential. Along with the first month of incubation the sulfate depletion followed similar rates in both the OCV and all the stimulated circuits. This trend reflects the homogeneity in the relative abundance profiles of putative SRB among all samples (Fig. 4A). Later on, between the first and third month of incubation, the rate of sulfate depletion considerably decreased in all microcosms (Fig. 4D). 2AP triggered a slightly more pronounced sulfate depletion compared to the single circuit and open circuit system, with an effect proportional to the intensity of the current. Indeed, average sulfate depletion percentages were 80 ± 3 % and 92 ± 2 % in the 2AP with 0.025 and 0.05 $mA \cdot cm^{-2}$ applied, whereas in OCV and single circuit microcosms stimulated with a current of 0.025 and 0.05 $mA \cdot cm^{-2}$ the average sulfate depletion were 54 ± 4 %, 74 ± 1 % and 75 ± 7 %, respectively. Such differences were mirrored by changes in the biodiversity of putative SRB at 95 days, when families *Desulfocapsaceae* and *Desulfobulbaceae* showed higher relative abundances in the double circuit systems and in the anodes of the METs compared to the OCV (Fig. 4B, Supplementary Table S10). Notably, in all microcosms the family of *Desulfosarcinaceae* was the most abundant putative SRB,

reaching 15.9 ± 4.9 % at 95 days in G0.05_A. Overall, a rearrangement in terms of putative SRB community was observed under all the studied conditions with the abundance of the SRB belonging to the Firmicutes phylum decreasing under the limit of detection along the experimental timeline. During the last two months of incubation (95-159 days), sulfates were furtherly depleted being reduced of the 67 ± 3 % in the OCV at the end of the experiment. Higher sulfate depletion was observed in the METs, ranging between 81% of the initial concentration in the system poised at -0.7 V to 96% in the 2AP stimulated with 0.05 mA·cm^{-2} (Supplementary Table S4 and S5). At the end of the experiment, major differences in the putative SRB community were detected between the cathodic and anodic areas, being characterized the former by a bloom in *Desulfotomaculales* and increased abundance of reads assigned to uncultured Thermoanaerobacterales (Firmicutes), and the latter by higher abundance of *Desulfuromonadaceae* and Nitrospirota members (Fig. 4C, Supplementary Table S11).

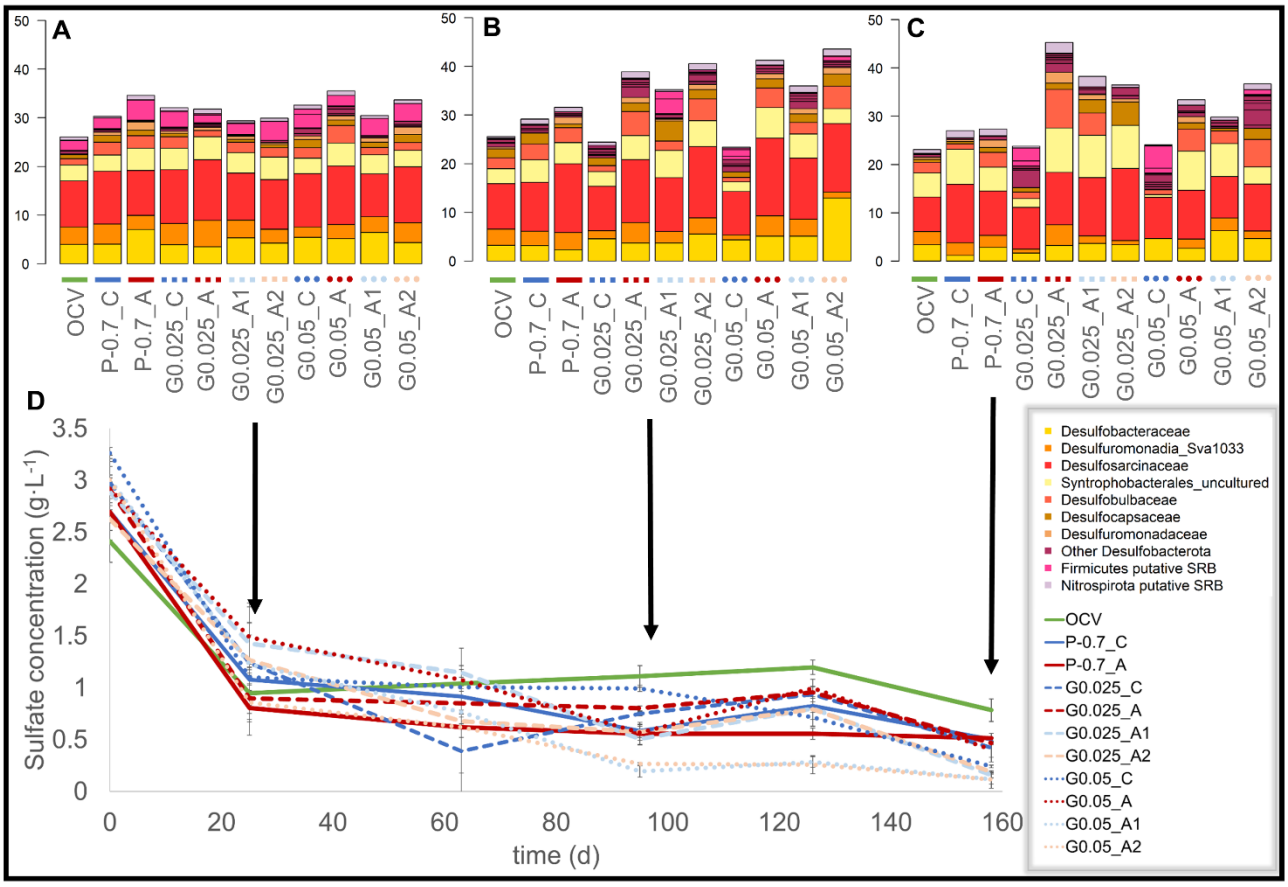

Figure 4 *Temporal dynamic of sulfate depletion from the sediments (D) in relation to changes in compositional profiles of putative SRB population (A-C). Microbial community profiles of bacteria identified as potential SRB according to the literature at 25 (A), 95 (B) and 159 (C) days is reported in relation to the temporal dynamic of sulfate concentration in the different microcosms (D), with black arrows indicating sampling times at which microbial community analysis was performed. Color legend*

is shown in the right panel for all plots. Within Desulfobacterota phylum only the top 7 families in terms of relative abundance are reported in different colors (shades of yellow, orange and red) whereas the other subdominant families (relative abundance <1.0%) are all depicted in dark purple (please see Table S9-S11 for the complete list). Percentage of bacterial relative abundance is represented as the mean of three replicates. OCV indicates open circuit microcosms. P-0.7 indicates MET poised at -0.7 V. G0.025 indicates MET stimulated with an applied current of 0.025 mA·cm$^{-2.}$ G0.05 indicates MET stimulated with an applied current of 0.05 mA·cm^{-2}. C indicates the cathode. A indicates the anode. A1 indicates area 1 in double circuit systems. A2 indicates area 2 in double circuit systems. Separate graphs for the studied conditions are reported in Supplementary Figures S14-S16, for improving clarity.

In order to assess the impact of the bioelectrochemical stimulation on the PCBs reductive dechlorination, the temporal variation in the chlorination degree was evaluated in relation to the compositional profile of commonly accepted OHRB potentially active in dechlorinating PCBs, i.e. ASV ascribed to members of the class Dehalococcoidia (Fig. 5B) (Kalogerakis et al., 2015; Zanaroli et al., 2012). An initial phase in which reductive dechlorination was not observed lasted 2 months (Supplementary Figure S17). Subsequently, reductive dehalogenation took place in all the microcosms. After 3 months of incubation, the chlorination degree of the PCBs mixture in the open circuit control was reduced by 11 ± 2 % (Fig. 5A). As for the electrified microcosms, the bioelectrochemical stimulation did not enhance reductive dechlorination whereas in some cases it exerted an inhibiting effect. In the cathodic area of the MET stimulated with -0.7 V and with a current density of 0.025 mA·cm^{-2}, dehalogenation proceeded similarly to the OCV showing reduction percentages of 11.2 ± 0.6 % and 7 ± 3 % (p values > 0.05, Supplementary Table S7). While around the anode the reductive dechlorination was slightly inhibited, being 7 ± 1 % and 4 ± 2 % in the -0.7 V and 0.025 mA·cm^{-2} microcosms. Applying a current density of 0.05 mA·cm^{-2} showed an even more negative effect on OHRB, resulting in reduction percentages of the chlorination degree of 4 ± 1 % and 2.4 ± 0.1 % at the cathode and anode. The double circuit systems mitigated the inhibition compared to the single circuit systems especially when applying 0.05 mA·cm^{-2}. In particular, reduction percentages after 95 days were: 6 ± 1 % and 5 ± 1 % at A1 and A2 of the 0.025 mA·cm^{-2} system; 8 ± 1 % and 9 ± 2 % at A1 and A2 of the 0.05 mA·cm^{-2}system. The effectiveness of the double circuit was demonstrated also on a long term. After 159 days of incubation, reduction percentages of the chlorination degree at the cathode and anode of the microcosm stimulated with 0.05 mA·cm^{-2} were 8 ± 1 % and 10 ± 4 %. In the 2AP system, the chlorination degree was reduced by 23 ± 5 % and 24 ± 4 % in A1 and A2, values not significantly different from the OCV (29.3 ± 0.4 %; p values > 0.05, Supplementary Table S7). Dehaloccoccoidia members putatively involved in PCB dechlorination maintained total abundance below 2% in all the studied conditions at 25 and 95 days. Conversely, at the

end of the experiment (159 days) Dehalococcoidia showed higher relative abundances (up to 3.5 %) that was positively correlated to the increase in the percentage reduction of the chlorination degree between 124 and 159 days (Spearman rank correlation coefficient, $\rho = 0.8$; p value ≤ 0.005). Indeed, at 159 days, the major increase of reductive dechlorination compared to the previous sampling point (124 days) was recorded in anodic samples of circuit poised at -0.7 V in line with the highest abundance of Dehalococcoidia observed at 159 days (Fig. 5B). Except for this condition, all the METs had a lower abundance of PCB OHRB compared to the OCV.

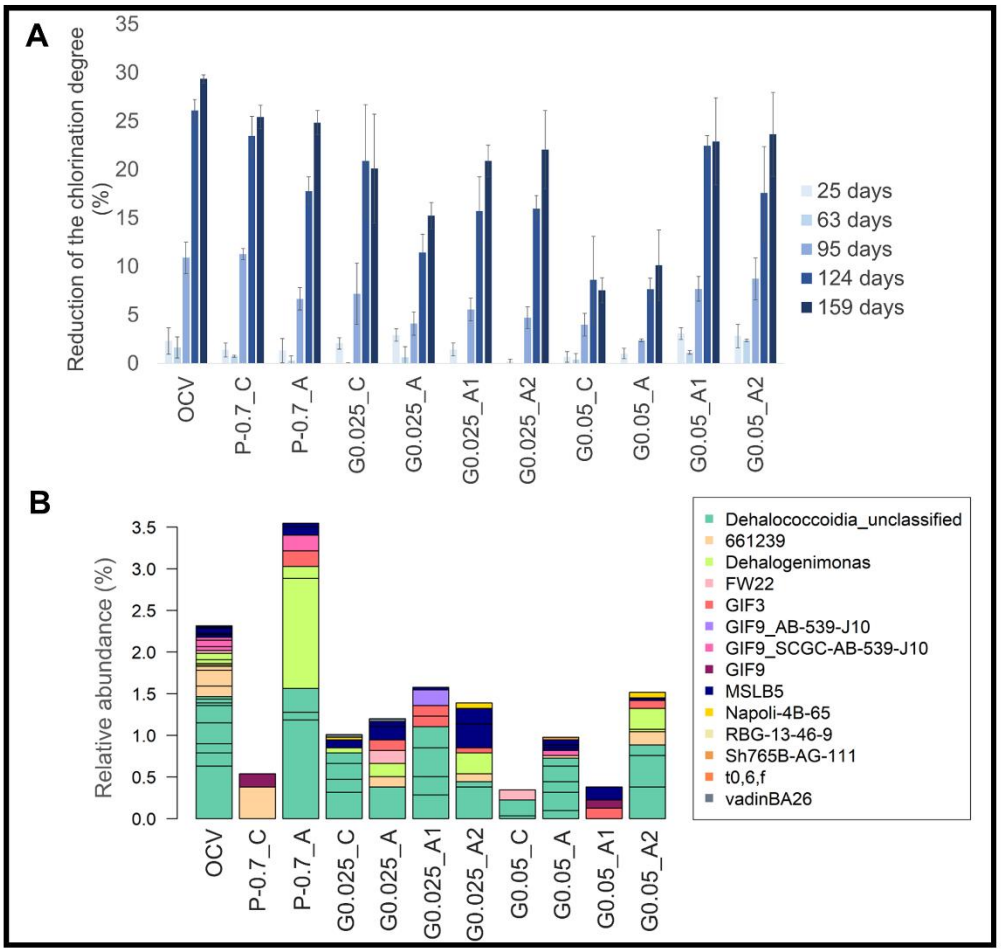

Figure 5 *Impact of bioelectrochemical stimulation on the chlorination degree of the PCBs mixture (A) and composition of microbial community members putatively involved in PCBs dechlorination (B). The reduction percentages of the chlorination degree in the studied microcosms throughout the length of the experiment is reported as bar plot with standard deviation (A). The mean relative abundance of Dehalococcoidia members in the studied microcosms at the end of the experiment (159 days) is depicted as barplot; detected Dehalococcoidia ASVs are reported using colors according to their Silva database v. 138 highest taxonomical assignation (please see color legend, right panel). Percentage of bacterial*

relative abundance is represented as the mean of three replicates. OCV indicates open circuit microcosms. P-0.7 indicates MET poised at -0.7 V. G0.025 indicates MET stimulated with an applied current of 0.025 mA·cm^{-2}. G0.05 indicates MET stimulated with an applied current of 0.05 mA·cm^{-2}. C indicates the cathode. A indicates the anode. A1 indicates area 1 in double circuit systems. A2 indicates area 2 in double circuit systems.

4.3.3 Electron balance of the sulfate reduction

In order to better understand the positive influence of the bioelectrochemical stimulation on the sulfate reduction, an electron balance was calculated to distinguish between chemoorganotrophic and chemolithotrophic sulfate reduction. The chemoorganotrophic sulfate reduction was estimated considering the activity of the OCV, where organic matter acted as electron donor (Blázquez et al., 2018). The chemolithotrophic contributions were calculated assuming that all the supplied electrons were delivered to sulfate reducers (Blázquez et al., 2018; Gacitúa et al., 2018; Luo et al., 2014; Su et al., 2012). The electron balance was calculated on the entire system without differentiating between cathode/anode or A1/A2 since no significant differences were observed in terms of sulfate reduction for each system (Supplementary Table S4). The electron balance (EB) showed that most of sulfates were removed via chemoorganotrophic reduction, which accounted for more than 50% of the sulfate removed (Fig. 6). Conversely, the chemolithotrophic contributions were: 7.3 ± 0.1 % when applying -0.7 V; 18.9 ± 0.5 % and 18.4 ± 0.2 % when applying 0.025 mA·cm^{-2} in single system and double system mode; 34 ± 2 % and 33 ± 1 % when applying 0.05 mA·cm^{-2} in single system and double system mode. It should be noticed that under galvanostatic conditions, the current flow was imposed by the operator, and it was not a consequence of the bioelectrochemical processes. Consequently, the higher chemolithotrophic contributions might be due to an artefact of the mathematical expression as higher current were imposed. In all the METs, the chemolithotrophic and chemoorganotrophic contributions were lower than the theoretical amount to reduce the sulfate, resulting in an EB lower than 100%. Additionally, coulombic efficiencies were calculated obtaining values higher than 100 % for all the METs (Supplementary Table S6).

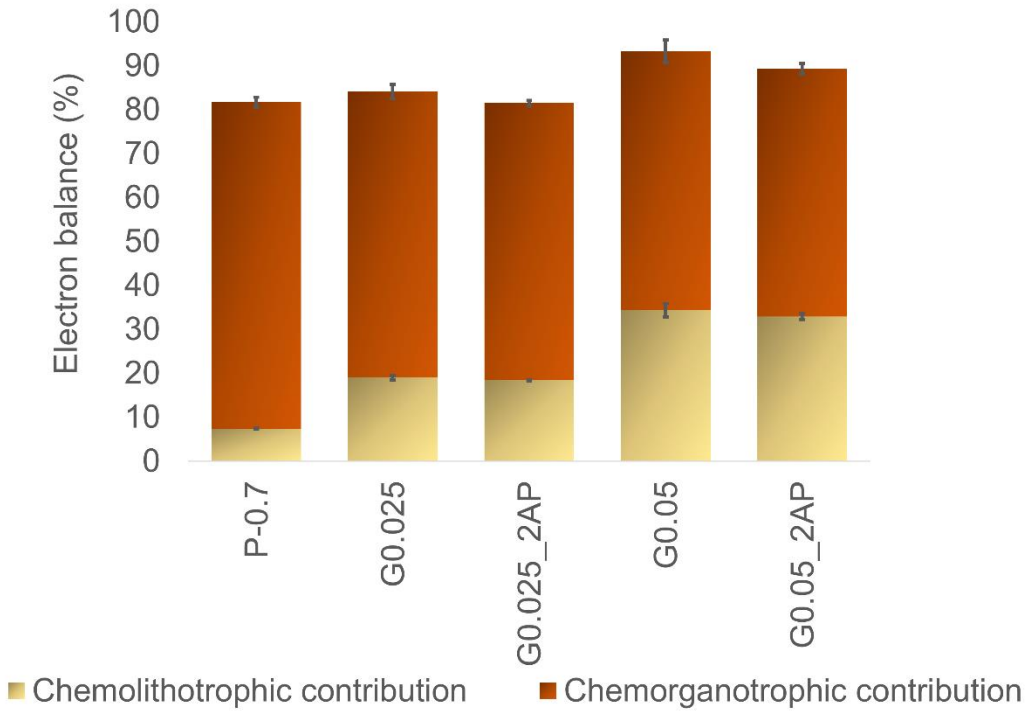

Figure 6 *Electron balance of the bioelectrochemical systems at the end of the experiment (159 days). Chemoorganotrophic contributions (dark orange): chemoorganotrophic sulfate reduction due to the oxidation of organic matter in the sediment, calculated considering the sulfate reduction activity in the open circuit microcosms. Chemolithotrophic contributions (light yellow): the theoretical contributions of the bioelectrochemical stimulation to the sulfate depletion calculated using the accumulated charge. P-0.7 indicates MET poised at -0.7 V. G0.025 indicates MET stimulated with an applied current of 0.025 mA·cm$^{-2.}$ G0.05 indicates MET stimulated with an applied current of 0.05 mA·cm^{-2}. 2AP indicates the double circuit systems.*

4.4 Discussion

Within the perspective of finding innovative solution for the remediation of polluted marine sediments, the present paper shows a first application of a MET on PCBs polluted sediments. Differently from previous experiments that successfully applied METs to freshwater environments (Chun et al., 2013; Liu et al., 2017; Yu et al., 2017, 2016) or synthetic media (Zhang et al., 2021), observing an increase of the dehalogenation rate of the pollutants, in this study the dehalogenation did not benefit from the electrochemical input. The process was slowed down in all the METs and longer times were required to observe a plateau of the chlorination degree when working with the closed circuits compared to the microcosm with no current applied. The electrochemical input inevitably led to variations of the sediments' conditions, such as raise of pH in the proximity of the cathodic area. Change in pH contributed

in modifying the microbiota composition, selecting for a subset of species able to tolerate the environmental stress induced by electrochemical stimulation. For instance, in the single circuit systems, bacteria belonging to the Peptostreptococcales-Tissierellales group, within the Firmicutes phylum, were enriched in the proximity of the cathodes, where values of pH up to 11.5 were reached. Peptostreptococcales-Tissierellales are fermentative bacteria (Yan et al., 2020), known to be active at alkaline pH (Owusu-agyeman et al., 2022). The detection of the family *Synergistaceae* also hints at a role played by pH in shaping the microbial community, since members of this family are known to tolerate alkaline environment (Wei et al., 2022). Conversely, OHRB grow preferentially at neutral pH (Chang et al., 2004; Holliger et al., 1998; Philips et al., 2013). The pH variation might then explain the lower degree of dehalogenation observed after 159 days in the electrochemically stimulated microcosms and the lower abundance of bacteria putatively involved in dechlorination with respect to the OCV, observed in almost all the METs. Only in the microcosm posed at -0.7 V, higher counts of bacteria linked to PCB dehalogenation were observed. The abundance of this class of bacteria was positively correlated to the increase of reductive dechlorination within the last month of incubation. The correlation suggested that the relative abundance profile of the putative OHRB portion of microbial community, registered at that final timepoint, reflected the degree of metabolic activity (and consequently of ability to proliferate) of that specific subset of bacteria. Indeed, in the OCV the PCB dehalogenation proceeded faster reaching a plateau after 159 days of incubation, possibly leading to a maintenance or a decline in the abundance of putative OHRB. On the other hand, longer times were required to observe the onset of dehalogenation in the METs, resulting in higher abundances of putative OHRB at the end of the incubation. The role of pH in shaping the microbial community and activities was supported also by the milder inhibition of reductive dechlorination observed in the 2AP compared to the single circuits. Indeed, the inversion of the electrode polarization mitigated the working pH contributing at maintaining the pH values in proximity to the neutrality even after long incubation time. In this perspective, the employment of double circuits revealed its efficacy compared to previous set up, as the one applied by Bellagamba *et al.* (2017). The stimulation strategy applied in their study was based on alternating periods with current applied and period with no current flows. Compared to our configuration, their system could not restore the original pH yet only slowing down the variation. Additionally, 2AP do not require the use of electrode materials that are both cathodically and anodically stable, typicals of system based on periodic inversion of polarity (Jiang et al., 2016; Li et al., 2014; Sun et al., 2015), thus allowing the use of a wider and cheaper range of materials.

A subset of microbiota members that showed to thrive within the imposed conditions were putative SRB, typically abundant in marine sediments due to the high concentrations of electron acceptors, i.e. SO_4^{2-}. The high abundance of these bacteria might have contributed in slowing down the remediation process in the electrified microcosms compared to the control, due to the competition between SRB and OHRB for the supplied electrons. Coulombic efficiencies and electron balances revealed that the provided equivalents were lower than the theoretical amount required to sustain the sulfate reduction activity. Consequently, SRB might have completely consumed the supplied reducing equivalents thus preventing electrons to be delivered to OHRB. The proliferation of this portion of the microbial community, which thrived in the presence of an electrochemical input, was also confirmed by the molecular characterization. For instance, the family *Desulfuromonadaceae*, which includes taxa capable of bioelectrochemically assisted sulfate reduction (X. Zhang et al., 2022), was enriched in the METs. Similarly, bacteria belonging to the families *Desulfobulbaceae* and *Desulfobacteraceae*, known sulfate reducers (Klein et al., 2001; Pan et al., 2022) and putative electroactive bacteria (Ishii et al., 2013; Matturro et al., 2017; H. Zhang et al., 2022), were enriched in METs. Despite the majority of sulfate were depleted within the first month of incubation (25 days) in all the METs as well as in the OCV, an enrichment of the taxa putatively including SRB was observed after 95 and 159 days of incubation in the electrified microcosms. Analogous increase in abundance of putative SRB was observed also around the anodic area, where electrons were not supplied. To address this phenomena, the model of the sulfur cycle depicted in Fig. 7 was elaborated. In the closed circuit METs, sulfate reduction was electrochemically stimulated at the cathode, possibly driven by *Desulfuromonadaceae* (Camacho, 2009), *Desulfobacteraceae* (Camacho, 2009), *Desulfobulbaceae* (Camacho, 2009), *Desulfosarcinaceae* (Watanabe et al., 2021) and *Syntrophobacterales* (Ma et al., 2021), leading to lower sulfate concentrations and to an enrichment of these taxa. On the other hand, several processes might have contributed in restoring sulfate, establishing a local sulfur cycle and guaranteeing the maintenance of the sulfate reduction process along the whole experimental timeline. Indeed, the low sulfate concentrations and the presence of sulfide scavengers, as Fe(II) coming from the oxidation of the anode that precipitates as FeS (Finster et al., 1998), might have made the sulfur disproportionation, possibly mediated by *Desulfobulbaceae* (Finster, 2008) and *Desulfocapsaceae* (Finster et al., 1998), thermodynamically feasible. Additionally, the oxidation of the iron plate might have led to the presence of iron oxide, e.g. Fe_2O_3, which could have acted as electron acceptor for the sulfide oxidation mediated by *Desulforomonas* (Zhang et al., 2014). Lastly, sulfate might had been restored by bacteria belonging to the family of *Chlorobiaceae*, chemolithoautotrophic bacteria able to oxidize sulfur or sulfide to sulfate (Camacho, 2009; Loy et al., 2009). Consequently, the plateau

in sulfate concentration, observed after the intense sulfate depletion occurred at the end of the first month, could had been guaranteed by the simultaneous presence of bacteria able to employ sulfur species both as electron acceptors and donors.

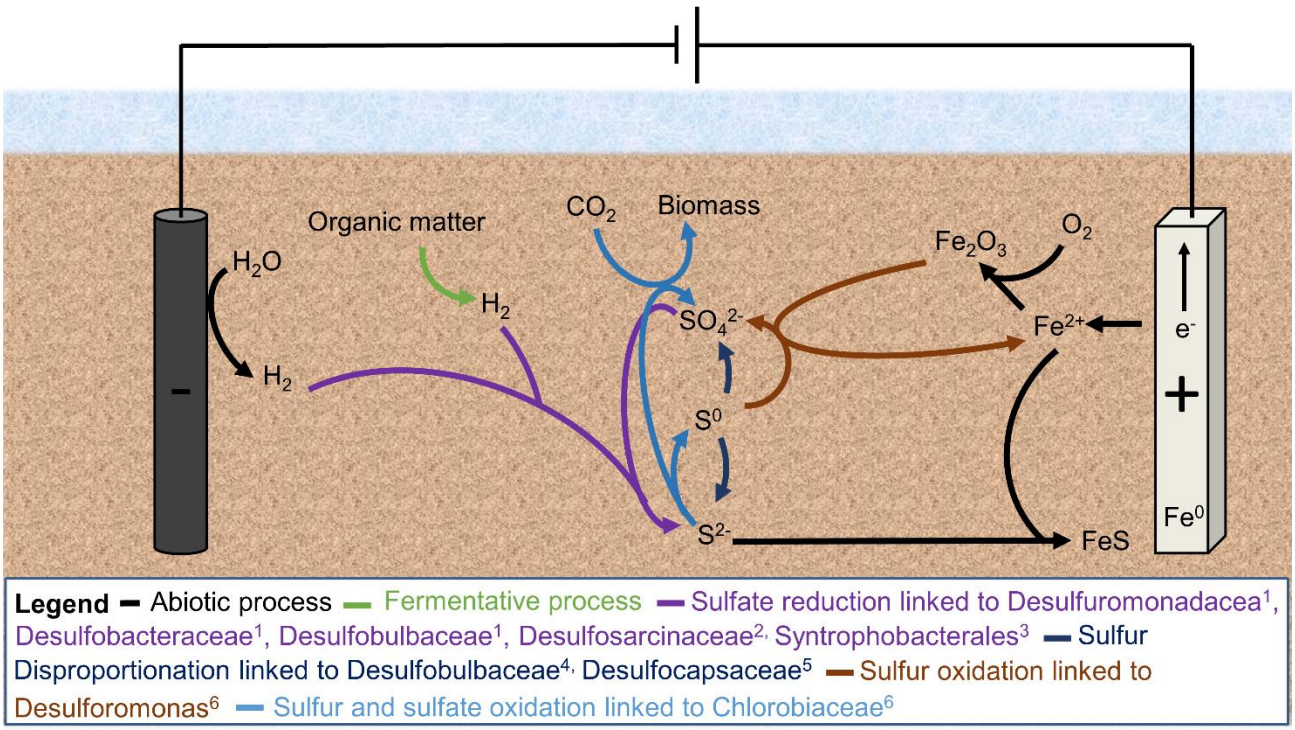

Figure 7 *Theoretical model depicting the sulfur cycle in the studied MET, highlighting the role of the bacteria and electrodes involved. Briefly, sulfate reduction is stimulated at the cathode, leading to the formation of sulfide. Sulfate are restored thanks to the disproportionation of sulfur and to the oxidation of sulfur and sulfide. Sulfur disproportionation is led by the scavenging effect of the Fe(II), anodically produced. Superscript numbers refer to the literature used to associate specific metabolisms to bacterial families as follows: 1* (Camacho, 2009)*, 2* (Watanabe et al., 2021)*, 3* (Ma et al., 2021)*, 4* (Finster, 2008)*, 5* (Finster et al., 1998) *and 6* (Zhang et al., 2014).

The presence of a competitive group of SRB might account for the scarce performance of the MET employed in this experiment compared to previous studied METs. In fact, the initial hypothesis that METs might had stimulated dehalogenation of PCBs polluted marine sediments was braced by literature about their application on synthetic (Chen et al., 2019) or real (Dell'Armi et al., 2022) freshwater environments polluted by chlorinated solvents, as PCE (Aulenta et al., 2009), and characterized by relevant biogeochemical differences, with respect to the marine environment. Analogously, earlier

studies about dechlorination of PCBs stimulated by METs showed effectiveness in freshwater environments, such as river sediments (Chun et al., 2013; Liu et al., 2017; Yu et al., 2017, 2016). Differently from freshwaters, marine environments are rich in SRB (Wang et al., 2012) thanks to the high concentration of SO_4^{2-}, resulting in highly competitive environment for OHRB, in terms of hydrogen availability. In this experiment it was not possible to selectively stimulate OHRB. It is known that at low hydrogen concentration OHRB might outcompete SRB (Hoelen and Reinhard, 2004), yet sulfate reduction was primed also when cathode was poised at -0.7 V, a value of potential that allows for negligible hydrogen production (Aulenta et al., 2009; Villano et al., 2010). This might be due to the ability of SRB to perform chemolithotrophic sulfate reduction with direct electron transfer (Su et al., 2012), as reported for *Desulfobulbaceae, Desulfobacteraceae* and *Desulfuromonadaceae* (Ishii et al., 2013; Matturro et al., 2017; H. Zhang et al., 2022; X. Zhang et al., 2022), or via hydrogen mediation (Luo et al., 2014), thus being competitive at a various range of working potential and even at low sulfate concentrations (0.25 $g \cdot L^{-1}$) (Daghio et al., 2018). One last point to be considered to explain the lack of stimulation of reductive dehalogenation is the role of PCBs as electron acceptors. Compared to other chlorinated compounds as PCE, PCBs are less efficient in sustaining microbial growth of OHRB due to their scarce water solubility and low Gibbs free energy of the reduction reaction (Chen and He, 2018; Holmes et al., 1993; Lombard et al., 2014), resulting in a less favorable respiration and thus yielding lower growth rates (Wang et al., 2014). All these factors might explain the inefficacy of METs for bioelectrochemical stimulation of PCBs reductive dechlorination in environments characterized by high concentrations of anaerobic competitors, despite they proved to be applicable in freshwater environment or other chlorinated solvents (e.g. PCE).

4.5 Conclusions

To the best of our knowledge, the experiment presented here represents the first application of bioelectrochemical systems to stimulate PCBs microbial dehalogenation in real marine sediments. Applying METs to static lab-scale microcosms showed to be ineffective to prime bioremediation. In fact SRB showed an impressive adaptability, exploiting the electrochemical stimulation and competing with OHRB even under the extreme pH conditions imposed by the electrochemical input. Future studies aimed at adapting the bioelectrochemical set-up to marine environment will have to focus on enhancing the selectivity of METs towards the stimulation of dehalorespiration to the detriment of sulfate reduction. For instance, METs could be operated at lower potential so as to reduce the stimulation of SRB, as observed also in this experiment, but this might affect OHRB too. Yu *et al.* (2016) posed the biocathode

at -0.46 V over a period of one year without observing stimulation of PCBs reductive dechlorination. Another approach could be providing an excess of reducing equivalents, which is a common strategy applied for bioremoval of chlorinated solvents (Sandefur and Koenigsberg, 1999). Though, this would require applying higher current and consequently need for a better pH control, for example by using automated systems and on line sensors. In the perspective of finding smart solutions to control physical-chemical variation of METs working under static conditions, alternating the circuits demonstrated to be a promising approach to mitigate pH's variation. Additionally, it would be fundamental to develop anodic materials for *in situ* oxygen production, since aerobic degradation can largely contribute in diminishing the environmental concentration of the pollutants (Payne et al., 2013). The cation exchange membrane studied herein showed impressive results, although several technical limitations still retain its application for long term experiments and further studies should be conducted to deeply evaluate its potential as, for example, determining the role of the membrane's thickness on the anode's endurance. As alternatives to physical barrier, selective catalysts are being designed to exert a repellent action towards Cl^-, obtaining promising results even in real seawater (Liu, 2022). Currently, materials able to selectively catalyze OER and sufficiently stable for long term applications in real seawater haven't been identified yet and despite further efforts are required to identify optimal configurations, it is believed that the scientific achievements obtained up to now will guarantee the development of effective solutions (Liu et al., 2022). In general, it was demonstrated that when applying METs in environments characterized by strong competitors and under static conditions, several elements should be taken into account to obtain an effective and selective stimulation.

4.6 Bibliography

Aulenta, F., Canosa, A., Reale, P., Rossetti, S., Panero, S., Majone, M., 2009. Microbial reductive dechlorination of trichloroethene to ethene with electrodes serving as electron donors without the external addition of redox mediators. Biotechnol. Bioeng. 103, 85–91. https://doi.org/10.1002/bit.22234

Aulenta, F., Fuoco, M., Canosa, A., Papini, M.P., Majone, M., 2008. Use of poly-β-hydroxy-butyrate as a slow-release electron donor for the microbial reductive dechlorination of TCE. Water Sci. Technol. 57, 921–925. https://doi.org/10.2166/wst.2008.073

Aulenta, F., Tocca, L., Verdini, R., Reale, P., Majone, M., 2011. Dechlorination of Trichloroethene in a

Continuous-Flow Bioelectrochemical Reactor : Effect of Cathode Potential on Rate , Selectivity , and Electron Transfer Mechanisms. Environ. Sci. Technol. 45, 8444–8451.

Balaji, R., Kannan, B.S., Lakshmi, J., Senthil, N., Vasudevan, S., Sozhan, G., Shukla, A.K., Ravichandran, S., 2009. An alternative approach to selective sea water oxidation for hydrogen production. Electrochem. commun. 11, 1700–1702. https://doi.org/10.1016/j.elecom.2009.06.022

Bard, A.J., Faulkner., L.R., 2001. Electrochemical Methods Fundamentals and Applications, Second. ed, Physics. John Wiley & Sons, Texas, Austin.

Baric, M., Pierro, L., Pietrangeli, B., Papini, M.P., 2014. Polyhydroxyalkanoate (PHB) as a slow-release electron donor for advanced in situ bioremediation of chlorinated solvent-contaminated aquifers. N. Biotechnol. 31, 377–382. https://doi.org/10.1016/j.nbt.2013.10.008

Bellagamba, M., Viggi, C.C., Ademollo, N., Rossetti, S., Aulenta, F., 2017. Electrolysis-driven bioremediation of crude oil-contaminated marine sediments. N. Biotechnol. 38, 84–90. https://doi.org/10.1016/j.nbt.2016.03.003

Blázquez, E., Guisasola, A., Gabriel, D., Baeza, J.A., 2018. Application of bioelectrochemical systems for the treatment of wastewaters with sulfur species, in: Biomass, Biofuels, Biochemicals: Microbial Electrochemical Technology: Sustainable Platform for Fuels, Chemicals and Remediation. Elsevier B.V., pp. 641–663. https://doi.org/10.1016/B978-0-444-64052-9.00026-1

Bolyen, E., Rideout, J.R., Dillon, M.R., Bokulich, N.A., Abnet, C.C., Al-Ghalith, G.A., Alexander, H., Alm, E.J., Arumugam, M., Asnicar, F., Bai, Y., Bisanz, J.E., Bittinger, K., Brejnrod, A., Brislawn, C.J., Brown, C.T., Callahan, B.J., Caraballo-Rodríguez, A.M., Chase, J., Cope, E.K., Da Silva, R., Diener, C., Dorrestein, P.C., Douglas, G.M., Durall, D.M., Duvallet, C., Edwardson, C.F., Ernst, M., Estaki, M., Fouquier, J., Gauglitz, J.M., Gibbons, S.M., Gibson, D.L., Gonzalez, A., Gorlick, K., Guo, J., Hillmann, B., Holmes, S., Holste, H., Huttenhower, C., Huttley, G.A., Janssen, S., Jarmusch, A.K., Jiang, L., Kaehler, B.D., Kang, K. Bin, Keefe, C.R., Keim, P., Kelley, S.T., Knights, D., Koester, I., Kosciolek, T., Kreps, J., Langille, M.G.I., Lee, J., Ley, R., Liu, Y.X., Loftfield, E., Lozupone, C., Maher, M., Marotz, C., Martin, B.D., McDonald, D., McIver, L.J., Melnik, A. V., Metcalf, J.L., Morgan, S.C., Morton, J.T., Naimey, A.T., Navas-Molina, J.A., Nothias, L.F., Orchanian, S.B., Pearson, T., Peoples, S.L., Petras, D., Preuss, M.L., Pruesse, E., Rasmussen, L.B., Rivers, A., Robeson, M.S., Rosenthal, P., Segata, N., Shaffer, M., Shiffer, A.,

Sinha, R., Song, S.J., Spear, J.R., Swafford, A.D., Thompson, L.R., Torres, P.J., Trinh, P., Tripathi, A., Turnbaugh, P.J., Ul-Hasan, S., van der Hooft, J.J.J., Vargas, F., Vázquez-Baeza, Y., Vogtmann, E., von Hippel, M., Walters, W., Wan, Y., Wang, M., Warren, J., Weber, K.C., Williamson, C.H.D., Willis, A.D., Xu, Z.Z., Zaneveld, J.R., Zhang, Y., Zhu, Q., Knight, R., Caporaso, J.G., 2019. Reproducible, interactive, scalable and extensible microbiome data science using QIIME 2. Nat. Biotechnol. 37, 852–857. https://doi.org/10.1038/s41587-019-0209-9

Botti, A., Biagi, E., Musmeci, E., Breglia, A., Degli Esposti, M., Fava, F., Zanaroli, G., 2023. Effect of polyhydroxyalkanoates on the microbial reductive dechlorination of polychlorinated biphenyls and competing anaerobic respirations in a marine microbial culture. Mar. Pollut. Bull. 186, 114458. https://doi.org/10.1016/j.marpolbul.2022.114458

Camacho, A., 2009. Sulfur Bacteria. Encycl. Inl. Waters 261–278. https://doi.org/10.1016/B978-012370626-3.00128-9

Chang, Chao Chien, Tseng, S.K., Chang, Chih Cheng, Ho, C.M., 2004. Degradation of 2-chlorophenol via a hydrogenotrophic biofilm under different reductive conditions. Chemosphere 56, 989–997. https://doi.org/10.1016/j.chemosphere.2004.04.051

Chen, C., He, J., 2018. Strategy for the Rapid Dechlorination of Polychlorinated Biphenyls (PCBs) by Dehalococcoides mccartyi Strains. Environ. Sci. Technol. 52, 13854–13862. https://doi.org/10.1021/acs.est.8b03198

Chen, F., Li, Z.L., Liang, B., Yang, J.Q., Cheng, H.Y., Huang, C., Nan, J., Wang, A.J., 2019. Electrostimulated bio-dechlorination of trichloroethene by potential regulation: Kinetics, microbial community structure and function. Chem. Eng. J. 357, 633–640. https://doi.org/10.1016/j.cej.2018.09.191

Chun, C.L., Payne, R.B., Sowers, K.R., May, H.D., 2013. Electrical stimulation of microbial PCB degradation in sediment. Water Res. 47, 141–152. https://doi.org/10.1016/j.watres.2012.09.038

Daghio, M., Espinoza Tofalos, A., Leoni, B., Cristiani, P., Papacchini, M., Jalilnejad, E., Bestetti, G., Franzetti, A., 2018. Bioelectrochemical BTEX removal at different voltages: assessment of the degradation and characterization of the microbial communities. J. Hazard. Mater. 341, 120–127. https://doi.org/10.1016/j.jhazmat.2017.07.054

Dai, S., Korth, B., Schwab, L., Aulenta, F., Vogt, C., Harnisch, F., 2022. Deciphering the fate of sulfate

in one- and two-chamber bioelectrochemical systems. Electrochim. Acta 408, 139942. https://doi.org/10.1016/j.electacta.2022.139942

Dell'Armi, E., Zeppilli, M., Di Franca, M.L., Matturro, B., Feigl, V., Molnár, M., Berkl, Z., Németh, I., Yaqoubi, H., Rossetti, S., Papini, M.P., Majone, M., 2022. Evaluation of a Bioelectrochemical Reductive/Oxidative Sequential Process for Chlorinated Aliphatic Hydrocarbons (Cahs) Removal from a Real Contaminated Groundwater. J. Water Process Eng. 49, 103101. https://doi.org/10.2139/ssrn.3981653

Dionigi, F., Reier, T., Pawolek, Z., Gliech, M., Strasser, P., 2016. Design Criteria, Operating Conditions, and Nickel-Iron Hydroxide Catalyst Materials for Selective Seawater Electrolysis. ChemSusChem 9, 962–972. https://doi.org/10.1002/cssc.201501581

Dolfing, J., 2003. Thermodynamic considerations for dehalogenation, in: Häggblom, M.M., Bossert, I.D. (Eds.), Dehalogenation, Microbial Processes and Environmental Applications. Kluwer Academic Publishers, Rutgers University, USA, pp. 89–114.

Fagervold, S.K., Watts, J.E.M., May, H.D., Sowers, K.R., 2011. Effects of bioaugmentation on indigenous PCB dechlorinating activity in sediment microcosms. Water Res. 45, 3899–3907. https://doi.org/10.1016/j.watres.2011.04.048

Fava, F., Zanaroli, G., Young, L.Y., 2003. Microbial reductive dechlorination of pre-existing PCBs and spiked 2,3,4,5,6-pentachlorobiphenyl in anaerobic slurries of a contaminated sediment of Venice Lagoon (Italy). FEMS Microbiol. Ecol. 44, 309–318. https://doi.org/10.1016/S0168-6496(03)00069-2

Finster, K., 2008. Microbiological disproportionation of inorganic sulfur compounds. J. Sulfur Chem. 29, 281–292. https://doi.org/10.1080/17415990802105770

Finster, K., Liesack, W., Thamdrup, B., 1998. Elemental sulfur and thiosulfate disproportionation by Desulfocapsa sulfoexigens sp. nov., a new anaerobic bacterium isolated from marine surface sediment. Appl. Environ. Microbiol. 64, 119–125. https://doi.org/10.1128/aem.64.1.119-125.1998

Frame, G.M., 1997. A collaborative study of 209 PCB congeners and 6 Aroclors on 20 different HRGC columns: 1. Retention and coelution database. Fresenius. J. Anal. Chem. 357, 701–713. https://doi.org/10.1007/s002160050237

Gacitúa, M.A., Muñoz, E., González, B., 2018. Bioelectrochemical sulphate reduction on batch reactors: Effect of inoculum-type and applied potential on sulphate consumption and pH. Bioelectrochemistry 119, 26–32. https://doi.org/10.1016/j.bioelechem.2017.08.006

Häggblom, M.M., Bossert, I.D., 2003. Dehalogenation, Microbial processes and environmental applications. Kluwer Academic Publishers, Rutgers University, USA.

Hall, M., Beiko, R.G., 2018. 16S rRNA Gene Analysis with QIIME2, in: Methods in Molecular Biology. Humana Press Inc., pp. 113–129.

Hoelen, T.P., Reinhard, M., 2004. Complete biological dehalogenation of chlorinated ethylenes in sulfate containing groundwater. Biodegradation 15, 395–403. https://doi.org/10.1023/B:BIOD.0000044592.33729.d6

Holliger, C., Hahn, D., Harmsen, H., Ludwig, W., Schumacher, W., Tindall, B., Vazquez, F., Weiss, N., Zehnder, A.J.B., 1998. Dehalobacter restrictus gen. nov. and sp. nov., a strictly anaerobic bacterium that reductively dechlorinates tetra- and trichloroethene in an anaerobic respiration. Arch. Microbiol. 169, 313–321. https://doi.org/10.1007/s002030050577

Holmes, D.A., Harrison, B.K., Dolfing, J., 1993. Estimation of Gibbs Free Energies of Formation for Polychlorinated Biphenyls. Environ. Sci. Technol. 27, 725–731. https://doi.org/10.1021/es00041a017

Ishii, S., Suzuki, S., Norden-Krichmar, T.M., Wu, A., Yamanaka, Y., Nealson, K.H., Bretschger, O., 2013. Identifying the microbial communities and operational conditions for optimized wastewater treatment in microbial fuel cells. Water Res. 47, 7120–7130. https://doi.org/10.1016/j.watres.2013.07.048

Jiang, S., Suo, H., Zhang, T., Liao, C., Wang, Y., Zhao, Q., Lai, W., 2022. Recent Advances in Seawater Electrolysis. Catalysts 12, 123.

Jiang, Y., Liang, P., Zhang, C., Bian, Y., Sun, X., Zhang, H., Yang, X., Zhao, F., Huang, X., 2016. Periodic polarity reversal for stabilizing the pH in two-chamber microbial electrolysis cells. Appl. Energy 165, 670–675. https://doi.org/10.1016/j.apenergy.2016.01.001

Kalogerakis, N., Arff, J., Banat, I.M., Broch, O.J., Daffonchio, D., Edvardsen, T., Eguiraun, H., Giuliano, L., Handå, A., López-de-Ipiña, K., Marigomez, I., Martinez, I., Øie, G., Rojo, F.,

Skjermo, J., Zanaroli, G., Fava, F., 2015. The role of environmental biotechnology in exploring, exploiting, monitoring, preserving, protecting and decontaminating the marine environment. N. Biotechnol. 32, 157–167. https://doi.org/10.1016/j.nbt.2014.03.007

Karlsson, R.K.B., Cornell, A., 2016. Selectivity between Oxygen and Chlorine Evolution in the Chlor-Alkali and Chlorate Processes. Chem. Rev. 116, 2982−3028. https://doi.org/10.1021/acs.chemrev.5b00389

Li, W., Sun, J., Hu, Y., Zhang, Y., Deng, F., Chen, J., 2014. Simultaneous pH self-neutralization and bioelectricity generation in a dual bioelectrode microbial fuel cell under periodic reversion of polarity. J. Power Sources 268, 287–293. https://doi.org/10.1016/j.jpowsour.2014.06.047

Lin, X.Q., Li, Z.L., Liang, B., Zhai, H.L., Cai, W.W., Nan, J., Wang, A.J., 2019. Accelerated microbial reductive dechlorination of 2,4,6-trichlorophenol by weak electrical stimulation. Water Res. 162, 236–245. https://doi.org/10.1016/j.watres.2019.06.068

Liu, X., Wan, H., Xue, Y., Feng, C., Wei, C., 2017. Addition of iron oxides in sediments enhances 2,3,4,5-tetrachlorobiphenyl (PCB 61) dechlorination by low-voltage electric fields. RSC Adv. 7, 26019–26027. https://doi.org/10.1039/c7ra02849k

Logan, B.E., Hamelers, B., Rozendal, R., Shroder, U., Keller, J., Freguia, S., Aelterman, P., Verstraete, W., Rabaey, K., 2006. Critical Review Microbial Fuel Cells : Methodology and Technology. Environ. Sci. Technol. 40, 5181–5192.

Logan, B.E., Rossi, R., Ragab, A., Saikaly, P.E., 2019. Electroactive microorganisms in bioelectrochemical systems. Nat. Rev. Microbiol. 17, 307–319. https://doi.org/10.1038/s41579-019-0173-x

Lombard, N.J., Ghosh, U., Kjellerup, B. V., Sowers, K.R., 2014. Kinetics and threshold level of 2,3,4,5-tetrachlorobiphenyl dechlorination by an organohalide respiring bacterium. Environ. Sci. Technol. 48, 4353–4360. https://doi.org/10.1021/es404265d

Loy, A., Duller, S., Baranyi, C., Mußmann, M., Ott, J., Sharon, I., Béjà, O., Le Paslier, D., Dahl, C., Wagner, M., 2009. Reverse dissimilatory sulfite reductase as phylogenetic marker for a subgroup of sulfur-oxidizing prokaryotes. Environ. Microbiol. 11, 289–299. https://doi.org/10.1111/j.1462-2920.2008.01760.x

Lu, Q., Liu, J., He, H., Liang, Z., Qiu, R., Wang, S., 2021. Waste activated sludge stimulates in situ microbial reductive dehalogenation of organohalide-contaminated soil. J. Hazard. Mater. 411, 125189. https://doi.org/10.1016/j.jhazmat.2021.125189

Luo, H., Fu, S., Liu, G., Zhang, R., Bai, Y., Luo, X., 2014. Autotrophic biocathode for high efficient sulfate reduction in microbial electrolysis cells. Bioresour. Technol. 167, 462–468. https://doi.org/10.1016/j.biortech.2014.06.058

Ma, L., She, W., Wu, G., Yang, J., Phurbu, D., Jiang, H., 2021. Influence of temperature and sulfate concentration on the sulfate/sulfite reduction prokaryotic communities in the tibetan hot springs. Microorganisms 9, 1–15. https://doi.org/10.3390/microorganisms9030583

Mao, X., Ciblak, A., Amiri, M., Alshawabkeh, A.N., 2011. Redox control for electrochemical dechlorination of trichloroethylene in bicarbonate aqueous media. Environ. Sci. Technol. 45, 6517–6523. https://doi.org/10.1021/es200943z

Matturro, B., Viggi, C.C., Aulenta, F., Rossetti, S., 2017. Cable bacteria and the bioelectrochemical Snorkel: The natural and engineered facets playing a role in hydrocarbons degradation in marine sediments. Front. Microbiol. 8, 1–13. https://doi.org/10.3389/fmicb.2017.00952

Mondello, F.J., 1989. Cloning and expression in Escherichia coli of Pseudomonas strain LB400 genes encoding polychlorinated biphenyl degradation. J. Bacteriol. 171, 1725–1732. https://doi.org/10.1128/jb.171.3.1725-1732.1989

Nuzzo, A., Hosseinkhani, B., Boon, N., Zanaroli, G., Fava, F., 2017. Impact of bio-palladium nanoparticles (bio-Pd NPs) on the activity and structure of a marine microbial community. Environ. Pollut. 220, 1068–1078. https://doi.org/10.1016/j.envpol.2016.11.036

Owusu-agyeman, I., Plaza, E., Cetecioglu, Z., 2022. Long-term alkaline volatile fatty acids production from waste streams : Impact of pH and dominance of Dysgonomonadaceae. Bioresour. Technol. 346, 126621. https://doi.org/10.1016/j.biortech.2021.126621

Palacky, G.J., 1987. Resistivity characteristics of geologic targets, in: Corbett, J.D., Nabighian, M.N. (Eds.), Electromagnetic Methods in Applied Geophysics - Theory Volume 1. Society of Exploration Geophysicists, Tulsa, Oklahoma, U.S.A., pp. 53–131.

Paquete, C.M., Rosenbaum, M.A., Baneras, L., Rotaru, A., Puig, S., 2022. Let ’ s chat :

Communication between electroactive microorganisms. Bioresour. Technol. 347. https://doi.org/10.1016/j.biortech.2022.126705

Philips, J., Maes, N., Springael, D., Smolders, E., 2013. Acidification due to microbial dechlorination near a trichloroethene DNAPL is overcome with pH buffer or formate as electron donor: Experimental demonstration in diffusion-cells. J. Contam. Hydrol. 147, 25–33. https://doi.org/10.1016/j.jconhyd.2013.02.002

Puggioni, G., Milia, S., Dessì, E., Unali, V., Pous, N., Balaguer, M.D., Puig, S., Carucci, A., 2021. Combining electro-bioremediation of nitrate in saline groundwater with concomitant chlorine production. Water Res. 206, 117736. https://doi.org/10.1016/j.watres.2021.117736

Riis, V., Babel, W., 1999. Removal of sulfur interfering in the analysis of organochlorines by GC-ECD. Analyst 124, 1771–1773. https://doi.org/https://doi.org/10.1039/A907504F

Rognes, T., Flouri, T., Nichols, B., Quince, C., Mahé, F., 2016. VSEARCH: A versatile open source tool for metagenomics. PeerJ 2016, 1–22. https://doi.org/10.7717/peerj.2584

Rosato, A., Barone, M., Negroni, A., Brigidi, P., Fava, F., Xu, P., Candela, M., Zanaroli, G., 2020. Microbial colonization of different microplastic types and biotransformation of sorbed PCBs by a marine anaerobic bacterial community. Sci. Total Environ. 705, 135790. https://doi.org/10.1016/j.scitotenv.2019.135790

Sandefur, C.A., Koenigsberg, S.S., 1999. The use of hydrogen Release Compound for the accelerated bioremediation of anaerobically degradable contaminants: The advent of time-release electron donors. Remediat. J. 10, 31–53. https://doi.org/10.1002/rem.3440100104

Song, M., Luo, C., Li, F., Jiang, L., Wang, Y., Zhang, D., Zhang, G., 2015. Anaerobic degradation of Polychlorinated Biphenyls (PCBs) and Polychlorinated Biphenyls Ethers (PBDEs), and microbial community dynamics of electronic waste-contaminated soil. Sci. Total Environ. 502, 426–433. https://doi.org/10.1016/j.scitotenv.2014.09.045

Sowers, K.R., May, H.D., 2013. In situ treatment of PCBs by anaerobic microbial dechlorination in aquatic sediment: Are we there yet? Curr. Opin. Biotechnol. 24, 482–488. https://doi.org/10.1016/j.copbio.2012.10.004

Su, W., Zhang, L., Tao, Y., Zhan, G., Li, Dongxun, Li, Daping, 2012. Sulfate reduction with electrons

directly derived from electrodes in bioelectrochemical systems. Electrochem. commun. 22, 37–40. https://doi.org/10.1016/j.elecom.2012.04.030

Sun, J., Hu, Y., Li, W., Zhang, Y., Chen, J., Deng, F., 2015. Sequential decolorization of azo dye and mineralization of decolorization liquid coupled with bioelectricity generation using a pH self-neutralized photobioelectrochemical system operated with polarity reversion. J. Hazard. Mater. 289, 108–117. https://doi.org/10.1016/j.jhazmat.2015.02.010

Viggi, C.C., Tucci, M., Resitano, M., Matturro, B., Crognale, S., Feigl, V., Molnár, M., Rossetti, S., Aulenta, F., 2022. Passive electrobioremediation approaches for enhancing hydrocarbons biodegradation in contaminated soils. Sci. Total Environ. 845. https://doi.org/10.1016/j.scitotenv.2022.157325

Villano, M., Aulenta, F., Ciucci, C., Ferri, T., Giuliano, A., Majone, M., 2010. Bioelectrochemical reduction of CO2 to CH4 via direct and indirect extracellular electron transfer by a hydrogenophilic methanogenic culture. Bioresour. Technol. 101, 3085–3090. https://doi.org/10.1016/j.biortech.2009.12.077

Wang, S., Chng, K.R., Wilm, A., Zhao, S., Yang, K.L., Nagarajan, N., He, J., 2014. Genomic characterization of three unique Dehalococcoides that respire on persistent polychlorinated biphenyls. Proc. Natl. Acad. Sci. 111, 12103–12108. https://doi.org/10.1073/pnas.1404845111

Wang, Y., Sheng, H.F., He, Y., Wu, J.Y., Jiang, Y.X., Tam, N.F.Y., Zhou, H.W., 2012. Comparison of the levels of bacterial diversity in freshwater, intertidal wetland, and marine sediments by using millions of illumina tags. Appl. Environ. Microbiol. 78, 8264–8271. https://doi.org/10.1128/AEM.01821-12

Watanabe, M., Galushko, A., Fukui, M., Kuever, J., 2021. Desulfosarcinaceae . Bergey's Man. Syst. Archaea Bact. 1–4. https://doi.org/10.1002/9781118960608.fbm00329

Wei, D., Zhang, X., Li, C., Zhao, M., Wei, L., 2022. Efficiency and bacterial diversity of an improved anaerobic baffled reactor for the remediation of wastewater from alkaline-surfactant-polymer (ASP) flooding technology. PLoS One 17, 1–16. https://doi.org/10.1371/journal.pone.0261458

Widdicombe, S., Spicer., J., Kitidis, V., 2011. Effects of ocean acidification on sediment fauna, in: Gattuso, J.-P., Hansson, L. (Eds.), Ocean Acidification. Oxford University Press, Oxford, UK, pp. 176–191.

Yan, M., Treu, L., Campanaro, S., Tian, H., Zhu, X., Khoshnevisan, B., Tsapekos, P., Angelidaki, I., Fotidis, I.A., 2020. Effect of ammonia on anaerobic digestion of municipal solid waste : Inhibitory performance , bioaugmentation and microbiome functional reconstruction. Chem. Eng. J. 401, 126159. https://doi.org/10.1016/j.cej.2020.126159

Yilmaz, P., Parfrey, L.W., Yarza, P., Gerken, J., Pruesse, E., Quast, C., Schweer, T., Peplies, J., Ludwig, W., Glöckner, F.O., 2014. The SILVA and "all-species Living Tree Project (LTP)" taxonomic frameworks. Nucleic Acids Res. 42, 643–648. https://doi.org/10.1093/nar/gkt1209

Yu, H., Feng, C., Liu, X., Yi, X., Ren, Y., Wei, C., 2016. Enhanced anaerobic dechlorination of polychlorinated biphenyl in sediments by bioanode stimulation. Environ. Pollut. 211, 81–89. https://doi.org/10.1016/j.envpol.2015.12.039

Yu, H., Feng, C., Liu, X., Yi, X., Ren, Y., Wei, C., Wan, H., Xue, Y., Feng, C., Wei, C., Yu, H., Wan, H., Feng, C., Yi, X., Liu, X., Ren, Y., Wei, C., 2017. Microbial polychlorinated biphenyl dechlorination in sediments by electrical stimulation: The effect of adding acetate and nonionic surfactant. Sci. Total Environ. 580, 1371–1380. https://doi.org/10.1039/c7ra02849k

Zanaroli, G., Balloi, A., Negroni, A., Borruso, L., Daffonchio, D., Fava, F., 2012. A Chloroflexi bacterium dechlorinates polychlorinated biphenyls in marine sediments under in situ-like biogeochemical conditions. J. Hazard. Mater. 209–210, 449–457. https://doi.org/10.1016/j.jhazmat.2012.01.042

Zhang, D., Li, X., Zhang, C., Xiao, Z., Li, Y., Liang, Y., Dang, H., 2021. Electrostimulated bio-dechlorination of a PCB mixture (Aroclor 1260) in a marine-originated dechlorinating culture. Environ. Pollut. 291, 118157. https://doi.org/10.1016/j.envpol.2021.118157

Zhang, H., Quan, H., Zhou, S., Sun, L., Lu, H., 2022. Enhanced performance and electron transfer of sulfur-mediated biological process under polyethylene terephthalate microplastics exposure. Water Res. 223, 119038. https://doi.org/10.1016/j.watres.2022.119038

Zhang, T., Bain, T.S., Barlett, M.A., Dar, S.A., Snoeyenbos-West, O.L., Nevin, K.P., Lovley, D.R., 2014. Sulfur oxidation to sulfate coupled with electron transfer to electrodes by Desulfuromonas strain TZ1. Microbiol. (United Kingdom) 160, 123–129. https://doi.org/10.1099/mic.0.069930-0

Zhang, X., Wei, S., Zhang, D., Lu, P., Huang, Y., 2022. Efficient sulfur cycling improved the performance of flowback water treatment in a microbial fuel cell. J. Environ. Manage. 323,

116368. https://doi.org/10.1016/j.jenvman.2022.116368

Zhou, J., He, Q., Hemme, C.L., Mukhopadhyay, A., Hillesland, K., Zhou, A., He, Z., Van Nostrand, J.D., Hazen, T.C., Stahl, D.A., Wall, J.D., Arkin, A.P., 2011. How sulphate-reducing microorganisms cope with stress: Lessons from systems biology. Nat. Rev. Microbiol. 9, 452–466. https://doi.org/10.1038/nrmicro2575

4.7 Supplementary materials

S1 - Preliminary study to evaluate OER in high chlorine concentrated water

S2- Figure S2 – pH profile in time of the open circuit voltage microcosm

S3– Figure S3 - pH profile in time of the bioelectrochemical system working at a potential of -0.7 V vs Ag/AgCl (3M KCl)

S4 – Figure S4 – pH profile in time of the single circuit bioelectrochemical system working with an applied current density of 0.025 $mA \cdot cm^{-2}$

S5 – Figure S5 - pH profile in time of the double circuit bioelectrochemical system working with an applied current density of 0.025 $mA \cdot cm^{-2}$

S6– Figure S6 – pH profile in time of the single circuit bioelectrochemical system working with an applied current density of 0.05 $mA \cdot cm^{-2}$

S7 – Figure S7 - pH profile in time of the double circuit bioelectrochemical system working with an applied current density of 0.05 $mA \cdot cm^{-2}$

S8 – Figure S8 - redox potential profile in time of the open circuit voltage microcosm

S8 – Figure S9 – redox potential profile in time of the bioelectrochemical system working at a potential of -0.7 V vs Ag/AgCl (3M KCl)

S10 – Figure S10 - redox potential profile in time of the single circuit bioelectrochemical system working with an applied current density of 0.025 $mA \cdot cm^{-2}$

S11 – Figure S11 - redox potential profile in time of the double circuit bioelectrochemical system working with an applied current density of 0.025 $mA \cdot cm^{-2}$

S12 – Figure S12 - redox potential profile in time of the single circuit bioelectrochemical system working with an applied current density of 0.05 $mA \cdot cm^{-2}$

S13 – Figure S13 - redox potential profile in time of the double circuit bioelectrochemical system working with an applied current density of 0.05 $mA \cdot cm^{-2}$

S14 – Figure S14 - sulfate concentration profile in time of the open circuit control and of the bioelectrochemical system working at a potential of -0.7 V vs Ag/AgCl (3M KCl)

S15 – Figure S15 - sulfate concentration profile in time of the open circuit control and of the bioelectrochemical systems with one circuit and two circuits working with an applied current density of 0.025 $mA \cdot cm^{-2}$

S16 – Figure S16 - sulfate concentration profile in time of the open circuit control and of the bioelectrochemical systems with one circuit and two circuits working with an applied current density of 0.05 $mA \cdot cm^{-2}$

S17 – Figure S17 - Profile of the chlorination degree of the PCB mixture in the studied microcosms

S18 – Figure S18 - Profile of the current flow in time of the bioelectrochemical system working at a potential of -0.7 V vs Ag/AgCl (3M KCl)

S19 – Figure S19 - Profile of the cathodic potential in time of the single circuit bioelectrochemical system working with an applied current density of 0.025 $mA \cdot cm^{-2}$

S20 – Figure S20 - Profile of the cathodic potential in time of the double circuit bioelectrochemical system working with an applied current density of 0.025 $mA \cdot cm^{-2}$

S21 – Figure S21 - Profile of the cathodic potential in time of the single circuit bioelectrochemical system working with an applied current density of 0.05 $mA \cdot cm^{-2}$

S22 – Figure S22 - Profile of the cathodic potential in time of the double circuit bioelectrochemical system working with an applied current density of 0.05 $mA \cdot cm^{-2}$

S23 – Figure S23 - PCoA based on weighted UniFrac distance among sediments microbiota profiles of the studied microcosms at 25, 95 and 159 days

S24 – Figure S24 - PCoA based on unweighted UniFrac distance among sediments microbiota profiles of the studied microcosms at 25, 95 and 159 days

S25 – Figure S25 - Phylogenetic profiles at the family level of the inoculated sediment at the beginning of the experiment and of the studied microcosms at 25, 95 and 159 days

S26 – Table S4 – adjusted p-values of the two tailed t-tests (0.05 significance threshold) performed with the data of the sulfate depletion percentages at 159 days of the bioelectrochemical systems

S27 – Table S5 - adjusted p-values of two tailed t-test (0.05 significance threshold) between the sulfate depletion percentages at 159 days of each bioelectrochemical system and the open circuit control

S28 – Table S6 - Coulombic efficiencies of the BES, calculated at the end of the experiment (159 days)

S29 – Table S7 - adjusted p-values of the two tailed t-tests (0.05 significance threshold) performed with the data of the reduction percentages of the chlorination degree

S30 – Table S8 - Potentiostatic data of the bioelectrochemical systems

S31 - Table S9 - Relative abundance profiles of bacteria selected as potential SRB in marine sediments at 25 days

S32 - Table S10 - Relative abundance profiles of bacteria selected as potential SRB in marine sediments at 95 days

S33 - Table S11 - Relative abundance profiles of bacteria selected as potential SRB in marine sediments at 159 days

(S1) Preliminary study to evaluate OER in high chlorine concentrated water

The aim of this experiment was to assess the durability of the anodic Nafion^{TM} coverage reported by Balaji *et al.* (2009), in order to develop a simple electrode modification to enhance oxygen evolution reaction. Stainless steel 316 as plate was chosen as an easy to modify electrode, since the hot press required a flat and robust material. During test I, the anodic oxygen production of the SS was initially measured using the pristine electrode. After 45 min of electrolysis, the oxygen concentration in the blank solution ($NaNO_3$ 0.5 M) reached a 57 ± 4 % of air saturation (Table S1). Conversely, the electrolysis of synthetic marine water (NaCl 0.5M) led to a negligible oxygen level (0.5 ± 0.5 %). In the synthetic marine

water, the presence of chlorine probably led to the electrode corrosion, which resulted in low working potential (Figure S1), not sufficient to perform water electrolysis.

Table S1 *Oxygen level obtained in test I (45 min, 5 mA·cm^{-2}) in the blank solution and in the synthetic marine water*

Blank solution, $NaNO_3$ 0.5 M		**Synthetic marine water, NaCl 0.5 M**	
O_2 in solution (air saturation %)	O_2 in the headspace (mM)	O_2 in solution (air saturation %)	O_2 in the headspace (mM)
57 ± 4	2 ± 1	0.5 ± 0.5	Not detected

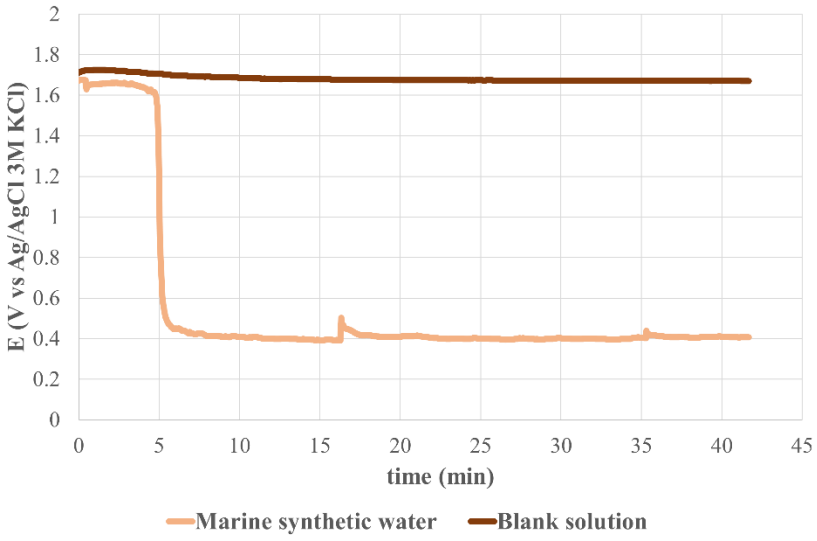

Figure S1 *Anodic potential measured during test I (45 min, 5 mA·cm^{-2}), using synthetic marine water and blank solution as electrolyte*

Subsequently, during test II, SS electrodes were covered with a Nafion^{TM} membrane to prevent diffusion of anions through the polymeric membrane, mitigating CLER. The electrochemical oxygen production of the coated anodes was assessed in the blank solution as well as in the synthetic marine water. As expected, the oxygen production obtained in the $NaNO_3$ electrolyte was lower in the presence of membrane, probably due to the physical barrier that limited the mass transfers: air saturation percentage was equal to 20.1 ± 3.2 % (Table S2). On the other hand, the oxygen production in synthetic marine water showed a similar value to the one obtained with the blank solution: 21.8 ± 2.7 %, confirming the

ability of the cation exchange membrane to limit the diffusion of Cl^- from the bulk of the medium to the electrode.

Table S2 *Oxygen level obtained in test II (5 mA·cm^{-2}) in the blank solution and in the synthetic marine water*

Time (min)	Blank solution, $NaNO_3$ 0.5 M		Synthetic marine water, NaCl 0.5 M	
	O_2 in solution (air saturation %)	O_2 in the headspace (mM)	O_2 in solution (air saturation %)	O_2 in the headspace (mM)
90	6.3 ± 0.2	0.0 ± 0	3.1 ± 0.3	1.0 ± 0.1
150	18.8 ± 0.5	6.7 ± 0.3	19.2 ± 0.7	6.8 ± 0.4
210	20.1 ± 3.2	10.3 ± 0.9	21.8 ± 2.7	5.5 ± 0.7

After having determined the potential of the Nafion membrane in preventing the CLER, the endurance of the modified electrodes was studied. In test III, a coated SS plate was repeatedly used in different cycles to oxygenate a synthetic marine water solution for 150 min with a current applied of 5 mA·cm^{-2}, until the exhaustion of the electrode. During the first three cycles, saturation levels of the electrolyte solution around 20% were obtained with all the replicates. Yet, the average durability of the modified electrode was of 3 cycles (Table S3), which was not considered compatible for an application of the system in real conditions. Following these experiments, the current density was diminished to 1 mA·cm^{-2}, 0.4 mA·cm^{-2} and 0.2 mA·cm^{-2} so as to reduce the kinetic of the process and enlarge the durability of the system. During these trials, no oxygen was produced due to the low anodic potentials (0.3-0.01 V, data not showed), not sufficient for OER (Karlsson and Cornell, 2016).

Table S3 *Oxygen level obtained in test III (150 min, 5 mA·cm^{-2}) for the three replicates used for the electrochemical oxygenation cycles*

Cycle	Replicate 1		Replicate 2		Replicate 3	
	O_2 in solution (air saturation %)	O_2 in the headspace (mM)	O_2 in solution (air saturation %)	O_2 in the headspace (mM)	O_2 in solution (air saturation %)	O_2 in the headspace (mM)

1°	20.3	3.37	23.0	1.82	17.8	2.91
2°	24.0	4.31	21.1	3.06	23.0	4.00
3°	25.4	3.69	24.2	3.99	31.9	4.02
4°	Overload		23.0	3.06	Overload	
			Overload			

(S2)

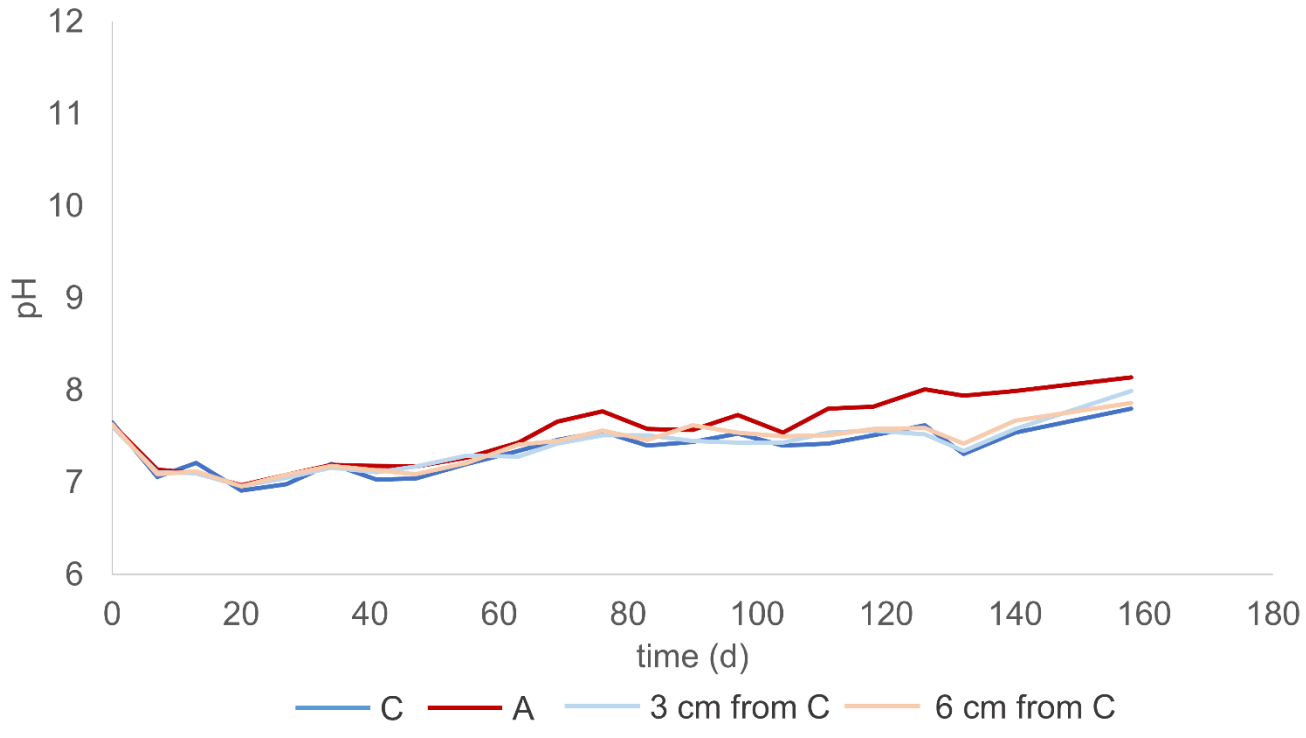

Figure S2 *pH profile in time of the open circuit voltage microcosm*

(S3)

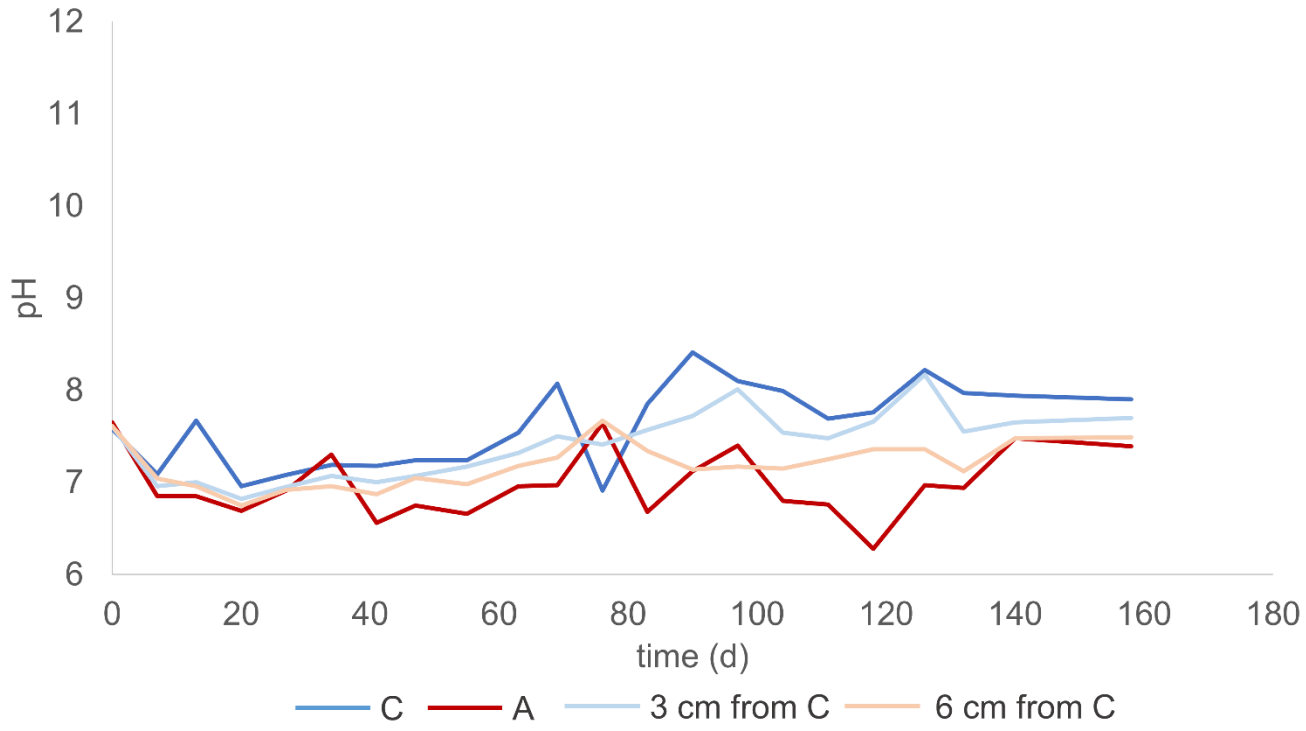

Figure S3 *pH profile in time of the bioelectrochemical system working at a potential of -0.7 V vs Ag/AgCl (3M KCl)*

(S4)

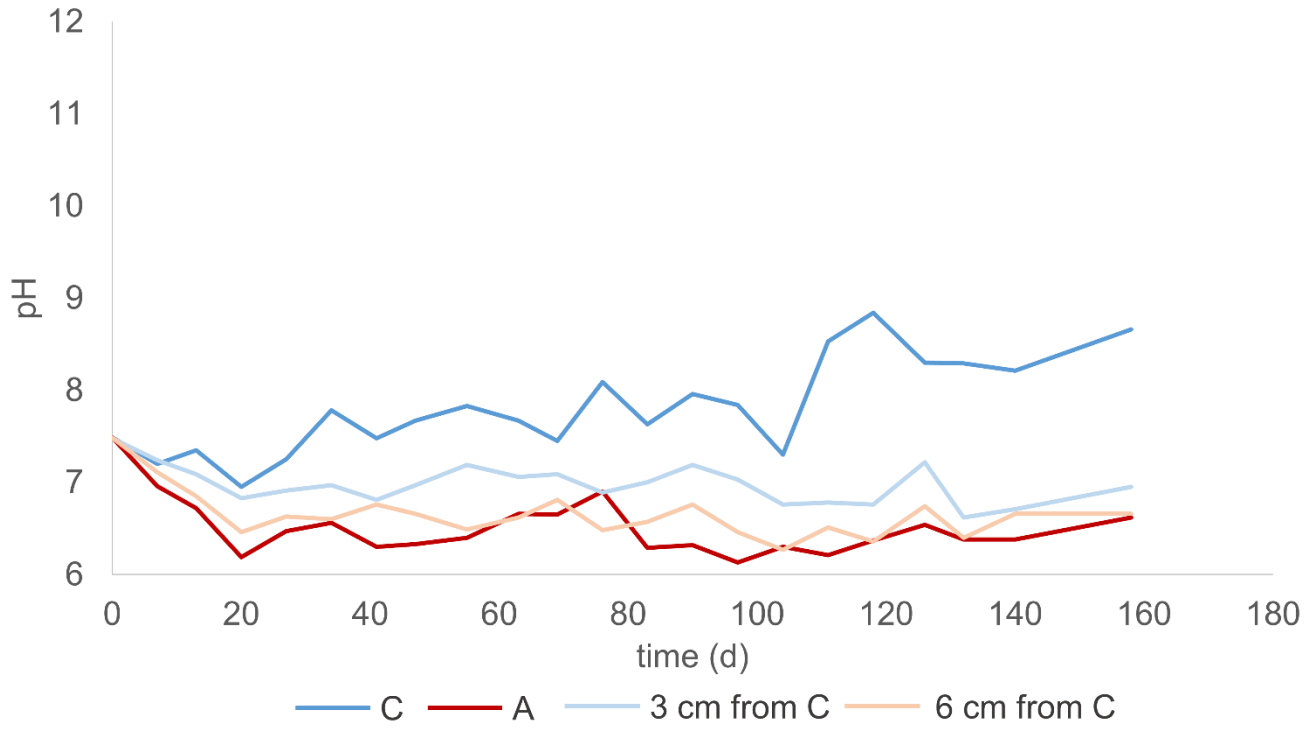

Figure S4 *pH profile in time of the single circuit bioelectrochemical system working with an applied current density of 0.025 mA·cm*$^{-2}$

(S5)

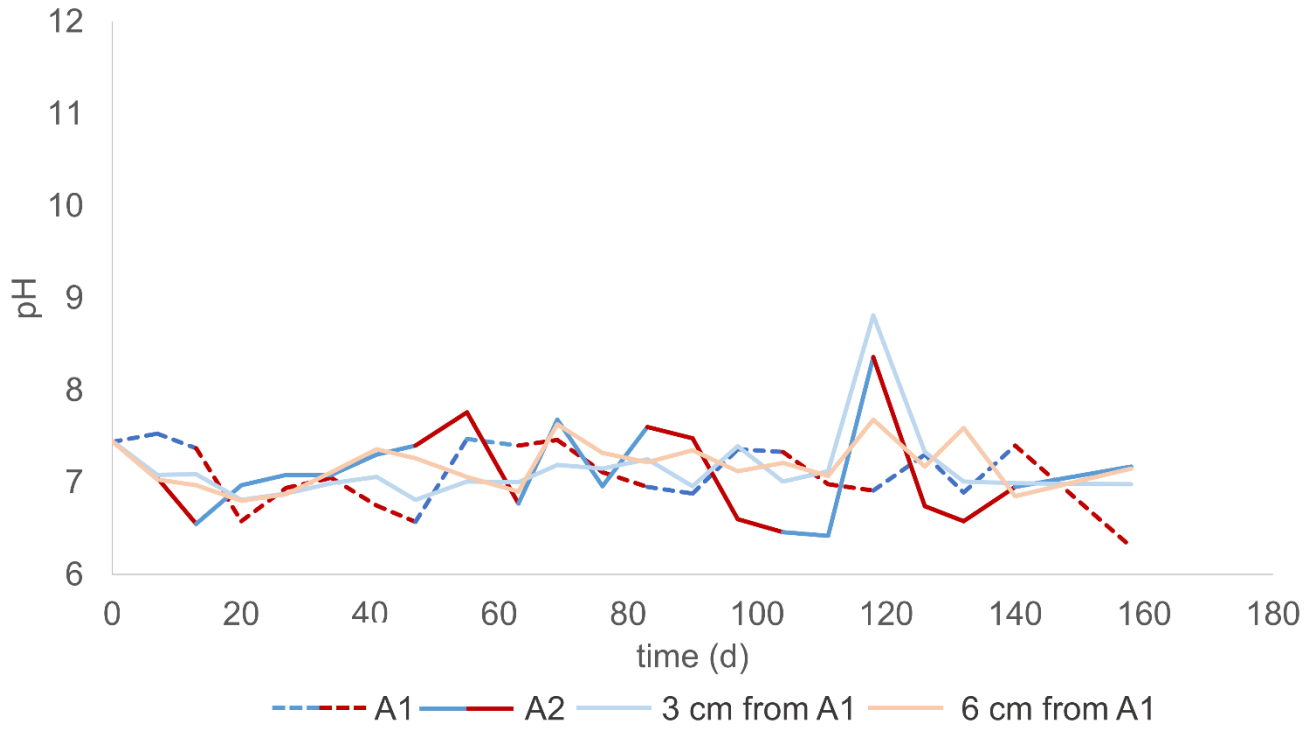

Figure S5 *pH profile in time of the double circuit bioelectrochemical system working with an applied current density of 0.025 mA·cm^{-2}*

dashed line blue or red: area 1; bold line blue or red: area 2; blue indicates a cathodic stimulation; red indicates an anodic stimulation

(S6)

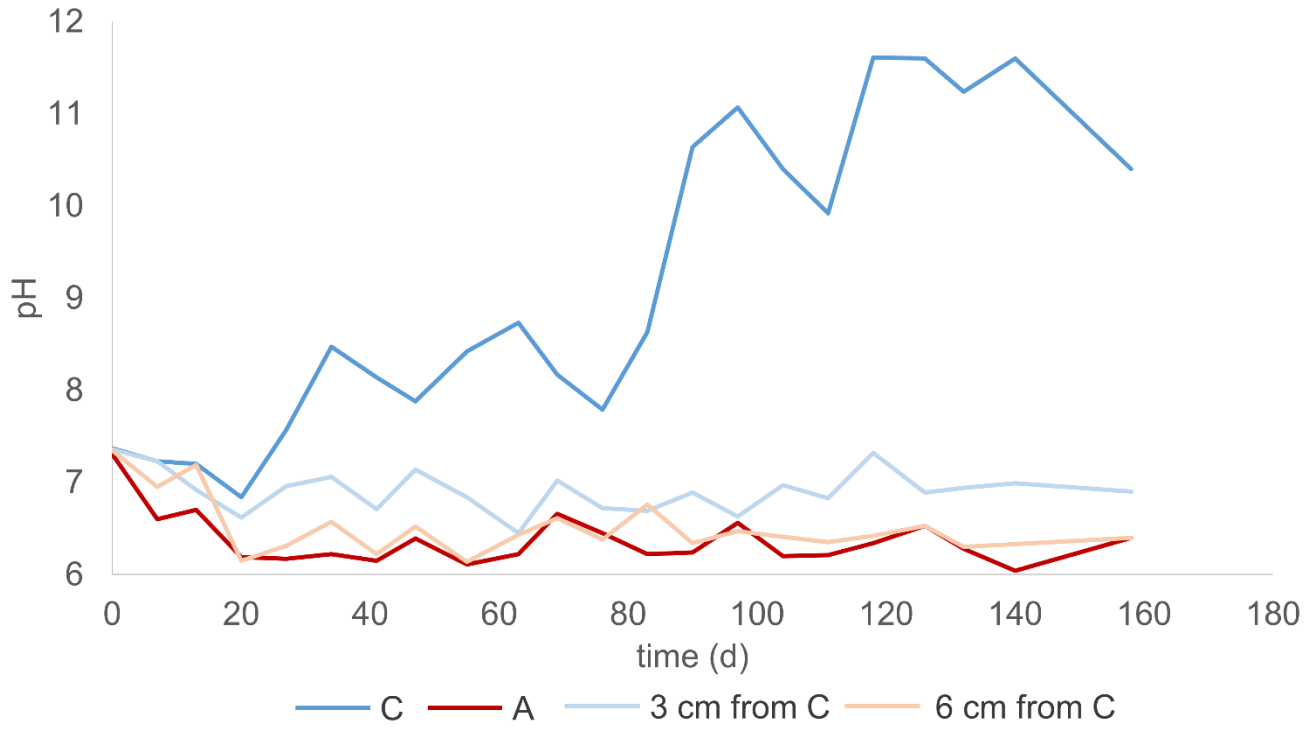

Figure S6 *pH profile in time of the single circuit bioelectrochemical system working with an applied current density of 0.05 mA·cm*$^{-2}$

(S7)

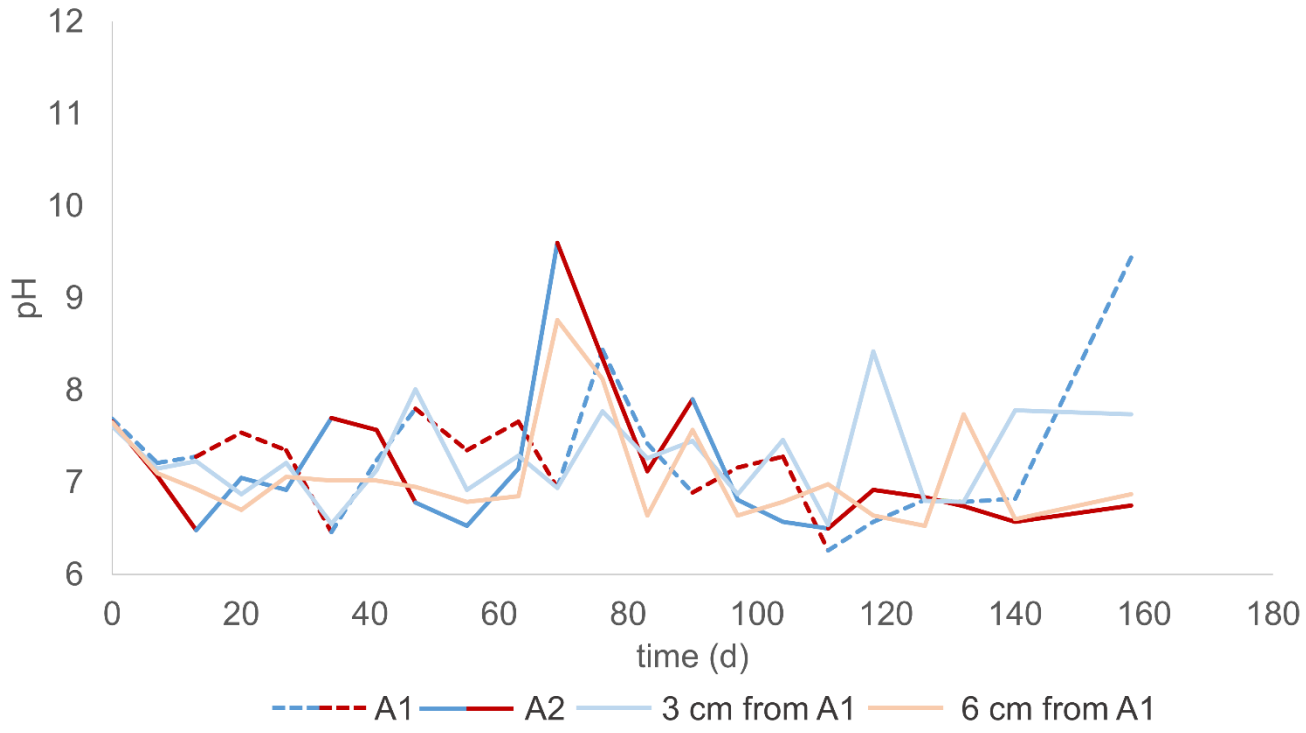

Figure S7 *pH profile in time of the double circuit bioelectrochemical system working with an applied current density of 0.05 mA·cm^{-2}*

dashed line blue or red: area 1; bold line blue or red: area 2; blue indicates a cathodic stimulation; red indicates an anodic stimulation

(S8)

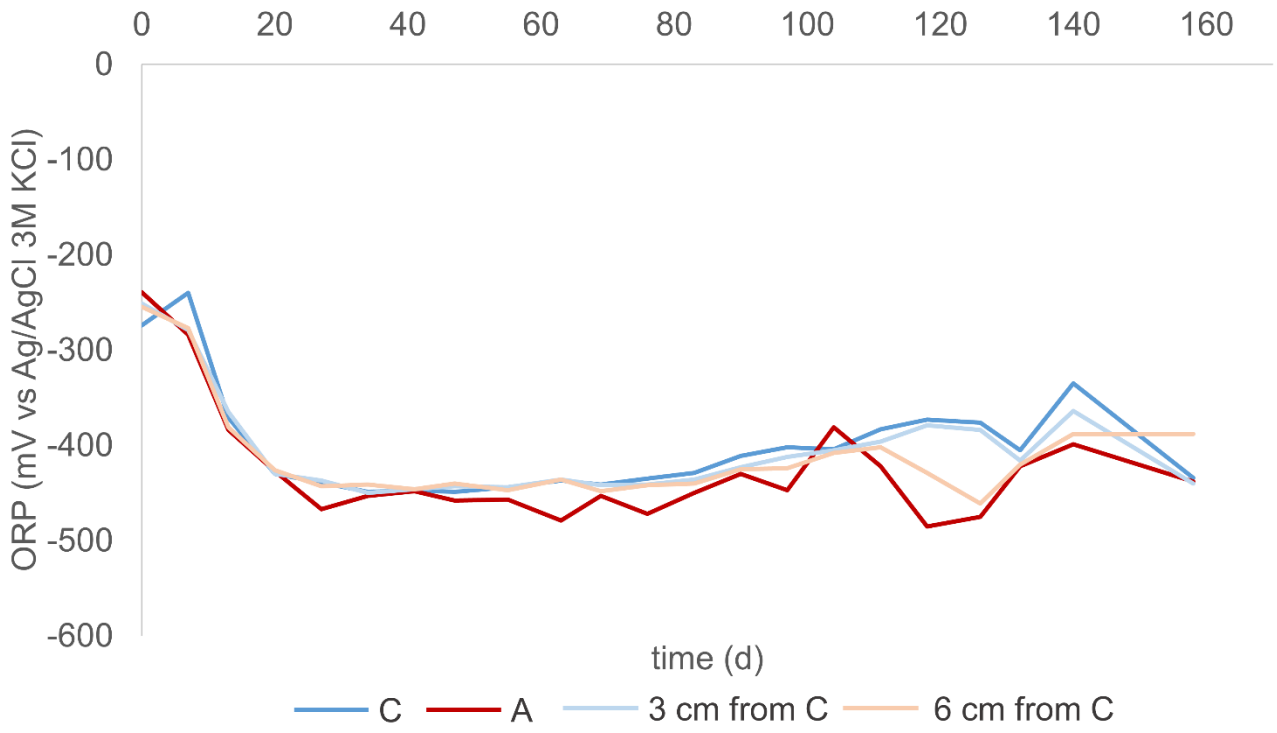

Figure S8 *redox potential profile in time of the open circuit voltage microcosm*

(S9)

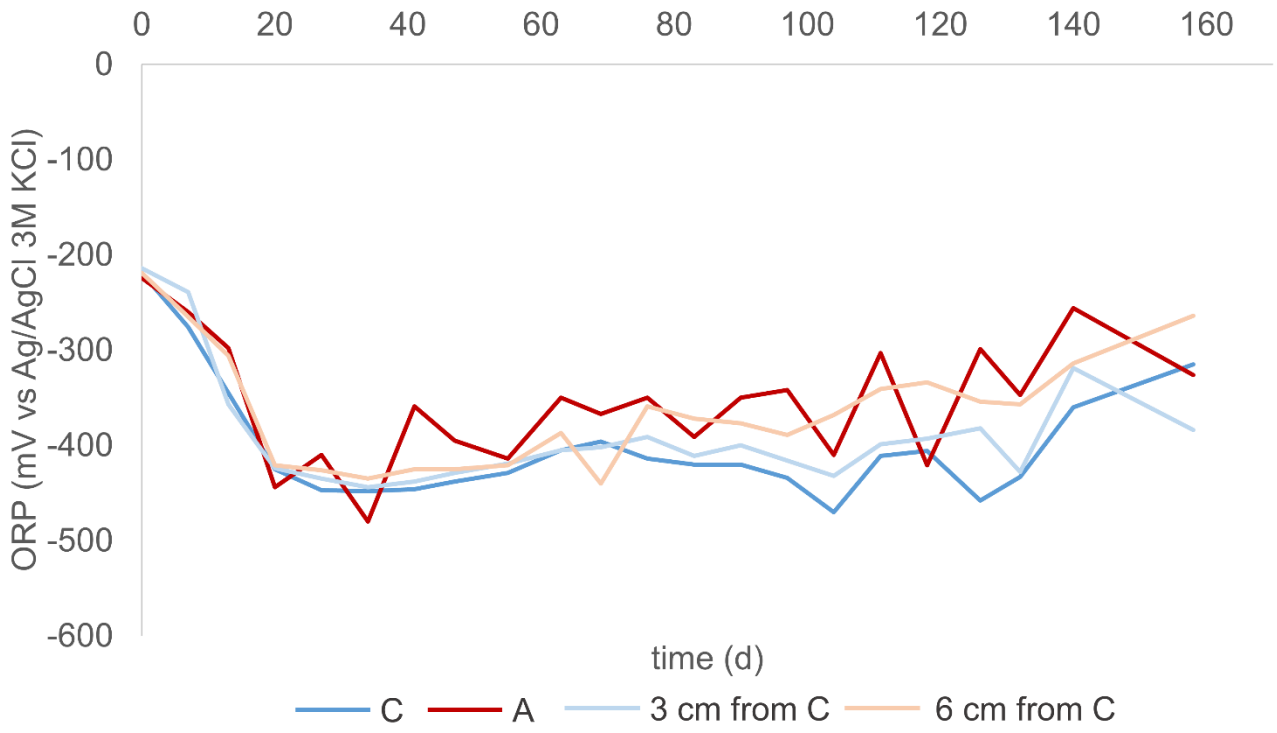

Figure S9 *redox potential profile in time of the bioelectrochemical system working at a potential of -0.7 V vs Ag/AgCl (3M KCl)*

(S10)

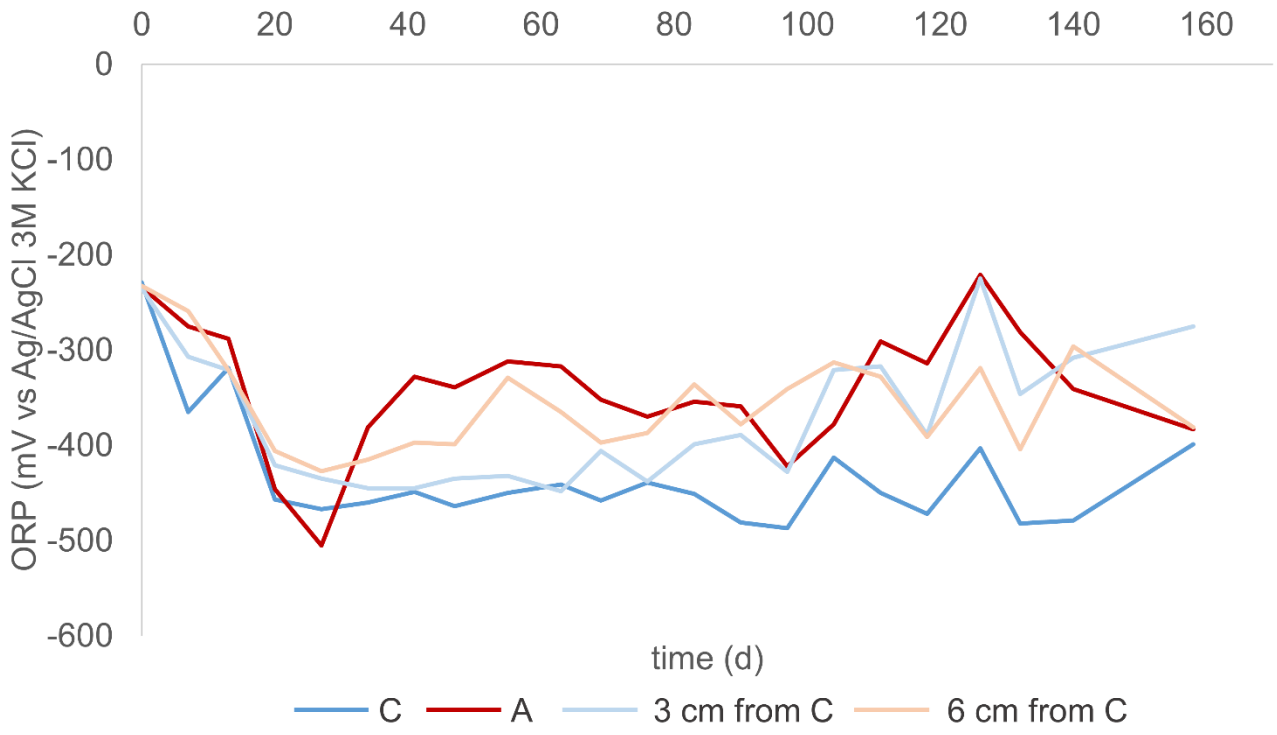

Figure S10 *redox potential profile in time of the single circuit bioelectrochemical system working with an applied current density of 0.025 mA·cm*$^{-2}$

(S11)

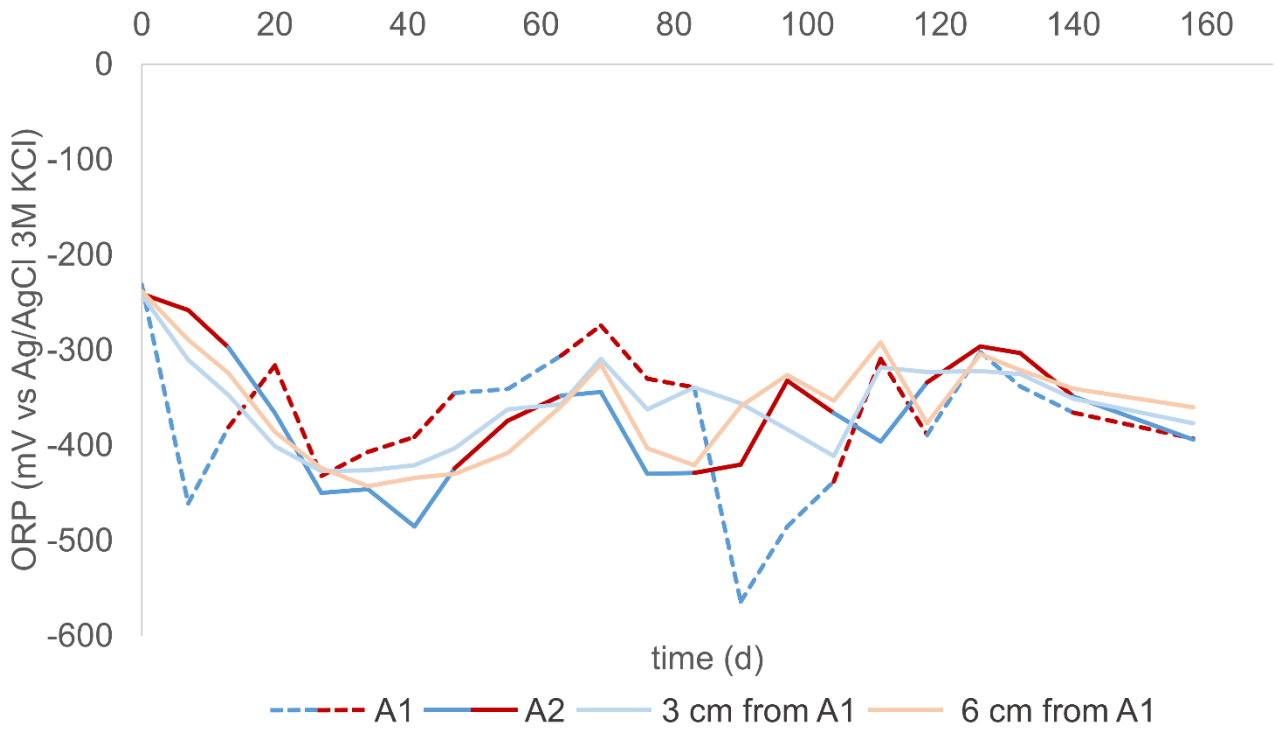

Figure S11 *redox potential profile in time of the double circuit bioelectrochemical system working with an applied current density of 0.025 mA·cm^{-2}*

dashed line blue or red: area 1; bold line blue or red: area 2; blue indicates a cathodic stimulation; red indicates an anodic stimulation

(S12)

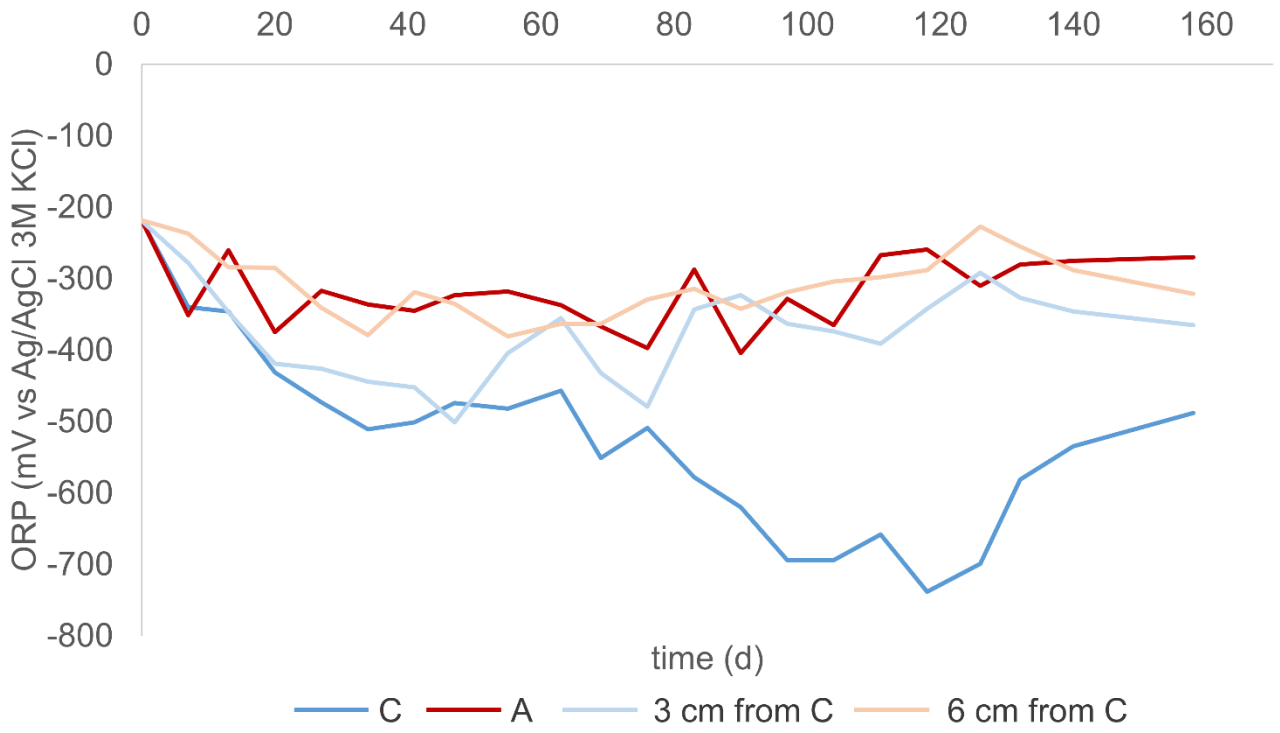

Figure S12 *redox potential profile in time of the single circuit bioelectrochemical system working with an applied current density of 0.05 mA·cm^{-2}*

(S13)

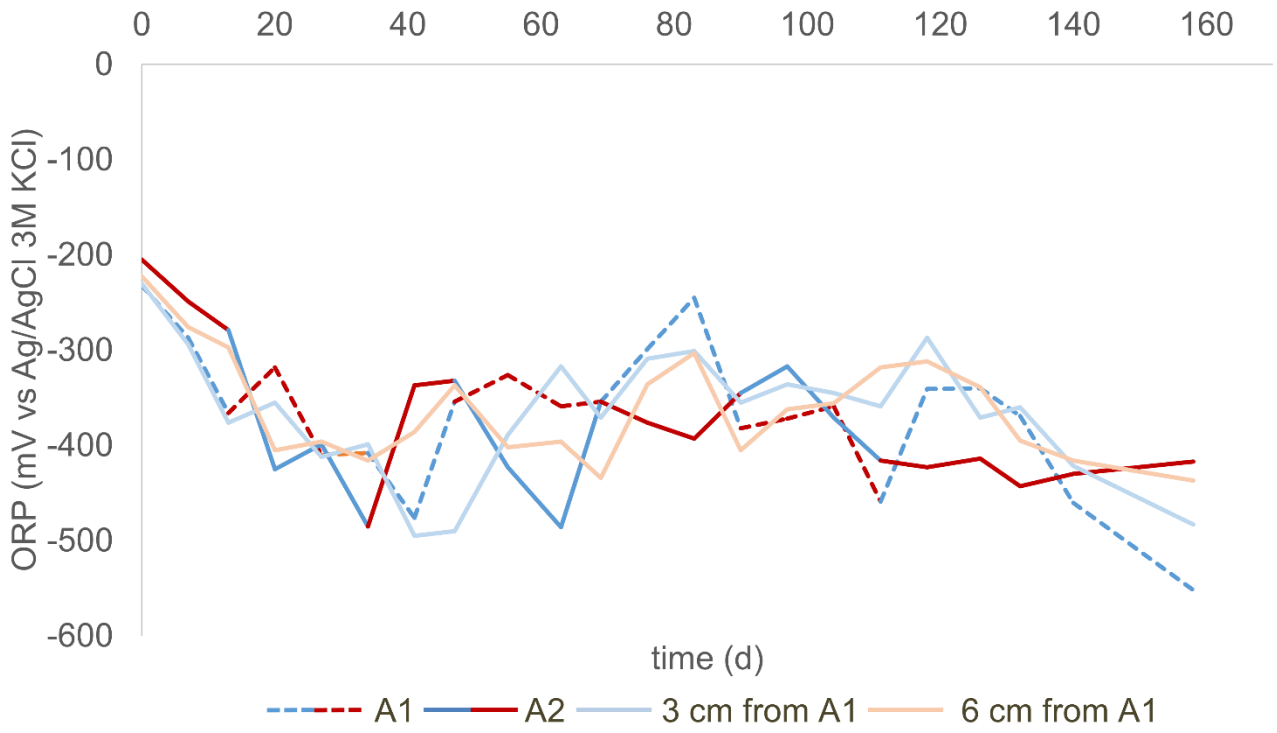

Figure S13 *redox potential profile in time of the double circuit bioelectrochemical system working with an applied current density of 0.05 mA·cm^{-2}*

dashed line blue or red: area 1; bold line blue or red: area 2; blue indicates a cathodic stimulation; red indicates an anodic stimulation

(S14)

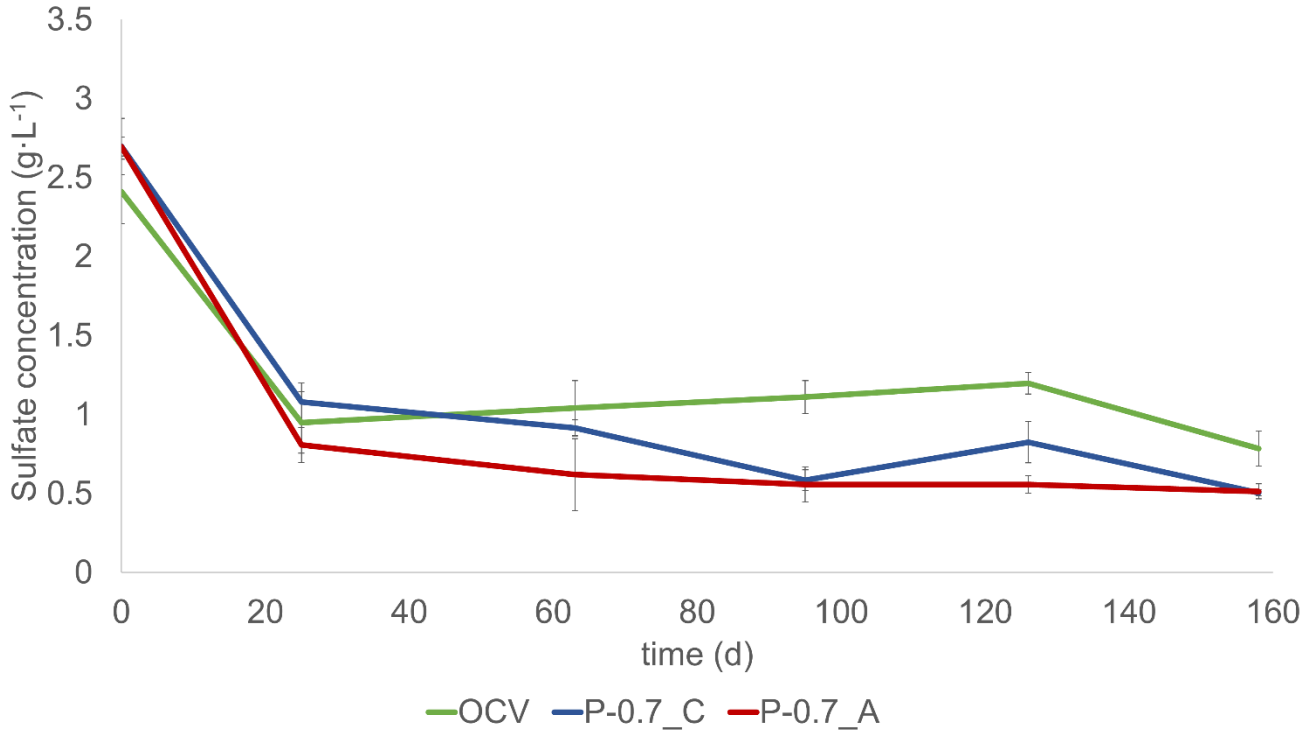

Figure S14 *sulfate concentration profile in time of the open circuit control and of the bioelectrochemical system working at a potential of -0.7 V vs Ag/AgCl (3M KCl)*

(S15)

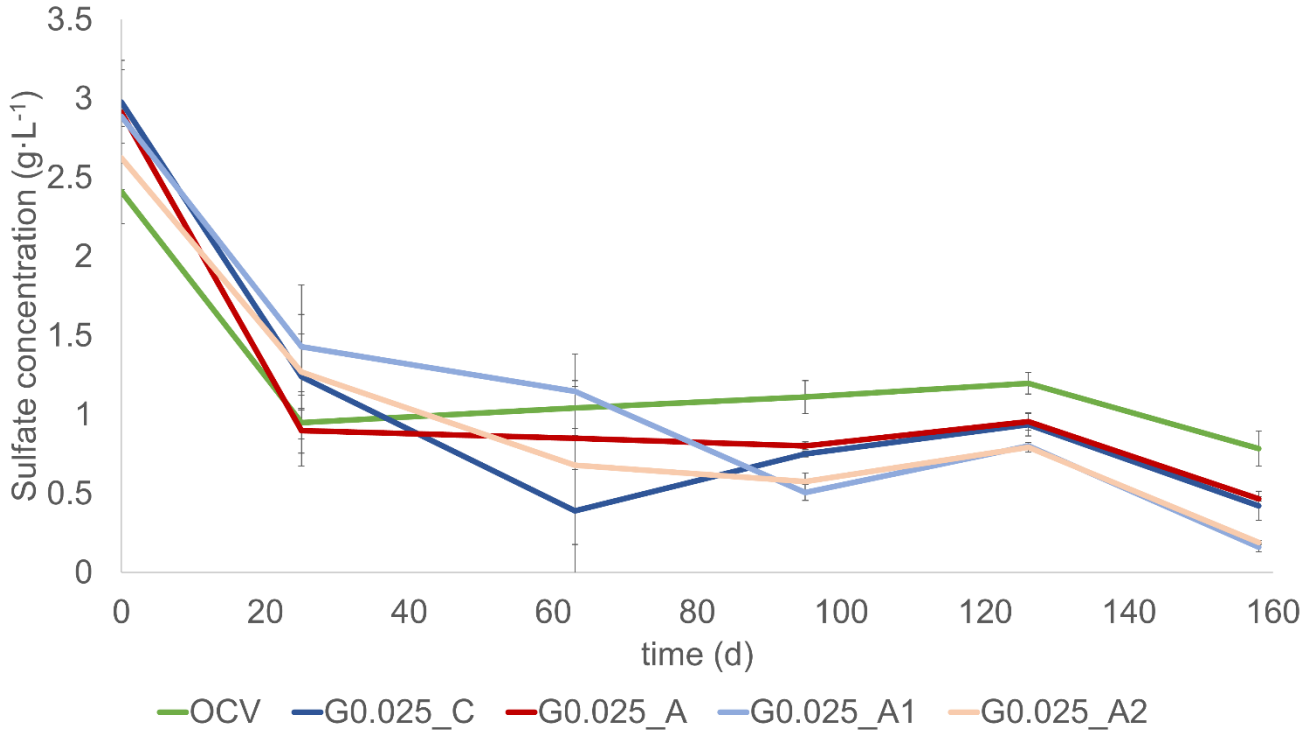

Figure S15 *sulfate concentration profile in time of the open circuit control and of the bioelectrochemical systems with one circuit and two circuits working with an applied current density of 0.025 mA·cm*$^{-2}$

(S16)

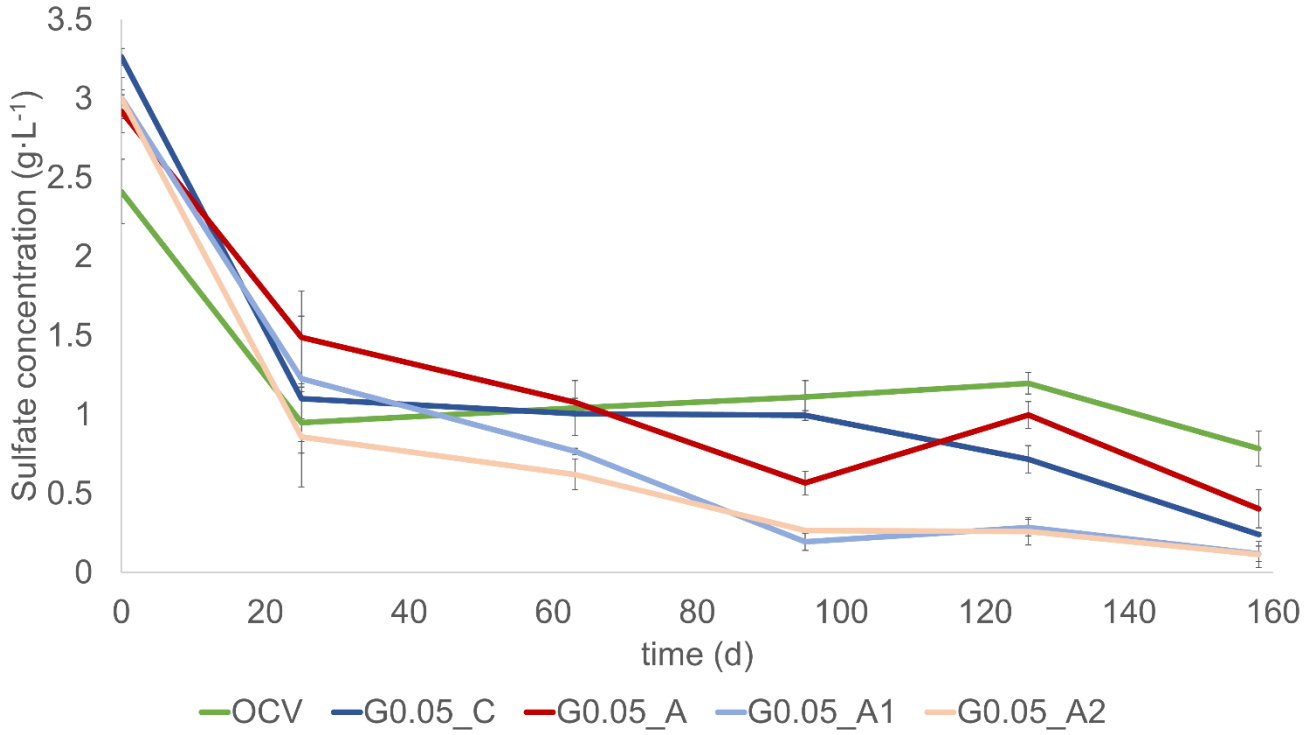

Figure S16 *sulfate concentration profile in time of the open circuit control and of the bioelectrochemical systems with one circuit and two circuits working with an applied current density of 0.05 mA·cm*$^{-2}$

(S17)

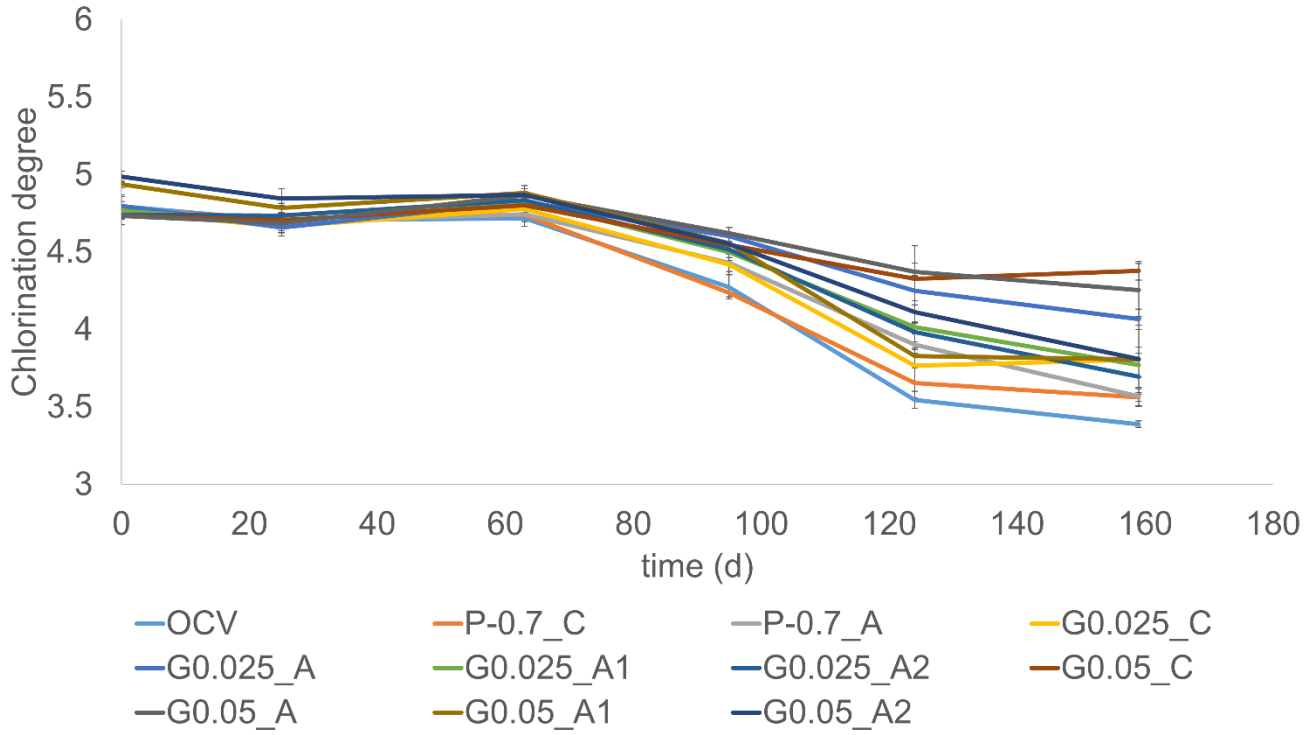

Figure S17 *Profile of the chlorination degree of the PCBs mixture in the studied microcosms*

(S18)

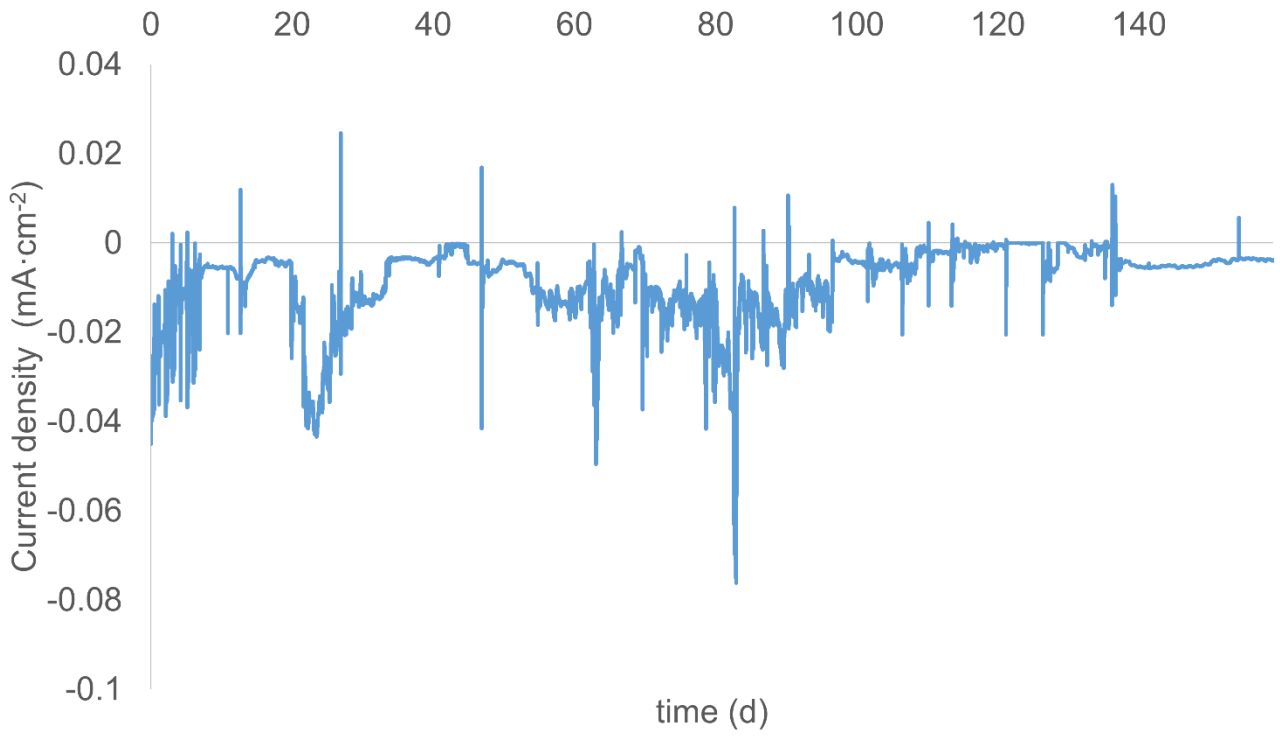

Figure S18 *Profile of the current flow in time of the bioelectrochemical system working at a potential of -0.7 V vs Ag/AgCl (3M KCl)*

(S19)

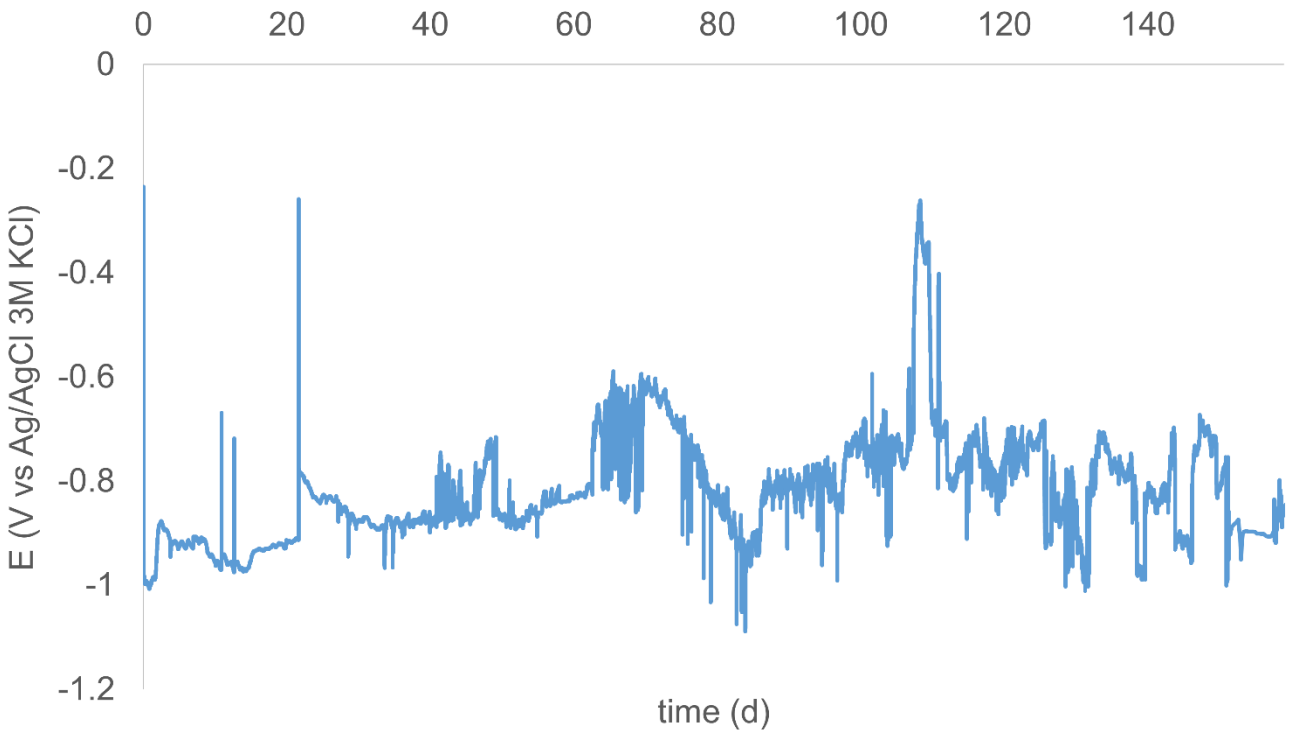

Figure S19 *Profile of the cathodic potential in time of the single circuit bioelectrochemical system working with an applied current density of 0.025 mA·cm^{-2}*

(S20)

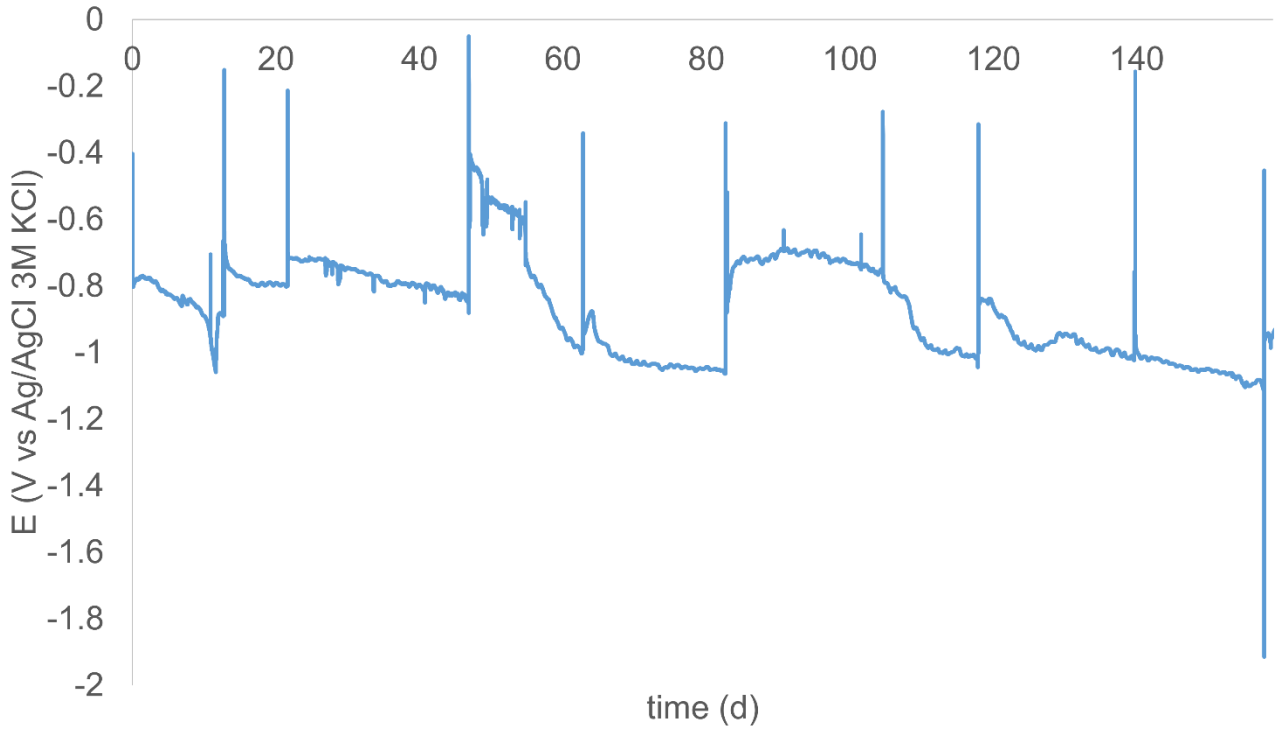

Figure S20 *Profile of the cathodic potential in time of the double circuit bioelectrochemical system working with an applied current density of 0.025 mA·cm*$^{-2}$

(S21)

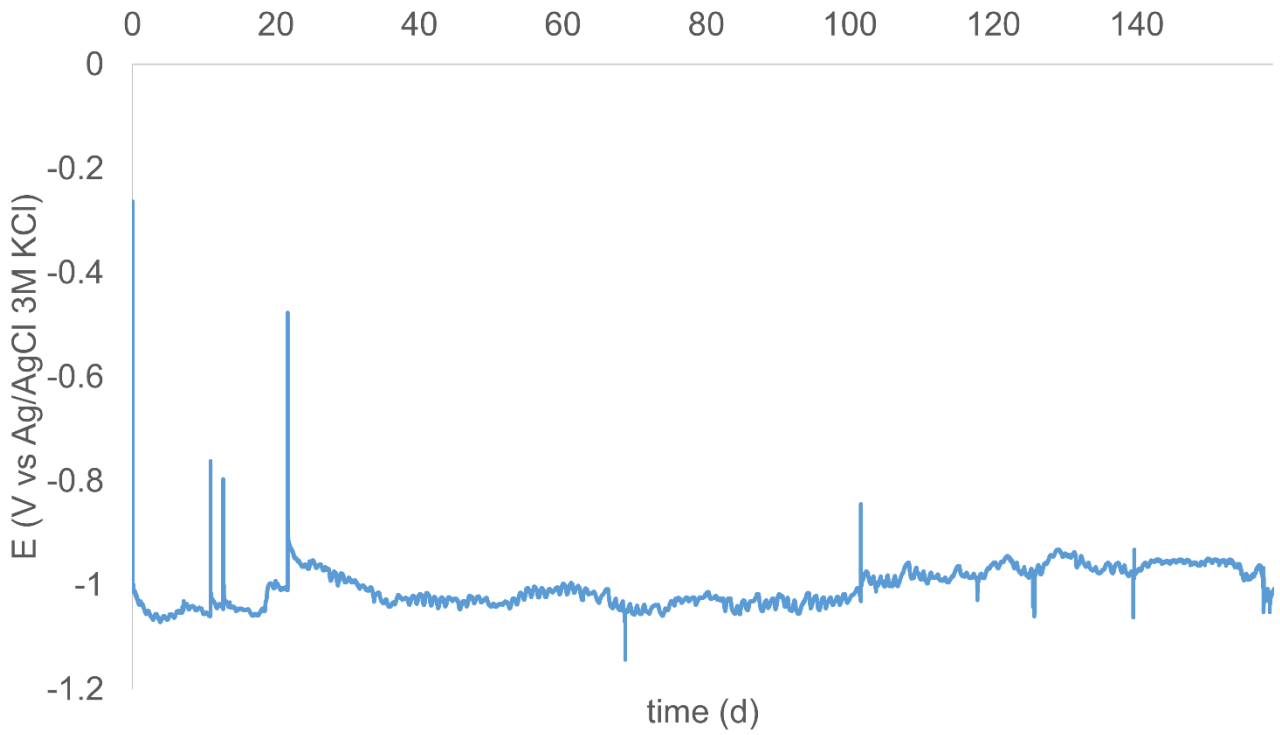

Figure S21 *Profile of the cathodic potential in time of the single circuit bioelectrochemical system working with an applied current density of 0.05 mA·cm^{-2}*

(S22)

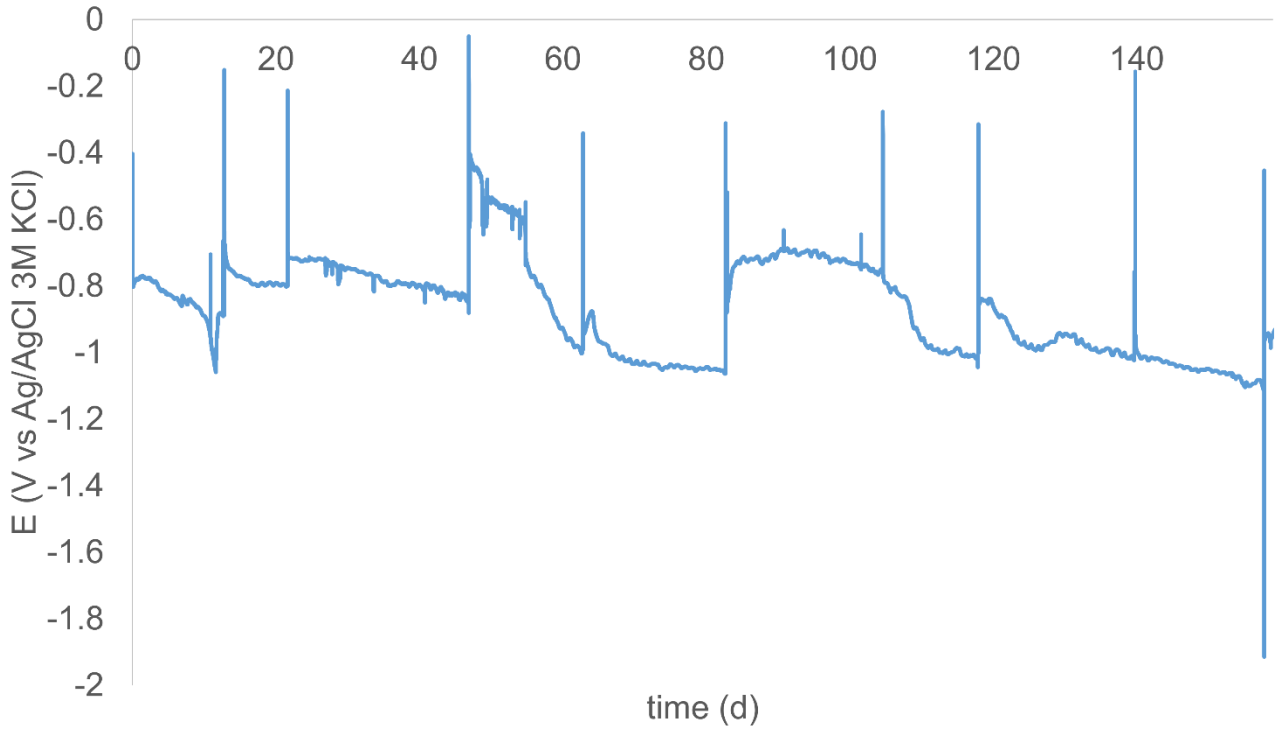

Figure S22 *Profile of the cathodic potential in time of the double circuit bioelectrochemical system working with an applied current density of 0.05 mA·cm^{-2}*

(S23)

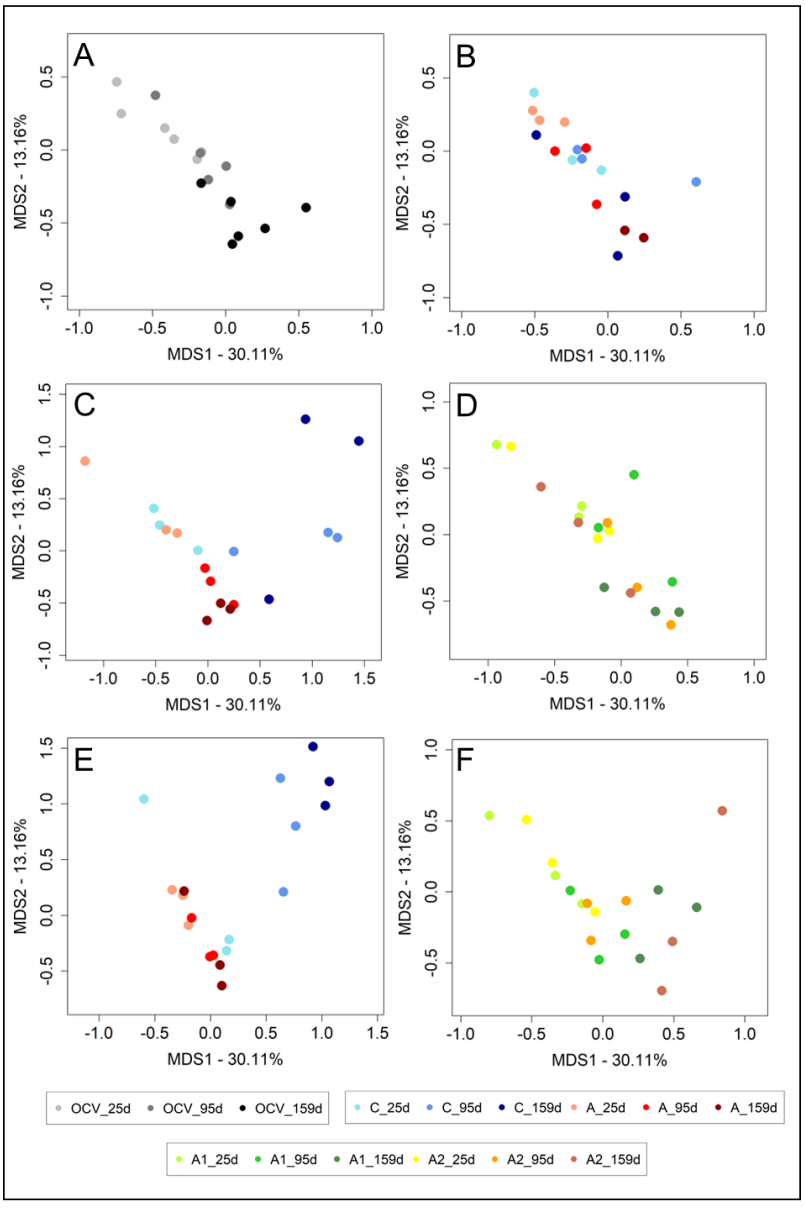

Figure S23 *Impact of bioelectrochemical stimulation on the composition of the sediments' microbial community. PCoA based on weighted UniFrac distances among sediments microbiota profiles of control circuit (OCV) (A) and of the MET circuits stimulated with a potential of -0.7 V vs Ag/AgCl (P-.07) (B). For the galvanostatic conditions a current density of 0.025 mA·cm^{-2} (G0.025) and of 0.05 mA·cm^{-2}*

(G0.05) was applied and monitored as single (C-E. respectively) and double circuits (A1 and A2) (D-F, respectively). Color code (bottom) for samples representation has been used to identify in single circuit MET cathode and anode at 25, 95, and 159 days, displayed with blue and red shaped, and in double circuit Area1 (A1) and Area2 (A2) at 25, 95, and 159 days, displayed with green and yellow shades. First and second coordination axes (MDS1 and MDS2) are plotted for each analysis. Percentages of variance in the dataset accounted for by MDS1 and MDS2 are reported.

(S24)

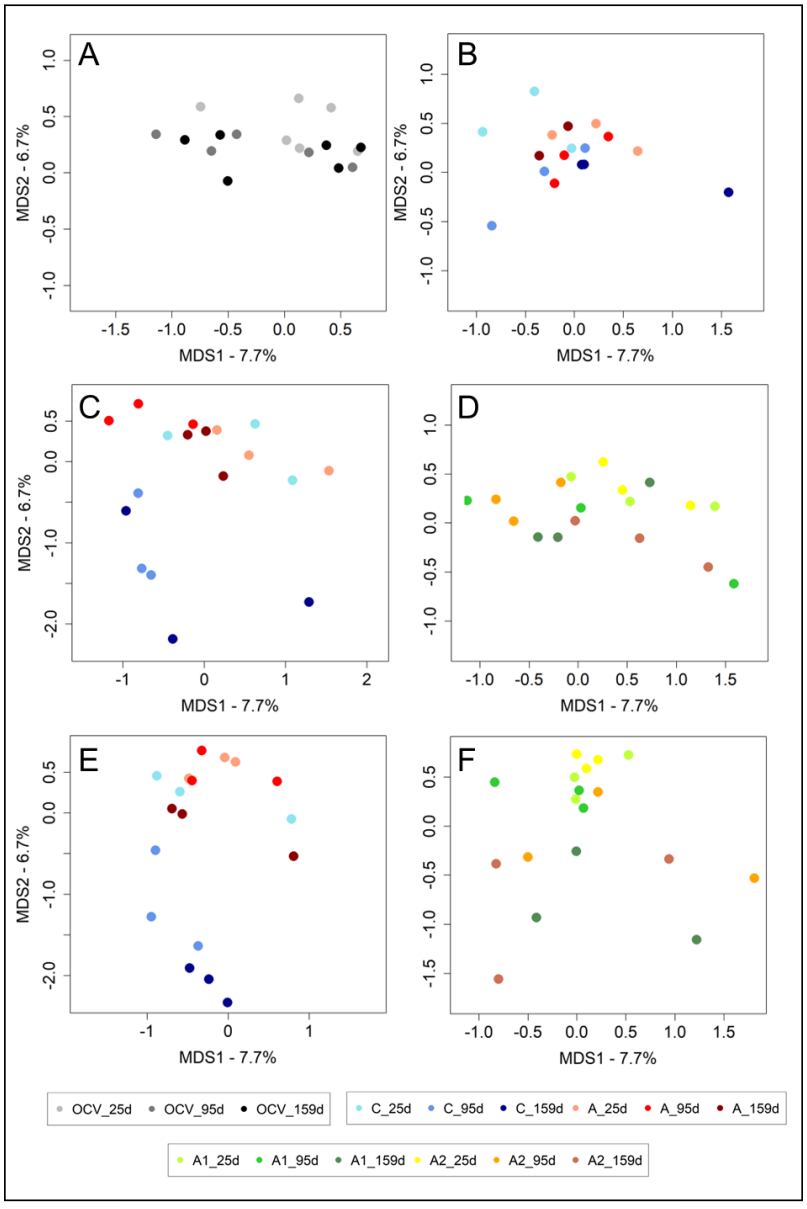

Figure S24 *Impact of bioelectrochemical stimulation on the composition of the sediments' microbial community PCoA based on unweighted UniFrac distances among sediments microbiota profiles of*

control circuit (OCV) (A) and of the MET circuits assessed with a potential of -0.7 V vs Ag/AgCl (P-.07) (B). For the galvanostatic conditions a current density of 0.025 mA·cm^{-2} (G0.025) and of 0.05 mA·cm^{-2} (G0.05) was applied and monitored as single (C-E. respectively) and double circuits (A1 and A2) (D-F, respectively). Color legend for samples representation is reporter (bottom). For each single circuit MET, cathode and anode at 25, 95, and 159 days are displayed with blue and red shaped, while double circuit Area1 (A1) and Area2 (A2) at 25, 95, and 159 days are displayed with green and yellow shades. First and second coordination axes (MDS1 and MDS2) are plotted for each analysis. Percentages of variance in the dataset accounted for by MDS1 and MDS2 are reported.

(S25)

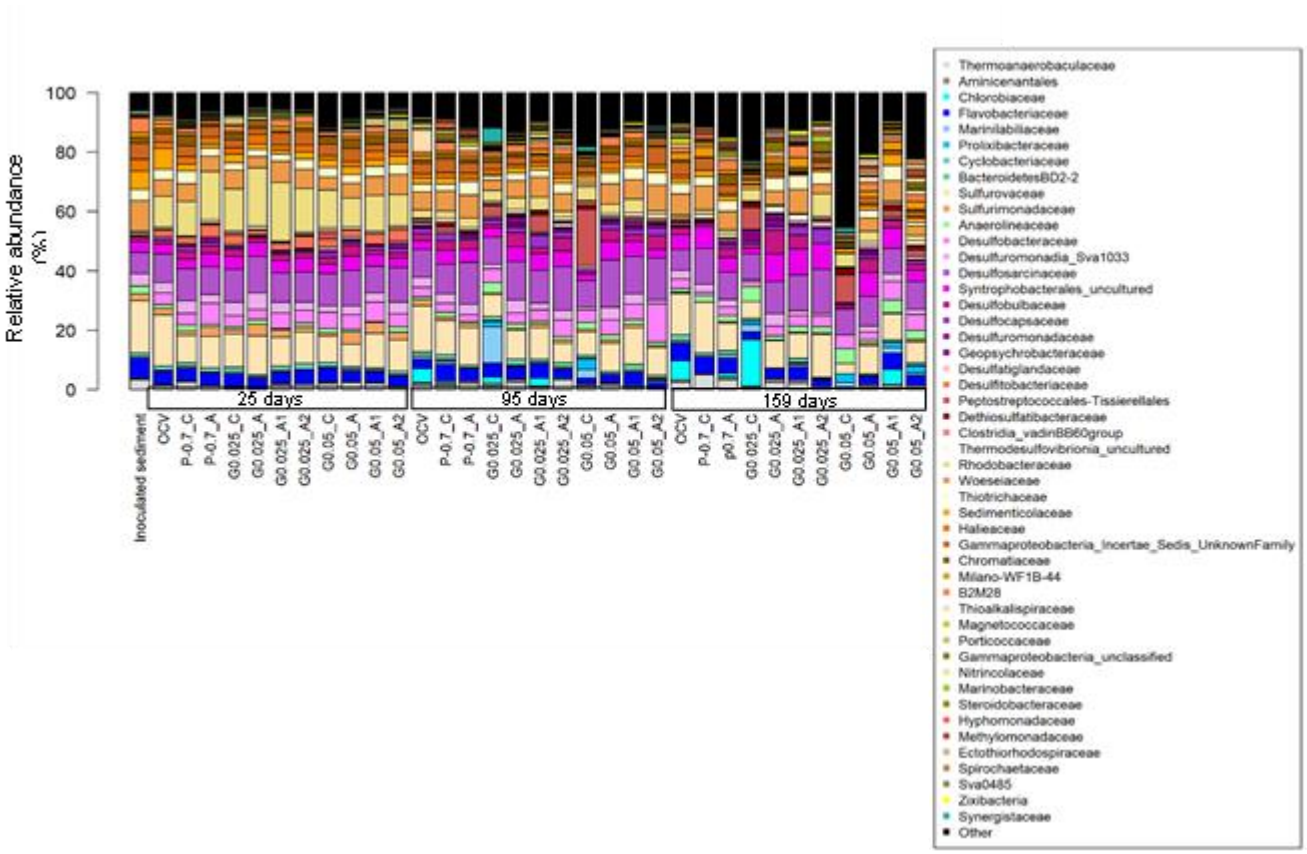

Figure S25 *Phylogenetic profiles at the family level of the inoculated sediment at the beginning of the experiment, the control circuit (OCV), sediments stimulated with potential of -0.7 V vs Ag/AgCl (P-.07) and with a current density of 0.025 mA·cm^{-2} (G0.025) or 0.05 mA·cm^{-2} (G0.05) in single and double circuit conditions (A1 and A2) at 25, 95, and 159 days.). Percentage of bacterial relative abundance is represented as the mean of three replicates. Bacterial families having relative abundance >1% in at least 10 sample are depicted in the barplots, for which color legend is reported in the right panel. Black color is used to indicate the percentage of "Other" reads, including unassigned sequences and families with a relative abundance which did not pass the mentioned threshold.*

(S26)

Table S4 *adjusted p-values of the two tailed t-tests (0.05 significance threshold) performed with the data of the sulfate depletion percentages at 159 days of the bioelectrochemical systems*

Comparison between the sulfate depletion percentages of cathode and anode or area 1 and area 2				
-0.7 V cathode vs anode	0.025 mA·cm^{-2} cathode vs anode	0.025 mA·cm^{-2} 2AP area 1 vs area 2	0.05 mA·cm^{-2} cathode vs anode	0.05 mA·cm^{-2} 2AP area 1 vs area 2
1	1	0.4	0.6	1
Comparison between the sulfate depletion percentages of the single circuit systems				
-0.7 V vs 0.025 mA·cm^{-2}	-0.7 V vs 0.05 mA·cm^{-2}		0.025 mA·cm^{-2} vs 0.05 mA·cm^{-2}	
0.02	0.01		0.01	
Comparison between the sulfate depletion percentages of the single circuit systems and double circuit systems				
0.025 mA·cm^{-2} single circuit vs double circuit		0.05 mA·cm^{-2} single circuit vs double circuit		
0.00008		0.02		
Comparison between the sulfate depletion percentages of the double circuit systems				
0.025 mA·cm^{-2} double circuit vs 0.05 mA·cm^{-2}double circuit				
0.03				

(S27)

Table S5 *adjusted p-values of two tailed t-test (0.05 significance threshold) between the sulfate depletion percentages at 159 days of each bioelectrochemical system and the open circuit control*

-0.7 V, Cathode	-0.7 V, Anode	0.025 mA·cm^{-2} Cathode	0.025 mA·cm^{-2}, Anode	0.025 mA·cm^{-2}, Area 1	0.025 mA·cm^{-2}, Area 2	0.05 mA·cm^{-2}, Cathode	0.05 mA·cm^{-2}, Anode	0.05 mA·cm^{-2}, Area 1	0.05 mA·cm^{-2}, Area 2
0.005	0.004	0.004	0.002	0.0001	0.0003	0.0003	0.02	0.00003	0.0002

(S28)

Table S6 *Coulombic efficiencies of the BES, calculated at the end of the experiment (159 days)*

-0.7 V	0.025 mA·cm^{-2}	0.025 mA·cm^{-2} 2AP	0.05 mA·cm^{-2}	0.05 mA·cm^{-2} 2AP
350 ± 20 %	184 ± 13 %	201 ± 5 %	120 ± 12 %	132 ± 6 %

(S29)

Table S7 *adjusted p-values of the two tailed t-tests (0.05 significance threshold) performed with the data of the reduction percentages of the chlorination degree*

Comparison between the reduction percentages of the chlorination degree around the electrodes of the bioelectrochemical systems and the control, after 95 days									
-0.7 V, Cathode	-0.7 V, Anode	0.025 mA·cm^{-2} Cathode	0.025 mA·cm^{-2}, Anode	0.025 mA·cm^{-2}, Area 1	0.025 mA·cm^{-2}, Area 2	0.05 mA·cm^{-2}, Cathode	0.05 mA·cm^{-2}, Anode	0.05 mA·cm^{-2}, Area 1	0.05 mA·cm^{-2}, Area 2
1	0.05	1	0.005	0.02	0.006	0.004	0.0005	0.22	1
Comparison between the reduction percentages of the chlorination degree around the electrodes of the bioelectrochemical systems and the control, after 159 days									
-0.7 V, Cathode	-0.7 V, Anode	0.025 mA·cm^{-2} Cathode	0.025 mA·cm^{-2}, Anode	0.025 mA·cm^{-2}, Area 1	0.025 mA·cm^{-2}, Area 2	0.05 mA·cm^{-2}, Cathode	0.05 mA·cm^{-2}, Anode	0.05 mA·cm^{-2}, Area 1	0.05 mA·cm^{-2}, Area 2
0.2	0.2	1	0.02	0.1	0.9	0.007	0.1	1	1

(S30)

Table S8 *Potentiostatic data of the bioelectrochemical systems*

-0.7 V Current	0.025 mA·cm^{-2} Voltage	0.025 mA·cm^{-2} 2AP Voltage	0.05 mA·cm^{-2} Voltage	0.05 mA·cm^{-2} 2AP Voltage

(mA)	(V vs Ag/AgCl 3 M KCl)	(V vs Ag/AgCl 3 M KCl)	(V vs Ag/AgCl 3 M KCl)	(V vs Ag/AgCl 3 M KCl)
-0.2 ± 0.2	-0.8 ± 0.1	-0.8 ± 0.1	-1.01 ± 0.03	-0.9 ± 0.1

(S31)

Table S9 *Relative abundance profiles of bacteria selected as potential SRB in marine sediments at 25 days. Sediments' microbiota members involved in sulfate reduction in the open circuit (OCV) and in those circuits poised with -0.7V (P-0.7) or 0.025 (G0.025) and 0.05 mA·cm^{-2} (G0.05) in single and double systems (area 1 A1 and area 2 A2). A and C abbreviation indicate the cathode and anode area of each circuit, respectively. According to the literature, members of Desulfobacterota (Waite et al., 2020), few families from the phyla Firmicutes (Desulfitobacteriaceae, Desulfotomaculales, Desulfallas-Sporotomaculum, Fusibacteraceae and reads ascribed to the order Thermoanaerobacterales) and Nitrospirota (Thermodesulfovibrionia) (Zhou et al., 2011). Color legend (right) according to Fig.4 is displayed to clearly identify groups of samples. Within Desulfobacterota phylum only the top 7 families in terms of relative abundance are reported in different colors (shades of yellow, orange and red) whereas the other subdominant families (relative abundance < 1.0) are all depicted in dark purple.*

	SRB families	relative abundance (%, mean)										
		OCV 25d	P-0.7_C 25d	P-0.7_A 25d	G0.025_C 25d	G0.025_A 25d	G0.025_A1 25d	G0.025_A2 25d	G0.05_C 25d	G0.05_A 25d	G0.05_A1 25d	G0.05_A2 25d
	Desulfobacteraceae	4,0	4,0	7,1	3,9	3,5	5,3	4,2	5,4	5,1	6,5	4,3
	Desulfuromonadia Sva1033	3,6	4,2	2,9	4,3	5,5	3,7	2,9	2,1	2,9	3,2	4,1
	Desulfosarcinaceae	9,5	10,8	9,3	11,1	12,4	9,7	10,2	11,0	12,0	8,8	11,5
	Syntrophobacterales uncultured	3,3	3,3	4,6	4,4	4,8	4,2	4,7	3,2	4,8	3,9	3,4
	Desulfobulbaceae	1,3	2,6	2,6	2,4	1,3	2,1	1,9	2,1	3,6	1,5	1,6
	Desulfocapsaceae	0,8	1,4	1,1	0,7	0,0	0,6	0,7	1,7	1,1	1,1	1,6
	Desulfuromonadaceae	0,0	0,6	1,7	0,4	0,6	0,6	0,3	0,8	0,9	0,9	1,5
	Geopsychrobacteraceae	0,0	0,0	0,1	0,0	0,2	0,0	0,0	0,0	0,2	0,0	0,2
	Desulfovibrionaceae	0,0	0,0	0,0	0,0	0,0	0,0	0,0	0,0	0,0	0,0	0,0
	Desulfococcaceae	0,1	0,1	0,0	0,0	0,3	0,1	0,1	0,5	0,3	0,1	0,3
	Desulfomicrobiaceae	0,0	0,0	0,0	0,0	0,0	0,0	0,0	0,0	0,0	0,0	0,0
	Desulfonatronaceae	0,0	0,0	0,0	0,0	0,0	0,0	0,0	0,0	0,0	0,0	0,0
	Desulfobacterales unknown	0,0	0,0	0,0	0,0	0,0	0,0	0,0	0,0	0,0	0,0	0,0
	Desulfatiglandaceae	0,6	0,4	0,0	0,5	0,3	0,2	0,4	1,0	0,9	0,0	0,7
	Desulfobaccaceae	0,1	0,2	0,2	0,1	0,0	0,0	0,0	0,1	0,5	0,3	0,0

	Desulfarculaceae	0,0	0,0	0,0	0,0	0,0	0,0	0,0	0,0	0,0	0,0	0,0
	Syntrophales uncultured	0,0	0,0	0,0	0,0	0,0	0,0	0,0	0,0	0,0	0,0	0,0
	Desulfobulbales unknown	0,0	0,1	0,0	0,0	0,0	0,0	0,0	0,0	0,0	0,0	0,0
	Desulfuromonadia PB19	0,0	0,0	0,0	0,2	0,2	0,0	0,0	0,0	0,0	0,0	0,0
	Desulfobulbales uncultured	0,0	0,0	0,0	0,0	0,0	0,0	0,0	0,0	0,1	0,0	0,0
	Desulfurivibrionaceae	0,0	0,1	0,1	0,0	0,1	0,0	0,0	0,0	0,0	0,0	0,0
	Desulfobacterales uncultured	0,0	0,0	0,0	0,0	0,0	0,0	0,0	0,0	0,0	0,0	0,0
	Desulfovibrionales unknown	0,0	0,0	0,0	0,0	0,0	0,0	0,0	0,0	0,0	0,0	0,0
	Syntrophaceae	0,0	0,0	0,0	0,0	0,0	0,0	0,0	0,0	0,0	0,0	0,0
	Desulfomonilaceae	0,0	0,0	0,0	0,0	0,0	0,0	0,0	0,0	0,1	0,0	0,0
	Desulfobacterota unknown	0,0	0,0	0,0	0,0	0,0	0,0	0,0	0,0	0,0	0,0	0,0
	Syntrophotaleaceae	0,0	0,0	0,0	0,0	0,0	0,0	0,0	0,0	0,0	0,0	0,0
	Dissulfuribacteraceae	0,0	0,0	0,0	0,0	0,0	0,0	0,0	0,0	0,0	0,0	0,0
	Bradymonadaceae	0,0	0,0	0,0	0,0	0,0	0,0	0,0	0,0	0,0	0,0	0,0
	Bradymonadales	0,0	0,0	0,0	0,0	0,0	0,0	0,0	0,0	0,0	0,0	0,0
	Geobacteraceae	0,0	0,0	0,0	0,0	0,0	0,0	0,0	0,0	0,0	0,0	0,0
	Desulfolunaceae	0,0	0,0	0,0	0,0	0,0	0,0	0,0	0,0	0,0	0,0	0,0
	Syntrophorhabdaceae	0,0	0,0	0,0	0,0	0,0	0,0	0,0	0,0	0,0	0,0	0,0
	Desulfobacterota uncultured	0,0	0,0	0,0	0,0	0,0	0,0	0,0	0,0	0,0	0,0	0,0
	Desulfobacteria unknown	0,0	0,0	0,0	0,0	0,0	0,0	0,0	0,0	0,0	0,0	0,0
	Desulfitobacteriaceae	2,0	2,2	4,1	3,2	1,6	2,3	3,9	2,7	2,1	3,5	3,6
	Desulfotomaculales	0,0	0,0	0,0	0,0	0,0	0,0	0,0	0,0	0,0	0,0	0,0
	Desulfallas-Sporotomaculum	0,0	0,0	0,0	0,0	0,0	0,0	0,0	0,0	0,0	0,0	0,0
	Thermoanaerobacterales SRB2	0,0	0,0	0,0	0,0	0,0	0,0	0,0	0,0	0,0	0,0	0,0
	Fusibacteraceae	0,1	0,0	0,0	0,2	0,3	0,1	0,0	1,2	0,0	0,0	0,0
	Thermodesulfovibrionia uncultured	0,7	0,3	0,9	0,7	1,0	0,4	0,7	0,8	0,9	0,6	0,8

(S32)

Table S10 *Relative abundance profiles of bacteria selected as potential SRB in marine sediments at 95 days. Sediments' microbiota members involved in sulfate reduction in the open circuit (OCV) and in those circuits poised with -0.7V (P-0.7) or 0.025 (G0.025) and 0.05 mA·cm^{-2} (G0.05) in single and double systems (area 1 A1 and area 2 A2). A and C abbreviation indicate the cathode and anode area of each circuit, respectively. According to the literature, members of Desulfobacterota (Waite et al., 2020), few families from the phyla Firmicutes (Desulfitobacteriaceae, Desulfotomaculales, Desulfallas-Sporotomaculum, Fusibacteraceae and reads ascribed to the order Thermoanaerobacterales) and Nitrospirota (Thermodesulfovibrionia) (Zhou et al., 2011). Color legend (right) according to Fig.4 is displayed to clearly identify groups of samples. Within Desulfobacterota phylum only the top 7 families in terms of relative abundance are reported in different colors (shades of yellow, orange and red) whereas the other subdominant families (relative abundance < 1.0) are all depicted in dark purple.*

	SRB families	relative abundance (%, mean)										
		OCV 95d	P-0.7_C 95d	P-0.7_A 95d	G0.025_C 95d	G0.025_A 95d	G0.025_A1 95d	G0.025_A2 95d	G0.05_C 95d	G0.05_A 95d	G0.05_A1 95d	G0.05_A2 95d
	Desulfobacteraceae	3,2	3,2	2,3	4,6	3,7	3,7	5,5	4,3	5,1	5,1	12,9
	Desulfuromonadia Sva1033	3,4	3,0	3,6	1,7	4,2	2,3	3,3	1,0	4,2	3,5	1,3
	Desulfosarcinaceae	9,3	10,0	14,1	9,1	12,9	11,1	14,7	8,9	15,9	12,6	14,1
	Syntrophobacterales uncultured	3,1	4,6	4,3	3,0	5,0	5,6	5,3	2,0	6,3	5,0	3,1
	Desulfobulbaceae	2,3	3,3	3,1	1,2	4,9	1,9	4,4	0,9	4,0	2,3	4,6
	Desulfocapsaceae	1,8	2,2	0,8	1,6	1,8	4,2	2,0	1,1	1,9	1,8	2,5
	Desulfuromonadaceae	0,4	0,1	1,4	0,0	1,2	0,4	1,0	0,0	1,1	1,1	1,3
	Geopsychrobacteraceae	0,8	0,0	0,0	0,4	2,1	0,2	0,5	0,0	0,5	1,5	0,3
	Desulfovibrionaceae	0,0	0,4	0,0	0,0	0,0	0,0	0,0	1,1	0,0	0,0	0,0
	Desulfococcaceae	0,1	0,3	0,0	0,1	0,4	0,1	0,2	0,2	0,5	0,5	0,4
	Desulfomicrobiaceae	0,0	0,2	0,0	0,2	0,0	0,0	0,0	0,0	0,0	0,0	0,4
	Desulfonatronaceae	0,0	0,0	0,0	0,0	0,0	0,0	0,0	0,0	0,0	0,0	0,0
	Desulfobacterales unknown	0,0	0,0	0,0	0,4	0,0	0,0	0,0	0,3	0,0	0,0	0,0
	Desulfatiglandaceae	0,7	0,6	0,3	0,6	0,4	0,6	1,3	0,9	0,7	0,7	0,3
	Desulfobaccaceae	0,1	0,0	0,2	0,2	0,7	0,1	0,3	0,0	0,0	0,4	0,0
	Desulfarculaceae	0,0	0,0	0,0	0,0	0,0	0,0	0,0	0,0	0,0	0,0	0,0
	Syntrophales uncultured	0,0	0,0	0,0	0,0	0,0	0,0	0,0	0,0	0,0	0,0	0,0
	Desulfobulbales unknown	0,0	0,0	0,3	0,0	0,0	0,0	0,0	0,0	0,0	0,0	0,0
	Desulfuromonadia PB19	0,0	0,0	0,4	0,0	0,0	0,0	0,0	0,0	0,0	0,0	0,0
	Desulfobulbales uncultured	0,0	0,0	0,0	0,0	0,0	0,0	0,0	0,0	0,1	0,0	0,0

	Desulfurivibrionaceae	0,1	0,1	0,0	0,0	0,2	0,1	0,2	0,0	0,0	0,2	0,0
	Desulfobacterales uncultured	0,0	0,0	0,0	0,0	0,0	0,0	0,0	0,0	0,0	0,0	0,0
	Desulfovibrionales unknown	0,0	0,0	0,0	0,0	0,0	0,0	0,0	0,0	0,0	0,0	0,0
	Syntrophaceae	0,0	0,0	0,0	0,0	0,0	0,0	0,0	0,0	0,0	0,0	0,0
	Desulfomonilaceae	0,0	0,0	0,0	0,0	0,0	0,0	0,0	0,0	0,0	0,0	0,0
	Desulfobacterota unknown	0,0	0,0	0,0	0,0	0,0	0,0	0,0	0,0	0,0	0,0	0,0
	Syntrophotaleaceae	0,0	0,0	0,0	0,0	0,0	0,0	0,0	0,0	0,0	0,0	0,0
	Dissulfuribacteraceae	0,0	0,0	0,0	0,0	0,0	0,0	0,0	0,0	0,0	0,0	0,1
	Bradymonadaceae	0,0	0,0	0,0	0,0	0,0	0,0	0,0	0,0	0,0	0,0	0,0
	Bradymonadales	0,0	0,0	0,0	0,0	0,0	0,0	0,0	0,0	0,0	0,0	0,0
	Geobacteraceae	0,0	0,0	0,0	0,0	0,0	0,0	0,0	0,0	0,0	0,0	0,0
	Desulfolunaceae	0,0	0,0	0,0	0,0	0,1	0,0	0,0	0,0	0,0	0,0	0,0
	Syntrophorhabdaceae	0,0	0,0	0,0	0,0	0,0	0,0	0,0	0,0	0,0	0,0	0,0
	Desulfobacterota uncultured	0,0	0,0	0,0	0,0	0,0	0,0	0,0	0,0	0,0	0,0	0,0
	Desulfobacteria unknown	0,0	0,0	0,0	0,0	0,0	0,0	0,0	0,0	0,0	0,0	0,0
	Desulfitobacteriaceae	0,1	0,0	0,0	0,0	0,0	0,0	0,0	0,0	0,0	0,0	0,0
	Desulfotomaculales	0,0	0,1	0,0	0,3	0,0	3,0	0,0	0,7	0,0	0,0	0,8
	Desulfallas-Sporotomaculum	0,0	0,0	0,0	0,0	0,0	0,0	0,0	0,0	0,0	0,0	0,0
	Thermoanaerobacterales SRB2	0,0	0,0	0,0	0,0	0,0	0,0	0,0	1,4	0,0	0,0	0,0
	Fusibacteraceae	0,0	0,1	0,0	0,3	0,1	1,5	0,4	0,3	0,0	0,1	0,2
	Thermodesulfovibrionia uncultured	0,3	1,0	0,9	0,7	1,3	0,4	1,3	0,2	1,0	1,4	1,4

(S33)

Table S11 *Relative abundance profiles of bacteria selected as potential SRB in marine sediments at 159 days. Sediments' microbiota members involved in sulfate reduction in the open circuit (OCV) and in those circuits poised with -0.7V (P-0.7) or 0.025 (G0.025) and 0.05 mA·cm^{-2} (G0.05) in single and double systems (area 1 A1 and area 2 A2). A and C abbreviation indicate the cathode and anode area of each circuit, respectively. According to the literature, members of Desulfobacterota (Waite et al., 2020), few families from the phyla Firmicutes (Desulfitobacteriaceae, Desulfotomaculales, Desulfallas-Sporotomaculum, Fusibacteraceae and reads ascribed to the order Thermoanaerobacterales) and Nitrospirota (Thermodesulfovibrionia) (Zhou et al., 2011). Color legend (right) according to Fig.4 is displayed to clearly identify groups of samples. Within Desulfobacterota phylum only the top 7 families in terms of relative abundance are reported in different colors (shades of yellow, orange and red) whereas the other subdominant families (relative abundance < 1.0) are all depicted in dark purple.*

	SRB families	relative abundance (%, mean)										
		OCV 159d	P-0.7_C 159d	P-0.7_A 159d	G0.025_C 159d	G0.025_A 159d	G0.025_A1 159d	G0.025_A2 159d	G0.05_C 159d	G0.05_A 159d	G0.05_A1 159d	G0.05_A2 159d
	Desulfobacteraceae	3,4	1,2	2,8	1,7	3,2	3,6	3,4	4,6	2,6	6,3	4,7
	Desulfuromonadia Sva1033	2,8	2,6	2,5	0,8	4,3	1,6	0,9	0,0	1,9	2,6	1,5
	Desulfosarcinaceae	7,1	12,1	9,2	8,7	10,9	12,1	14,9	8,6	10,1	8,6	9,7
	Syntrophobacterale uncultured	5,0	7,2	4,9	1,8	9,2	8,7	8,9	0,5	8,1	6,8	3,5
	Desulfobulbaceae	2,2	1,1	3,1	1,4	8,0	4,7	0,0	1,0	4,6	2,6	5,7
	Desulfocapsaceae	0,6	0,5	1,0	0,9	1,3	2,7	4,8	0,1	1,3	0,5	2,3
	Desulfuromonadaceae	0,4	0,4	1,6	0,1	2,2	1,1	0,7	0,0	1,3	0,0	0,0
	Geopsychrobacteraceae	0,0	0,0	0,0	3,7	1,8	0,1	0,0	0,6	0,8	0,0	0,7
	Desulfovibrionaceae	0,0	0,0	0,0	0,0	0,6	0,0	0,0	0,0	0,1	0,0	3,2
	Desulfococcaceae	0,0	0,1	0,0	0,2	0,3	0,0	0,7	0,4	0,3	0,0	0,0
	Desulfomicrobiaceae	0,0	0,0	0,0	0,0	0,0	0,0	0,0	0,0	0,0	0,3	1,3
	Desulfonatronaceae	0,0	0,0	0,0	0,0	0,0	0,0	0,0	0,4	0,0	0,0	0,0
	Desulfobacterales unknown	0,0	0,0	0,0	0,1	0,0	0,0	0,0	1,5	0,0	0,2	0,0
	Desulfatiglandaceae	0,6	0,0	0,7	0,5	0,3	0,9	1,7	0,0	1,1	0,7	0,7
	Desulfobaccaceae	0,0	0,0	0,0	0,0	0,3	0,4	0,0	0,2	0,0	0,0	0,0
	Desulfarculaceae	0,0	0,0	0,0	0,0	0,4	0,0	0,0	0,0	0,0	0,0	0,9
	Syntrophales uncultured	0,0	0,0	0,0	0,0	0,0	0,0	0,0	0,1	0,0	0,5	0,0
	Desulfobulbales unknown	0,0	0,0	0,0	0,0	0,0	0,0	0,0	0,0	0,0	0,0	0,1
	Desulfuromonadia PB19	0,0	0,0	0,0	0,0	0,0	0,0	0,0	0,0	0,0	0,0	0,0
	Desulfobulbales	0,1	0,3	0,0	0,0	0,0	0,3	0,0	0,0	0,0	0,0	0,1

	uncultured											
	Desulfurivibrionaceae	0,0	0,0	0,0	0,0	0,0	0,0	0,0	0,0	0,0	0,0	0,2
	Desulfobacterales uncultured	0,0	0,0	0,0	0,0	0,0	0,0	0,0	0,0	0,0	0,0	0,0
	Desulfovibrionales unknown	0,0	0,0	0,0	0,0	0,0	0,0	0,0	0,0	0,0	0,0	0,0
	Syntrophaceae	0,0	0,0	0,0	0,0	0,0	0,0	0,0	0,0	0,0	0,0	0,0
	Desulfomonilaceae	0,0	0,1	0,0	0,0	0,0	0,0	0,0	0,1	0,0	0,0	0,0
	Desulfobacterota unknown	0,0	0,0	0,1	0,0	0,0	0,0	0,0	0,0	0,0	0,0	0,0
	Syntrophotaleaceae	0,0	0,0	0,0	0,0	0,0	0,0	0,0	0,0	0,0	0,0	0,0
	Dissulfuribacteraceae	0,0	0,0	0,0	0,0	0,1	0,0	0,0	0,0	0,0	0,0	0,0
	Bradymonadaceae	0,0	0,0	0,0	0,0	0,0	0,0	0,0	0,0	0,0	0,0	0,0
	Bradymonadales	0,0	0,0	0,0	0,0	0,0	0,0	0,0	0,0	0,0	0,0	0,0
	Geobacteraceae	0,0	0,0	0,0	0,0	0,0	0,0	0,0	0,0	0,0	0,0	0,0
	Desulfolunaceae	0,0	0,0	0,0	0,0	0,0	0,0	0,0	0,0	0,0	0,0	0,0
	Syntrophorhabdaceae	0,0	0,0	0,0	0,0	0,0	0,0	0,0	0,0	0,0	0,0	0,0
	Desulfobacterota uncultured	0,0	0,0	0,0	0,0	0,0	0,0	0,0	0,0	0,0	0,0	0,0
	Desulfobacteria unknown	0,0	0,0	0,0	0,0	0,0	0,0	0,0	0,0	0,0	0,0	0,0
	Desulfitobacteriaceae	0,0	0,0	0,0	0,0	0,0	0,0	0,0	0,0	0,1	0,0	0,0
	Desulfotomaculales	0,0	0,0	0,0	1,0	0,0	0,0	0,0	1,0	0,0	0,0	0,0
	Desulfallas-Sporotomaculum	0,0	0,0	0,0	0,0	0,0	0,0	0,0	0,0	0,0	0,0	0,0
	Thermoanaerobacterales SRB2	0,0	0,0	0,0	2,7	0,0	0,0	0,0	4,6	0,0	0,0	1,0
	Fusibacteraceae	0,0	0,0	0,0	0,0	0,0	0,0	0,0	0,0	0,0	0,0	0,0
	Thermodesulfovibrionia uncultured	0,8	1,4	1,4	0,4	2,3	2,1	0,5	0,2	1,1	0,7	1,2

Chapter 5

Threshold of PCBs concentration to sustain reductive dechlorination in marine sediments

5.1 Introduction

PCBs polluted sediment's toxicity can be reduced via a biological process named reductive dehalogenation, mediated by a class of bacteria defined as organohalide respiring bacteria (OHRB) (Dolfing, 2003). Though, natural attenuation of sediment's toxicity is thought to be constrained by the environmental concentration of the pollutants (Passatore et al., 2014), which it might not be sufficient to sustain growth of OHRB in the polluted site (Cho et al., 2003). In this regard, bioaugmentation, the addition of endogenous bacteria to the treated site, has been proven as an effective technique to bioremediate PCBs polluted sediments (Payne et al., 2011). However, it should be questioned whether or not the inoculated bacteria could process low amount of pollutants in sediments. Indeed, previous studies identified threshold concentrations of 35-40 $mg \cdot Kg_{drysediment}^{-1}$ as values below which it was not observed reductive dechlorination (Cho et al., 2003; Sokol et al., 1998). Needham *et al.* (2019) speculated that these values were the result of a growth threshold whereas reductive dechlorination can take place even at PCBs concentration of 0.035 $mg \cdot Kg_{drysediment}^{-1}$. In particular, they suggested that the growth threshold could be avoided by growing OHRB *ex situ* and proceeding via bioaugmenting the sediment. Payne *et al.* confirmed this hypothesis by demonstrating that bioaugmenting a polluted freshwater site at a PCBs concentration lower than 5 $mg \cdot Kg_{drysediment}^{-1}$ reduced the concentration of pollutants (Payne et al., 2019). Yet, when bioaugmenting marine sediments, the abundant competitive anaerobic bacteria of OHRB, as sulfate reducing bacteria (SRB) (Leloup et al., 2007), might contend the available electron donors of the sediment possibly mining the efficacy of the remediation strategy (Varadhan et al., 2011). Moreover, the kinetic studies carried on by Needham *et al.* (2019) were performed with single congeners, whereas threshold values for PCBs concentration should be tested under conditions more similar to polluted sites, which are commonly characterized by a mixture of congeners (Quero et al., 2015) that can be more or less recalcitrant to dechlorination thus introducing several threshold concentrations (Cho et al., 2003). Therefore, in this study it was studied the effectiveness of a bioaugmentation strategy in marine sediments under *in situ* like conditions, spiked at different Aroclor concentrations to better assess the influence of the pollutants concentration on the bioremediation process.

5.2 Materials and methods

5.2.1 Microcosms preparation, sampling and maintenance

Sediments were collected in the Pialassa della Baiona, Ravenna (Ravenna, Italy, 44.2938 N 11.2034 E). Microcosms were prepared in 100 mL glass serum bottles with 70 mL of sediment slurry (20% w/v of sediment and overlaying water) under anaerobic conditions (nitrogen gas in the headspace) and sealed with butyl rubber stopper and aluminum crimp. Under stirring and nitrogen flow, the anaerobic slurry was spiked with a 20'000 $mg \cdot L^{-1}$ stock solution of Aroclor 1254 in acetone to final PCBs concentrations of 5, 10, 50, 100 and 500 $mg \cdot kg_{dry\ sediment}^{-1}$ and inoculated (5% v/v) with a marine culture previously enriched with OHRB able to reductively dechlorinate PCBs (Nuzzo et al., 2017). Set of microcosms not inoculated (NI) and sterile (STR) were prepared as well having final PCBs concentration of 500 $mg \cdot kg_{dry\ sediment}^{-1}$. Sterile microcosms were prepared by autoclaving the sediment three times at 121 °C for 1 h. Between each autoclave cycle microcosms were incubated statically at 30°C for 24 h. Throughout the experiment, microcosms were incubated statically in the dark at 30°C for 178 days. Sampling was performed after 25, 61, 94, 122 and 178 days to analyze the concentration of PCBs in the sediment. In addition, consumed SO_4^{2-} were replenished periodically to maintain microcosms under actual site biogeochemical conditions, avoiding the alteration of the natural competition for electron donors between different terminal-electron accepting processes. In particular, sulfates were replenished by adding a 2.1 M stock solution of Na_2SO_4.

5.2.2 Extraction and analysis of PCBs

PCBs in the sediment were extracted following a modified method from Rosato *et al.* (2020). Batch extraction was performed overnight at 30°C and 150 rpm from 1 mL of sediment slurry, with 3 mL of a hexane:acetone (9:1) mixture and octachloronaphtalene (OCN) (0.04 $mg \cdot L^{-1}$) as internal standard. The recovered organic phase was filtered on an Extrabond® Silica column (Scharlab, Barcelona, Spain) and added with 10 mg of elemental copper (Sigma Aldrich, St. Luis, Missouri, USA) as described in (Riis and Babel, 1999). An aliquot of the sample was placed in 1.5 mL vials for gas-chromatography (GC) equipped with Teflon coated screw caps (LLG-Labware, Meckenheim, Germany). The qualitative and quantitative analysis of the extracted PCBs was performed with a gas chromatograph (6890 series II) equipped with a HP-5 capillary column (30 m by 0.25 mm), a ^{63}Ni electron capture detector (μECD) and a 6890 series II automatic sampler (Agilent Technologies, Santa Clara, CA, USA). The column was operated at the following conditions: initial temperature 60°C; isothermal for 1 min; initial temperature

rate 40°C/min; final temperature 140°C; isothermal for 2 min; initial temperature rate 1.5°C/min; final temperature 185°C; initial temperature rate 4.5°C/min; final temperature 275°C; isothermal for 5 min; injector (splitless mode), 250°C; detector ECD, 320°C; carrier gas flow rate (N_2) 1.5 mL/min; sample volume 1 µl. Aroclor PCBs, injected in the presence of OCN, were identified as described in Fava *et al.* (2003) by matching the detected peaks with the chromatographic profiles of the standard PCBs mixtures Aroclor 1254 and Aroclor 1242 previously characterized (Frame et al., 1996) and comparing the retention time (relative to OCN) of each peak with those of PCBs of the same standard Aroclors analyzed under identical conditions. Quantitative analysis of the freshly spiked PCBs and their possible dechlorination products was performed by using the GC-ECD response factor of each target PCB congener or group of co-eluting congeners obtained from six-points calibration curves (0.5-50 $mg \cdot L^{-1}$) of Aroclors 1254 and 1242 and the weight percentage of each congener occurring in the same Aroclors reported elsewhere (Frame, 1997). PCBs concentrations were expressed as µmol of $PCBs \cdot kg_{dry\ sediment}^{-1}$. The chlorination degree was calculated as average number of chlorines per biphenyl molecule, as follows,

(**1**)
$$Chlorination\ degree = \frac{\mu mol\ of\ organic\ chlorine}{\mu mol\ of\ total\ PCBs} = \frac{\sum C_i \times n_i}{\sum C_i}$$

where C_i is the molar concentration of each detected PCB congener ($\mu mol \cdot kg_{dry\ sediment}^{-1}$) and n_i is the number of its Cl substituents.

5.2.3 Dechlorination rates, kinetic constants of the dechlorination reactions and threshold concentrations

Dechlorination rates were calculated as the variation of the chlorination degree over the incubation time and expressed as $mol\text{-}Cl^-_{removed} \cdot mol\text{-}biphenyl \cdot d^{-1}$. Dechlorination reactions were considered to proceed via first order kinetic (Cho et al., 2003; Needham et al., 2019). Dechlorination constants were calculated as the slope of the following linear function:

(**2**)
$$ln\frac{C_o}{C_t} = kt$$

where C_0 is the initial concentration of the dechlorinated congener and C_t is the concentration at time t. Dechlorination constants were reported as average of the k measured at each Aroclor 1254 concentration (5, 10, 50, 100 and 500) and expressed as d^{-1}. The threshold concentration (q) at which the theoretical degradation rate would be 0 was calculated as reported by Cho *et al.* (2003), by plotting the

dechlorination rates of the single congeners versus their initial concentrations. The threshold concentration was then calculated as the intercept of the following equation, when $-\frac{dC}{dt} = 0$:

(**3**) $$-\frac{dC}{dt} = k(C_0 - C) + q$$

5.2.4 Analysis of sulfates

The concentration of SO_4^{2-} in the water phase of the sediment slurry was determined using a Dionex ICS-1000 ion chromatograph equipped with an IonPac AS14 4 mm × 250 mm column, a conductivity detector combined to an AERS-500 suppressor system (Dionex, Sunnyvale, CA, USA). Quantitative analysis were performed by using the conductivity detector response factor obtained from a five points calibration curve (0.5-50 $mg \cdot L^{-1}$) of Na_2SO_4.

5.2.5 Chemicals

Aroclor 1242, Aroclor 1254 and octachloronaphtalene were provided by Ultra-Scientific. Acetone and hexane (both for pesticide analysis in capillary column GC systems) as well as the ultra-resi analyzed water for ion chromatography were supplied by Mallinckrodt-Baker.

5.3 Results

No signs of dechlorination were observed in the sterile controls and in the not inoculated microcosms at the end of the experiment (178 days) (Fig. 1). Conversely, in the bioaugmented microcosms the chlorination degree decreased below 4 at all the studied concentrations. Different incubation times were required to observe reductive dechlorination of PCBs according to the concentration of pollutants. In particular, lag-phase ranged from 1 month in the 500 ppm microcosms up to 3 months in the 5 ppm ones. The reductive dechlorination involved mainly flanked *meta* and *para* positions, resulting in the accumulation of congeners with unflanked or *orto* chlorine atoms. Dehalogenation was observed also at concentrations of single congeners or group of co-eluting congeners in the order of 10^{-3} $mg \cdot Kg_{drysediment}^{-1}$ (Supplementary Table S1). The dechlorination rate was a linear function of the initial PCBs concentration (r^2 = 0.996), with values between 0.016 ± 0.009 and 7.8 ± 0.5 $mol\text{-}Cl^-_{removed} \cdot mol\text{-}biphenyl \cdot d^{-1}$ (Fig. 2). Kinetic constants of the reductive dechlorination were then calculated considering the reductive dechlorination as a first order reaction. Obtained k were comprised between 0.003 and

0.017 d^{-1} (Supplementary Table S2), with an average dechlorination rate constant of 0.011 ± 0.003 d^{-1}. Threshold concentrations to observe reductive dechlorination were calculated plotting the dechlorination rate versus the initial concentration of the congeners. The average value was equal to 0.01 ± µmol·$Kg_{drysediment}^{-1}$ or 0.001 ± 0.001 mg·$Kg_{drysediment}^{-1}$.

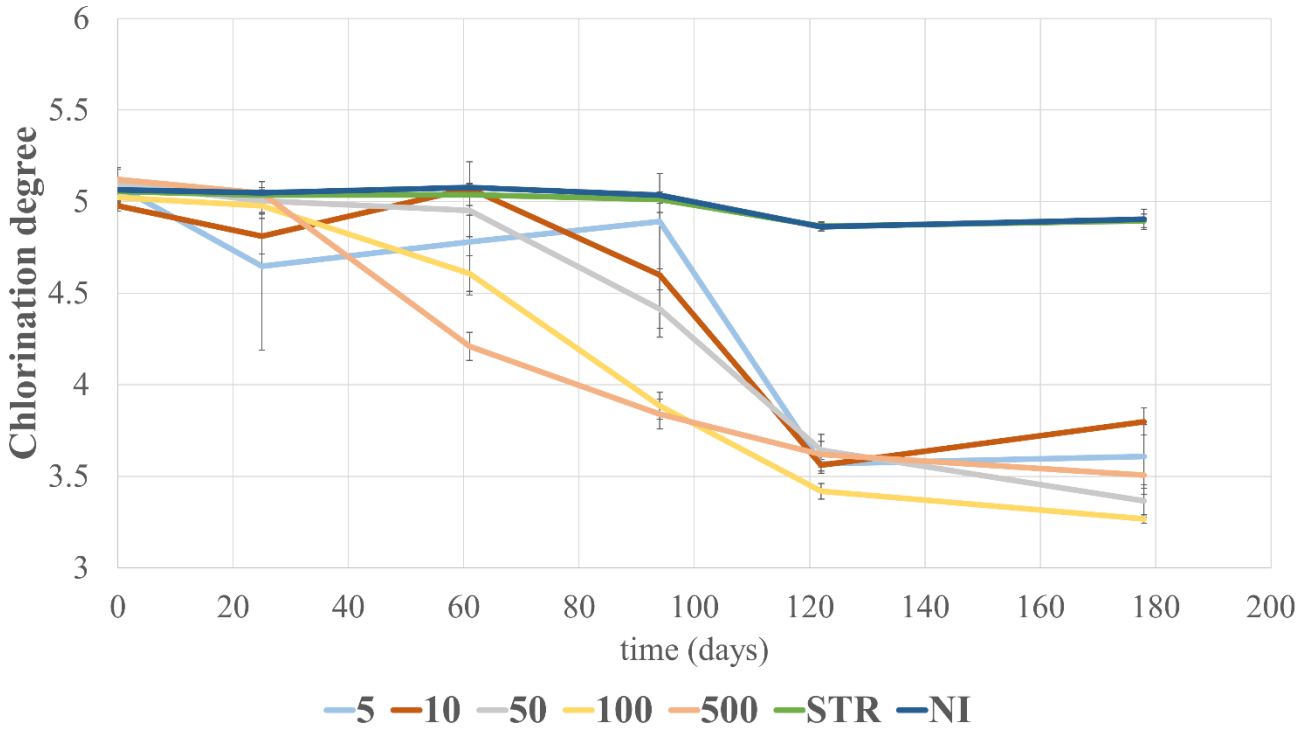

Figure 7 *Profile of the chlorination degree in time for the PCBs mixture in the studied microcosms. 5, 10, 50, 100 and 500 indicate the Aroclor 1254 concentration, expressed in mg·$Kg_{drysediment}^{-1}$, in the bioaugmented sediments. STR are the microcosms containing sterile sediments. NI are the microcosms not bioaugmented, both containing 500 mg·$Kg_{drysediment}^{-1}$ of PCBs.*

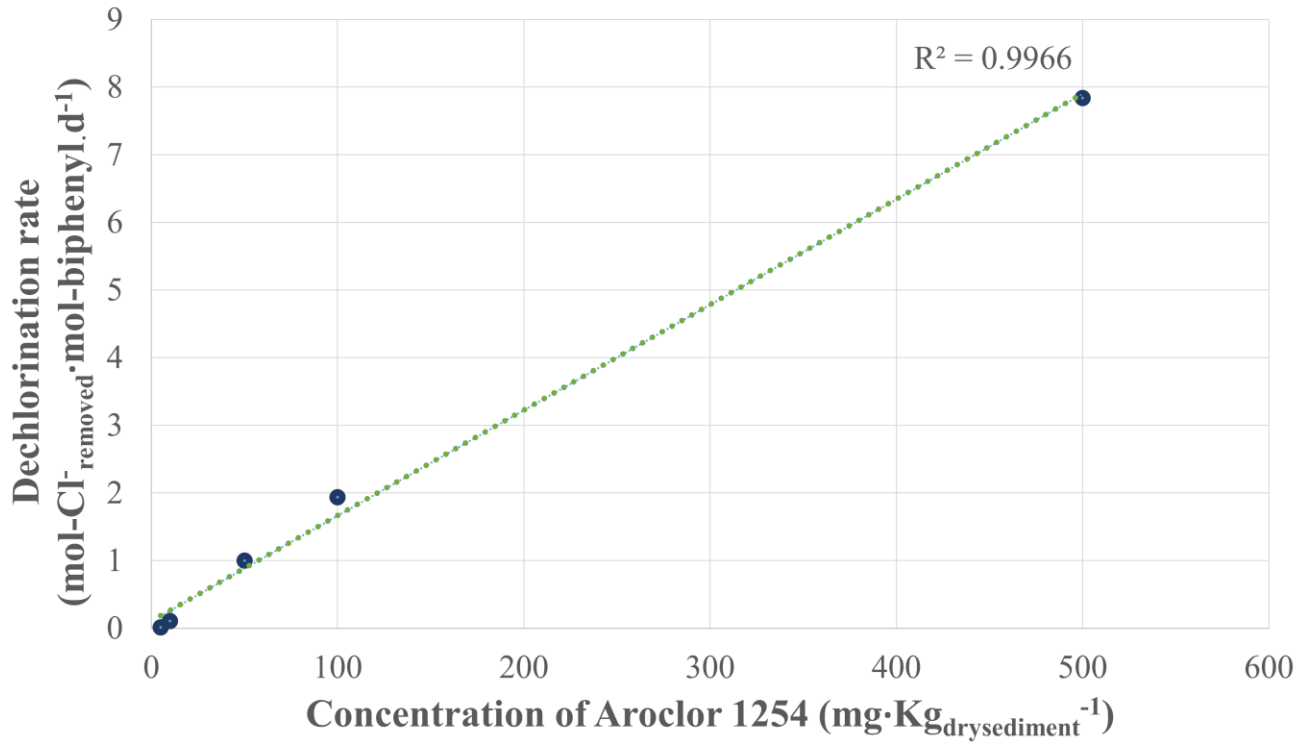

Figure 8 *Dechlorination rate as a function of the initial concentration of Aroclor 1254*

5.4 Discussion

The PCBs concentration in the polluted sediment has been recognized as one of the limiting factors for an effective bioremediation action (Dolfing, 2003; Passatore et al., 2014). Conflicting concentration thresholds to observe PCBs reductive dechlorination were reported in the literature (Cho et al., 2003; Lombard et al., 2014; Needham et al., 2019; Sokol et al., 1998). Recently, it was demonstrated that PCBs reductive dechlorination can proceed at low concentration as 0.035 mg·$Kg_{drysediment}^{-1}$, working on single congeners and with sediment supplemented with synthetic medium (Needham et al., 2019). In this study, it was observed that PCBs can be dechlorinated in marine sediments under *in situ* like conditions at concentrations typically found in polluted sites (Guerra, 2012; Todaro et al., 2020). Furthermore, dechlorination proceeded at values of single congeners below the safety limits stated by international guidelines (0.1-1 mg·$Kg_{drysediment}^{-1}$) (Alzieu et al., 2003; Brien et al., 2003; MacDonald et al., 2000). Considering the negligible signs of dehalogenation in the not inoculated control, the presence of an active microbial community able to reductively dechlorinate PCBs was identified as the fundamental factor to observe reductive dechlorination, as previously pointed out (Lombard et al., 2014; Needham et al., 2019).

Additionally, the indigenous amount of organic matter was sufficient to sustain the bioremediation process.

The kinetic of reductive dechlorination measured in this experiment was comparable to data reported by Cho *et al.* (2003), who worked with freshly spiked river sediment, and by Lombard *et al.* (2014), who worked with free-sediment synthetic medium, and that respectively observed dechlorination constant ranging between 0.006-0.067 d^{-1} and 0.027-0.043 d^{-1}. Yet, Needham *et al.* (2019) detected faster kinetics, reaching values between 0.08-0.17 d^{-1}. It should be noticed that the process was studied in river sediment supplied with synthetic nutrients, freshly spiked with a single PCB congener and inoculated with highly concentrated pure culture. Differently, in this experiment, the complexity of the real matrix and indigenous microbial community introduces competitors of OHRB which might slow down the dechlorination process by subtracting electron donors. Secondly, the dechlorination kinetic is specific for the single congener (Cho et al., 2003), thus in a complex PCBs mixture as the one studied herein, congeners more recalcitrant to dechlorination are present and account for lower kinetic constants. Lastly, more accurate results could be obtained by considering the initial amount of OHRB (Needham et al., 2019; Sokol et al., 1998), which were not monitored during this experiment and would normalize the calculated constants.

As for the higher previously reported threshold concentrations compared to the one obtained in this study, values around 35-40 $mg \cdot Kg_{drysediment}^{-1}$ were identified when working with real sediments freshly spiked with complex PCBs mixtures (Cho et al., 2003; Sokol et al., 1998). It was speculated that the absence of dehalogenation was not directly related to the low amount of pollutants, yet to a concentration insufficient to trigger and sustain the growth of OHRB (Cho et al., 2003; Needham et al., 2019). In this regard, this experiment confirms that bioaugmenting with an enriched microbial community able to reductively dechlorinate PCBs reduces the time for the growth of OHRB, resulting in shorter length of bioremediation and allowing the bioremoval of lower pollutants concentrations (Needham et al., 2019). The variable incubation times required to detect dechlorination at the different Aroclor concentrations observed during this experiment suggest that the inoculated microbial community was not enriched enough with OHRB to avoid the initial lag-phase. In fact, according to the concentration of respiring bacteria in the polluted site the bioremediation time can vary from few days (Needham et al., 2019) up to months (this experiment) or several years (Pakdeesusuk et al., 2005), supporting the fact that attaining high concentrated inoculum might guarantee a feasible approach to bioremediate polluted sediments.

5.5 Conclusions

In the perspective of clarifying limits and possibilities of bioremediation of PCBs polluted sediments, this study demonstrated that dechlorination of this class of compounds can proceed at experimentally detectable time scale even at typical environmental concentration of pollutants in competitive environments as marine sediments. Despite the sediments were inoculated with a microbial community enriched with OHRB able to reductively dechlorinate PCBs, incubation length of monthly time scale were required to observe dechlorination, underlying the need of an optimization of the inoculum concentration. Nonetheless, this experiment highlighted once more that *in situ* bioremediation can proceed relying solely on PCBs dehalorespiring bacteria without external dosage of chemical compounds that could affect the indigenous microbial community furtherly impacting the polluted site.

5.6 Bibliography

Alzieu, C., Bocquené, G., Régis, D., Dhainaut-Courtois, N., Empis, A., Forget, J., Glémarec, M., Jean François, Pavillon Chrystèle, P., Françoise, Q., 2003. Evaluation des risques liés à l'immersion des boues de dragage des ports maritimes.

Brien, G.O., Behnke, H.F., Poulson, H.D., Ela, J.P., Willett, S.D., Hassett, S., 2003. Consensus-Based Sediment Quality Guidelines Recommendations for Use & Application Interim Guidance Developed by the Contaminated Sediment Standing Team James Tiefenthaler Jr ., Vice Chair Wisconsin Department of Natural Resources, Wisconsin department of natural resources.

Cho, Y.C., Sokol, R.C., Frohnhoefer, R.C., Rhee, G.Y., 2003. Reductive Dechlorination of Polychlorinated Biphenyls: Threshold Concentration and Dechlorination Kinetics of Individual Congeners in Aroclor 1248. Environ. Sci. Technol. 37, 5651–5656. https://doi.org/10.1021/es034600k

Dolfing, J., 2003. Thermodynamic considerations for dehalogenation, in: Häggblom, M.M., Bossert, I.D. (Eds.), Dehalogenation, Microbial Processes and Environmental Applications. Kluwer Academic Publishers, Rutgers University, USA, pp. 89–114.

Fava, F., Zanaroli, G., Young, L.Y., 2003. Microbial reductive dechlorination of pre-existing PCBs and spiked 2,3,4,5,6-pentachlorobiphenyl in anaerobic slurries of a contaminated sediment of Venice Lagoon (Italy). FEMS Microbiol. Ecol. 44, 309–318. https://doi.org/10.1016/S0168-6496(03)00069-2

Frame, G.M., 1997. A collaborative study of 209 PCB congeners and 6 Aroclors on 20 different HRGC columns: 1. Retention and coelution database. Fresenius. J. Anal. Chem. 357, 701–713. https://doi.org/10.1007/s002160050237

Guerra, R., 2012. Polycyclic aromatic hydrocarbons, polychlorinated biphenyls and trace metals in sediments from a coastal lagoon (Northern Adriatic, Italy). Water. Air. Soil Pollut. 223, 85–98. https://doi.org/10.1007/s11270-011-0841-6

Leloup, J., Loy, A., Knab, N.J., Borowski, C., Wagner, M., Jørgensen, B.B., 2007. Diversity and abundance of sulfate-reducing microorganisms in the sulfate and methane zones of a marine sediment, Black Sea. Environ. Microbiol. 9, 131–142. https://doi.org/10.1111/j.1462-2920.2006.01122.x

Lombard, N.J., Ghosh, U., Kjellerup, B. V., Sowers, K.R., 2014. Kinetics and threshold level of 2,3,4,5-tetrachlorobiphenyl dechlorination by an organohalide respiring bacterium. Environ. Sci. Technol. 48, 4353–4360. https://doi.org/10.1021/es404265d

MacDonald, D.D., Dipinto, L.M., Field, J., Ingersoll, C.G., Long, E.R., Swartz, R.C., 2000. Development and evaluation of consensus-based sediment effect concentrations for polychlorinated biphenyls. Environ. Toxicol. Chem. 19, 1403–1413. https://doi.org/10.1002/etc.5620190524

Needham, T.P., Payne, R.B., Sowers, K.R., Ghosh, U., 2019. Kinetics of PCB microbial dechlorination explained by freely dissolved concentration in sediment microcosms. Environ. Sci. Technol. 53, 7432–7441. https://doi.org/10.1021/acs.est.9b01088

Nuzzo, A., Hosseinkhani, B., Boon, N., Zanaroli, G., Fava, F., 2017. Impact of bio-palladium nanoparticles (bio-Pd NPs) on the activity and structure of a marine microbial community. Environ. Pollut. 220, 1068–1078. https://doi.org/10.1016/j.envpol.2016.11.036

Pakdeesusuk, U., Lee, C.M., Coates, J.T., Freedman, D.L., 2005. Assessment of natural attenuation via in situ reductive dechlorination of polychlorinated biphenyls in sediments of the Twelve Mile

Creek arm of Lake Hartwell, SC. Environ. Sci. Technol. 39, 945–952. https://doi.org/10.1021/es0491228

Passatore, L., Rossetti, S., Juwarkar, A.A., Massacci, A., 2014. Phytoremediation and bioremediation of polychlorinated biphenyls (PCBs): State of knowledge and research perspectives. J. Hazard. Mater. 278, 189–202. https://doi.org/10.1016/j.jhazmat.2014.05.051

Payne, R.B., Ghosh, U., May, H.D., Marshall, C.W., Sowers, K.R., 2019. A Pilot-Scale Field Study: In Situ Treatment of PCB-Impacted Sediments with Bioamended Activated Carbon. Environ. Sci. Technol. 53, 2626–2634. https://doi.org/10.1021/acs.est.8b05019

Payne, R.B., May, H.D., Sowers, K.R., 2011. Enhanced reductive dechlorination of polychlorinated biphenyl impacted sediment by bioaugmentation with a dehalorespiring bacterium. Environ. Sci. Technol. 45, 8772–8779. https://doi.org/10.1021/es201553c

Quero, G.M., Cassin, D., Botter, M., Perini, L., Luna, G.M., 2015. Patterns of benthic bacterial diversity in coastal areas contaminated by heavy metals, polycyclic aromatic hydrocarbons (PAHs) and polychlorinated biphenyls (PCBs). Front. Microbiol. 6, 1–15. https://doi.org/10.3389/fmicb.2015.01053

Riis, V., Babel, W., 1999. Removal of sulfur interfering in the analysis of organochlorines by GC-ECD. Analyst 124, 1771–1773. https://doi.org/https://doi.org/10.1039/A907504F

Rosato, A., Barone, M., Negroni, A., Brigidi, P., Fava, F., Xu, P., Candela, M., Zanaroli, G., 2020. Microbial colonization of different microplastic types and biotransformation of sorbed PCBs by a marine anaerobic bacterial community. Sci. Total Environ. 705, 135790. https://doi.org/10.1016/j.scitotenv.2019.135790

Sokol, R.C., Bethoney, C.M., Rhee, G.Y., 1998. Effect of aroclor 1248 concentration on the rate and extent of polychlorinated biphenyl dechlorination. Environ. Toxicol. Chem. 17, 1922–1926. https://doi.org/10.1897/1551-5028(1998)017’1922:EOACOT’2.3.CO;2

Todaro, F., De Gisi, S., Notarnicola, M., 2020. Contaminated marine sediment stabilization/solidification treatment with cement/lime: leaching behaviour investigation. Environ. Sci. Pollut. Res. 27, 21407–21415. https://doi.org/10.1007/s11356-020-08562-1

Varadhan, A.S., Khodadoust, A.P., Brenner, R.C., 2011. Effect of biostimulation on the microbial

community in PCB-contaminated sediments through periodic amendment of sediment with iron. J. Ind. Microbiol. Biotechnol. 38, 1691–1707. https://doi.org/10.1007/s10295-011-0959-y

4.7 Supplementary materials

Summary

S1 – Table S1 - Concentration of single congeners or group of co-eluting congeners in the sediment spiked with Aroclor 1254 at 5 mg·$Kg_{drysediment}^{-1}$

S2 – Table S2 - Dechlorination constant and threshold concentrations of the reductively dechlorinated single congeners or group of co-eluting congeners

(S1)

Table S1 *Concentration of single congeners or group of co-eluting congeners in the sediment spiked with Aroclor 1254 at 5 mg·$Kg_{drysediment}^{-1}$*

PCBs congeners	Concentration expressed as µmol·$Kg_{drysediment}^{-1}$		Concentration expressed as mg·$Kg_{drysediment}^{-1}$	
	0 days	178 days	0 days	178 days
2-2, 26	0.1 ± 0.2	n.d.	0.02 ± 0.04	n.d.
24, 25	0.01 ± 0.01	n.d.	0.002 ± 0.003	n.d.
2-3,	n.d.	n.d.		n.d.
23, 2-4	n.d.	n.d.	n.d.	n.d.
26-2,	n.d.	0.1 ± 0.2	n.d.	0.03 ± 0.04
4-4, 25-2	n.d.	1.0 ± 0.3	n.d.	0.24 ± 0.08
24-2	n.d.	0.5 ± 0.2	n.d.	0.12 ± 0.05
236, 26-3	n.d.	0.01 ± 0.02	n.d.	0.003 ± 0.004
23-2, 26-4	n.d.	0.7 ± 0.3	n.d.	0.18 ± 0.08
245	0.002 ± 0.002	0.01 ± 0.01	0.0005 ± 0.0005	0.004 ± 0.004
234	n.d.	1.0 ± 0.2	n.d.	0.25 ± 0.04
25-3, 24-3	n.d.	2.1 ± 0.5	n.d.	0.5 ± 0.1
25-4, 24-4, 246-2	n.d.	0.41 ± 0.04	n.d.	0.11 ± 0.01
23-3, 234, 34-2, 25-26	n.d.	1.4 ± 0.4	n.d.	0.37 ± 0.09
23-4, 24-26	n.d.	1.1 ± 0.3	n.d.	0.29 ± 0.07
236-2	0.05 ± 0.03	0.08 ± 0.09	0.014 ± 0.008	0.02 ± 0.03

23-26	0.003 ± 0.006	n.d.	0.001 ± 0.002	n.d.
25-25, 246-3	0.08 ± 0.03	n.d.	0.024 ± 0.007	n.d.
235-2, 24-25	n.d.	n.d.	n.d.	n.d.
245-2, 246-4	0.02 ± 0.02	1.8 ± 0.3	0.007 ± 0.007	0.54 ± 0.08
23-25	0.14 ± 0.006	0.03 ± 0.02	0.041 ± 0.002	0.009 ± 0.006
34-4, 23-24, 236-3	0.07 ± 0.08	0.4 ± 0.2	0.02 ± 0.02	0.12 ± 0.06
234-2, 236-4, 26-34, 25-35	0.3 ± 0.4	2 ± 2	0.1 ± 0.1	0.7 ± 0.6
23-23	0.014 ± 0.009	0.07 ± 0.06	0.004 ± 0.003	0.02 ± 0.02
235-3, 246-25	n.d.	0.08 ± 0.05	n.d.	0.02 ± 0.01
235-4	0.04 ± 0.04	n.d.	0.01 ± 0.01	n.d.
245-4, 235-26	0.38 ± 0.05	n.d.	0.11 ± 0.02	n.d.
25-34	0.92 ± 0.07	n.d.	0.27 ± 0.02	n.d.
35-35, 2356-2, 236-25, 245-26	0.35 ± 0.02	n.d.	0.112 ± 0.008	n.d.
234-3, 236-24, 246-35	0.09 ± 0.04	0.06 ± 0.02	0.02 ± 0.01	0.020 ± 0.006
23-34, 234-4	0.26 ± 0.05	n.d.	0.08 ± 0.01	n.d.
236-23, 235-25, 246-246	0.28 ± 0.21	0.07 ± 0.06	0.09 ± 0.07	0.03 ± 0.02
235-24, 245-25	0.7 ± 0.1	n.d.	0.22 ± 0.04	n.d.
34-35, 245-24, 236-35	0.7 ± 0.2	n.d.	0.21 ± 0.05	n.d.
345-3, 235-23, 2356-3	0.05 ± 0.02	n.d.	0.017 ± 0.007	n.d.
345-4, 234-25, 2356-4, 345-26	0.44 ± 0.04	0.11 ± 0.04	0.14 ± 0.01	0.04 ± 0.01
234-24	0.1 ± 0.1	n.d.	0.03 ± 0.03	n.d.
236-34, 235-246	0.9 ± 0.1	0.34 ± 0.08	0.32 ± 0.03	0.12 ± 0.3
234-23	0.35 ± 0.03	0.11 ± 0.03	0.11 ± 0.01	0.04 ± 0.01
234-35, 235-34, 2356-24	0.15 ± 0.05	n.d.	0.05 ± 0.02	n.d.
2345-3, 245-34, 2346-24, 236-245	1.7 ± 0.3	0.04 ± 0.04	0.6 ± 0.1	0.02 ± 0.01
2345-4, 2356-23, 2345-26, 345-23, 2346-23, 235-235, 23456-2	0.06 ± 0.04	n.d.	0.02 ± 0.01	n.d.
235-245, 2356-35, 2356-246	0.04 ± 0.02	n.d.	0.01 ± 0.01	n.d.
234-34, 234-236, 2346-35	1.0 ± 0.2	n.d.	0.36 ± 0.08	0.02 ± 0.03
245-245	0.35 ± 0.03	0.20 ± 0.04	0.12 ± 0.01	0.07 ± 0.02
2345-25	0.08 ± 0.02	0.021 ± 0.005	0.030 ± 0.008	0.007 ± 0.002
234-235	0.05 ± 0.02	0.024 ± 0.002	0.018 ± 0.008	0.0086 ± 0.0009
234-245, 2356-34, 236-345	0.54 ± 0.09	0.16 ± 0.03	0.19 ± 0.03	0.06 ± 0.01
23456-4, 2356-235	0.07 ± 0.08	0.004 ± 0.004	0.03 ± 0.03	0.001 ± 0.002

234-234, 235-345	0.066	± 0.003	n.d.		0.024	± 0.001	n.d.	
2345-236, 23456-24	0.019	± 0.017	n.d.		0.008	± 0.007	n.d.	
2345-34, 2346-234	0.12	± 0.02	0.02	± 0.02	0.047	± 0.009	0.007	± 0.007
2345-235, 23456-246	0.02	± 0.02	0.01	± 0.02	0.009	± 0.008	0.005	± 0.008
2345-245	0.05	± 0.02	n.d.		0.019	± 0.009	n.d.	
2345-234	0.04	± 0.02	0.09	± 0.01	0.015	± 0.007	0.037	± 0.005
Total	10.8	± 2.9	14.4	± 5.6	3.5	± 0.9	4.0	± 1.6

n.d. not detected

(S2)

Table S2 *Dechlorination constant and threshold concentrations of the reductively dechlorinated single congeners or group of co-eluting congeners*

PCBs congeners	k (d^{-1})		q ($\mu mol \cdot Kg_{drysediment}^{-1}$)		q ($mg \cdot Kg_{drysediment}^{-1}$)	
236-2	0.004	± 0.007	0.0004	± 0.0001	0.00012	± 0.00004
25-25, 246-3	0.0035	± 0.0009	0.0002	± 0.0005	0.0001	± 0.0001
23-25	0.013	± 0.009	0.0013	± 0.0009	0.0004	± 0.0003
235-4	0.003	± 0.001	0.00141	± 0.00009	0.00041	± 0.00003
245-4, 235-26	0.013	± 0.007	0.099	± 0.005	0.0030	± 0.002
25-34	0.009	± 0.004	0.008	± 0.005	0.002	± 0.001
35-35, 2356-2, 236-25, 245-26	0.007	± 0.003	0.003	± 0.004	0.001	± 0.001
234-3, 236-24, 246-35	0.010	± 0.007	0.001	± 0.002	0.0002	± 0.0005
23-34, 234-4	0.012	± 0.006	0.002	± 0.001	0.0007	± 0.0004
236-23, 235-25, 246-246	0.016	± 0.009	0.004	± 0.007	0.001	± 0.002
235-24, 245-25	0.013	± 0.007	0.01	± 0.01	0.003	± 0.003
34-35, 245-24, 236-35	0.012	± 0.007	0.01	± 0.01	0.004	± 0.004
345-3, 235-23, 2356-3	0.011	± 0.007	0.001	± 0.0003	0.00033	± 0.00009

345-4, 234-25, 2356-4, 345-26	0.016	± 0.009	0.005	± 0.008	0.001	± 0.003
234-24	0.012	± 0.007	0.004	± 0.006	0.001	± 0.002
236-34, 235-246	0.01	± 0.01	0.01	± 0.01	0.002	± 0.004
234-23	0.017	± 0.008	0.002	± 0.005	0.001	± 0.001
234-35, 235-34, 2356-24	0.008	± 0.005	0.0016	± 0.0001	0.00055	± 0.00004
2345-3, 245-34,2346-24, 236-245	0.012	± 0.007	0.02	± 0.03	0.006	± 0.009
2345-4, 2356-23, 2345-26, 345-23, 2346-23, 235-235, 23456-2	0.012	± 0.007	0.001	± 0.001	0.0003	± 0.0004
235-245, 2356-35, 2356-246	0.012	± 0.005	0.001	± 0.001	0.0004	± 0.0004
234-34, 234-236, 2346-35	0.01	± 0.01	0.006	± 0.009	0.002	± 0.003
245-245	0.015	± 0.009	0.003	± 0.006	0.001	± 0.002
2345-25	0.012	± 0.007	0.001	± 0.001	0.0002	± 0.0004
234-235	0.011	± 0.007	0.0002	± 0.0007	0.0001	± 0.0002
234-245, 2356-34, 236-345	0.012	± 0.007	0.004	± 0.008	0.001	± 0.003
23456-4, 2356-235	0.011	± 0.007	0.001	± 0.002	0.0004	± 0.0006
234-234, 235-345	0.013	± 0.007	0.001	± 0.002	0.0005	± 0.0009
2345-236, 23456-24	0.011	± 0.006	0.0004	± 0.0002	0.0001	± 0.0001
2345-34, 2346-234	0.011	± 0.006	0.001	± 0.002	0.0003	± 0.0006
2345-235, 23456-246	0.008	± 0.008	0.00005	± 0.00008	0.00002	± 0.00003
2345-245	0.009	± 0.005	0.0003	± 0.0004	0.0001	± 0.0001
2345-234	0.005	± 0.006	0.0002	± 0.0004	0.0001	± 0.0001
Average	0.011	± 0.003	0.01	± 0.02	0.001	± 0.001

Chapter 6

Bioaugmentation and biostimulation, what comes next for the bioremediation of PCBs polluted marine sediments?

6.1 The road so far, a summary of the work done

The present study aimed at exploring the possibility to enhance bioremediation of polychlorobiphenyls (PCBs) polluted marine sediments by adding polyhydroxyalkanoates (PHAs), employed as novel biostimulating agents, or by supplying the required electron donors via the assistance of electrodes. The effectiveness of biostimulating with PHAs depended on the features of the treated site, due to the influence of physical-chemical parameters of the sediment and competition of indigenous bacterial species. As for the bioelectrochemical stimulation, the technique mainly favored competitive anaerobic metabolisms of reductive dechlorination, as sulfate reduction, while negatively impacting OHRB due to the alteration of sediment's parameters as pH. In both the biostimulation experiments the presence of a microbial community able to reductively dechlorinate PCBs was the fundamental aspect so as to observe bioremediation of the polluted sites. It is then reasonable to wonder if proceeding by bioaugmenting would be a sufficient effective approach, relying on the indigenous nutrient substances of the sediment to carry on the bioremediation process and possibly adapting the biostimulation as an accessory treatment. In this regard, the next paragraph will try to define critical guidelines for further studies, starting from a deep review of the available literature about bioaugmentation and biostimulation,

6.2 Bioaugmentation and biostimulation, learning from the past

Ten years ago Sowers and May (2013) questioned if *in situ* bioremediation of PCBs polluted sites was becoming a feasible options, underlying that the operational setbacks were on their way to be overcome. They highlighted how the addition of external electron donors was secondary to the presence of organohalide respiring bacteria able to sustain PCBs bioremoval (Winchell and Novak, 2008), focusing on guaranteeing the presence of sufficient OHRB in the polluted site via biaugmentation. The challenge of bioaugmentation was to obtain highly concentrated sediment-free cultures to inoculate the site and find a proper vector to deliver the microorganisms (Sowers and May, 2013). Relying on the fact that in a polluted site the sediment acts as support for the biofilm formation, thus guaranteeing the contact with the contaminants (Sowers and May, 2013), activated carbon was studied as scaffold to concomitantly inoculate the bacteria, sustain microbial growth and sequester the pollutants from the sediment enhancing the contact with bacteria (Capozzi et al., 2019; Payne et al., 2013, 2011). Further on, the technique was studied on mesocosm scale (Payne et al., 2017) and then tested at pilot scale (Payne et al., 2019), via the assistance of 250 L scale bioreactor to obtain sufficient amount of highly enriched culture to use as inoculum. Therefore, biaugmentation moved from the lab scale experiments, with pollutants concentrations outlying the ones occurring in the environment, up to pilot scale treatment under real *in*

situ conditions (Fagervold et al., 2011; Kjellerup et al., 2012; Krumins et al., 2009; Payne et al., 2019, 2017, 2013, 2011; Sudjarid et al., 2012; Winchell and Novak, 2008; Yan et al., 2006). Combining bioaugmentation and biostimulation approaches furtherly enhanced the remediation rates (Payne et al., 2019, 2017). Regarding the biostimulation approach, a variety of substrates as readily fermentable molecules (Chang et al., 2006; Di Gregorio et al., 2013; Krumins et al., 2009; Lu et al., 2021; Song et al., 2015; Sudjarid et al., 2012), oxidizable metals (Xu et al., 2021; Zanaroli et al., 2012b) and vegetable matrixes (Lehtinen et al., 2014) were studied as amendments. Electrochemical inputs were demonstrated to prime the dehalogenation process as well (Chun et al., 2013; Liu et al., 2017; Yu et al., 2017). Despite all these efforts, biostimulation studies of PCBs polluted sites remained at lab-scale with microcosms mimicking *in situ* conditions. Strategies that aim at performing microbial remediation of PCBs polluted sediments should then rely on bioaugmentation approaches, with the possibility to further enhancing the remediation process via a combination of the two techniques. The advantages of bioaugmentation have been widely demonstrated. In fact, similar remediation rates can be obtained either by biostimulating (Chang et al., 2006; Chun et al., 2013; Di Gregorio et al., 2013; Krumins et al., 2009; Liu et al., 2017; Lu et al., 2021; Song et al., 2015; Xu et al., 2021; Yu et al., 2017; Zanaroli et al., 2012b) or bioaugmenting (Fagervold et al., 2011; Kjellerup et al., 2012; Krumins et al., 2009; Payne et al., 2019, 2017, 2013, 2011; Sudjarid et al., 2012; Winchell and Novak, 2008; Yan et al., 2006), as illustrated in Chapter 1. Bioaugmentation can exert a beneficial effect on the microbial community of the polluted site, priming indigenous dehalogenators of the treated sediment (Payne et al., 2017). On the other hand, biostimulation can sort null (Lehtinen et al., 2014; Winchell and Novak, 2008) or negative (Sudjarid et al., 2012; Zanaroli et al., 2012a) effects on the bioremediation process. A further implication to be considered for the biostimulation approach is the instauration of unfavorable growth conditions driven by the exogenous chemicals or electrochemical input. For instance, it was reported that zero valent iron inhibited anaerobic bacteria as organohalide respiring bacteria (Summer et al., 2020) and that the application of a potential for a prolonged period led to extreme pH variations (Chun et al., 2013). Considering the difficulties of biostimulating the microbial degradation of PCBs in aquatic sediments, it should be wondered why use of sole biostimulation techniques as the injection of slow fermentable compounds or zero valent iron in sites contaminated by chlorinated solvents are currently being applied at field scale (Kocur et al., 2016; Koenigsberg et al., 2006; Zemb et al., 2010). The reason may lie in the intrinsic features of the process, in particular in the low bioavailability of PCBs compared to other chlorinated compounds (Wang et al., 2019, 2014). Indeed, when trying to stimulate PCBs reductive dechlorination at environmental concentration, the growth rate will be always dependent on the electron acceptor concentration (Rhee et

al., 2001). Therefore, an excess of electron donors might partially speed up the process up to the maximal growth rate defined by the PCBs concentration (Fagervold et al., 2011; Payne et al., 2017). OHRB which respire PCBs would always be poorly competitive due to the low bioavailability of the pollutants compared to other substrates. Thus biostimulation can be a feasible option under particular conditions. For instance in freshwater sites, where anaerobic competitors are less abundant. In fact, the effectiveness of biostimulation was proved on a lab scale with river sediments from Keelung river (Taiwan), Fox River (Wisconsin) and Anacostia river (Washington) (Chang et al., 2006; Chun et al., 2013; Krumins et al., 2009). Other conditions favorable for effective biostimulation processes are sites polluted with high PCBs concentrations, which guarantee higher growth rates. In this regard, PCBs concentrations in the order of magnitudes of 10^1 mg·$Kg_{drysediment}^{-1}$ for single congeners (Xu et al., 2021; Yu et al., 2017) or 10^3 mg·$Kg_{drysediment}^{-1}$ for complex mixtures (Zanaroli et al., 2012b) are commonly obtained when working on a lab scale by freshly spiking the contaminants so as to perform the proof of concept of the biostimulation technique. Yet environmental concentrations are usually lower, being in the order of magnitude of 10^0-10^1 mg·$Kg_{drysediment}^{-1}$ of total PCBs (Kjellerup et al., 2012; Pakdeesusuk et al., 2005; Šrédlová and Cajthaml, 2022). When trying to identify an efficient, general approach for *in situ* bioremediation of PCBs polluted site, bioaugmentation might be considered as a realistic option and might have more chance to be employed at full scale. In this perspective, the use of biostimulating agents that can selectively favor OHRB and aerobic degraders would be an effective tool to further prime the inoculated cultures. It should be noticed that the need to increase the concentration of organohalide respiring bacteria and aerobic degraders in the treated sediment is not a new perspective, since it has been highlighted already fifteen years ago (Bedard et al., 2007). What differs now is that the limits and possibilities of biostimulation and bioaugmentation have been largely proven at laboratory scale, paving the way to strategies that lead to full scale applications.

6.3 A focus on biaugmentation

Although scientific progresses are leading to a deeper comprehension of bacteria able to metabolize PCBs, on how to cultivate them and employ them in the real world, some key points should still be addressed. Regarding OHRB, the knowledge built so far demonstrated that bioaugmentation should rely on sediment-free cultures of these bacteria, equipped with reductive dehalogenases active both on PCBs and PCE. In fact, growing OHRB on PCE yields faster growth rates and higher biomass titer, obtaining culture that can be inoculated *in situ* (Chen and He, 2018). Furthermore, before inoculating the treated site, the chlorinated solvent can be removed by purging the culture medium thanks to its volatility (Payne

et al., 2019). In this regard, the bioaugmentation strategy applied for the experiments reported in this manuscript had some limitations. The inoculum employed was constituted by a marine sediment containing microbial culture enriched with PCBs dehalorespiring bacteria. Bioaugmenting via a marine culture that links its growth to the sediment necessarily meant inserting in the treated site the products of the reductive dechlorination of the inoculum, namely low chlorinated PCBs, which even if characterized by lower toxicity compared to higher chlorinated congeners (Dolfing, 2003), might affect the applicability of the treatment *in situ* (Krumins et al., 2009). Consequently, this bioaugmentation approach should not be employed for real *in situ* application. Up to now, only few sediment-free cultures able to grow on PCBs and PCE have been obtained, as *Dehalobium chlorocoercia* DF-1 (May et al., 2008), *Dehalococcoides mccartyi* strains CG1, CG4 and CG5 (Wang et al., 2014), Chloroflexi phylotypes SF1, DEH10 (Fagervold et al., 2007; Payne et al., 2017) and o-17 (Cutter et al., 2001; Payne et al., 2017) and *D. mccartyi* strains JNA (Laroe et al., 2014; Wang et al., 2015) and MB (Cheng and He, 2009; Xu et al., 2022b). Yet, based on the available literature, the only strain applied in field is DF-1 (Payne et al., 2019). In fact, obtaining culture sufficiently enriched to be amended to the sediment is not enough, since the bacteria have to be competitive in the inoculated environment. For instance, strain MB grows on PCBs only co-metabolically, requiring PCE to sustain microbial growth (Xu et al., 2022b). Additionally, strain isolated from freshwater environments, as JNA and CG1 (Bedard et al., 2006; Laroe et al., 2014; Wang et al., 2014; Wang and He, 2013), or terrestrial environments, as CG3 and CG4 (Wang et al., 2014; Wang and He, 2013), might not have the capability to survive in more competitive ecosystems as marine ones, pointing out the need to isolate OHRB from diverse environments and evaluate their applicability (Xu et al., 2022a). Finally, for a comprehensive view of full scale bioaugmentation, it should be wondered if bioaugmentation approaches could be versatile or dependent on the characteristic of the treated site. In fact, despite this approach has been demonstrated successful on a pilot-scale in river sediments (Payne et al., 2019) and cost effective compared to other treatments as dredging and *ex-situ* disposal, capping or reactive capping (Sowers et al., 2018), the results achieved might be related to the coexistence of several factors, as the competitiveness of indigenous microbiota and the intrinsic features of the site. Indeed, the microbiota of freshwater environment is usually anaerobically poorly competitive. As for the characteristic of the treated drainage pond (Payne et al., 2019), the sandy composition of river sediments (Abeshu et al., 2022) and the low water depth of the polluted site (1.2-1.8 m) (Payne et al., 2019), might have guaranteed sufficient oxygen exchanges from the surface water to the sediment to sustain aerobic degradation of the pollutants (Huettel et al., 2014). On the other hand, in contaminated sites as the highly polluted Bay of Mar Piccolo, where concentrations above the values identified by the Italian sediment

quality guidelines (APAT, 2006) were detected (Cotecchia et al., 2021), the more competitive biota of seawater might reduce the extent of reductive dechlorination. Additionally, the muddier composition and higher water depth (12 m) (Cotecchia et al., 2021; Lisco et al., 2016), might reduce the oxygen transfer to the sediment, lowering the activity of the aerobic community and dramatically affecting the effectiveness of the bioaugmentation strategy (Payne et al., 2013). It should be noted that up to now, sustainable strategies to supply oxygen *in situ* have not been found yet. Consequently, even though bioaugmentation appears as the more feasible strategy for an effective and economically sustainable bioremediation approach, the scarcity of sediment-free culture that can be used as inoculum, the poor knowledge of interactions between PCBs bioremoval processes and features of the treated site require more studies to assess the applicability of bioaugmentation in harsh environments and under real *in situ* conditions. It should be kept in mind that further steps still lie ahead and that given the complexity of the factors involved, there might not be a panacea but specific solutions should be found according to the different requirements of each treated site.

6.4 The story of PCBs, a warning for the scientific community

There is one last lesson that we can learn from these pollutants, related to their story and to how we have dealt with them, considering that after decades of studies about remediation techniques, PCBs still represent an unsolved problem. Indeed, bioremediation is just one of the many paths that have been followed trying to find an optimal solution, yet discovering many obstacles. It all started in 1966, when almost half a century after their industrial employment (1929), PCBs were detected for the first time in environmental samples (Jensen, 1972). Sören Jensen (1972) described the discovery of this environmental and global contamination as a fortuitous case given the not clear evidence of the impact of pollutants on the environment, which differed from other chemicals initially applied as insecticides like DDT or mercury. After realizing the consequences of the PCBs usage on the environment, Sweden banned their use (Jensen, 1972) and other countries did as well (Abraham Wolf-Reiner et al., 2002), but almost a century of industrial activities led to a severe contamination, that has not found a solution yet (Šrédlová and Cajthaml, 2022). At that time, Jensen (1972) suggested that the PCBs story should have thought us how to deal with new chemicals and substances, proceeding by cooperating with different scientific profiles to be as much aware as possible of the risks involved in their utilization. We should then question ourselves if we, as scientist and as humans, are learning this lesson. Indeed, apart from the knowledge acquired during all these years about how these pollutants interact with the environment and how we can deal with them, the PCBs story should have thought us that prevention rather than fixing

might be the most sustainable approach, avoiding impressive health and remediation costs. In fact, industrial molecules as environmentally persistent as PCBs are currently being employed. For instance, PFAs, per- and poly-fluoroalkyl substances, are a group of thousands of molecules (OECD/UNEP, 2018) widely applied in the industry since 1940 (Glüge et al., 2020). In the last years lots of attention has been payed to PFAs, identifying the polluted sites and assessing the impact of PFAs on the environment and on the human life (Bonato et al., 2020), reporting the difficulties to find proper removal strategies (Garg et al., 2023). Up to now, regulatory limits are being set for specific molecules, resulting in not effective restrictions (Dean et al., 2020; European Commission, 2020; European Parliament and council of the European Union, 2021), despite the enormous society costs. For example estimated costs for the EEA countries, including health and remediation costs, range between 52 and 84 billion euros (European Commission, 2020). Only recently, an ambitious law has been enacted by an Italian region, Piemonte, defining environmental limits for the whole group of PFAs (Giunta Regionale del Piemonte, 2022). Yet, it appears that countries are reacting slowly to the PFAs problem, trying to find a balance between advantages and risks in the daily employ of these compounds (Brennan et al., 2021). We should then wonder if we are reacting quickly enough to prevent the problem rather than setting the conditions to deal with it, if as we should, had we really learnt the lesson from our struggle in dealing with PCBs pollution.

6.5 Bibliography

Abeshu, G.W., Li, H.Y., Zhu, Z., Tan, Z., Leung, L.R., Li, H.Y., 2022. Median bed-material sediment particle size across rivers in the contiguous US. Earth Syst. Sci. Data 14, 929–942. https://doi.org/10.5194/essd-14-929-2022

Abraham Wolf-Reiner, Nogales Balbina, Golyshin Peter N, Pieper Dietmar H, Timmis Kenneth N, 2002. Polychlorinated biphenyl-degrading microbial communities in soils and sediments. Curr. Opin. Microbiol. 5, 246–253. https://doi.org/10.1016/s1369-5274(02)00323-5 Abstract

APAT, 2006. Diossine Furani e PCB. Rome, Italy.

Bedard, D.L., Bailey, J.J., Reiss, B.L., Van Slyke Jerzak, G., 2006. Development and characterization of stable sediment-free anaerobic bacterial enrichment cultures that dechlorinate aroclor 1260. Appl. Environ. Microbiol. 72, 2460–2470. https://doi.org/10.1128/AEM.72.4.2460-2470.2006

Bedard, D.L., Ritalahti, K.M., Löffler, F.E., 2007. The Dehalococcoides population in sediment-free mixed cultures metabolically dechlorinates the commercial polychlorinated biphenyl mixture Aroclor 1260. Appl. Environ. Microbiol. 73, 2513–2521. https://doi.org/10.1128/AEM.02909-06

Bonato, M., Corrà, F., Bellio, M., Guidolin, L., Tallandini, L., Irato, P., Santovito, G., 2020. Pfas environmental pollution and antioxidant responses: An overview of the impact on human field. Int. J. Environ. Res. Public Health 17, 1–45. https://doi.org/10.3390/ijerph17218020

Brennan, N.M., Evans, A.T., Fritz, M.K., Peak, S.A., von Holst, H.E., 2021. Trends in the regulation of per-and polyfluoroalkyl substances (PFAS): A scoping review. Int. J. Environ. Res. Public Health 18. https://doi.org/10.3390/ijerph182010900

Capozzi, S.L., Bodenreider, C., Prieto, A., Payne, R.B., Sowers, K.R., Kjellerup, B.V., 2019. Colonization and growth of dehalorespiring biofilms on carbonaceous sorptive amendments. Biofouling 35, 50–58. https://doi.org/10.1080/08927014.2018.1563892

Chang, B.-V., Chiu, T.-C., Yuan, S.-Y., 2006. Dechlorination of Polychlorinated Biphenyl Congeners by Anaerobic Microorganisms From River Sediment. Water Environ. Res. 78, 764–769. https://doi.org/10.2175/106143006x107380

Chen, C., He, J., 2018. Strategy for the Rapid Dechlorination of Polychlorinated Biphenyls (PCBs) by Dehalococcoides mccartyi Strains. Environ. Sci. Technol. 52, 13854–13862. https://doi.org/10.1021/acs.est.8b03198

Cheng, D., He, J., 2009. Isolation and characterization of "Dehalococcoides" sp. strain MB, which dechlorinates tetrachloroethene to trans-1,2-dichloroethene. Appl. Environ. Microbiol. 75, 5910–5918. https://doi.org/10.1128/AEM.00767-09

Chun, C.L., Payne, R.B., Sowers, K.R., May, H.D., 2013. Electrical stimulation of microbial PCB degradation in sediment. Water Res. 47, 141–152. https://doi.org/10.1016/j.watres.2012.09.038

Cotecchia, F., Vitone, C., Sollecito, F., Mali, M., Miccoli, D., Petti, R., Milella, D., Ruggieri, G., Bottiglieri, O., Santaloia, F., De Bellis, P., Cafaro, F., Notarnicola, M., Todaro, F., Adamo, F., Di Nisio, A., Lanzolla, A.M.L., Spadavecchia, M., Moretti, M., Agrosì, G., De Giosa, F., Fago, P., Lacalamita, M., Lisco, S., Manzari, P., Mesto, E., Romano, G., Scardino, G., Schingaro, E., Siniscalchi, A., Tempesta, G., Valenzano, E., Mastronuzzi, G., Cardellicchio, N., Di Leo, A., Spada, L., Giandomenico, S., Calò, M., Uricchio, V.F., Mascolo, G., Bagnuolo, G., Ciannarella, R., Tursi, A., Cipriano, G., Cotugno, P., Sion, L., Carlucci, R., Capasso, G., De Chiara, G., Pisciotta, G., Velardo, R., Corbelli, V., 2021. A geo-chemo-mechanical study of a highly polluted marine system (Taranto, Italy) for the enhancement of the conceptual site model. Sci. Rep. 11, 1–26. https://doi.org/10.1038/s41598-021-82879-w

Cutter, L.A., Watts, J.E.M., Sowers, K.R., May, H.D., 2001. Identification of a microorganism that links its growth to the reductive dechlorination of 2,3,5,6-chlorobiphenyl. Environ. Microbiol. 3, 699–709. https://doi.org/10.1046/j.1462-2920.2001.00246.x

Dean, W.S., Adejumo, H.A., Caiati, A., Garay, P.M., Harmata, A.S., Li, L., Rodriguez, E.E., Sundar, S., 2020. A Framework for Regulation of New and Existing PFAS by EPA. J. Sci. Policy Gov. 16. https://www.sciencepolicyjournal.org/article_1038126_jspg_16_01_03.html

Di Gregorio, S., Azaizeh, H., Lorenzi, R., 2013. Biostimulation of the autochthonous microbial community for the depletion of polychlorinated biphenyls (PCBs) in contaminated sediments. Environ. Sci. Pollut. Res. 20, 3989–3999. https://doi.org/10.1007/s11356-012-1350-x

Dolfing, J., 2003. Thermodynamic considerations for dehalogenation, in: Häggblom, M.M., Bossert, I.D. (Eds.), Dehalogenation, Microbial Processes and Environmental Applications. Kluwer

Academic Publishers, Rutgers University, USA, pp. 89–114.

European Commission, 2020. Poly- and perfluoroalkyl substances (PFAS), Communication from the commission to the European Parliament, the Council, the European Committee and the Committee of the Regions. Bruxelles.

European Parliament and council of the European Union, 2021. DIRECTIVE (EU) 2020/2184. Bruxelles.

Fagervold, S.K., May, H.D., Sowers, K.R., 2007. Microbial reductive dechlorination of Aroclor 1260 in Baltimore Harbor sediment microcosms is catalyzed by three phylotypes within the Phylum chloroflexi. Appl. Environ. Microbiol. 73, 3009–3018. https://doi.org/10.1128/AEM.02958-06

Fagervold, S.K., Watts, J.E.M., May, H.D., Sowers, K.R., 2011. Effects of bioaugmentation on indigenous PCB dechlorinating activity in sediment microcosms. Water Res. 45, 3899–3907. https://doi.org/10.1016/j.watres.2011.04.048

Garg, A., Shetti, N.P., Basu, S., Nadagouda, M.N., Aminabhavi, T.M., 2023. Treatment technologies for removal of per- and polyfluoroalkyl substances (PFAS) in biosolids. Chem. Eng. J. 453. https://doi.org/10.1016/j.cej.2022.139964

Giunta Regionale del Piemonte, 2022. DGR 60-5220. Piemonte.

Glüge, J., Scheringer, M., Cousins, I.T., Dewitt, J.C., Goldenman, G., Herzke, D., Lohmann, R., Ng, C.A., Trier, X., Wang, Z., 2020. An overview of the uses of per- And polyfluoroalkyl substances (PFAS). Environ. Sci. Process. Impacts 22, 2345–2373. https://doi.org/10.1039/d0em00291g

Huettel, M., Berg, P., Kostka, J.E., 2014. Benthic exchange and biogeochemical cycling in permeable sediments. Ann. Rev. Mar. Sci. 6, 23–51. https://doi.org/10.1146/annurev-marine-051413-012706

Jensen, S., 1972. The PCB story. Ambio 1, 123–131. https://www.jstor.org/stable/4311963

Kjellerup, B. V., Paul, P., Ghosh, U., May, H.D., Sowers, K.R., 2012. Spatial distribution of PCB dechlorinating bacteria and activities in contaminated soil. Appl. Environ. Soil Sci. 2012. https://doi.org/10.1155/2012/584970

Kocur, C.M.D., Lomheim, L., Molenda, O., Weber, K.P., Austrins, L.M., Sleep, B.E., Boparai, H.K., Edwards, E.A., O'Carroll, D.M., 2016. Long-Term Field Study of Microbial Community and Dechlorinating Activity Following Carboxymethyl Cellulose-Stabilized Nanoscale Zero-Valent Iron Injection. Environ. Sci. Technol. 50, 7658–7670. https://doi.org/10.1021/acs.est.6b01745

Koenigsberg, S., Willett, A., Sutherland, M., 2006. Controlled release electron donors: Hydrogen release compound (HRC)-an overview of a decade of case studies. Bioremediat. J. 10, 45–57. https://doi.org/10.1080/10889860600842837

Krumins, V., Park, J.W., Son, E.K., Rodenburg, L.A., Kerkhof, L.J., Häggblom, M.M., Fennell, D.E., 2009. PCB dechlorination enhancement in Anacostia River sediment microcosms. Water Res. 43, 4549–4558. https://doi.org/10.1016/j.watres.2009.08.003

Laroe, S.L., Fricker, A.D., Bedard, D.L., 2014. Dehalococcoides mccartyi strain JNA in pure culture extensively dechlorinates aroclor 1260 according to polychlorinated biphenyl (PCB) dechlorination process N. Environ. Sci. Technol. 48, 9187–9196. https://doi.org/10.1021/es500872t

Lehtinen, T., Mikkonen, A., Sigfusson, B., Ólafsdóttir, K., Ragnarsdóttir, K.V., Guicharnaud, R., 2014. Bioremediation trial on aged PCB-polluted soils-a bench study in Iceland. Environ. Sci. Pollut. Res. 21, 1759–1768. https://doi.org/10.1007/s11356-013-2069-z

Lisco, S., Corselli, C., De Giosa, F., Mastronuzzi, G., Moretti, M., Siniscalchi, A., Marchese, F., Bracchi, V., Tessarolo, C., Tursi, A., 2016. Geology of Mar Piccolo, Taranto (southern Italy): the physical basis for remediation of a polluted marine area. J. Maps 12, 173–180. https://doi.org/10.1080/17445647.2014.999136

Liu, X., Wan, H., Xue, Y., Feng, C., Wei, C., 2017. Addition of iron oxides in sediments enhances 2,3,4,5-tetrachlorobiphenyl (PCB 61) dechlorination by low-voltage electric fields. RSC Adv. 7, 26019–26027. https://doi.org/10.1039/c7ra02849k

Lu, Q., Liu, J., He, H., Liang, Z., Qiu, R., Wang, S., 2021. Waste activated sludge stimulates in situ microbial reductive dehalogenation of organohalide-contaminated soil. J. Hazard. Mater. 411, 125189. https://doi.org/10.1016/j.jhazmat.2021.125189

May, H.D., Miller, G.S., Kjellerup, B. V., Sowers, K.R., 2008. Dehalorespiration with polychlorinated biphenyls by an anaerobic ultramicrobacterium. Appl. Environ. Microbiol. 74, 2089–2094. https://doi.org/10.1128/AEM.01450-07

OECD/UNEP, 2018. Toward a new comprehensive global database of per- and polyfluoroalkyl substances (PFASs): Summary report on updating the OECD 2007 list of per- and polyfluoroalkyl substances (PFASs), Organisation for Economic Co-operation and Development.

Pakdeesusuk, U., Lee, C.M., Coates, J.T., Freedman, D.L., 2005. Assessment of natural attenuation via in situ reductive dechlorination of polychlorinated biphenyls in sediments of the Twelve Mile Creek arm of Lake Hartwell, SC. Environ. Sci. Technol. 39, 945–952. https://doi.org/10.1021/es0491228

Payne, R.B., Fagervold, S.K., May, H.D., Sowers, K.R., 2013. Remediation of polychlorinated biphenyl impacted sediment by concurrent bioaugmentation with anaerobic halorespiring and aerobic degrading bacteria. Environ. Sci. Technol. 47, 3807–3815. https://doi.org/10.1021/es304372t

Payne, R.B., Ghosh, U., May, H.D., Marshall, C.W., Sowers, K.R., 2019. A Pilot-Scale Field Study: In Situ Treatment of PCB-Impacted Sediments with Bioamended Activated Carbon'. Environ. Sci. Technol. 53, 6104–6105. https://doi.org/10.1021/acs.est.9b02107

Payne, R.B., Ghosh, U., May, H.D., Marshall, C.W., Sowers, K.R., 2017. Mesocosm Studies on the Efficacy of Bioamended Activated Carbon for Treating PCB-Impacted Sediment. Environ. Sci. Technol. 51, 10691–10699. https://doi.org/10.1021/acs.est.7b01935

Payne, R.B., May, H.D., Sowers, K.R., 2011. Enhanced reductive dechlorination of polychlorinated biphenyl impacted sediment by bioaugmentation with a dehalorespiring bacterium. Environ. Sci. Technol. 45, 8772–8779. https://doi.org/10.1021/es201553c

Rhee, G.Y., Sokol, R.C., Bethoney, C.M., Cho, Y.C., Frohnhoefer, R.C., Erkkila, T., 2001. Kinetics of polychlorinated biphenyl dechlorination and growth of dechlorinating microorganisms. Environ. Toxicol. Chem. 20, 721–726. https://doi.org/10.1002/etc.5620200405

Song, M., Luo, C., Li, F., Jiang, L., Wang, Y., Zhang, D., Zhang, G., 2015. Anaerobic degradation of

Polychlorinated Biphenyls (PCBs) and Polychlorinated Biphenyls Ethers (PBDEs), and microbial community dynamics of electronic waste-contaminated soil. Sci. Total Environ. 502, 426–433. https://doi.org/10.1016/j.scitotenv.2014.09.045

Sowers, K.R., Ghosh, U., May, H.D., 2018. Evaluating the Efficacy of Bioaugmentation for In-Situ Treatment of PCB Impacted Sediments ESTCP Project ER-201215.

Sowers, K.R., May, H.D., 2013. In situ treatment of PCBs by anaerobic microbial dechlorination in aquatic sediment: Are we there yet? Curr. Opin. Biotechnol. 24, 482–488. https://doi.org/10.1016/j.copbio.2012.10.004

Šrédlová, K., Cajthaml, T., 2022. Recent advances in PCB removal from historically contaminated environmental matrices. Chemosphere 287, 132096. https://doi.org/10.1016/j.chemosphere.2021.132096

Sudjarid, W., Chen, I.M., Monkong, W., Anotai, J., 2012. Reductive dechlorination of 2,3,4-chlorobiphenyl by biostimulation and bioaugmentation. Environ. Eng. Sci. 29, 255–261. https://doi.org/10.1089/ees.2011.0228

Summer, D., Schöftner, P., Watzinger, A., Reichenauer, T.G., 2020. Inhibition and stimulation of two perchloroethene degrading bacterial cultures by nano- and micro-scaled zero-valent iron particles. Sci. Total Environ. 722, 137802. https://doi.org/10.1016/j.scitotenv.2020.137802

Wang, S., Chen, C., Zhao, S., He, J., 2019. Microbial synergistic interactions for reductive dechlorination of polychlorinated biphenyls. Sci. Total Environ. 666, 368–376. https://doi.org/10.1016/j.scitotenv.2019.02.283

Wang, S., Chng, K.R., Chen, C., Bedard, D.L., He, J., 2015. Genomic Characterization of Dehalococcoides mccartyi Strain JNA That Reductively Dechlorinates Tetrachloroethene and Polychlorinated Biphenyls. Environ. Sci. Technol. 49, 14319–14325. https://doi.org/10.1021/acs.est.5b01979

Wang, S., Chng, K.R., Wilm, A., Zhao, S., Yang, K.L., Nagarajan, N., He, J., 2014. Genomic characterization of three unique Dehalococcoides that respire on persistent polychlorinated biphenyls. Proc. Natl. Acad. Sci. 111, 12103–12108. https://doi.org/10.1073/pnas.1404845111

Wang, S., He, J., 2013. Phylogenetically Distinct Bacteria Involve Extensive Dechlorination of Aroclor 1260 in Sediment-Free Cultures. PLoS One 8. https://doi.org/10.1371/journal.pone.0059178

Winchell, L.J., Novak, P.J., 2008. Enhancing polychlorinated biphenyl dechlorination in fresh water sediment with biostimulation and bioaugmentation. Chemosphere 71, 176–182. https://doi.org/10.1016/j.chemosphere.2007.10.021

Xu, G., Zhang, N., Zhao, X., Chen, C., Zhang, C., He, J., 2022a. Offshore Marine Sediment Microbiota Respire Structurally Distinct Organohalide Pollutants. Environ. Sci. Technol. 56, 3065–3075. https://doi.org/10.1021/acs.est.1c06680

Xu, G., Zhao, S., Chen, C., Zhao, X., Ramaswamy, R., He, J., 2022b. Dehalogenation of Polybrominated Diphenyl Ethers and Polychlorinated Biphenyls Catalyzed by a Reductive Dehalogenase in Dehalococcoides mccartyi Strain MB. Environ. Sci. Technol. 56, 4039–4049. https://doi.org/10.1021/acs.est.1c05170

Xu, Y., Tang, Y., Xu, L., Wang, Y., Liu, Z., Qin, Q., 2021. Effects of iron-carbon materials on

microbial-catalyzed reductive dechlorination of polychlorinated biphenyls in Taihu Lake sediment microcosms: Enhanced chlorine removal, detoxification and shifts of microbial community. Sci. Total Environ. 792, 148454. https://doi.org/10.1016/j.scitotenv.2021.148454

Yan, T., LaPara, T.M., Novak, P.J., 2006. The impact of sediment characteristics on polychlorinated biphenyl-dechlorinating cultures: Implications for bioaugmentation. Bioremediat. J. 10, 143–151. https://doi.org/10.1080/10889860601021381

Yu, H., Wan, H., Feng, C., Yi, X., Liu, X., Ren, Y., Wei, C., 2017. Microbial polychlorinated biphenyl dechlorination in sediments by electrical stimulation: The effect of adding acetate and nonionic surfactant. Sci. Total Environ. 580, 1371–1380. https://doi.org/10.1016/j.scitotenv.2016.12.102

Zanaroli, G., Balloi, A., Negroni, A., Borruso, L., Daffonchio, D., Fava, F., 2012a. A Chloroflexi bacterium dechlorinates polychlorinated biphenyls in marine sediments under in situ-like biogeochemical conditions. J. Hazard. Mater. 209–210, 449–457. https://doi.org/10.1016/j.jhazmat.2012.01.042

Zanaroli, G., Negroni, A., Vignola, M., Nuzzo, A., Shu, H.Y., Fava, F., 2012b. Enhancement of microbial reductive dechlorination of polychlorinated biphenyls (PCBs) in a marine sediment by nanoscale zerovalent iron (NZVI) particles. J. Chem. Technol. Biotechnol. 87, 1246–1253. https://doi.org/10.1002/jctb.3835

Zemb, O., Lee, M., Low, A., Manefield, M., 2010. Reactive iron barriers: A niche enabling microbial dehalorespiration of 1,2-dichloroethane. Appl. Microbiol. Biotechnol. 88, 319–325. https://doi.org/10.1007/s00253-010-2740-y

Chapter 7

Microbial electrochemical technologies to upgrade wastewater treatment plants

Preface

Within the context of the ELECTRA project [grant agreement no. 826244], financially supported by the Horizon 2020 programme of the European Union, and in order to gain insights on the application of bioelectrochemical systems for bioremediation purposes, I spent a research period abroad of 6 months in the laboratory of Prof. Sebastià Puig, at Lequia (Laboratory of Chemical and Environmental Engineering), Girona, Spain. The results collected during the staying, in collaboration also with Prof. Cheng, from the State Key Lab of Urban Water Resource and Environment of Shenzhen, China, led to a publication in the Chemical Engineering Journal (https://doi.org/10.1016/j.cej.2022.138949), which is reported below.

7.1 Introduction

Secondary effluents of wastewater treatment plants (WWTPs) are commonly characterized by the presence of total nitrogen (TN) (Díaz et al., 2003; Li et al., 2015). High TN values can compromise the discharge in the environment and the reuse of these effluents. Indeed, Directive 91/271/EEC which regulates urban wastewater (WW) clearly states a maximum of 15 mg N-TN·L^{-1} for discharging in sensitive areas (e.g. eutrophic areas) (Council Directive, 1991). Water reuse from urban wastewater discharges is also promoted from the perspective of facing water scarcity and droughts (Sanz and Gawlik, 2014). A key parameter for water reuse is the pathogens content, which has to meet strict thresholds, specific for each European country (Sanz and Gawlik, 2014). For instance, the limit for urban uses ranges from 0.3 to 1.3 log(CFU·100mL^{-1}) of total coliforms (TC) in Greece and absence to 2 log(CFU·100mL^{-1}) of E. coli in Spain (Ilias et al., 2014; Pous et al., 2021). The more stringent Italian law requires a maximum threshold of 1 log(CFU·100mL^{-1}) of E. coli for any reuse applications (M.D. 185/2003, 2003). It becomes necessary to guarantee that secondary WWTP effluents match the target values to be either reused or released into the environment (Council Directive, 1991; Dulio et al., 2018).

Technologies meant to polish the contaminant content in excess are defined as tertiary treatments (TT). Nowadays, even though 91.2 % of the European continent population has access to urban wastewater collecting and treatment systems, only 70% can rely on WWTPs equipped with tertiary treatments. The remaining slice of the population has access to primary treatments (PT, 3.5%), secondary treatments (ST, 19.5%), and decentralized WWTPs (DEWATS, 7%) (Eurostat, 2019). PT and ST are often not sufficient to reduce the nitrogen content to environmentally acceptable values (Haandel and Lubbe, 2012), while tertiary treatments are meant to meet the nitrogen discharge criteria and to furtherly reduce the pathogens content according to the water reuse or the discharge site (Gerba and Pepper, 2015). Adding a treatment step inevitably increases costs and space requirements, which makes retrofitting solutions less attractive and highlights the need of finding alternative approaches (Díaz et al., 2003). Microbial Electrochemical Technologies (METs) might contribute to enhancing the polishing power of WWTPs, without being necessary the implementation of additional tertiary treatments.

METs couple solid-state electrodes with bacteria, using the latter as a biocatalyst (Rabaey et al., 2007). Electrodes can then act as electron donors/acceptors to stimulate the different microbial metabolisms, without the need for external chemical dosage. METs are considered a promising approach to reducing nitrogen content in WW, where microbial activity is used as a tool to reach the required quality standards

for nitrate (NO_3^-), nitrite (NO_2^-) and ammonium (NH_4^+). Ammonium is conventionally removed aerobically by a process named nitrification, which transforms NH_4^+ to NO_3^- (Haandel and Lubbe, 2012). Nitrate is subsequently converted via denitrification, a heterotrophic or autotrophic anaerobic cascade mechanism that requires a source of electrons to reduce NO_3^- to dinitrogen gas (N_2), via sequential steps that go through NO_2^-, nitric oxide (NO) and nitrous oxide (N_2O) (Rout et al., 2021). It is known that METs can prime biological nitrogen removal processes, such as NO_3^- reduction to dinitrogen gas or NH_4^+ oxidation to N_2 via anammox (Osset-Álvarez et al., 2019; Shaw et al., 2020). Autotrophic denitrification can be assisted by electrodes, which act as direct electron donors (Clauwaert et al., 2007). This concept has started to move toward engineering applications. For example, Sander *et al.* used a three-electrode system placed in a plug-flow reactor as a tertiary treatment to reduce the TN content of real WWTPs' secondary effluents. The nitrogen removal was mainly limited to denitrification, reducing the NO_3^- amount below 0.5 mg $N\text{-}NO_3^- \cdot L^{-1}$ (Sander et al., 2017). As for ammonium, a pilot-scale METs was coupled with a nitrifying reactor and used to treat real urban WW and centrate from anaerobic digestors with total-nitrogen removal efficiencies ranging between 10 and 95 % depending on the influent content (40-1460 mg N-TN $\cdot L^{-1}$) (Isabel San-Martín et al., 2018). A similar set-up was applied to concomitantly remove COD, NH_4^+ and NO_3^- from synthetic WW. The electrons supplied by the anodic oxidation of the organic matter were used to reduce the nitrate at the cathode, which was previously obtained by converting the ammonium in an external nitrifying reactor (Virdis et al., 2008). The concomitant nitrate and ammonium removals were observed also by integrating a METs with a membrane bioreactor to treat synthetic WW with high NH_4^+ content (Li et al., 2017). Moreover, simultaneous nitrification and denitrification have been enhanced in the cathodic chamber of a bioelectrochemical system, when working with a synthetic medium (Virdis et al., 2010). In respect to the pathogens, the use of electrochemical oxidation (ECO) as disinfecting technique is becoming a feasible alternative to traditional methods (e.g. chemicals dosage or UV) (Chen et al., 2021; Hand and Cusick, 2021). Electrochemical oxidation can proceed via the anodic production of oxidant agents, such as chlorine when an anolyte (e.g. wastewater) contains chloride (Costa and Olivi, 2009; Fang et al., 2006). ECO as tertiary treatment showed an efficacy up to 99.5% when disinfecting real wastewater containing E.coli (> 5 $\log(CFU \cdot 100mL^{-1})$) (Pérez et al., 2010). Electrochemical disinfection using Ti-MMO anode was demonstrated effective also for treating low chloride WW as stormwater (9 mg $Cl^- \cdot L^{-1}$) (Feng et al., 2018).

METs can become a reasonable stand-alone nitrogen removal technology soon, but their implementation in existing WWTPs might accelerate its adoption (Osset-Álvarez et al., 2019). The replacement of existing infrastructures is not feasible due to the high costs invested in them, but the versatility of METs could allow their integration into already existing biological processes by the simply immersion of electrodes in the bioreactors. Sander *et al.* demonstrated how a simple bioelectrochemical configuration increased the polishing of real WW (Sander et al., 2017). Yet, they studied the MET as a tertiary treatment and not retrofit secondary WW treatments. To the best of the authors' knowledge, there is only one paper showing the potential to merge MET in existing WWTPs for nitrogen removal. Tejedor-Sanz *et al* adapted a three-electrode configuration to an activated sludge to increase the nitrogen removal rate of the system. The applied potential induced an anaerobic zone at the cathode and aerobic zone at the anode to concomitantly stimulate denitrification and nitrification (Tejedor-Sanz et al., 2016). However, the implementation in secondary settlers, where a natural redox stratification exists, could allow an easier implementation of MET-based applications. In addition, the previously studied systems were meant to enhance the sole nitrogen removal and the disinfectant power of the MET was not assessed.

For the first time, a lab-scale model of a bioelectrochemical reactor coupled with a secondary settler, labelled as e-settler, was built to study how the immersion of polarized electrodes can enhance the polishing of real secondary wastewater. First, the usage of an immersed anode/cathode was explored as a method to stimulate nitrogen removal processes. Second, anode electrochemical oxidation will be explored to disinfect wastewater. The coupling of the two techniques in a simple configuration, which could allow an economic retrofit of existing WWTPs, has not been assessed previously. The set-up of the kit was meant to be placed in the upper part of the secondary settler to avoid the strict aerobic conditions of the activated sludge tank, which would compromise the growth of denitrifying bacteria as well as to avoid electrode clogging due to sludge accumulation (Li et al., 2014).

7.2 Materials and methods

7.2.1 Reactors set-up

Two piston flow reactor replicates were built to study e-settlers, as depicted in Figure 1. A Plexiglas tube (40 cm length, 2.5 cm inner diameter) was sealed to two PVC t-connectors (6.5 cm length, 2.5 cm inner diameter). The upper part was closed with a PVC cap (3 cm in length, 2.5 cm inner diameter). The length

of the reactor was 55 cm, with a net volume of 170 mL. The cathode was made of a graphite-coated stainless steel mesh, prepared by Cheng et al. as described elsewhere (Xu et al., 2020). Cathode features were: total cathodic area, TCA: 468 cm^2; total cathodic volume, TCV: 24.5 mL; net cathodic volume, NCV: 2 mL; total cathodic length: 5 cm. A stainless steel wire was used as the current collector. Initially, graphite rods (total surface area: 8.8 cm^2; Mersen Ibérica, Spain) were used as the anode. On day 64, graphite rods were substituted with Ti-MMO (total surface area: 3.9 cm^2; NMT electrodes, South Africa) to assess the anodic hypochlorite evolution as a disinfection action. An Ag/AgCl sat. KCl (+ 0.197 V vs. standard hydrogen electrode, SHE, SE 11, Xylem Analytics Germany Sales GmbH & Co. KG Sensortechnik Meinsberg, Germany) was introduced at a height of 3 cm as the reference electrode. The distance between the cathode and the anode was set at 7.5 cm. The Influent was pumped with a peristaltic pump.

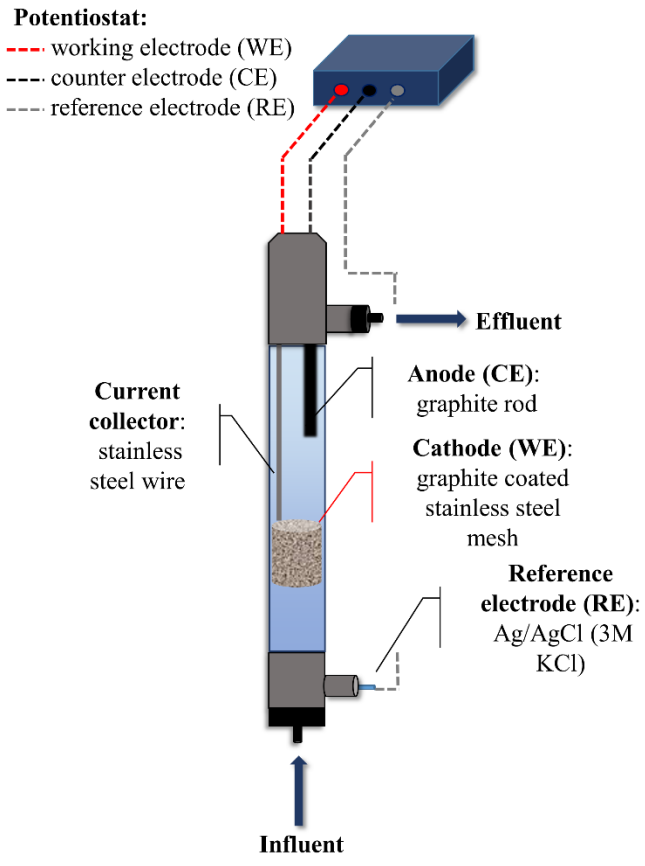

Figure 9 *Scheme of the lab-scale e-settler used for the experiment, details are reported in the text.*

7.2.2 Wastewater characteristics

The effluent coming from the secondary settler of an urban WWTP (Quart, Girona, Spain) was used as the e-settlers' influent. Inorganic nitrogen composition is given as a range of values, observed due to the natural biological processes. Three different WW samplings were performed and addressed as low nitrogen wastewater (NO_3^--WW), used from day 1 to day 50, high nitrogen wastewater (NH_4^+-NO_3^--WW), used from day 50 to day 85, and low nitrogen wastewater 2 (NO_3^--2-WW), used from day 85 to day 102. WW was stored in a refrigerated stirring tank at 4 °C to preserve its characteristics. Chemical physical parameters of NO_3^--WW were: BOD_5 (biological oxygen demand) 2 ± 1 mg $O_2 \cdot L^{-1}$; BOD_{30} 11 ± 1 mg $O_2 \cdot L^{-1}$; COD (chemical oxygen demand) 20 – 76 mg $O_2 \cdot L^{-1}$; 18.7 – 31.5 mg N-$NO_3^- \cdot L^{-1}$; 0 – 4.1 mg N-$NO_2^- \cdot L^{-1}$; 0 – 8.9 mg N-$NH_4^+ \cdot L^{-1}$. Chemical physical parameters of NH_4^+-NO_3^--WW were: BOD_5 5.7 ± 0.5 mg $O_2 \cdot L^{-1}$; BOD_{30} 23 ± 5 mg $O_2 \cdot L^{-1}$; COD 29.5 – 178 mg $O_2 \cdot L^{-1}$; NO_3^- 19.3 – 40.8 mg N-$NO_3^- \cdot L^{-1}$; NO_2^- 0.12 – 4.2 mg N-$NO_2^- \cdot L^{-1}$; NH_4^+ 0.17 – 33.7 mg N-$NH_4^+ \cdot L^{-1}$. Chemical physical parameters of NO_3^--2-WW were: COD 56.6 - 128 mg $O_2 \cdot L^{-1}$; NO_3^- 32.9 – 37.1 mg N-$NO_3^- \cdot L^{-1}$; NO_2^- 0.03 – 0.67 mg N-$NO_2^- \cdot L^{-1}$; NH_4^+ 0.16 – 1.8 mg N-$NH_4^+ \cdot L^{-1}$.

7.2.3 Operational mode

For the inoculation period, the reactors were poised at – 0.321 V vs Ag/AgCl sat. KCl in batch mode to promote the development of an electroactive population (Pous et al., 2015). A 1:1 solution of wastewater and effluent from a denitrifying MET reactor (Pous et al., 2017), adjusted to a final nitrate concentration of 33 mg N-$NO_3^- \cdot L^{-1}$, was used to inoculate the reactors. The media was recirculated at 25 $L \cdot d^{-1}$ for 3 weeks.

After the inoculation period, the two reactor replicates were operated in continuous mode to study the functioning of the e-settlers. The influent used was a 9:1 solution of wastewater and effluent from a denitrifying MET reactor (Pous et al., 2017), and stored into a 10 L tank connected to the reactors, previously flushed with N_2 gas. After changing from inoculation mode to continuous mode, the current flow between the electrodes was negligible. For this reason, the potentiostat was switched to galvanostatic mode to guarantee a constant electron flow to prime biological denitrification. Data presented are reported as the average of the two replicates.

Two different operational phases can be distinguished. During phase I, wastewater with a low ammonium content (NO_3^--WW) was fed to the reactors. The composition of WW resembled a WWTPs with good nitrification performance, allowing studying the polishing power of the e-settlers in an ideal condition. During this phase, the effect of the current density and flow rate was studied. Each parameter was modified separately, to better identify the different contributions. The current applied was initially set to

a value high enough to perform complete denitrification, 26 mA·L^{-1}_{TCV}, and subsequently adjusted to 20 mA· L^{-1}_{TCV}, to mild the electrode potentials. HRT, calculated on the cathode length, was set at 7.4 ± 0.6 h. Subsequently, the inflow's rate was increased step wisely, to a final HRT of 2.9 ± 0.2 h. Later on, the current applied was raised to 61 mA· L^{-1}_{TCV}, maintaining the same HRT, aiming to increase nitrogen polishing.

During phase II, the composition of the influent presented a high concentration of ammonium (NH_4^+-NO_3^--WW). The NH_4^+ content of the secondary effluent is representative of WWTPs with an inefficient aerobic stage, thus allowing us to assess the e-settler removal ability under non-ideal conditions. Initially, HRT was set at 2.2 ± 0.1 h with a current of 98 mA· L^{-1}_{TCV}, a theoretical value necessary to reduce the nitrate content. Yet, considering the only partial removal of TN, it was decided to increase the current flow to perform also denitrification of the NO_3^- coming from NH_4^+ nitrification. Before doing so, anodes were replaced with Ti-MMO to evaluate the electrochemical anodic disinfection. The current was raised to 214 mA· L^{-1}_{TCV}. Subsequently, wastewater composition changed again (NO_3^--2-WW) and the current was switched off to evaluate the open-circuit voltage (OCV) contributions (days 84-95). Finally, the potentiostat was turned on again to assess the possibility to restore the bioelectrochemical stimulation (days 95-102).

7.2.4 Abiotic tests

The abiotic contribution of the graphite-coated stainless steel mesh cathode to nitrogen removal was assessed in a two-compartment H-cell. This was composed of two 300 mL glass bottles separated by a cation membrane (CEM, CMI-7000, Membranes Int., USA). A graphite-coated stainless steel mesh was placed in the cathodic chamber (total cathodic volume: 39.25 mL; net cathodic volume: 3 mL; total cathodic area: 448 cm^2) and stainless steel wire was used as the current collector. Graphite rods (18 cm^2; Mersen Ibérica, Spain) were used as anode electrode. Ag/AgCl sat. KCl (+ 0.197 V vs. standard hydrogen electrode, SHE, SE 11, Xylem Analytics Germany Sales GmbH & Co. KG Sensortechnik Meinsberg, Germany) was used as the reference electrode. The synthetic media described by (Ceballos-Escalera et al., 2021) was used as abiotic media, with a concentration of 33 mg N-NO_3^-·L^{-1} and 2.7 mg N-NH_4^+·L^{-1}. The working electrode was poised at -0.3 V and -0.9 V vs Ag/AgCl sat. KCl as they were the potentials commonly found in the running e-settlers. Tests were run for a minimum of 7 days.

7.2.5 Analytical methods and calculations

A minimum of three samples of effluent and influent were taken and analysed from both reactors for each tested condition. The same procedure was kept for the abiotic test, analysing cathodic and anodic chambers. All liquid samples were analysed according to APHA standard water measurements (APHA, 2005) for nitrate ($N\text{-}NO_3^-$), nitrite ($N\text{-}NO_2^-$), and ammonium ($N\text{-}NH_4^+$) by ionic chromatography (ICS 5000, Dionex, USA). The pH and electrical conductivity of the samples were measured with a pH-meter (pH-meter basic 20+, Crison, Spain) and a conductivity meter (EC-meter basic 30+, Crison, Spain), respectively. Nitrous oxide (N_2O) was measured using an N_2O liquid-phase microsensor (Unisense, Denmark). COD was measured via a colourimetric kit (Hach, Iowa, USA). BOD was determined according to the standard methods (APHA, 2005). The hydraulic retention time was calculated considering the total cathodic length volume and the flow rate. All removal rates were calculated as reported in the supplementary material (Supplementary equations S1-S5). The coulombic efficiency (CE) was calculated considering all reduction steps from nitrate to dinitrogen gas considering nitrite, nitrous oxide accumulation and ammonium nitrification (Supplementary equation S6). The COD electron balance (COD-EB) was calculated considering COD removal and it was used to evaluate the maximum contribution from heterotrophic denitrification, as reported in the supplementary material (Supplementary equation S7). The theoretical maximum COD-EB was calculated considering the effluent COD equal to 0, while the real maximum COD-EB was calculated considering the real effluent's COD. In both cases, COD was considered to be biodegradable and heterotrophically removed from denitrifiers bacteria. Total coliforms, E. coli and Enterococcus were analysed in an external laboratory following standard procedures for wastewater examinations (CECAM, Girona) (APHA, 2005).

7.3 Results and discussion

7.3.1 Nitrogen removal performance of e-settlers treating low ammonium content wastewater (NO_3^--WW)

After the inoculation period, the system was set on continuous mode to begin "phase I". Real wastewater, labelled as NO_3^--WW, was pumped into the reactors. At the initial conditions, HRT of 7.4 ± 0.6 h and current applied of 20 $mA \cdot L^{-1}_{TCV}$, the nitrogen content decreased below the 15 mg $N \cdot L^{-1}$ threshold, going from 31 ± 4 mg $N \cdot L^{-1}$ to 2 ± 3 mg $N \cdot L^{-1}$ of TN (Fig. 3), with a removal rate of 94 ± 17 g $N \cdot m^{-3}_{TCV} \cdot d^{-1}$ (Fig. 2). The flow rate was then increased (of 5.1 ± 0.6 h HRT), observing a rise in the TN removal rate

(115 ± 16 g $N \cdot m^{-3}_{TCV} \cdot d^{-1}$), with an effluent presenting a TN concentration of 3 ± 3 mg $N \cdot L^{-1}$. The HRT was further reduced to 2.9 ± 0.2 h, reaching a TN removal rate of 156 ± 60 g $N \cdot m^{-3}_{TCV} \cdot d^{-1}$. At this condition, e-settlers showed the highest nitrate removal rate during phase I, equivalent to 146 ± 62 g $N\text{-}NO_3^- \cdot m^{-3}_{TCV} \cdot d^{-1}$, and TN effluent standards were fulfilled (8 ± 6 $mg \cdot L^{-1}$). Then, the applied current was increased and set to the theoretical flow required to fully reduce the nitrate content (61 $mA \cdot L^{-1}_{TCV}$). Consequently, the effluent TN decreased to 4 ± 3 mg $N \cdot L^{-1}$.

During phase I, NH_4^+ was fully removed, with neither NO_2^- nor N_2O accumulation (Table S1). To identify the contribution of the applied current to the nitrogen removal processes, CE was taken into account. It has to be reminded that the system worked under galvanostatic conditions: the current supplied was chosen by the operator, not as a result of the bioelectrochemical activity of the reactor. At the initial current density (20 $mA \cdot L^{-1}_{TCV}$), the value was adjusted to nitrogen availability, and CEs around 100% were observed. As the HRT was decreased from 7 to 3 h while keeping the current density stable, the CE dropped to 37 % (Table 1), suggesting the co-occurrence of heterotrophic NO_3^- reduction (Xiao et al., 2015). The gradual decrease in CE revealed that electrochemical stimulation was partially contributing to the overall nitrogen removal. Then, when the current was raised to 68 $mA \cdot L^{-1}_{TCV}$ to balance the theoretical nitrogen removal requirements, CE went up to 124 %. The succeeding increase of CE observed after incrementing the current might be related to an artefact of the mathematical expression. In order to better understand the role of heterotrophic denitrification on nitrogen depletion, COD was identified as an index to evaluate the organic matter content of WW, acting as an indigenous organic source of electrons. However, an increase of the COD in the effluent of the e-settlers was observed, due to the electrochemical oxidation of the graphite anode, which allowed only to speculate about the heterotrophic denitrification role in the system. Indeed, inlet COD ranged from 35 to 64 mg $O_2 \cdot L^{-1}$, while outlet COD presented values between 62 and 89 mg $O_2 \cdot L^{-1}$ (Supplementary Table S1). An electron balance was calculated considering that: i) all inlet COD was consumed by denitrifiers (theoretical COD-EB); ii) all inlet COD was biodegradable despite being the effluent of a secondary treatment. The results showed a hypothetical maximum contribution of heterotrophic denitrification that went from 82% to 58% (table 1), suggesting necessary electrochemical assistance. It has to be considered that COD measurements for this range of values can suffer from low accuracy. Moreover, the real contribution of heterotrophic denitrification could be negligible considering that the BOD was around 10 mg $O_2 \cdot L^{-1}$. At the end of phase I, e-settlers demonstrated the ability to simultaneously remove ammonium and nitrate, under mild conditions of HRT and pollutant concentration.

Table 1 *Details, coulombic efficiency and energy consumption of e-settlers at the different tested conditions*

	Tested conditions					
	HRT (h)	Current applied ($mA \cdot L^{-1}_{TCV}$)	Anode	CE (%)	COD - EB (%)	Energy ($KWh/gN_{removed}$)
Phase I	7.4 ± 0.6	20	Graphite	63 ± 24	82 ± 31^{T}	$1.5 \cdot 10^{-2} \pm 2 \cdot 10^{-3}$
	5.1 ± 0.6	20	Graphite	45 ± 6	64 ± 16^{T}	$1.2 \cdot 10^{-2} \pm 2 \cdot 10^{-3}$
	2.9 ± 0.2	20	Graphite	37 ± 14	50 ± 18^{T}	$1.0 \cdot 10^{-2} \pm 4 \cdot 10^{-3}$
	3.1 ± 0.6	61	Graphite	124 ± 40	58 ± 38^{T}	$5 \cdot 10^{-2} \pm 2 \cdot 10^{-2}$
Phase II	2.2 ± 0.1	98	Graphite	100 ± 12	83 ± 51^{T}	$610^{-2} \pm 1 \cdot 10^{-2}$
	2.1 ± 0.1	98	Ti-MMO	194 ± 106	121 ± 92^{T}	$1.0 \cdot 10^{-1} \pm 3 \cdot 10^{-2}$
	2.3 ± 0.3	214	Ti-MMO	352 ± 81	201 ± 93^{R}	$3.9 \cdot 10^{-1} \pm 7 \cdot 10^{-2}$
O.C.V.	2.0 ± 0.2	/	Ti-MMO	/	170 ± 89^{R}	/
Validation test	2.1 ± 0.2	214	Ti-MMO	353 ± 17	91 ± 35^{R}	$4.9 \cdot 10^{-1} \pm 2 \cdot 10^{-2}$

T: theoretical COD-EB, based on total COD removal; R: calculated COD-EB, based on the measured COD removal

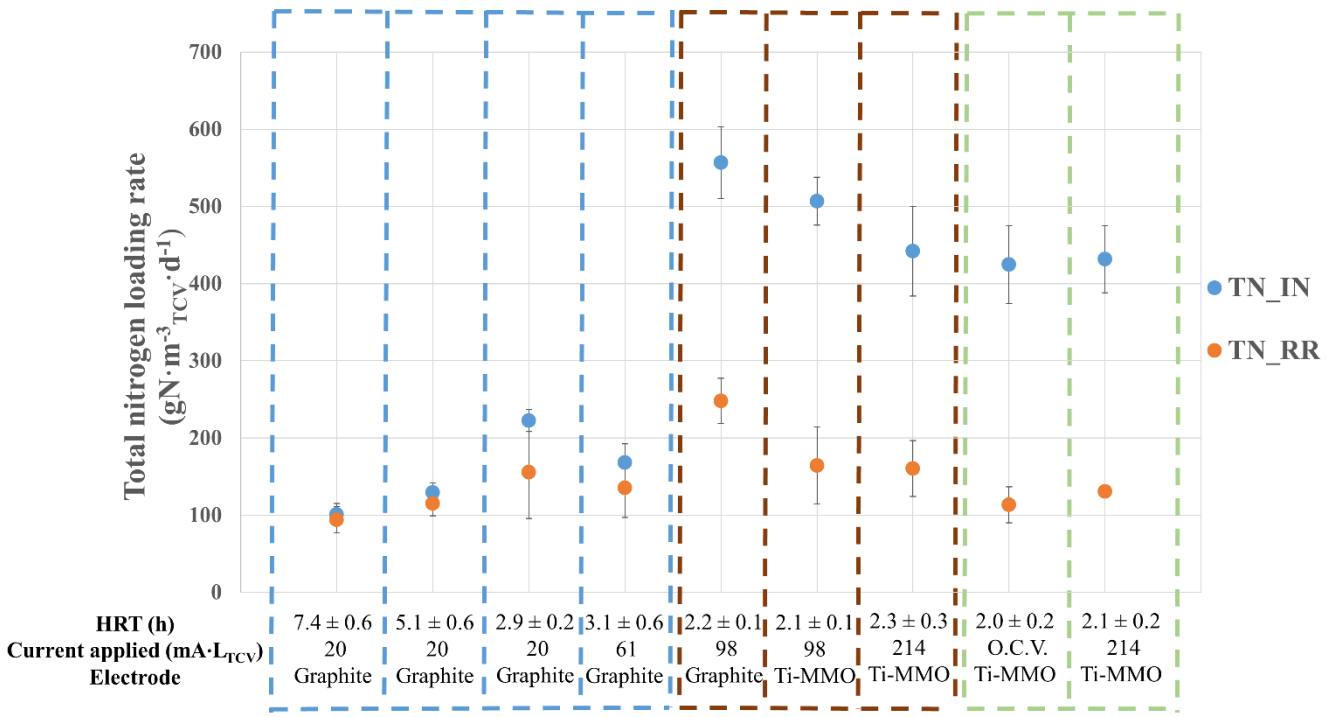

Figure 1 *Inlet flows and removal rates of the total nitrogen in the e-settlers, at the different tested conditions: TN, total nitrogen; IN, influent; RR, removal rate; Dashed blue lines: phase 1, NO3 —WW; Dashed brown lines: phase 1I, NH4 +–NO3 —WW; Dashed green lines: open circuit and validation tests, NO3 − -2-WW.*

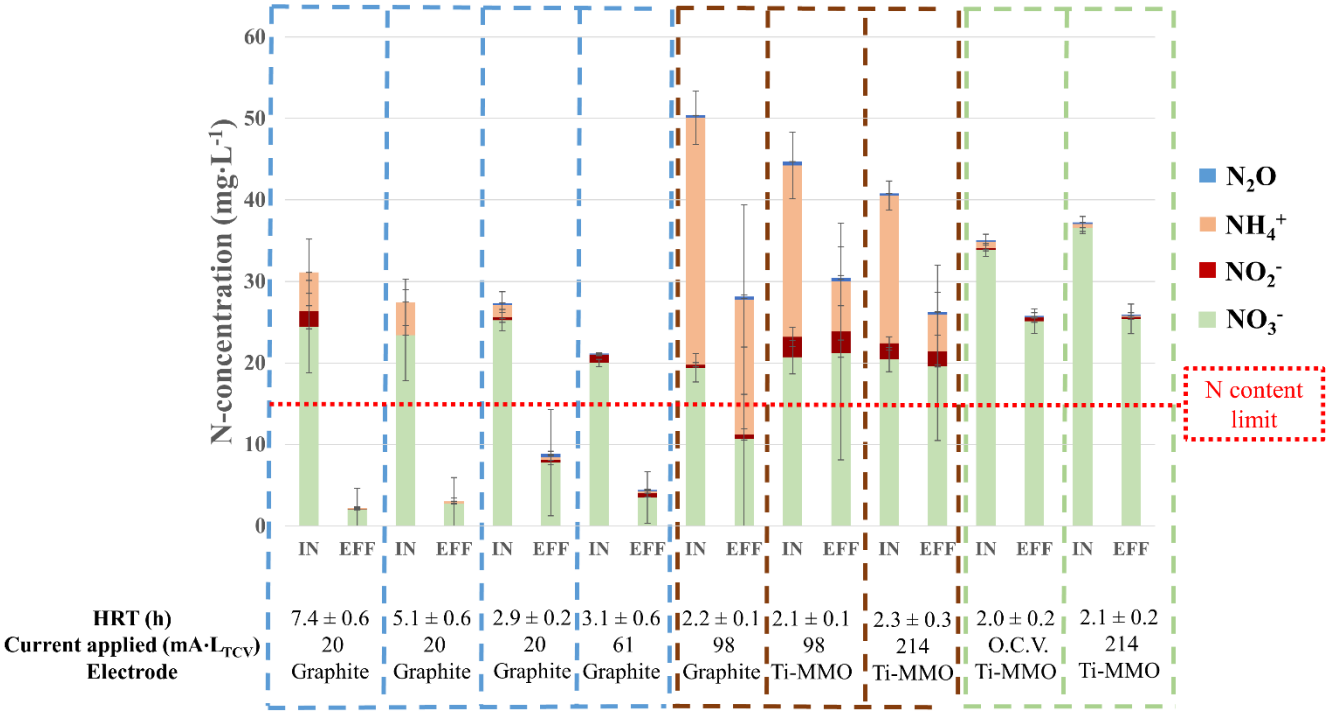

Figure 2 *Influent and effluent compositions of the e-settlers at the different tested conditions: IN, influent; EFF, effluent; Dashed blue lines: phase 1, NO3 —WW; Dashed brown lines: phase 1I, NH4 +–NO3 —WW; Dashed green lines: open circuit and validation tests, NO3 − -2-WW*

7.3.2 e-settlers behaviour treating rich ammonium wastewater (NH_4^+-NO_3^--WW)

When phase I finished, the composition of WW changed. Phase II was characterized by effluent of secondary settlers with a high content of ammonium (up to 31 ± 3 mg N-NH_4^+·L^{-1}, Table S1). At the initial conditions, HRT of 2.2 ± 0.1 h and 98 mA·L^{-1}_{TCV}, e-settlers reported the highest nitrogen removal rate observed, 248 ± 29 g N·m^{-3}_{TCV}·d^{-1} (Fig. 2). The CE, 100 ± 12 %, suggested a good correspondence between electrons supplied and reduced nitrogen (Table 1). However, the effluent composition was largely over the guideline value, being 28 ± 3 mg N·L^{-1} (Fig. 3). The supplied current was enough to reduce the initial NO_3^- but not for removing the whole of the inlet NH_4^+ (31 ± 3 mg N-NH_4^+·L^{-1}).

Before increasing the current density, graphite anodes were replaced with Ti-MMO to compare the disinfecting abilities of the two materials. The electrodes substitution led to a drop in the performance of the e-settlers. TN removal rate decreased to 164 ± 50 g N·m^{-3}_{TCV}·d^{-1} (Fig. 1). Denitrification became less marked, with an effluent composition of 21 ± 13 mg N-NO_3^-·L^{-1} compared to 20 ± 2 mg N-NO_3·L^{-1} of the influent, while ammonium was still clearly reduced, going from 23 ± 3 mg N-NH_4^+·L^{-1} in the influents

to 6 ± 7 mg $N\text{-}NH_4^+ \cdot L^{-1}$ in the effluents (Supplementary Table S1). To explain the variation of the e-settlers performance, a cathodic and anodic combined mechanism was considered. When the inlet was pumped into the reactors, wastewater was first exposed to the cathode, where denitrification took place transforming the available NO_3^- into N_2. As wastewater moved up, it reached the anode, where electrochemical oxygen promoted aerobic nitrification, which converts ammonium into nitrate (Lai et al., 2017). At low ammonium contents or high HRTs, the nitrate content of the effluent was either negligible orcould still be cathodically reduced thanks to back-diffusion, as observed during phase I. When the ammonium content was high (Phase II), ammonium was solely converted to nitrate, but the e-settlers were not able to completely remove it.

The reactors' performance decreased after the anode replacement probably because Ti-MMO raised the electrochemical production of oxidant agents, which resulted to be harmful to the biocathode. The current density was then set to 214 $mA \cdot L^{-1}_{TCV}$, to verify that an increase in the current would not have positively primed the e-settlers performance in presence of the titanium anode. Indeed, after having raised the current, no significant changes were observed in terms of nitrogen polishing, with an average value of TN removal rate of 160 ± 36 g $N \cdot m^{-3}_{TCV} \cdot d^{-1}$ (Fig 1). Similar effluent compositions were obtained compared to the previous test (20 ± 9 mg $N\text{-}NO_3^- \cdot L^{-1}$; 4 ± 6 mg $N\text{-}NH_4^+ \cdot L^{-1}$, Table S1). At these conditions, a high coulombic efficiency was observed, 352 ± 81 %, indicating that the bacterial community was not able to utilise the whole of the current supplied to the system (Table 1). By replacing the graphite electrode with Ti-MMO, electrochemical anodic oxidation was avoided, allowing to estimate the real COD removal. The estimated COD-EB was 390 ± 96 % (Table 1). Such high value suggested that the majority of the supplied electrons were delivered to other chemical reactions (e.g. H_2 production). The CE and the electron balance inferred an inefficient nitrogen removal stimulation, possibly due to a high anodic oxygen production that limited the cathodic denitrification mechanism, and to high ammonium content that could not be completely polished in the studied set-up leading to an accumulation of nitrate, as depicted in Figure S5.

7.3.3 Control tests

After having assessed the nitrogen removal abilities of the e-settlers, wastewater was changed again (NO_3^--2-WW) and the electricity supply was switched off to identify the effect of the current on the microbial activity (OCV test). Without electrical stimulation, the TN removal rates dropped to 113 ± 23 g $N \cdot m^{-3}_{TCV} \cdot d^{-1}$ (Fig. 2), a value between 1.5 and 2 times lower than the ones observed with electricity

supply. This was a proof of the influence of the applied current on the nitrogen removal processes. However, as the current was restored to 214 $mA \cdot L^{-1}_{TCV}$, the activity was not recovered (131 ± 6 $g\ N \cdot m^{-3}_{TCV} \cdot d^{-1}$) (Fig. 2). Indicating that the absence of current negatively affected the microbial cathodic activity. This is in line with what was observed in a previous study, where long starvation periods (> 10 days) decreased the performance of the bioelectrochemical system (Ruiz et al., 2015).

Regarding abiotic contributions, no significant nitrogen removal was observed when working at the lowest cathodic potential reached during the experiment, -0.9 vs Ag/AgCl sat. KCl (Table S2). An increase in the TN content was detected, especially in terms of ammonium, which raised from 1 to 6 and 7 mg $N\text{-}NH_4^+ \cdot L^{-1}$ in the cathodic and anodic chambers, respectively, after 7 days. Such a raise was possibly due to a trace of ammonia in the coating of the electrode, as a result of the manufacturing process (Xu et al., 2020).

7.3.4 Evaluating the removal of pathogens

The e-settlers concept was born as a technique to promote WW polishing. For this purpose, disinfection ability was also monitored to evaluate the treatment potential of this technology. The total content of coliforms of WW was characterized, reporting an influent concentration >2 $log(CFU \cdot 100mL^{-1})$ (Supplementary Table S3). The e-settlers equipped with graphite anodes showed a similar removal of the total coliforms content compared to the open circuit condition, resulting in an average effluent concentration of 1.3 ± 0.9 $log(CFU \cdot 100mL^{-1})$ for the graphite test and 1.3 ± 0.4 $log(CFU \cdot 100mL^{-1})$ for the open circuit test. Instead, e-settlers integrated with Ti-MMO anodes reduced the total coliforms to 0.4 ± 0.1 $log(CFU \cdot 100mL^{-1})$. The better result obtained with the Ti-MMO anode is likely to be due to the higher anodic stability, which favours the formation of oxidizing agents rather than the oxidation of the anodic material itself. This hypothesis is in line with the data reported in the literature. Lai *et al.* compared graphite and Ti-MMO as anode materials (Lai et al., 2017). Higher CO_2 production was detected when working with a graphite rod, which was linked to the degradation of the carbon electrode. Conversely, Ti-MMO promoted oxygen evolution, with an efficiency of 90%. A comparative study of anode materials reported that Ti-MMO increased the active chlorine production up to 3 times more than graphite (Khelifa et al., 2004). Bare titanium was demonstrated to be more effective than graphite for the electrochemical disinfection of water (Rahmani et al., 2019), probably due to the formation of oxidant agents. It has been demonstrated that sodium chloride at concentrations higher than 0.2 $g \cdot L^{-1}$ enhanced the electrochemical oxidation power of Ti-MMO anodes due to the evolution of active chlorine (Tavares

et al., 2012). Considering the relevant NaCl amount in wastewater, which can range from 0.5 to a few $g \cdot L^{-1}$ (Fontenot et al., 2013; Hamoda and Al-Attar, 1995), e-settlers probably performed a WW disinfection via the presence of oxidant agents such as active chlorine.

7.3.5 Implications

Towards the development of technologies and smart solutions to upgrade already existing WWTPs, e-settlers appeared to be competitive compared to treatments based on conventional biological processes as well as to treatments equipped with bioelectrochemical systems (Table 2). The highest nitrogen removal rate observed in this experiment was 248 ± 29 g $N \cdot m^{-3}_{TCV} \cdot d^{-1}$, which is a value comparatively higher than those found in the literature for tertiary nitrogen polishing. Some of the conventional methods used as tertiary treatments rely on nature-based solutions. The usage of a bioreactor filled with plant substrates showed denitrification rates of 17.5 g $N\text{-}NO_3^- \cdot m^{-3} \cdot d^{-1}$ (Díaz et al., 2003) while floating wetland removed nitrogen at a rate of 12.2 g $N \cdot m^{-3} \cdot d^{-1}$ (Gao et al., 2017). The main strength of the e-settler is its compact configuration which minimize the space requirements. Moving to more technological/intensive treatments applicable as ST for nitrogen removal, fixed-film reactors showed a TN removal rate of 29 g $N\text{-}NO_3^- \cdot m^{-3} \cdot d^{-1}$ (Shewa et al., 2022) and membrane bioreactors had a TN removal rate of 82 g $N\text{-}NO_3^- \cdot m^{-3} \cdot d^{-1}$ (Khastoo et al., 2021). Those technologies are close to market or already being applied, while bioelectrochemical systems are still in a process of development. Taking into account this, the data obtained in the current work (248 ± 29 g $N \cdot m^{-3}_{TCV} \cdot d^{-1}$) were higher than the removal rates reported by Sander *et al*, who worked with a plug-flow MET reactor as tertiary treatment removing 150 g $N \cdot m^{-3} \cdot d^{-1}$ from real secondary settler's effluents (Sander et al., 2017). As for the small portfolio of studies about the integration of bioelectrochemical systems with already existing technology, MET were inserted into activated sludge for treating synthetic WW, showing a TN removal rate of 18.7 g $N\text{-}NO_3^- \cdot m^{-3} \cdot d^{-1}$ (Tejedor-Sanz et al., 2016). Instead, coupling polarized electrodes with constructed wetlands resulted in stimulation of the nitrogen removal, with a rate of 39.1 g $N_{TCC} \cdot m^{-3} \cdot d^{-1}$ removed (Aguirre-Sierra et al., 20116), and represents an improvement over other nature-based solutions (Díaz et al., 2003; Gao et al., 2017). Other MET-based studies have evaluated different configurations, that could be applied as secondary or tertiary treatments and would require a high degree of modifications of current WWTPs. For example, San-Martín *et al.* used a pilot-scale six-chambers MET to treat effluent from primary treatment and obtained a TN removal rate of 28 g $N \cdot m^{-3} \cdot d^{-1}$ (Isabel San-Martín et al., 2018). A two

chambers system used to treat synthetic WW was based on the coupling of electrochemical production of oxygen and hydrogen to stimulate nitrification and denitrification, showing a removal rate of 14 g $N \cdot m^{-3} \cdot d^{-1}$ (Goel and Flora, 2005). High nitrogen removal rates, 3900 g $N \cdot m^{-3}_{TCC} \cdot d^{-1}$, were obtained using a MET, but the system was supplemented with sulphur and iron and high currents were applied (100 mA) (Zhu et al., 2021).

A relevant point for the e-settler application is the durability of the system. In this experiment, this study aimed to tune the working parameters to increase nitrogen and pathogens removal whereas the durability of the MET kit was not deeply assessed (total operation of 102 days). First of all, electrode clogging should be evaluated and maintenance could be required (e.g. backwashing of trapped sludge). Placing the electrodes in the upper part of the secondary settler and optimizing the cathode dimension could decrease the clogging. It was demonstrated that in the bioelectrochemical systems for WW treatment, a smaller electrode dimensions decreased the occlusion (Brunschweiger et al., 2020). Moreover, it has been suggested that the current itself can prevent the clogging of the electrodes when using METs for WW treatment, either by enhancing the degradation of the suspended particles (Khalfbadam et al., 2016) or by decreasing the agglomeration of the sludge particles (Ding et al., 2018). A second parameter to be considered for system durability is the long-term stability of electrodes. The electrodes could partially lose their electrochemical characteristics, reducing the removal performance, e.g. as observed during Phase II. This work has explored a total of 3 electrodes: graphite anode, Ti-MMO anode and graphite-coated stainless steel cathode. Graphite anode worked as a sacrificial electrode, and thus a regular replacement would be required. When using a Ti-MMO anode, a longer life-span is expected. For example, the resistance of a Ti-MMO anode has been assessed during a long-term experiment (> 200 days), using it for oxygen evolution in a marine environment (Cappello et al., 2019). Regarding the cathode, the relevant risk would come from the presence of anodic oxidizing agents. Before the replacement of the graphite rods with Ti-MMO, the bioelectrochemical systems had been operated for 64 days showing an increasing nitrogen removal rate by tuning the different operational parameters. During this period, e-settlers demonstrated their stability and room for improvement given by the optimization of the working conditions. Yet, the substitution of the anodes slightly decreased the e-settlers performance. At the last test with graphite, total nitrogen was removed at a rate of 248 g $N \cdot m^{-3}_{TCV} \cdot d^{-1}$, while at the first test with Ti-MMO, total nitrogen was removed at 164 g $N \cdot m^{-3}_{TCV} \cdot d^{-1}$ (nitrogen removal rate decreased by 34 %). A larger anode-cathode distance, together with higher water upflow velocity could reduce the effect of oxidizing agents over the biocathode. Moreover, in scaled-up e-settlers

a horizontal electrodes configuration would be used, as shown in the graphical abstract, which can allow a better control of the anode-cathode distance as it is homogeneous for the whole length of the electrodes. However, a compromise with smaller anode-cathode distances to ensure proper electrochemical stability would be required (i.e. minimization of ohmic losses). These factors could contribute to reduce the corrosion of the electrodes themselves but also provide higher protection over cathodic bacteria. After having optimized the working conditions, the performance of the scaled-up MET should be assessed in a long term to evaluate whether stability is preserved. In fact, during the operation of the studied e-settlers, mostly stable removal rates were observed for each tested condition. Deviations ranged between 6 and 60 g $N \cdot m^{-3}_{TCV} \cdot d^{-1}$ according to the different tests performed, with an average removal rate variation of 30 g $N \cdot m^{-3}_{TCV} \cdot d^{-1}$ (20% of the mean value).

The optimization of the water upflow velocity and the anode-cathode distance would not only increase the system durability, but also the nitrogen removal rates.

Another important aspect of the application of the e-settler is how the nitrogen removal performance changes depending on the influent characteristics. In the studied set-up, when operating with NO_3^--WW, the operational conditions (NH_4^+ content; low HRT) were optimal to guarantee the removal of the converted ammonium. However, as the WW composition fluctuated to higher NH_4^+ concentration (NH_4^+-NO_3^--WW) the system was not able to completely remove the nitrate produced through nitrification. To overcome this issue, it would be required to study the coupling of the e-settler with an activated sludge bioreactor. The ideal WW influent for e-settlers is mainly composed of NO_3^- and low dissolved O_2, to favour denitrifying bacteria. In the secondary treatment model, aeration can be improved by regulating the dissolved oxygen according to the ammonium content of the aerobic sludge effluent, which is a control system already demonstrated to be effective in real WWTPs (Bertanza et al., 2021). In this manner, ammonium content can be maintained within the required limits, i.e. 5 $mg \cdot L^{-1}$ for WW discharge (Bertanza et al., 2021) or 0.5 $mg \cdot L^{-1}$ in case of water reuse for human consumption (Council Directive, 1998). A further solution, not evaluated in the studied e-settler, to remove the NH_4^+ content is via anammox. If WW contains anammox bacteria and the operational conditions can sustain their growth (e.g. anoxic environment), autotrophic anaerobic oxidation of ammonium mediated by electrodes could occur. In this regard, it has been shown how anammox bacteria can transfer electrons directly to electrodes (Shaw et al., 2020) and how they can be used in METs to treat syntethic WW (Vilajeliu-Pons et al., 2018). In parallel, HRT should be also adjusted according to the dimension of the ST model. HRT, calculated on the cathodic volume, was used as the index to have a flow rate comparable to real secondary

settlers, which usually ranges from 1 to 3 h (Haandel and Lubbe, 2012). An application on a larger scale of the technique would mean adapting the electrochemical system to maintain the performance as high as possible while using an appropriate electrode dimension. Consequently, the HRT of the scaled-up technology should decrease, since it is not possible to think of a settler where the cathode occupies the entire space of the tank.

The MET kit is meant to be a versatile system that can be easily applied to existing plants. This retrofitting technology can play an important role in the perspective of water discharge and reuse, considering the relevant number of WWTPs unequipped with appropriate treatments for nitrogen and pathogens removal in the EU (Eurostat, 2019), the conspicuous amount of not safely treated household WW in the world (44%) (UN-Water, 2021) and the environmental costs associated to the introduction of additional installations in existing WWTPs (Faragò et al., 2021). The e-settler technology should not replace large-scale tertiary treatments but upgrade the efficiency of the overall WWTP. In the case of small-scale plants (e.g. decentralized WWTPs) smart solutions to guarantee proper nitrogen removal and sanitation of waste streams are needed (Grommen and Verstraete, 2002; Van Timmeren and Sidler, 2007). For instance, Singh *et al*. analyzed the polishing power of several DEWATS, currently widely employed in India (Singh et al., 2019). The majority of the plants were equipped with settlers, anaerobic baffled reactors and collecting tanks, which were not always efficient resulting in a TN content in the effluent higher than 15 $mg \cdot L^{-1}$ and a coliform amount over 2.5 $\log(CFU \cdot 100mL^{-1})$. The e-settler configuration is flexible (e.g. electrodes dimension) and it could be adapted to each plant. The use of electrochemical stimulation is expected to avoid the addition of chemicals, i.e. methanol, which is usually added to increase COD to enhance heterotrophic denitrification (Haandel and Lubbe, 2012), or oxidant agents for disinfection. This effect will not only reduce the operational costs associated but also increase sustainability in the broader sense, as no transport of chemicals will be required and electricity could be generated in-situ through renewable energy.

Table 2 *Summary of wastewater treatment technologies for nitrogen removal*

Bioelectrochemical systems or technologies equipped with MET					
Technology	Nitrogen		Working volume (L)	Applied current or potential	Reference
	Influent type and composition ($mgN \cdot L^{-1}$)	Removal rate			
This study	Secondary settler's effluent 50 (TN): 31 (NH_4^+); 19 (NO_3^-)	248 $gN \cdot m^{-3}_{TCV} \cdot d^{-1}$	0.17	98 $mA \cdot dm^{-3}_{TCV}$	
Activated sludge + MET	Synthetic WW 37 (TN)	[R]18.7 $gN \cdot m^{-3}_{TCC} \cdot d^{-1}$	22	-0.6 V vs Ag/AgCl 3 M KCl (70 $mA \cdot dm^{-2}$)	(Tejedor-Sanz et al., 2016)
MET + iron/sulfur mediated denitrification	Synthetic WW 35 (NO_3^-)	[C]3900 $gN \cdot m^{-3}_{TCC} \cdot d^{-1}$	0.3	353 $mA \cdot dm^{-3}$	(Zhu et al., 2021)
Wetland + MET	Urban WW 55 (TN): 47 (NH_4^+); 1 (NO_3^-)	[C]39.1 $gN \cdot m^{-3}_{TCC} \cdot d^{-1}$	34	0.3 V vs Ag/AgCl (16.7 $mA \cdot dm^{-3}$)	(Aguirre-Sierra et al., 20116)
MET	Secondary settler's effluent 3.5 (TN): 0.5 (NH_4^+); 3 (NO_3^-)	[R]150 $gN \cdot m^{-3} \cdot d^{-1}$	2	-0.9 V vs Ag/AgCl 3 M KCl (25 $mA \cdot dm^{-3}_{NCV}$)	(Sander et al., 2017)
MET	Primary treatment's effluent 40 (TN)	[C]28 $gN \cdot m^{-3} \cdot d^{-1}$	150	1 V (cell voltage)	(Isabel San-Martín

					et al., 2018)
MET	Synthetic WW 49 (NH_4^+)	[C]14 $gN \cdot m^{-3} \cdot d^{-1}$	1.6	50 $mA \cdot dm^{-2}$	(Goel and Flora, 2005)
Technologies not equipped with METs					
Bioreactor amended with organic matter	Secondary settler's effluent 17.7 (NO_3^-)	[R]17.5 $gN \cdot m^{-3} \cdot d^{-1}$	59	n.i.	(Díaz et al., 2003)
Floating wetlands	Synthetic WW 15 (TN): 3.5 (NH_4^+); 11.5 (NO_3^-)	[C]12.2 $gN \cdot m^{-3} \cdot d^{-1}$	224	n.i.	(Gao et al., 2017)
Fixed rope media	Primary treatment's effluent 24 (NH_4^+)	[C]29 $gN \cdot m^{-3} \cdot d^{-1}$	1890	n.i.	(Shewa et al., 2022)
Membrane bioreactor	Primary treatment's effluent 57 (TN)	[C]82 $gN \cdot m^{-3} \cdot d^{-1}$	140	n.i.	(Khastoo et al., 2021)

TCC: total cathodic compartment, R: reported in the paper, C: calculated using the data reported in the paper

7.4 Conclusions

The e-settler concept aims to retrofit WWTPs, avoiding the additional space required for the installation of conventional tertiary treatments. The potential of an e-settler was proved by coupling a bioelectrochemical system with a secondary settler. The applied current concomitantly increased the nitrogen removal rate and the disinfection power of the system. This is the first study that merges the ability of METs to stimulate nitrogen removal and perform electrochemical oxidation for WW disinfection while applying these techniques using a simple configuration suitable to retrofit existing WWTPs. For example, a similar set-up to the one used in this experiment was studied by Sander *et al* (Sander et al., 2017). A three-electrode system, with graphite granules both as anode and cathode, was

placed in a plug-flow reactor and used as a tertiary treatment for WW. The system increased the nitrogen removal of the treatment plant. But the so-constructed MET would require additional space to be implanted in an existing WWTPs and the system did not show disinfectant ability. Moreover, to the best of the authors' knowledge, the only other study about merging METs into existing WWTPs was conducted by Tejedor-Sanz *et al* (Tejedor-Sanz et al., 2016) which placed a three-electrode system in an activated sludge bioreactor. Although the coupled technologies showed enhanced polishing power, they had some limitations: the aerobic conditions of the reactor required a membrane to guarantee low oxygen levels in the cathodic chamber; the anode was meant to supply the oxygen for nitrification and could not be used to perform electrochemical disinfection. Instead, the e-settler can merge the increased nitrogen removal and WW disinfection since it is placed in the upper part of the secondary settler. Given the high amount of untreated water discharged into the environment and the number of WWTPs not equipped with tertiary treatments, the simplicity of the MET kit could become a feasible solution to upgrade existing plants, especially considering small-scale plants (e.g. decentralized WWTPs).

Further studies are required to improve the system. High ammonium content (> 30 mgN-$NH_4^+ \cdot L^{-1}$) could not be polished in the current e-settler, requiring better aeration in the activated sludge bioreactor. As for the electrochemical disinfection, the proximity of the two electrodes resulted in a diffusion of the oxidizing agents to the biocathode, requiring optimization of the anode-cathode distance. Although several parameters still need to be adjusted for a scale-up of the process, e-settler demonstrated as a feasible route to enhance the polishing action of secondary settlers.

7.5 Bibliography

Aguirre-Sierra, A., Bacchetti-De Gregoris, T., Bernà, A., Salas, J.J., Aragòn, C., Esteve-Núñez, A., 20116. Microbial Electrochemical Systems outperform fixed--bed biofilters for cleaning--up urban wastewater. Environ. Sci. Water Res. Technol. 2, 984–993. https://doi.org/10.2134/jeq2002.1757

APHA, 2005. Standard Methods for the Examination of Water and Wastewater, 19th ed. Am. Public Heal. Assoc. Washingt. DC, USA.

Bertanza, G., Baroni, P., Garzetti, S., Martinelli, F., 2021. Reducing energy demand by the combined application of advanced control strategies in a full scale WWTP. Water Sci. Technol. 83, 1813–

1823. https://doi.org/10.2166/wst.2021.109

Brunschweiger, S., Ojong, E.T., Weisser, J., Schwaferts, C., Elsner, M., Ivleva, N.P., Haseneder, R., Hofmann, T., Glas, K., 2020. The effect of clogging on the long-term stability of different carbon fiber brushes in microbial fuel cells for brewery wastewater treatment. Bioresour. Technol. Reports 11, 100420. https://doi.org/10.1016/j.biteb.2020.100420

Cappello, S., Cruz Viggi, C., Yakimov, M., Rossetti, S., Matturro, B., Molina, L., Segura, A., Marqués, S., Yuste, L., Sevilla, E., Rojo, F., Sherry, A., Mejeha, O.K., Head, I.M., Malmquist, L., Christensen, J.H., Kalogerakis, N., Aulenta, F., 2019. Combining electrokinetic transport and bioremediation for enhanced removal of crude oil from contaminated marine sediments: Results of a long-term, mesocosm-scale experiment. Water Res. 157, 381–395. https://doi.org/10.1016/j.watres.2019.03.094

Ceballos-Escalera, A., Pous, N., Chiluiza-Ramos, P., Korth, B., Harnisch, F., Bañeras, L., Balaguer, M.D., Puig, S., 2021. Electro-bioremediation of nitrate and arsenite polluted groundwater. Water Res. 190, 116748. https://doi.org/10.1016/j.watres.2020.116748

Chen, Y. di, Duan, X., Zhou, X., Wang, R., Wang, S., Ren, N. qi, Ho, S.H., 2021. Advanced oxidation processes for water disinfection: Features, mechanisms and prospects. Chem. Eng. J. 409, 128207. https://doi.org/10.1016/j.cej.2020.128207

Clauwaert, P., Rabaey, K., Aelterman, P., De Schamphelaire, L., Pham, T.H., Boeckx, P., Boon, N., Verstraete, W., 2007. Biological denitrification in microbial fuel cells. Environ. Sci. Technol. 41, 3354–3360. https://doi.org/10.1021/es062580r

Costa, C.R., Olivi, P., 2009. Effect of chloride concentration on the electrochemical treatment of a synthetic tannery wastewater. Electrochim. Acta 54, 2046–2052. https://doi.org/10.1016/j.electacta.2008.08.033

Council Directive, 1998. Council Directive 98/83/EC, COfficial Journal of the European Communities. https://doi.org/10.1017/cbo9780511610851.055

Council Directive, 1991. Council Directive 91/271/EEC, Official Journal of the European Communities. https://doi.org/10.1039/AP9842100196

Díaz, R., García, J., Mujeriego, R., Lucas, M., 2003. A Quick , Low-Cost Treatment Method for

Secondary Effluent Nitrate Removal through Denitrification. Environ. Eng. Sci. 20, 693–702. https://doi.org/10.1089/109287503770736195

Ding, A., Fan, Q., Cheng, R., Sun, G., Zhang, M., Wu, D., 2018. Impacts of applied voltage on microbial electrolysis cell-anaerobic membrane bioreactor (MEC-AnMBR) and its membrane fouling mitigation mechanism. Chem. Eng. J. 333, 630–635. https://doi.org/10.1016/j.cej.2017.09.190

Dulio, V., van Bavel, B., Brorström-Lundén, E., Harmsen, J., Hollender, J., Schlabach, M., Slobodnik, J., Thomas, K., Koschorreck, J., 2018. Emerging pollutants in the EU: 10 years of NORMAN in support of environmental policies and regulations. Environ. Sci. Eur. 30, 1–13. https://doi.org/10.1186/s12302-018-0135-3

Eurostat, 2019. Population connected to urban wastewater collecting and treatment systems, by treatment level [WWW Document]. Popul. Connect. to urban wastewater Collect. Treat. Syst. by Treat. Lev. URL https://ec.europa.eu/eurostat/databrowser/view/ten00020/default/table?lang=en

Fang, Q., Shang, C., Chen, G., 2006. MS2 Inactivation by Chloride-Assisted Electrochemical Disinfection. J. Environ. Eng. 132, 13–22. https://doi.org/10.1061/(asce)0733-9372(2006)132:1(13)

Faragò, M., Damgaard, A., Madsen, J.A., Andersen, J.K., Thornberg, D., Andersen, M.H., Rygaard, M., 2021. From wastewater treatment to water resource recovery: Environmental and economic impacts of full-scale implementation. Water Res. 204, 117554. https://doi.org/10.1016/j.watres.2021.117554

Feng, W., McCarthy, D.T., Wang, Z., Zhang, X., Deletic, A., 2018. Stormwater disinfection using electrochemical oxidation: A feasibility investigation. Water Res. 140, 301–310. https://doi.org/10.1016/j.watres.2018.04.059

Fontenot, S., Lee, S., Asche, K., 2013. The effects of chloride from waste water on the environment, The Effects of Chloride from Waste Water on the Environment. City of Morris.

Gao, L., Zhou, W., Huang, J., He, S., Yan, Y., Zhu, W., Wu, S., Zhang, X., 2017. Nitrogen removal by the enhanced floating treatment wetlands from the secondary effluent. Bioresour. Technol. 234, 243–252. https://doi.org/10.1016/j.biortech.2017.03.036

Gerba, C.P., Pepper, I.L., 2015. Municipal Wastewater Treatment, in: Pepper, I., Gerba, C., Gentry, T. (Eds.), Environmental Microbiology: Third Edition. Elsevier Inc., Oxford, UK, pp. 583–606. https://doi.org/10.1016/B978-0-12-394626-3.00025-9

Goel, R.K., Flora, J.R.V., 2005. Sequential nitrification and denitrification in a divided cell attached growth bioelectrochemical reactor. Environ. Eng. Sci. 22, 440–449. https://doi.org/10.1089/ees.2005.22.440

Grommen, R., Verstraete, W., 2002. Environmental biotechnology: The ongoing quest. J. Biotechnol. 98, 113–123. http://ovidsp.ovid.com/ovidweb.cgi?T=JS&PAGE=reference&D=emed5&NEWS=N&AN=20022 61686

Haandel, A.C. van, Lubbe, J.G.M. van der, 2012. Handbook of Biological Wastewater Treatment, Second ed. ed. Iwa Publishing, London, UK.

Hamoda, M.F., Al-Attar, I.M.S., 1995. Effects of high sodium chloride concentrations on activated sludge treatment. Water Sci. Technol. 31, 61–72. https://doi.org/10.1016/0273-1223(95)00407-E

Hand, S., Cusick, R.D., 2021. Electrochemical Disinfection in Water and Wastewater Treatment: Identifying Impacts of Water Quality and Operating Conditions on Performance. Environ. Sci. Technol. 55, 3470–3482. https://doi.org/10.1021/acs.est.0c06254

Ilias, A., Panoras, A., Angelakis, A., 2014. Wastewater recycling in Greece: The case of Thessaloniki. Sustain. 6, 2876–2892. https://doi.org/10.3390/su6052876

Isabel San-Martín, M., Mateos, R., Carracedo, B., Escapa, A., Morán, A., 2018. Pilot-scale bioelectrochemical system for simultaneous nitrogen and carbon removal in urban wastewater treatment plants. J. Biosci. Bioeng. 126, 758–763. https://doi.org/10.1016/j.jbiosc.2018.06.008

Khalfbadam, H.M., Ginige, M.P., Sarukkalige, R., Kayaalp, A.S., Cheng, K.Y., 2016. Bioelectrochemical system as an oxidising filter for soluble and particulate organic matter removal from municipal wastewater. Chem. Eng. J. 296, 225–233. https://doi.org/10.1016/j.cej.2016.03.067

Khastoo, H., Hassani, A.H., Mafigholami, R., Mahmoudkhani, R., 2021. Comparing the performance of the conventional and fixed-bed membrane bioreactors for treating municipal wastewater. J.

Environ. Heal. Sci. Eng. 19, 997–1004. https://doi.org/10.1007/s40201-021-00664-3

Khelifa, A., Moulay, S., Hannane, F., Benslimene, S., Hecini, M., 2004. Application of an experimental design method to study the performance of electrochlorination cells. Desalination 160, 91–98. https://doi.org/10.1016/S0011-9164(04)90021-5

Lai, A., Aulenta, F., Mingazzini, M., Palumbo, M.T., Papini, M.P., Verdini, R., Majone, M., 2017. Bioelectrochemical approach for reductive and oxidative dechlorination of chlorinated aliphatic hydrocarbons (CAHs). Chemosphere 169, 351–360. https://doi.org/10.1016/j.chemosphere.2016.11.072

Li, H., Zuo, W., Tian, Y., Zhang, J., Di, S., Li, L., Su, X., 2017. Simultaneous nitrification and denitrification in a novel membrane bioelectrochemical reactor with low membrane fouling tendency. Environ. Sci. Pollut. Res. 24, 5106–5117. https://doi.org/10.1007/s11356-016-6084-8

Li, W.W., Yu, H.Q., He, Z., 2014. Towards sustainable wastewater treatment by using microbial fuel cells-centered technologies. Energy Environ. Sci. 7, 911–924. https://doi.org/10.1039/c3ee43106a

Li, X., Shi, H., Li, K., Zhang, L., 2015. Combined process of biofiltration and ozone oxidation as an advanced treatment process for wastewater reuse. Front. Environ. Sci. Eng. 9, 1076–1083. https://doi.org/10.1007/s11783-015-0770-5

M.D. 185/2003, 2003. Ministerial Decree 185/2003.

Osset-Álvarez, M., Rovira-Alsina, L., Pous, N., Blasco-Gómez, R., Colprim, J., Balaguer, M.D., Puig, S., 2019. Niches for bioelectrochemical systems on the recovery of water, carbon and nitrogen in wastewater treatment plants. Biomass and Bioenergy 130, 105380. https://doi.org/10.1016/j.biombioe.2019.105380

Pérez, G., Gómez, P., Ibañez, R., Ortiz, I., Urtiaga, A.M., 2010. Electrochemical disinfection of secondary wastewater treatment plant (WWTP) effluent. Water Sci. Technol. 62, 892–897. https://doi.org/10.2166/wst.2010.328

Pous, N., Barcelona, A., Sbardella, L., Hidalgo, M., Colomer, J., Serra, T., Salvadó, V., 2021. Zooplankton-based reactors for tertiary wastewater treatment: A pilot-scale case study. J. Environ. Manage. 278, 111538. https://doi.org/10.1016/j.jenvman.2020.111538

Pous, N., Puig, S., Balaguer, M.D., Colprim, J., 2017. Effect of hydraulic retention time and substrate

availability in denitrifying bioelectrochemical. Environ. Sci. Water Res. Technol. 3, 922–929. https://doi.org/10.1039/c7ew00145b

Pous, N., Puig, S., Dolors Balaguer, M., Colprim, J., 2015. Cathode potential and anode electron donor evaluation for a suitable treatment of nitrate-contaminated groundwater in bioelectrochemical systems. Chem. Eng. J. 263, 151–159. https://doi.org/10.1016/j.cej.2014.11.002

Rabaey, K., Rodríguez, J., Blackall, L.L., Keller, J., Gross, P., Batstone, D., Verstraete, W., Nealson, K.H., 2007. Microbial ecology meets electrochemistry: Electricity-driven and driving communities. ISME J. 1, 9–18. https://doi.org/10.1038/ismej.2007.4

Rahmani, A.R., Samarghandi, M.R., Nematollahi, D., Zamani, F., 2019. A comprehensive study of electrochemical disinfection of water using direct and indirect oxidation processes. J. Environ. Chem. Eng. 7, 102785. https://doi.org/10.1016/j.jece.2018.11.030

Rout, P.R., Shahid, M.K., Dash, R.R., Bhunia, P., Liu, D., Varjani, S., Zhang, T.C., Surampalli, R.Y., 2021. Nutrient removal from domestic wastewater: A comprehensive review on conventional and advanced technologies. J. Environ. Manage. 296, 113246. https://doi.org/10.1016/j.jenvman.2021.113246

Ruiz, Y., Ribot-Llobet, E., Baeza, J.A., Guisasola, A., 2015. Conditions for high resistance to starvation periods in bioelectrochemical systems. Bioelectrochemistry 106, 328–334. https://doi.org/10.1016/j.bioelechem.2015.06.010

Sander, E.M., Virdis, B., Freguia, S., 2017. Bioelectrochemical nitrogen removal as a polishing mechanism for domestic wastewater treated effluents. Water Sci. Technol. 76, 3150–3159. https://doi.org/10.2166/wst.2017.462

Sanz, L.A., Gawlik, B.M., 2014. Water Reuse in Europe. Publ. Off. Eur. Union 1–51.

Shaw, D.R., Ali, M., Katuri, K.P., Gralnick, J.A., Reimann, J., Mesman, R., van Niftrik, L., Jetten, M.S.M., Saikaly, P.E., 2020. Extracellular electron transfer-dependent anaerobic oxidation of ammonium by anammox bacteria. Nat. Commun. 11, 1–12. https://doi.org/10.1038/s41467-020-16016-y

Shewa, W.A., Sun, L., Gan, C., Bossy, K., Dagnew, M., 2022. Biological treatment of municipal wastewater using fixed rope media technology: Impact of aeration scheme. Environ. Technol.

Innov. 27, 102387. https://doi.org/10.1016/j.eti.2022.102387

Singh, A., Sawant, M., Kamble, S.J., Herlekar, M., Starkl, M., Aymerich, E., Kazmi, A., 2019. Performance evaluation of a decentralized wastewater treatment system in India. Environ. Sci. Pollut. Res. 26, 21172–21188. https://doi.org/10.1007/s11356-019-05444-z

Tavares, M.G., da Silva, L.V.A., Sales Solano, A.M., Tonholo, J., Martínez-Huitle, C.A., Zanta, C.L.P.S., 2012. Electrochemical oxidation of Methyl Red using Ti/Ru 0.3Ti 0.7O 2 and Ti/Pt anodes. Chem. Eng. J. 204–205, 141–150. https://doi.org/10.1016/j.cej.2012.07.056

Tejedor-Sanz, S., Bacchetti De Gregoris, T., Salas, J.J., Pastor, L., Esteve-Núñez, A., 2016. Integrating a microbial electrochemical system into a classical wastewater treatment configuration for removing nitrogen from low COD effluents. Environ. Sci. Water Res. Technol. 2, 884–893. https://doi.org/10.1039/c6ew00100a

UN-Water, 2021. Summary Progress Update 2021 : SDG 6 — water and sanitation for all, Summary progress update 2021: SDG 6 - water and sanitation for all. Geneva, Switzerland.

Van Timmeren, A., Sidler, D., 2007. The sustainable implant: Decentralised sanitation and energy reuse (Desaer) in the built environment. Constr. Innov. 7, 22–37. https://doi.org/10.1108/14714170710721278

Vilajeliu-Pons, A., Koch, C., Balaguer, M.D., Colprim, J., Harnisch, F., Puig, S., 2018. Microbial electricity driven anoxic ammonium removal. Water Res. 130, 168–175. https://doi.org/10.1016/j.watres.2017.11.059

Virdis, B., Rabaey, K., Rozendal, R.A., Yuan, Z., Keller, J., 2010. Simultaneous nitrification, denitrification and carbon removal in microbial fuel cells. Water Res. 44, 2970–2980. https://doi.org/10.1016/j.watres.2010.02.022

Virdis, B., Rabaey, K., Yuan, Z., Keller, J., 2008. Microbial fuel cells for simultaneous carbon and nitrogen removal. Water Res. 42, 3013–3024. https://doi.org/10.1016/j.watres.2008.03.017

Xiao, Y., Zheng, Y., Wu, S., Yang, Z.H., Zhao, F., 2015. Bacterial Community Structure of Autotrophic Denitrification Biocathode by 454 Pyrosequencing of the 16S rRNA Gene. Microb. Ecol. 69, 492–499. https://doi.org/10.1007/s00248-014-0492-4

Xu, D.C., Zhai, S.Y., Cheng, H.Y., Guadie, A., Wang, H.C., Han, J.L., Liu, C.Y., Wang, A.J., 2020.

Wire-drawing process with graphite lubricant as an industrializable approach to prepare graphite coated stainless-steel anode for bioelectrochemical systems. Environ. Res. 191, 110093. https://doi.org/10.1016/j.envres.2020.110093

Zhu, M., Zhang, M., Yuan, Y., Zhang, P., Du, S., Ya, T., Chen, D., Wang, X., Zhang, T., 2021. Responses of microbial communities and their interactions to ibuprofen in a bio-electrochemical system. J. Environ. Manage. 289, 112473. https://doi.org/10.1016/j.jenvman.2021.112473

7.6 Supplementary materials

S1 – Equation S1 - Nitrate removal rate

S2 – Equation S2 - Nitrite removal rate

S3 – Equation S3 - Nitrous oxide production rate

S4 – Equation S4 - Ammonium removal rate

S5 – Equation S5 - Total nitrogen removal rate

S6 – Equation S6 - Coulombic efficiency (CE)

S7 – Equation S7 - Electron balance for heterotrophic denitrification based on COD (COD-EB)

S8 – Table S1 - Influent and effluent concentrations of total nitrogen, nitrate, nitrite, ammonium, nitrogen dioxide and COD of e-settlers

S9 – Table S2 - Chemical composition of cathodic and anodic chambers for the abiotic tests

S10 – Table S3 - Pathogens concentration as log(CFU·100mL^{-1}) in the influents and effluents of the e-settlers with the two different anodes

(S1-S7)

Equations for the calculation of removal rates, coulombic efficiencies and electron balances

Legend: $\dot{Q}$, flow rate expressed as L·d^{-1}; $C_{NO_3^- influent}$, nitrate concentration of the influent; $C_{NO_3^- effluent}$, nitrate concentration of the effluent; rNO_3^-, nitrate removal rate; V_{TCV}, total cathodic volume expressed as m^3;

$C_{NO_2^-\,influent}$, nitrite concentration of the influent; $C_{NO_2^-\,effluent}$, nitrite concentration of the effluent; rNO_2^-, nitrite removal rate; $C_{N_2O_{influent}}$, nitrous oxide concentration of the influent; $C_{N_2O_{effluent}}$, nitrous oxide concentration of the effluent; rN_2O, nitrous oxide production rate; $C_{NH_4^+\,influent}$, ammonium concentration of the influent; $C_{NH_4^+\,effluent}$, ammonium concentration of the effluent; rNH_4^+, ammonium removal rate; rTN, total nitrogen removal rate. Concentrations are expressed as $g \cdot L^{-1}$; removal rates or production rates are expressed as $gN \cdot m_{TCV}^{-3} \cdot d^{-1}$.

(S1) Nitrate removal rate

$$rNO_3^- = \frac{C_{NO_3^-\,influent} - C_{NO_3^-\,effluent}}{V_{TCV}} \cdot \dot{Q}$$

(S2) Nitrite removal rate

$$rNO_2^- = rNO_3^- + \frac{C_{NO_2^-\,influent} - C_{NO_2^-\,effluent}}{V_{TCV}} \cdot \dot{Q}$$

(S3) Nitrous oxide production rate

$$rN_2O = rNO_2^- + \frac{C_{N_2O_{influent}} - C_{N_2O_{effluent}}}{V_{TCV}} \cdot \dot{Q}$$

(S4) Ammonium removal rate

$$rNH_4^+ = \frac{C_{NH_4^+\,influent} - C_{NH_4^+\,effluent}}{V_{TCV}} \cdot \dot{Q}$$

(S5) Total nitrogen removal rate

$$rTN = rNO_3^- + rNO_2^- + rN_2O + rNH_4^+$$

(S6) Coulombic efficiency (CE)

$$= \frac{accumulated\ charge\ (C)}{V \cdot MA_N^{-1} \cdot HRT \cdot F \cdot (n_{NO_3^-/NO_2^-} \cdot rNO_3^- + n_{NO_2^-/N_2O} \cdot rNO_2^- + n_{N_2O/N_2} \cdot rN_2O + n_{NO_3^-/N_2} \cdot rNH_4^+)} x\ 100$$

Where F is the Faraday constant (96 485 $C \cdot mol^{-1}$); V is the cathodic liquid volume (m^3); MA_N is the atomic weight of nitrogen (14 $g \cdot mol^{-1}$); HRT is the hydraulic retention time considering the cathodic volume (d); n represent the equivalent electrons required for each redox reaction

($n_{NO_3^-/NO_2^-}$=2; $n_{NO_2^-/N_2O}$=2; n_{N_2O/N_2}=1; $n_{NO_3^-/N_2}$ =5); rNO_3^-, rNO_2^-, rN_2O and rNH_4^+ are the nitrogen reduction rate in $gN \cdot m_{TCV}^{-3} \cdot d^{-1}$.

(S7) Electron balance for heterotrophic denitrification based on COD (COD-EB)

$$= \frac{(COD_{influent} - COD_{effluent}) \cdot {MM_{O_2}}^{-1} \cdot n_{O_2/H_2O} \cdot F \cdot V}{V \cdot F \cdot MA_N^{-1} \cdot HRT \cdot (n_{NO_3^-/NO_2^-} \cdot rNO_3^- + n_{NO_2^-/N_2O} \cdot rNO_2^- + n_{N_2O/N_2} \cdot rN_2O + n_{NO_3^-/N_2} \cdot rNH_4^+)} \; x\; 100$$

Where F is the Faraday constant (96 485 $C \cdot mol^{-1}$); V is the cathodic liquid volume (m^3); n is 4; molecular weight (MM) of oxygen is 32 g/mol; MA_N is the atomic weight of nitrogen (14 $g \cdot mol^{-1}$); HRT is the hydraulic retention time considering the cathodic volume (d); When the effluent's COD was higher than the inlet's COD, the COD-EB was addressed as theoretical COD-EB and calculated assuming the effluent's COD equal to 0 $mgO_2 \cdot L^{-1}$. When the effluent's COD was lower than the inlet's COD, the COD-EB was addressed as real COD-EB and calculated assuming the COD removal. In both cases the initial COD was considered to be biodegradable in spite of being the effluent of a secondary treatment.

(S8)

Table S1 *Influent and effluent concentrations of total nitrogen, nitrate, nitrite, ammonium, nitrogen dioxide and COD of e-settlers*

HRT (h); current applied ($mA \cdot L^{-1}_{TCV}$); electrode	Sample	NO_3^- (mgN-$NO_3^- \cdot L^{-1}$)	NO_2^- (mgN-$NO_2^- \cdot L^{-1}$)	NH_4^+ (mgN-$NH_4^+ \cdot L^{-1}$)	N_2O (mgN-$N_2O \cdot L^{-1}$)	TN ($mgN \cdot L^{-1}$)	COD ($mgO_2 \cdot L^{-1}$)
7.4 ± 0.6; 20 graphite	Influent	24 ± 6	2 ± 2	5 ± 4	n.d.	31 ± 4	64 ± 21
	Effluent	2 ± 3	0.1 ± 0.1	0.1 ± 0.2	n.d.	2 ± 3	89 ± 54
5.1 ± 0.6; 20 graphite	Influent	23 ± 6	0 ± 0	4 ± 3	n.d.	27 ± 3	43 ± 10
	Effluent	3 ± 3	0 ± 0	0.3 ± 0.4	n.d.	3 ± 3	83 ± 18
2.9 ± 0.2; 20 graphite	Influent	25 ± 1	0.4 ± 0.6	1.5 ± 1.6	0.3 ± 0.1	27.1 ± 0	24 ± 4
	Effluent	8 ± 7	0.3 ± 0.5	0.3 ± 0.4	0.5 ± 0.3	8 ± 6	62 ± 10
3.1 ± 0.6; 61 graphite	Influent	20.0 ± 0.5	0.9 ± 0.1	0.07 ± 0.08	0.1 ± 0.1	21.0 ± 0.5	35 ± 6
	Effluent	3 ± 3	0.5 ± 0.4	0.2 ± 0.2	0.2 ± 0.1	4 ± 3	65 ± 8
2.2 ± 0.1; 98 graphite	Influent	19 ± 2	0.4 ± 0.3	31 ± 3	0.3 ± 0.1	50 ± 4	66 ± 4
	Effluent	11 ± 11	0.6 ± 0.7	17 ± 12	0.4 ± 0.2	28 ± 3	89 ± 20
2.1 ± 0.1;	Influent	20 ± 2	2 ± 1	23 ± 3	0.2 ± 0.1	44 ± 1	56 ± 6

98 Ti-MMO	Effluent	21 ± 13	3 ± 3	6 ± 7	0.5 ± 0.2	30 ± 4	74 ± 24
2.3 ± 0.2; 214 Ti-MMO	Influent	20 ± 1	2 ± 1	18 ± 2	0.3 ± 0.1	52 ± 4	120 ± 64
	Effluent	20 ± 9	2 ± 2	4 ± 6	0.4 ± 0.2	26 ± 3	67 ± 25
2.1 ± 0.2; O.C.V. TiMMO	Influent	34 ± 1	0.2 ± 0.4	0.8 ± 0.9	0.2 ± 0.1	35 ± 1	92 ± 36
	Effluent	25 ± 1	0.4 ± 0.6	0.04 ± 0.1	0.2 ± 0.1	26 ± 1	46 ± 13
2.1 ± 0.2; 214 Ti-MMO	Influent	37 ± 0.1	0.01 ± 0.02	0.5 ± 0.4	0.2 ± 0.1	37 ± 1	74 ± 5
	Effluent	25 ± 2	0.2 ± 0.1	0.1 ± 0.1	0.2 ± 0.1	26 ± 2	44 ± 10

Legend: n.d., not determined

(S9)

Table S2 *Chemical composition of cathodic and anodic chambers for the abiotic tests*

Condition	Time						
		NO_3^- (mg N-$NO_3^-\cdot L^{-1}$)	NO_2^- (mgN-$NO_2^-\cdot L^{-1}$)	NH_4^+ (mgN-$NH_4^+\cdot L^{-1}$)	N_2O (mg N-$N_2O \cdot L^{-1}$)	Total Nitrogen (mg $N \cdot L^{-1}$)	COD ($mg\cdot L^{-1}$)
-0.9 V vs Ag/AgCl		Cathodic chamber					
	0 days	29.1	0.31	1.31	n.d.	30.7	7.15
	7 days	28.1	0.2	6.1	1.3	35.6	89.9
		Anodic chamber					
	0 days	29.1	0.31	1.31	n.d.	30.7	7.15
	7 days	31.1	2.02	7.2	n.d.	40.9	157

(S10)

Table S3 *Pathogens concentration as log(CFU·100mL^{-1}) in the influents and effluents of the e-settlers with the two different anodes*

Anode HRT Current applied		Bacterial count (log(CFU·100mL^{-1}))		
		Total coliforms	E.coli	Enterococcus
Graphite 2.2 ± 0.1 h 98 mA·L$^{-1}_{TCV}$	Influent	> 2	> 2	> 2
	Effluent	1.3 ± 0.9	0 ± 0	0 ± 0
Ti-MMO 2.3 ± 0.3 h 214mA·L$^{-1}_{TCV}$	Influent	2.3 ± 0.5	1.5 ± 0.7	1.7 ± 0.5
	Effluent	0.4 ± 0.1	0 ± 0	0 ± 0
O.C.V. 2.0 ± 0.2 h	Influent	2.8 ± 0.2	1 ± 0	1 ± 0
	Effluent	1.3 ± 0.4	1 ± 0	1 ± 0

Acnkowledgements

Almost 4 years have passed since I received the proposal to enter into the field of bioelectrochemistry. At the time, I knew it would not be an easy path. I was a bit scared but also fascinated by understanding how this field of science could work, how electrons could travel around surfaces, contributing in the growth of life. The path I followed has been rich of ups and downs, of days where I wanted to quit and days where I felt that there was something amazing. During this time, I have had the luck of sharing the road with many people who supported me and who were by my side to celebrate and rest.

First of all I thank prof. Zanaroli, for having believed in me and for having given me the chance to be a PhD student in his lab. I thank Elena, because even if we worked together only during the last part of this journey, I really felt trusted, supported and motivated. I want to thank also prof. Bertin, for having given me the opportunity to be the tutor of the organic chemistry course. I had the dream of teaching and I really enjoyed those moments, where I could talk about science, trying to simplify the mechanisms behind it so as to help students to understand it.

Many thanks go also to colleagues and friends. Thanks to Angela, for all the smiles and laughs. Thanks to Eliana, for the collaboration we have just started and for the effort we made to understand the reciprocal scientific worlds. Thanks to Emma, for sharing the office with laughs and advices. Thanks to Kejvin, for all the scientific discussions, talks and support. Thanks to Roberta, for having convinced all the people of the department to bring a cake for everybody. The world is a sweeter place thanks to you. Thanks to Sara, for having shared the long and hot summer days during the year of COVID. Thanks to Stefano, for all the discussion and support about electrochemistry, you really helped me. Thanks to all the new entries, Sara, Caterina, Rosaria, for all the laughs, discussions, advices and launches shared together. Lastly, I really thank Andrea, who supported me especially during the first year, when I still had to learn many things and few people were around to talk about science and bioelectrochemistry.

A special thanks goes to the Lequia group (Girona, Spain) who warmly welcomed me during my stay abroad. I'm very grateful to Narcis and Sebastià for all the trust, support, advices and wisdom that they shared and given to me. I will never thank them enough for what I've learnt, both as a person and as a scientist. I also thank Laura, Alba, Emma, Meri, Gaetan and all those who have made Girona my home.

Leaving the work field, I think I should still have to list so many people that I don't know if I'll finish in time to submit this thesis. Firstly I thank my parents, Marco and Patti, because they have started believing in me almost 28 years ago and still do it. I thank my sister Lucia, all the cousins, Fili and Ale, and wives,

Lisa and Co, with whom I've shared many dinners and nice talks. I thank my mentor, spiritual guide and psychologist, Raffa who helped me to go through this PhD, and helped me becoming the person I am today. You really supported me, so thank you. I thank Sara, who is both a friend and a sister, for all the thoughts and talks shared. Thank to the crew of Maranello, Alice, Cero, Cri, Debbi, Elia, Frenci, Laura, Piro, Schiavo, because it is always nice to share some time and boardgames with you. I thank Giulia, for being a great flatmate, friend, advice giver and for all the bottles of wine we shared. I thank Anna, for being my flatmate, adopted sister, friend and for having shared the amazing period of the lockdown (and many other experiences). Thanks to Fede, for all the mountains that we have conquered together in these years. I thank all the guys from Chimind, Pando, Ila, Ninho, Teo and many others.

I thank also the people from EVO. Thanks to Angelo, Chiara, Crippi, Dash, Debs, Ele, Federico, Federica, Fra, Fraschi, Ila, Lori, Jacopo, Margi, Marghe, Miri, Simo, Succo, Terry. Thanks to Loris who spent so much love and time for us.

Thanks to Diego, who became a spiritual father and friend to me. Many thanks to Noemi, Egidio, Laura and Ale for the gratuity of our relationships.

The most important thanks goes to you, Annalisa. I've started this journey meeting you at the Poggeschi. We first became friends, taking care of each other with tenderness. Then we've decided to spend our lives together, supporting each other and celebrating ourselves for the rest of our lives. You're a gift and if this journey has been softer, it has also been thanks to you.